EPFL

Thèse n° 9249

Orchestration of oscillatory activity to improve visual motion discrimination

Présentée le 20 décembre 2021

Faculté des sciences de la vie
Unité du Prof. Hummel
Programme doctoral en neurosciences

pour l'obtention du grade de Docteur ès Sciences

par

Roberto Felipe SALAMANCA GIRON

Acceptée sur proposition du jury

Prof. M. D. C. Sandi Perez, présidente du jury
Prof. F. C. Hummel, directeur de thèse
Prof. M. Murray, rapporteur
Prof. H. Bridge, rapporteuse
Prof. M. Herzog, rapporteur

École
polytechnique
fédérale
de Lausanne

2021

Acknowledgements

These lines will never be enough to thank and recognize the fundamental role that every single person that has passed through my life has played for me to achieve this. I have been extremely lucky to be in a position of choosing what I want to do and thus, build a path that has permitted me to have iconoclast interactions with amazing brains and very autoctonous personalities. To everyone that has given me a moment to remember, just my most sincere affection and my deepest gratitude, because you have immensely contributed to this version of me. Nevertheless, I think that the purpose of this thesis flies way beyond doing a long list of names that consciously or not, have helped me write this current document.

This being written, I think I rather prefer to just simply humble myself to this wonderful possibility that existence has given me and just dedicate this tiny contribution to the scientific knowledge to all those patients that pose their expectations, dreams and hopes in people like me, and wait uncomfortably to listen novel ideas, disruptive concepts and unimagined solutions that might help them overpass their dolences. My compromise is with you and it will always be the engine that moves me forward.

Abstract

This thesis describes advances in the use of novel configurations of non-invasive brain stimulation over the visual system allowing to modulate of modifying electro-physiological activity, interregional interactions and by it, visual behavior such as motion discrimination capacity in healthy subjects. These novel paradigms were conceived based on the idea of applying electric currents to the brain like an ordered symphony that ought to follow timed-motifs, precise dynamics and specific frequencies, as it happens when an orchestra plays. To this aim, we have implemented three experimental protocols that include the application of a motion discrimination and integration task in combination with bifocal transcranial Alternating Current Stimulation (i.e. tACS) over the primary visual cortex (i.e. V1) and medio-temporal areas (i.e. V5), while varying some of the “orchestra” parameters in each study. The common objective pursued in the three studies presented in the upcoming chapters was to evaluate physiological changes induced by tACS combined with the visual task, leading to enhanced visual performance expressed by the accurate distinction of the generalized movement orientation of a kinetogram.

After introducing the scientific rationale of this thesis in Chapter 1, Chapter 2 describes whether applying two phase-shifted (Alpha) α-tACS conditions (Anti-Phase and In-Phase tACS) within the V1-V5 network were able to positively modulate behavior compared to Sham tACS. Our results suggest that the active Anti-Phase condition significantly increased visual motion discrimination compared to In-phase tACS which rather tended to decrease performances. These two case scenarios were associated with opposite changes in Alpha-Gamma oscillatory modulation (i.e. V1 phase – V5 amplitude coupling) determined by multichannel EEG.

Based on these findings, in Chapter 3, we describe testing the effects of modulating Alpha-Gamma interregional interaction. Hence, two conditions V1αV5ɣ tACS and vice versa, V1ɣV5α tACS, were behaviorally and electrophysiologically evaluated. The results suggested that there was a common electrophysiological feature between the two Verum tACS, which contrasted with Sham tACS, expressed through WPLIɣ (i.e. Weighted Phase Locking Value) connectivity. Furthermore, WPLIα and ZPAC V1amplitude – V5phase (i.e. Z-scored Phase Amplitude Coupling) were the inter-areal mechanisms in which both Verum conditions differed to explain the variance of their corresponding group behavior. However, the electrophysiological changes did not lead to significant difference in behavioral measures.

In Chapter 4, we combined the knowledge gained in the first two studies and thus, we time-locked, short bursts of phase-shifted α-tACS to the visual stimulus onset. This permitted to find out that, despite the phase difference between the tACS conditions (i.e. In-Phase vs. Anti-Phase), there was a generalized augmentation of the performance after verum stimulation compared to the results with Sham. This amelioration was generally associated with changes in causal PSI (i.e. Phase Slope Index) flows in ɣ, whereas specifically the Θ-ɣ modulation permitted to explain the differences in behavior between Verum and Sham. Moreover, dynamic PSI-causal β bottom-up and top-down flows revealed the mechanisms behind each type of Verum stimulation.

These studies provided first interesting evidence that physiology-inspired bifocal tACS applied to the visual network might be used to modulate visual behavior and respective underlying mechanisms. The induced electrophysiological and behavioural

effects achieved are complex and need to be studied in more details in upcoming studies. Ultimately the present findings serve as a basis to keep exploring and defining parameters of stimulation inducing more pronounced behavioural effects with the potential of translating this knowledge into novel therapeutic approaches for visually-impaired patients such as patients after a stroke suffering from hemianopia.

Keywords : Oscillations, motion discrimination, tACS, orchestration

Résumé

Cette thèse décrit les avancées dans l'utilisation de nouvelles configurations de stimulation cérébrale non invasive sur le système visuel permettant de moduler ou modifier l'activité électrophysiologique, les interactions interrégionales et par elle, le comportement visuel tel que la capacité de discrimination du mouvement chez des sujets sains. Ces nouveaux paradigmes ont été conçus sur la base de l'idée d'appliquer des courants électriques au cerveau comme une symphonie ordonnée qui devrait suivre des motifs chronométrés, une dynamique précise et des fréquences spécifiques, comme cela se produit lorsqu'un orchestre joue. À cet effet, nous avons mis en œuvre trois protocoles expérimentaux qui incluent l'application d'une tâche de discrimination et d'intégration de mouvement en combinaison avec la stimulation bifocale transcrânienne à courant alternatif (i.e. tACS) sur le cortex visuel primaire (i.e. V1) et les zones médio-temporelles (i.e. V5), tout en faisant varier certains paramètres « d'orchestre » dans chaque étude. L'objectif commun poursuivi dans les trois études présentées dans les chapitres à venir était d'évaluer les changements physiologiques induits par le tACS combiné à la tâche visuelle, conduisant à une performance visuelle améliorée exprimée par la distinction précise de l'orientation généralisée du mouvement d'un kinétogramme.

Après avoir introduit la justification scientifique de cette thèse dans le chapitre 1, le chapitre 2 décrit si l'application de deux conditions α-tACS déphasées (Alpha) (tACS Anti-Phase et In-Phase) au sein du réseau V1-V5 a pu moduler positivement le comportement par rapport à Sham tACS. Nos résultats suggèrent que la condition Anti-Phase active augmente significativement la discrimination visuelle du mouvement par rapport au tACS In-Phase qui a plutôt tendance à diminuer les performances. Ces deux scénarios de cas étaient associés à des changements opposés dans la modulation oscillatoire Alpha-Gamma (i.e. le couplage phase V1 - amplitude V5) déterminés par EEG multicanal.

Sur la base de ces résultats, dans le chapitre 3, nous décrivons tester les effets de la modulation de l'interaction interrégionale Alpha-Gamma. Par conséquent, deux conditions V1αV5ɣ tACS et vice versa, V1ɣV5α tACS, ont été évaluées sur le plan comportemental et électrophysiologique. Les résultats suggèrent qu'il y avait une caractéristique électrophysiologique commune entre les deux tACS Verum, qui contrastait avec le tACS Sham, exprimé par la connectivité WPLIɣ (i.e. la valeur de verrouillage de phase pondérée). De plus, WPLIα et ZPAC V1amplitude - V5phase (i.e. le couplage d'amplitude de phase à score Z) étaient les mécanismes inter-zones dans lesquels les deux conditions de Verum différaient pour expliquer la variance de leur comportement de groupe correspondant. Cependant, les changements électrophysiologiques n'ont pas conduit à une différence significative dans les mesures comportementales.

Dans le Chapitre 4, nous avons combiné les connaissances acquises dans les deux premières études et ainsi, nous avons synchronisé des courtes rafales de α-tACS déphasés (*In-Phase* et *Anti-Phase*) à chaque présentation d’un stimulus visuel. Cela a

permis de découvrir que, malgré la différence de phase entre les conditions tACS (i.e. In-Phase vs. Anti-Phase), cette amélioration était généralement associée à des changements de connectivité directionelle mesurée par PSI (i.e. Phase Slope Index) en ɣ, alors que plus spécifiquement la modulation Θ-ɣ permettait d'expliquer les différences de comportement entre Verum et Sham. De plus, la connectivité ascendante et descendante en Beta (PSI-β) a révélé des mécanismes différents dans les deux type de stimulation Verum.

Ces études ont fourni la première preuve intéressante que le tACS bifocal inspiré de la physiologie appliqué au réseau visuel pourrait être utilisé pour moduler le comportement visuel et les mécanismes sous-jacents respectifs. Les effets électrophysiologiques et comportementaux induits obtenus sont complexes et doivent être étudiés plus en détail dans les études à venir. En fin de compte, les résultats actuels servent de base pour continuer à explorer et à définir des paramètres de stimulation induisant des effets comportementaux plus prononcés avec le potentiel de traduire ces connaissances en de nouvelles approches thérapeutiques pour les patients malvoyants tels que les patients après un AVC souffrant d'hémianopsie.

Mots-clés : Oscillations, discrimination de mouvement, tACS, orchestration

Contents

Preface

In this thesis, I present the results of a series of studies conducted during my doctoral studies. My projects are focused on the idea of orchestrating the oscillatory activity between areas V1 and V5 of healthy subjects, by means of bifocal tACS, with the goal of modulating motion perception.

At the time of writing, 1 review is published (Raffin et al., 2020), 1 study is published (Salamanca-Giron et al. 2021) and 2 are in preparation (Salamanca-Giron et al. 2022 a, Salamanca-Giron et al., 2022 b). The 3 studies included in this thesis main body :

Enhancing visual motion discrimination by desynchronizing bifocal oscillatory activity.
Roberto F. SALAMANCA-GIRON, Estelle RAFFIN, Sarah B. Zandvliet, Martin SEEBER, Christoph M. MICHEL, Paul Sauseng, Krystel R. HUXLIN, Friedhelm C. HUMMEL.
NeuroImage, 2021

Cross-frequency tACS modulates EEG coupling during a motion discrimination task.
Roberto F. SALAMANCA-GIRON, Martin SEEBER, Christoph M. MICHEL, Krystel R. HUXLIN, Estelle RAFFIN, Friedhelm C. HUMMEL.

Bursts of bifocal α-tACS improve visual motion discrimination.
Roberto F. SALAMANCA-GIRON, Martin SEEBER, Christoph M. MICHEL, Krystel R. HUXLIN, Friedhelm C. HUMMEL, Estelle RAFFIN.

Additional work associated to the field (Raffin et al., 2021) :

Adaptive changes in regional and network activity in response to TMS induced virtual lesions of the visual cortex.
Estelle RAFFIN, Roberto F. SALAMANCA-GIRON, Krystel R. HUXLIN, Olivier RENAUD, Loan MATTERA, Roberto MARTUZZI, Friedhelm C. HUMMEL.
Cerebral Cortex, 2021

1 Introduction

The human visual system constantly gets different types of inputs that ought to be processed in order to successfully behave in daily life. Among these types of incoming information, there is one visual feature whose correct interpretation is very relevant for common activities such as walking, navigating in space, grasping and even reading : motion perception. Therefore, given the broad palette of activities where this feature is involved, it is of importance to understand the underlying mechanisms of it, how its processing is implemented in the brain and thus, how can it be possibly modulated to ultimately pave the way towards the regulation of such a complex human behaviors.

1.1 Visual motion perception

1.1.1. Classical model of vision

The definition of a pathway related to motion perception involves several brain areas (e.g. striate, extrastriate cortices) that interact with each other in order to interpret different visual contextual variables (e.g. direction, sensitivity, integration of features, contrast, etc.), playing together a fundamental role to achieve perception. In support of this, current literature highlights the idea of a constant parallel interplay between the ventral (‘what’) stream and the dorsal (‘where’) stream in the visual cortex (Goodale and Milner, 1992), that actually permits to the motion perception pathway to receive and process information rapidly and efficiently (Gilaie-Dotan, 2016).

Specifically, Mortimer Mishkin and Leslie Ungerleider proposed this hypothesis of having two processing streams in the visual cortex. The two-pathways model describes how the visual cortex processes information. A dorsal pathway, located towards the posterior parietal cortex, processing where are the objects located in the visual field, and the ventral pathway, projecting into the infero-temporal cortex, carrying information about which objects are in the visual scene (Mishkin and Ungerleider, 1982).

Livingston and Hubbel extended this model to the earliest sensory input due to the discovery of parvocellular cells (P-cells) and magnocellular cells (M-cells) found on a first stage in the retina and posteriorly, in the thalamus (i.e. lateral geniculate nucleus, LGN) (Livingstone and Hubel, 1984). P-cells have small receptive fields, sensitivity to color (i.e. different wavelengths), high-spatial frequencies, medium conductance velocity and responses lasting only as long as the stimulus is present. M-cells have large receptive fields, no sensitivity to color, rapid conductance and transient responses, associated with motion perception. Essen and Gallant discovered that there is a constant crossover between the two streams when they tried to cut off the precortical path, this fact pointed strongly to connections between the two routes (Van Essen and Gallant, 1994).

The crossover of the two streams has been considered fundamental for the visual system (Maunsell et al., 1990). When the two streams work together, implying an interaction between the P-cells and M-cells, they permit an adequate interpretation of features, such as speed of motion in longer ranges. This feature that is essential to not only understand the trajectory and the direction of a moving stimulus, but also to define it in space according to other characteristics such as texture and depth (Felleman and Van Essen, 1991). (See Figure 1)

In general terms, a hierarchical but complementary organization describes the relationship between the basic features (e.g. orientation, speed, composition, etc) of an incoming visual stimulus in the lower visual areas, and the integrative aspects (e.g. direction, shape, texture, etc.) of visual perception in higher cognitive areas (DeYoe and Van Essen, 1988; Allman et al., 1985).

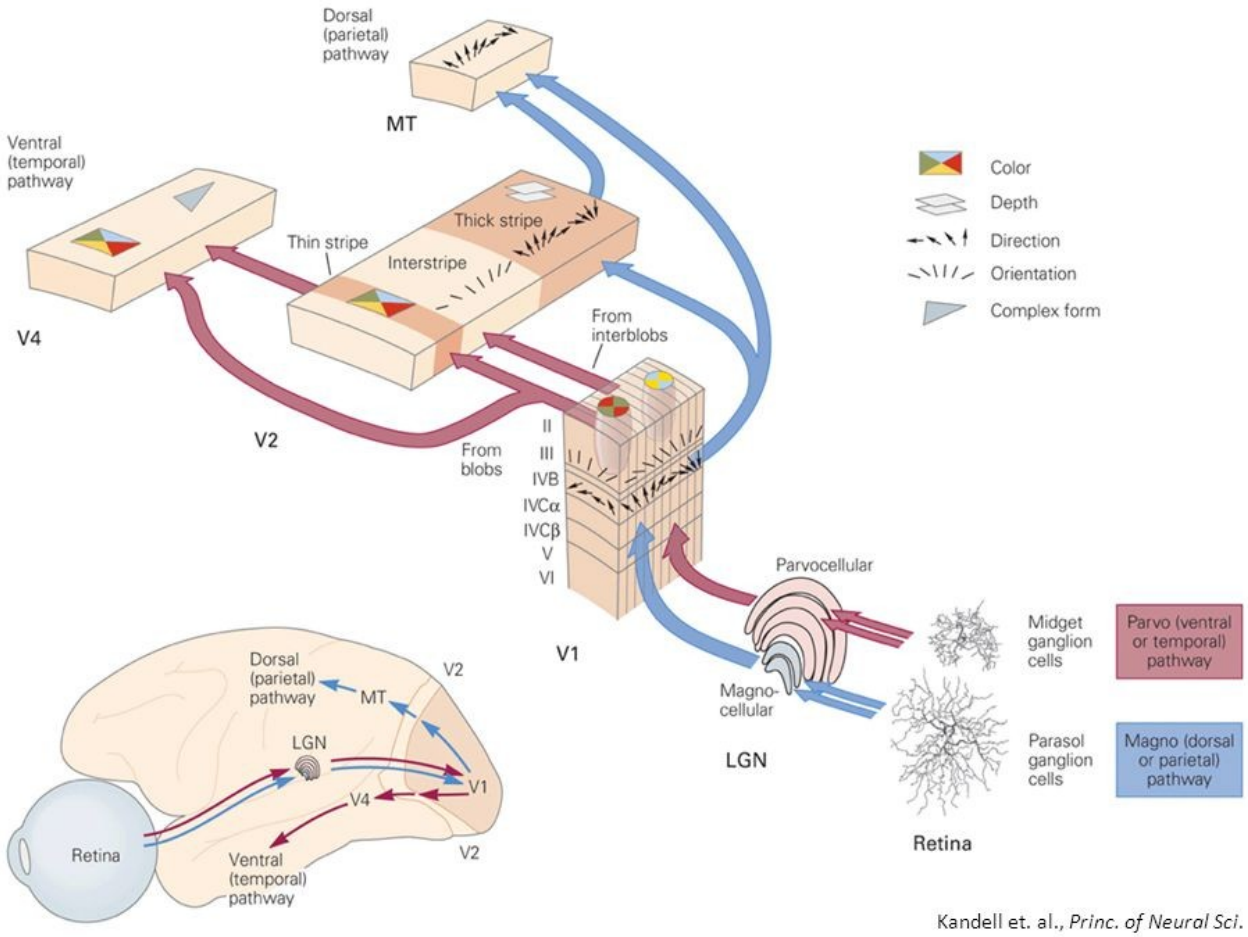

Figure 1. Classical two-streams model of vision. Dorsal and ventral streams and their different actors from the retina to respectively MT area and V4. Adapted from (Kandel et al., 2014).

In the upcoming subsections I will introduce the most known and accepted description of the basic morphological and physiological organization involved in motion perception. We center our focus on remarking the most canonical model discovered and tested in both humans and animal models (Orban et al., 2004), helping us building up our scientific framework around the modulation of a specific defined portion of this pathway in healthy subjects, with the expectation of carrying a clear behavioral associated response.

1.1.2. From the retina to the primary visual cortex (V1)

When photons reflected from an object excite the retina, two types of photo-receptors, i.e., cones and rods, transform the light into electrical impulses in a process that is known as photo-transduction (Tsin et al., 2018). Thanks to this photo-transduction process, the perception of motion is inferred by the visual system through the changes of incoming patterns of light in the retina (Johansson, 1975). The subsequent neuronal activation is possible when the photo-excitation provokes the separation of opsin proteins from Vitamin A molecules (Hubbard and Wald, 1951). This liberation generates an exchange of ions that lead to an electrical impulse within a chemical process known as Wald's visual cycle (Tsin et al., 2018; Wald, 1935).

The relationship between the photo-receptors and motion perception is as follows. Rods have shown to be primarily sensitive to moving stimuli benefitting from their distribution over the entire surface of the retina (Schaerer and Neumeyer, 1996). This might have occurred as an evolutionary response to rapidly amplify and detect surrounding danger or prey (Johansson, 1975), even in low intensity light environments (Hecht et al., 1942; Schaerer and Neumeyer, 1996). Cones rather located in the center of the retina (i.e. foveal area), are highly sensitive to color and fine details, thus needing a big amount of light to trigger an electro-chemical activation. Nonetheless, cones also sense motion in the fovea, but they contribute mainly to the refinement of the image that is seen (Hecht et al., 1942).

The electrical impulse, as an output from Wald's visual cycle, travels through a bundle formed by the axons from retinal ganglion cells (i.e. optic nerve) until the chiasma where it receives the input from the contra-lateral eye. From this point onward, there is a transmission of this impulse through a pathway that reaches the Lateral Geniculate Nucleus (i.e. LGN) in the Thalamus, where a direct connection to the primary visual cortex (i.e. V1) originates (v. Monakow, 1895). The LGN has been shown to be a structure that refines the topographical mapping that has been done previously in the retina (Weyand, 2016).

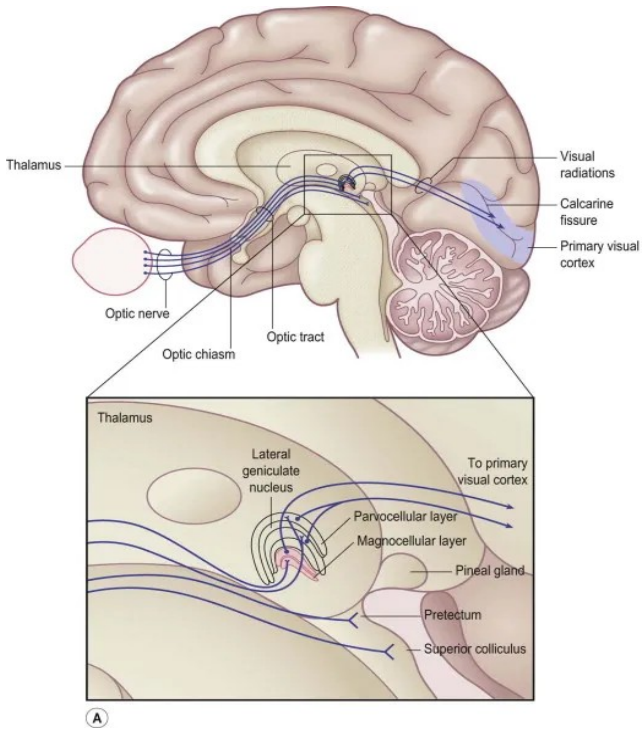

Figure 2. Graphical representation showing the main components of the retino-geniculate-striatal pathway (retina→ optic nerve → chiasm → LGN → V1). Figure adapted from (Kandel, 2014).

Contributing to the perception of motion, the LGN might play a role in locating a visual stimulus within the stereoscopic spatial representation via the modulation of the interaction of the separate outputs from the two eyes (Dougherty et al., 2019a), however whether there is an exclusive modulation of monocular neurons or also a complementary binocular cellular modulation, still remains an open question (Howarth et al., 2014; Dougherty et al. 2019b). Furthermore, the LGN modulates the perception of a stimulus and the integration of its features, as location in space and speed, via connections with higher-order anatomical levels in the cortex (Jones et al., 2015). From the 6 layers of cells in the LGN, composed predominantly by magnocellular cells (layers I and II) or parvocellular cells (layers III, IV, V, VI), there are axonal connections to the different subparts of the IV layer of V1, that in turn contribute to understanding stimulus features in a retinotopic manner (See figure 1).

In fact, this retinotopic characterization was demonstrated through invasive recordings in cats and monkeys by the winners of the Nobel Prize in 1981, David Hubel and Torsten Wiesel, who mapped the electrical response from cells in V1. Their experiments permitted to decompose the visual system in a hierarchy composed by simple, complex and hypercomplex cells (Hubel and Wiesel, 1962). Meaning that when the information arrives to V1, it is redistributed in bits of information according to the receptive field of each cell-type responding in complexity to a precise stimulus feature (e.g. direction, position, orientation, color, etc.). The neurons that are similarly

topographically activated by each characteristic are organized in columns/blobs that respond together to the specific attribute (Hubel and Wiesel, 1968, 1965, 1962).

Specifically in V1, the majority of cells are selective to directions and orientation and this has been shown to be a fundamental fact to perceive motion (Livingstone and Hubel, 1988). Nevertheless, the retinotopic organization in the LGN and in V1 is non-isometric, meaning that is weighted by the sensitivity due to the quantity and type of photo-receptors that were activated in the retina on the first place (Afgoustidis, 2015).

The description of these first steps is in line with the classic theory of motion perception suggesting a two-steps mechanism (Albright and Stoner, 1995). From one side, it implies that on the retino-geniculate-striatal pathway, there is a first basic interpretation of the direction of the visual stimulus features and its sensitivity to the motion of its respective contours. From the other side, in the extrastriate areas, an integration of basic features occurs and thus, a recognition of moving patterns take place, as it will be explained in the next section (Adelson and Movshon, 1982). Moreover, this two-steps model helps us to narrow down anatomical areas of interest because in order to have an effective influence in the pathway, we ought to take into the account the intercept between the first step where a first direction/orientation recognition is performed and the second step, where an information integration occurs. Therefore, given that the great majority of processed information through the retino-geniculate-striatal pathway leads to V1, this anatomical area was chosen as our first target.

1.1.3. From V1 to extrastriate areas

Extrastriate parts of the occipital visual cortex (e.g., V2, V3, V5/hMT+) play a fundamental role in motion perception, based on parallel integrative processes complementing the directionality sensitivity processing from early areas in the retino-geniculoate-striatal pathway (Li et al., 2001). Literature shows that there is not only a serial flow of information towards these areas after visual features have reached V1, but there are parallel flows among higher extrastriate areas (Andersen, 1997 ; Bullier and Nowak, 1995; Schroeder et al., 1998).

V2 extends the functionality of V1 but is organized in 4 quadrants and they are tuned to color, orientation, illusory contours and ground-figure differentiation (Cowey, 1964; Qiu and von der Heydt, 2005). In the case of V3, cells are tuned to orientation, depth and motion. Dorsal parts of V2 have shown to have a role in coherent motion processing linked to its projection towards the temporal lobe of the cortex (Braddick et al., 2001), while ventral sections of V3 are rather dedicated to color and shapes. Regarding the perception of motion, V2 demonstrates to better respond to high temporal frequencies (i.e. number of occurrences throughout time) and low spatial frequencies (i.e. number of perceived cycles per degree within a defined space) than V1 (Foster et al., 1985), whereas V3 presents a high receptive capacity of spatial frequencies plus a high contrast sensitivity, essential properties for interpreting motion (Gegenfurtner et al., 1997).

More importantly, the human motion middle-temporal complex (i.e. named interchangeably hMT+/V5), composed by the Middle Temporal Area (i.e. MT), with small receptive fields and organized retinotopically, plus the Superior Temporal Area (i.e. MST), rather with big receptive fields but with no retinotopic organization (Huk et al., 2002) has been characterized as the region by excellence responding to motion sensing (Dubner and Zeki, 1971). As a matter of fact, invasive recordings in the analogous brain area of primates, named complex MT+ (see figure 3), demonstrated that the majority of cells in this area were selective to directionality suggesting a columnar organization of this area (Zeki, 1974). Moreover, the experiments made possible to distinguish between cells that responded either to a single direction or to multiple directions regardless of the stimulus shape, plus cells rather sensitive to the movement of contours, suggesting that there is indeed a specialization of motion perception this area (Zeki, 1978, 1974).

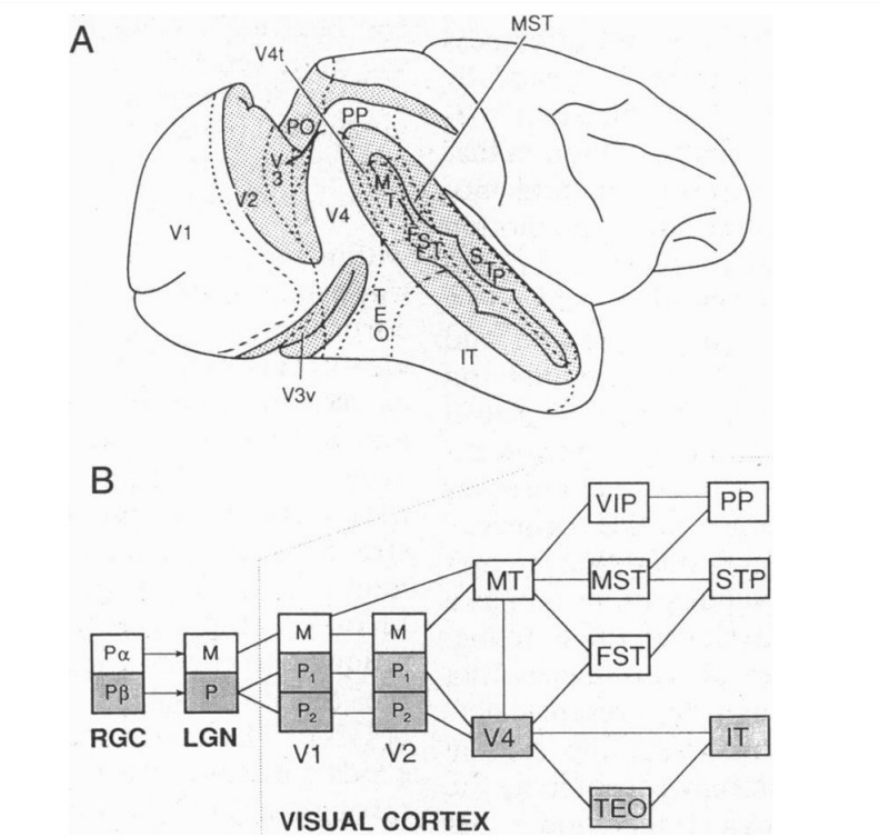

Figure 3. A. Lateral view of a monkey brain with primary visual and extrastriate visual areas. **B.** Anatomical connections of the motion perception pathways, originating from different retinal ganglion cells (RGN). The scheme underlines the

hierarchical arrangement, but also the parallel processing of different aspects of the stimuli. Magno (M, black) vs Parvocellular (P, white). VIP = ventral intraparietal, FST = fundus superior tempral, STP = superior temporal polysensory, PP = posterior parietal, MST = medial superior temporal. Taken from (Albright and Stoner, 1995).

Later experiments have permitted to confirm such a statement. From one side, trial-randomized invasive microstimulation augmenting the rate of cell discharge of the MT+ area while monkeys where undertaking a motion discrimination task, led to a more recurrent motion perception in the cells that tuned up to the specific direction in the task (Salzman et al., 1992). Complementary, antidromic microstimulation of MT+, allowed to show that cells from V1 to MT+ respond to complex motion patterns and they are definitely directionality selective (Movshon and Newsome, 1996). From another side, studies implying lesions of different extensions of MT+ in primates, resulted in the impairment of perceiving motion at different thresholds and difficulty at capturing the characteristics of the presented movement (Pasternak and Merigan, 1994). In a similar manner, small chemical lesions in monkey's brains enabled the understanding that saccadic and pursuing eye movements necessary to track motion, become deficient when MT+ is injured (Newsome et al., 1985). Additionally, virtual lesions studies in humans by means of Transcranial Magnetic Stimulation (TMS) knocking out / virtually lesioning MT+/V5 at the stimulus onset, demonstrated that it negatively affects the perception of motion in a random-dot discrimination task (Hotson et al., 1994). Highlighting with all these examples together the crucial role that the complex area hMT+ and MT+ plays in the perception of motion in humans and primates.

As a matter of fact, hMT+ has been shown to be capable of acting independently of V1 suggesting a parallel pathway involved in motion perception in humans. This has been widely described through experiments testing the effects of the Blindsight phenomenon (Ajina et al., 2015b, 2015a; Ajina and Bridge, 2018a). Blindsight implies the unconscious perception of visual stimulation despite the fact of not consciously perceiving it because of a lesion in V1, and it seems to actually be linked to the capacity of sensing movement in this extrastriate area through a direct functional connection from the LGN that permits to patients with a deranged visual field to perceive changes in speed (Ajina and Bridge, 2018b). Nevertheless, it is also important to remark that even though V5 could get activated through a different pathway away from V1, it has been demonstrated that its directionality sensitivity is greatly reduced when information has not passed through the serial path that involves V1, suggesting a precarious areal interplay to accomplish motion perception (Girard et al., 1992).

Under this principle of joined and separated action of V1 and V5, it has been possible to measure the latencies associated to the transmission of a visual stimulus from the retina to the visual cortex, that open further possibilities of precisely influencing the perception of motion in human subjects. Specifically, experiments with transcranial magnetic stimulation (TMS) over V1 and V5 in humans, permitted to demonstrate that it takes ~60ms for information to arrive to V1, whereas a considerably shorter timing of around ~30ms is needed to activate the hMT+ complex. This latter finding

complements the idea that there are V5 to V1 feedback signals appearing before the arrival of a visual stimulus to V1 (Hupé et al., 2001). Furthermore, the time that it takes for the motion associated signal to travel from V1 to V5 is around ~40ms. Setting up this way a precise framework of reference for interventions and a detailed understanding of motion perception (Beckers and Zeki, 1995).

Figure 4. Parallel pathways towards V5 and their respective timings measured by means of TMS applied over V1 and V5. Taken from (Zeki, 2015)

Apart from these extrastriate areas (e.i., V2, V3, V5/hMT+), there might be some other neuronal areas such as the superior temporal sulcus that extend the function of perceiving external motion towards the processing of self-motion, such as facial and body dynamic cues, and other complex motion-related scenarios (Rokszin et al., 2010). For instance, in the parietal cortex, the anterior intraparietal has been claimed to be in charge of movements like grasping or grabbing, whereas the lateral intraparietal cortex might serve as a controller of gaze that contributes to the perception of motion through the constant tracking of the position of a moving stimulus (Sakata et al., 1997). In the frontal lobe, the Frontal Eye Fields, possess pursuit neurons that have been implicated in tracking motion, sensitive to speed and tuned to a specific directionality (Akao et al., 2005).

In this order of ideas, it has been explicit how motion perception is a network process that implicates several actors depending on the source and characteristics of the motion. Nonetheless, in the current thesis we decided to minimize and focus on the complexity and focus on the following network of interest formed between two of the main zones that demonstrate to be relevant for visual perception and conscious motion sensing, respectively V1 and V5.

V1 as explained before, collects the output from the first processing stage, leading to a primary interpretation of directionality sensitivity (Adelson and Movshon, 1982; Girard et al., 1992; Livingstone and Hubel, 1988). V5 in turn, is by excellence, the area where a greater part of the motion signals falls into because of the characteristics of neurons to tune up to specific orientations, directionality and changes in speed, in other words, sensing of motion (Movshon and Newsome, 1996; Newsome et al., 1985;

Salzman et al., 1992; Zeki, 1978, 1974). Although these two areas can act independently and there are even alternative pathways (e.g. blindsight pathway) activated upon an incoming moving stimulus, the greatest portion of information debunked from the motion flows seem to fall into V1 and consecutively be transmitted to V5 (Felleman and Van Essen, 1991).

The main part of the motion perception might thus take place between V1 and V5 due to the functional hierarchical organization that implies that there are more enlarged receptive fields the more you advance in the pathway (Hubel and Wiesel, 1965, 1962), meaning that there is a process of refinement of information, that is composed by a first step of direction sensing in V1 that then in a second step it is integrated as a coherent pattern in V5 (Movshon and Newsome, 1996; Pasternak et al., 1985; Shipp and Zeki, 1989). Hence, we took these two core areas as our main targets for neuromodulation that impacts in the capacity of perceiving motion.

1.1.4. The aperture problem

It is important to remark that the perception of motion could be achieved by either eye movements pursuing the changes in position over time of a certain stimulus or instead, by having different parts of a non-moving retina excited by the same stimulus at different times. In the current thesis, given the experimental conditions demanded to the participants, i.e. central-dot gaze fixation during a motion discrimination task, we focus on understanding the neurological correlates linked to the second scenario.

This multiple-spots excitation of the retina at subsequent time-points has been modeled as a multiplication of time-lagged signals that result in a motion signal. Specifically, it has been proposed that there are motion-energy sensors capable of accounting for the bi-directional correlation in space and time associated to the change in position of a stimulus between to instants (Hassenstein and Reichardt, 1956). This model was further improved by assuming that there is rather a trace of activation throughout the retina that gets captured by bi-local sensors located in V1 and in the MT and MST areas. These sensors are sensitive to a certain speed that imply an excitation of two nearby receptive whose image coincide taken into account a time delay between the two. The direction of the retinal excitation implies a uni-directional correlation of consecutive sensors (van de Grind et al., 1986).

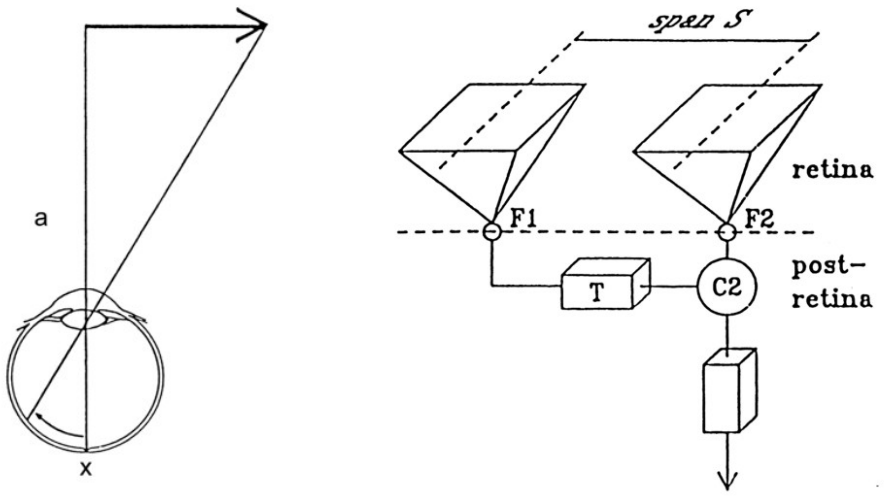

Figure 5. A. Vectorial scheme of the horizontal motion of a particle in space projected into the retina at two different points after a certain time-delay **B.** Blocks diagram representing a motion detector, where the excitation of two different reception fields (F1, F2) in the retina, with a time span (T) between both occurrences, at a specific distance (S), allow C2 to compute the uni-directional correlation of the dynamic trajectory. Adapted from (Ehrenstein, 2003).

These sensors of motion incur in what is known as the aperture problem, meaning that there might be an ambiguous perception of the speed of a stimulus given the reduced size of the receptive field that is capturing it. This fact implies that there are several portions of the retina that might elicit the same null estimation of the real movement of the stimulus, until some of these receptive fields detects changes in the edges, orthogonal or at a precise angle to the movement, that help inferring the direction of the stimulus (Wallach, 1935).

This aperture problem highlights as well the idea that motion processing requires not only the hierarchical pathway processing from V1 to MT characterized by small features processing, nor just the early activation of the bigger receptive fields in MT providing a better overview of the scene, but also the involvement of areas such as MST that might contribute to the integration of visual context and sensory information (Snowden and Freeman, 2004). Nevertheless, although we acknowledge the over-simplification of our approach by only taking into account two of the most prominent areas (i.e. V1 and V5) within the extensive network associated to motion perception, due to the experimental and ethical limitations from our non-invasive intervention we prefer to not involve further areas.

1.3. Visual processing through oscillatory activity

1.3.1. Evidence of oscillatory activity in visual processing

Endogenous electrical activation and deactivation in the brain can be defined by its periodicity, implying that it is patterned and time-modulated, and thus, interpreted as oscillatory traces of activity evolving through time and flowing among brain sites (Singer, 2018). This activity is favoured by the network-like organization and interconnection of several neuronal populations that debate themselves between excitatory and inhibitory motifs. These motifs ultimately are a representation of different encoding and gating processes that permit information transmission and its interpretation within or among several neuronal clusters (Singer, 2018).

In this order of ideas, neural oscillations could be taken as a representation of grouped synchronous cellular exchanges of charged ions through the membrane (Llinás and

Yarom, 1986), or instead as rhythmic firing of action potentials (Azouz and Gray, 2000). These oscillatory patterns can be perceived at meso/macroscopic level as local or inter-areal interactions of neuronal ensembles, representing collective bio-physical interactions embedded in a specific brain network (Buzsáki and Draguhn, 2004; Varela et al., 2001). Moreover, these cortical synchronized interactions have been suggested to be of interest for cognition (Fries, 2005; Wang, 2010) and perception (Cabral-Calderin and Wilke, 2019; Ronconi et al., 2017) as underlying correlates of behavior.

The firsts notions of oscillatory activity in visual processing come from the experiments from Hubel and Wiesel characterizing time simple visual fields depending on the variety of their cellular responses (e.g., indifference to movements, unilateral/bilateral response) as well as complex visual fields that were taking into account mixed behaviors, such as switching on-off areas. With this objective, they took into account the responses of excitatory moving stimuli at different speeds and exciting the different cells involved in the processing of a visual stimulus. This speed was taken as the rate of movement proportional to the time between 2 discharges. Like this they manage to discover that cells are tuned to specific directions and speeds (1°/s – 10°/s) and the discharge firing, sensed as oscillations, is synchronized to movement at a cadence of 5-10 spikes occurring at a frequency of 20 Hz (Hubel and Wiesel, 1962).

These studies were further developed with intracortical recordings in cats and in fact, they continued to demonstrate that not only the global features of the stimuli were relevant to characterize the information encoding in an oscillatory response, but it was also necessary to achieve a magnitude and/or phase synchronization of cells of different columns for optimal communication. This could even happen without phase difference between sites, however, the distance between them and, above all, the preferred orientation of the column, played a role (Gray et al., 1989).

For instance, distances longer than 7 mm in intracortical recordings showed an nonexistent inter-areal phase-locking, nonetheless when fitting damped sinusoidal gabors, the cat’s visual cortex would synchronously and significantly fire at 40-60 Hz. Moreover, different stimulus orientations provided different synchronization profiles, e.g. Angular difference until 22° of a preferred stimulus orientation has the highest correlation (0.4 mm to 7 mm), whereas 45° seemed to impair the correlation, and 90° guaranteed a medium correlation. Ultimately, what was shown here is that the time synchronization between columns established transient relationships that encode features of a visual input in really specific manners depending on the cytoarchitecture and the characteristics of the stimulus (Gray et al., 1989). Additional recordings in the primary visual cortex of kittens showed a consistent 40 Hz oscillation correlated with behavioral attention. In the absence of a sensory stimulus in the receptive field, oscillations were around 1-10 Hz. When visualizing an optimal stimulus, oscillations increased its frequency up until a velocity of 42 +/- 7 Hz. Furthermore, during periods of response, the oscillations were tuned at 35-50 Hz lasting 250ms in the feedforward direction and 500ms in the feedback direction, implying a specific timing to achieve the convey of information throughout the visual cortex (Gray and Singer, 1989).

In general terms, synchronized oscillations in the visual cortex (i.e. +/- 10-50 Hz) have been proven to appear in invasive recordings of neuronal assemblies when their

receptive fields are activated by specific orientations and directions from an observed stimulus (Gray and Singer, 1989). Fact of immense interest because it shows that visual context, defined by these specific properties of a stimulus, is of importance to lead towards an organized dynamical firing and synchronization within a neuronal cluster serving functionally to interpret incoming information (Singer, 1999).

This synchronization of oscillations that permit communication has been proposed to happen in two different mechanisms: First, coherence, meaning that neuronal clusters are co-activated in the same timing, encompassing equivalent magnitude and phase temporal dynamics for the clusters. This fact in turn, allows the existence of windows where the synchronized signals either, permit the processing of incoming information or output the results of this interpretation (Fries, 2005). Second, gating by inhibition, that proposes the pulsed inactivation of regions that are not of importance for a certain process, through the use of low-frequency oscillations. This implies as well the trace of a relevant pathway composed by the areas that are important for information interpretation, and where local stages of processing occur by means of high frequency oscillations (Jensen and Mazaheri, 2010). Therefore, this latter concept suggests that low frequency oscillations around 10 Hz are mainly used for inter-areal connections that imply longer distances and thus, longer wavelengths (Palva and Palva, 2011), and rapid oscillations above 30 Hz as local processes that encode specific stimulus features (Fries, 2009).

Complementary, synchronization could be also measured as a cross-frequency signal modulation, modality that helps supporting the inter-areal communication between areas as it is recruited by several perceptual modalities (Canolty et al., 2006). It has been proposed that these cross-frequency modulation motifs extend from just simply a synchronicity in time to actually be part of a full intermingling of two cross-frequency signals (e.g., amplitude-modulation). This fact is in line with the way endogenous brain activity behaves, given that there are no singular frequency components traveling from point A to B, to be instead a melange of signals that flow all around neuronal clusters. Under this premise, slow encoding of visual features from a stimulus has been described as an amplitude modulation phenomenon of Gamma activity spiking linked to membrane potential changes (Volgushev et al., 2003) and this notion has been complemented by temporal transitions in electrophysiological states where it is possible to see how high-frequency (<30 Hz) intermingles with low frequencies (>13 Hz) components in both amplitude-modulated and phase-modulated motifs, becoming fundamental for any interpretation of perceptive processes from the outer world (Freeman and Rogers, 2002).

In order to give a frame of reference of directionality of these oscillations, we have followed the definition of dynamicists in systems neuroscience that do not depend on fixed morpho-physiological hierarchy, thus avoiding its caveats (Rauss and Pourtois, 2013), but being aware of the specialization of each area (Kinchla and Wolfe, 1979). Hence, based on the temporal binding model (Engel et al., 1992; Engel and Singer, 2001; Singer, 1999; Singer and Gray, 1995), we determine a bottom-up flow as a feedforward stream that implies the recruitment of a more integrative and larger dynamical activity from a less complex processing area, meaning an area where really simple features are interpreted (e.g. V1→V5), whereas a top-down flow or feedback, implies the opposite interaction (e.g. V5→V1) (Haken and Stadler, 2012; Rauss and

Pourtois, 2013; Engel et al., 2001). As an example of the use of this framework, please refer to our already published papers (Salamanca-Giron et al., 2021, Raffin et al., 2021).

With these basic concepts of oscillatory activity in the visual cortex in the different factors and interactions that might define their relationships, what are then the most prominent rhythms involved in visual processing in the brain? In the upcoming section we present studies in favour of two frequency bands, Alpha (7-13 Hz) and Gamma (<30 Hz), that seem to be involved in the majority of vision-related processes.

1.3.2. Functional role of oscillatory activity in the Alpha and Gamma band in the visual cortex

Evoked Alpha-like and endogenous Alpha rhythms involved in vision perception of different types of visual stimuli have been elicited in a variety of behavioral tasks, where a peak resonant frequency in the visual cortex, at of 9-10 cycles per second, characterizing the stimulus features such as flickering, direction, etc. has appeared consistently (Childers and Perry, 1971).

This knowledge has been deepened by Varela and colleagues, who demonstrated that temporal framing in visual perception is correlated with the Alpha wave phase. In detail, what Varela *et al.* discovered was that the stimulus onset from an occipital Alpha wave marks the dynamic where the trough is linked to sequential perception, whereas the peak is rather linked to simultaneous perception. These events were characterized by flows of excitation and inhibition lasting between ~80 – 200 ms. In addition, their findings revealed that to separately perceive two consecutive stimuli, they should not occur at the peak of the Alpha oscillation, but at different phase onsets (Varela et al., 1981).

Complementary studies in the cat's visual cortex suggested that oscillations might be a second stage of coding complementary to the receptive field mapping in the primary visual cortex. The timing associated with these oscillations is the way of encoding specific features from an incoming visual stimulus and they might lead to resonance usually perceivable around 40-50 Hz (up until 80 Hz and belonging to the Gamma band) depending on the velocity of the stimulus (Eckhorn et al., 1988). Moreover, Eckhorn *et al.* argued that the phase synchronization of neuronal clusters of the network, where the oscillations flow, determine the relationships of synchronization and their inter- and intra-areal communication. This means that congruent and similar structurally-organized neuronal columns, in each one of the network’s nodes tune up to a certain specific feature from the visual stimulus (e.g., orientation, direction, speed, etc.) and this happens in one of three phase linking circumstances: Bottom-up entrainment by a common driver sharing excitatory connections, a top-down signal from higher ranked cortical areas or a mutual excitation from columns at the same rank in the hierarchy (Eckhorn et al., 1988).

Gamma activity has been described as one of the pillars of perception under the influence of several types of stimuli and contexts, more importantly it seems to play the fundamental role of linking segmented pieces of information from an incoming stimulus. Stimuli are generally composed of several features that ought to be understood by different connected neuronal clusters. This connection among neuronal clusters might be achieved through the elicitation of Gamma rhythms that serve as a local synchronizing tool (Fries, 2009). An example of this in the visual perception pathway in monkeys has been reported during a perceptual task. The results stated that feedforward Gamma activity accounted for the changes in reaction time of the animals, through an optimal inter-areal Gamma phase relationship (Rohenkohl et al., 2018).

As highlighted before, it is not only a matter of feedforward communication carrying the information associated to the input stimulus to higher processing areas, feedback signals are of extreme importance to comprehend the environmental context of the task. Thus, intracortical experiments in monkeys have been able to depict the oscillatory interplay that composes bilateral information transfer in the visual cortex. While feedforward communication seems to preferentially happen in the Gamma (30-80 Hz) range, the same team reported evidence that feedback is manifested in lower frequency bands, precisely in the Beta band (14-30 Hz) (Bastos et al., 2015). This study is backed up by similar results from laminar recordings and microstimulation in monkeys undertaking a segregation task where it was possible to see a feedforward signalling once more in the Gamma band, however in this case the feedback signals appeared to be in the Alpha band, instead of the Beta (van Kerkoerle et al., 2014).

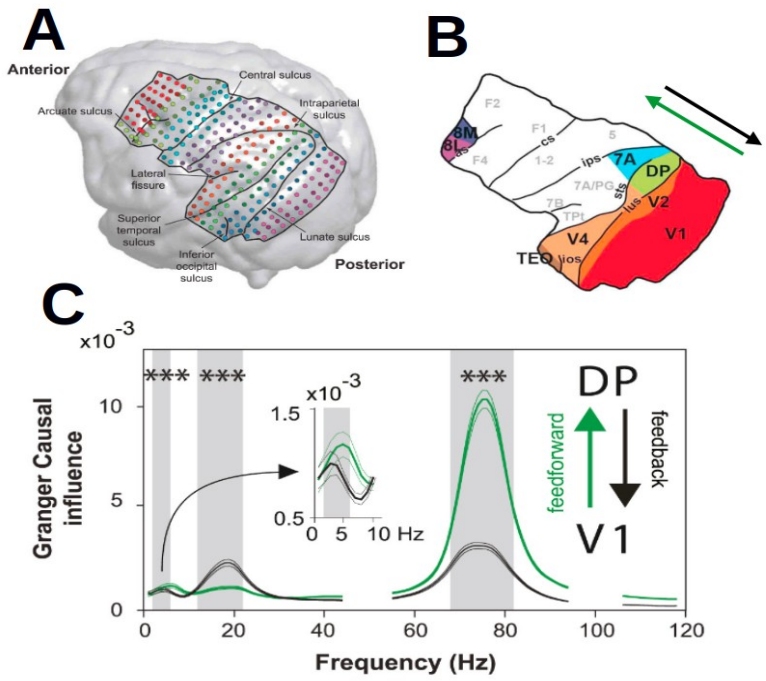

Figure 6. Adapted from (Bastos et al., 2015). Main directional oscillatory flows taken from intracranial recordings in a monkey's experiments linked to motion sensitive areas. **A.** Brain localization of the intracranial electrodes mesh **B.** Scheme representing the areas covered by the mesh **C.** Granger causality relationships between V1 and DP (i.e. approximate location of V5 in humans)

These experiments are supported by the outcome from an experiment with human participants engaged in an attentional-monitoring task eliciting both feedback and feedforward flows. Congruent with the set of monkey's experiments, magnetoencephalographic (MEG) results showed that feedforward directions are mostly governed by Gamma and the feedback signals are rather in the Alpha-Beta band. Directionality of information flow was drawn through Granger causality (Michalareas et al., 2016). Besides, in the specific case of motion discrimination in humans, it has been shown that there are specific low frequency components in Delta-Alpha, significantly appearing in both V1 and V5 associated to the characteristics of the movement and its specific timings. This accordance between oscillations and stimulus, might be a representation of a gating mechanism that permits integration of information in higher cortical areas (Händel et al., 2007).

Complementing these results, further experiments in monkeys showed that these causal cross-frequency interactions ruling the feedforward and feedback sweeps take place at precise timings. Likewise, they provide an orchestrated information flow in the visual cortex, suggesting that not only location and directionality are essential, but also timing between signals in order to achieve an optimal transmission. Specifically, the study proved that a top-down Beta band signal from the Parietal cortex to V1, precedes a bottom-up V1 to V4 Gamma signal during a visuo-attentional task in monkeys. This cross-frequency elicitation was optimal when there was a delay of 100 ms between both signals (Richter et al., 2017).

These earlier studies emphasize the existence of two prominent rhythms dominating within the visual cortex: Alpha and Gamma. Specifically, Alpha oscillations appear to be linked to the perceptive sampling of novel or changing features of visual incoming stimuli. This sampling seems to be regulated by adding a temporal context to visual events by means of the phase of the low-frequency waves, generating an impulse of the synchronization of neuronal columns. This time framework takes place through moments of excitation and inhibition at a rate of every couple of hundreds of milliseconds (Childers and Perry, 1971). Whereas Gamma oscillations are linked to the way each feature is ciphered and delivered to every specialized column (Eckhorn et al., 1988). But, how are these two frequency bands related to the perception of motion? In the upcoming section we reviewed the most important studies that relate oscillatory activity and motion perception.

1.3.3. Neural oscillations, potential signature of motion perception

In order to make sense of complex seen properties such as those decomposed from a moving stimulus, binding and synchronization of cellular columns processing complementary visual features takes place (Gray et al., 1989). This neuronal binding when unwrapped in the time domain, constitutes a mechanism to integrate and group processing information from different cortical stages of relevance, permitting an holistic interpretation of a visual input (Engel et al., 1997; Singer and Gray, 1995). Thus, coherent oscillatory neuronal activity appears to be a rapid and efficient manner

to code visual motion perception, given that different features that permit motion sensing, such as orientation, directionality, speed, etc. generate distinct resonant frequencies (35-85 Hz) across organized columns (Eckhorn et al., 1988; Fries et al., 2001)

.

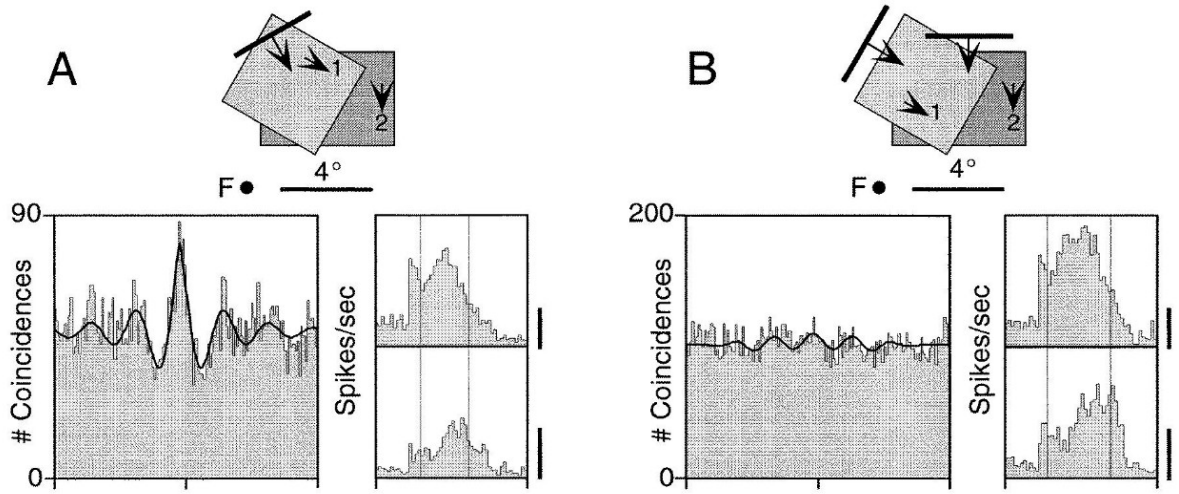

Figure 7. Intracortical recordings of a monkey brain during a motion perception task. F = Fixation point, Arrows = neuronal direction of preference, 1-2 = Receptive fields of V1 and V5 cells **A.** Synchronization of V1 and V5 after the presentation of a moving bar, please note the increased central peak in the cross-correlogram when the movement was between the two preferred directions **B.** Absence of synchronization when the movements where in the two preferred cellular directions. Adapted from (Kreiter and Singer, 1996).

Based on the previous ideas, several studies of specific oscillatory signatures accompanying several modalities of visual perception have been shown in animals and human literature. For example, monocular stimulus in strabismic cats demonstrated the elicitation of high frequency activity (<30 Hz), whereas its dichoptic presentation led to a neural synchronization of not only those neurons that directly responded to the stimulus but also those cells previously activated, thus highlighting the fundamental role of synchronicity for visual perception (Fries et al., 1997). Additionally, in a visual detection task applied to human subjects, it was shown that the maximum detection threshold depended on the phase concentration of low oscillatory (>13 Hz) activity that served as a predictor of behavior probably due to the fact of helping to frame perception in time (Busch et al., 2009). Complementary, it was later on demonstrated that this phase prediction was also associated with a phase-amplitude coupling interaction (i.e. low frequency phase modulates high frequency amplitude) that modulated performance and sensitivity of participants in a similar visual-target task (Fiebelkorn et al., 2013).

Thus, a condition of static-eyes perception of motion has most probably a specific oscillatory signature that tunes up to the characteristics of the stimulus. In favor of this idea, in an apparent motion task where stimuli were consecutive or presented at the same time, it was demonstrated that correct responses were maximized when they matched a specific phase-angle in the low-frequency oscillatory traces (7-13 Hz) from the visual cortex (Varela et al., 1981). Moreover, in the context of motion discrimination in humans, it has been shown that there is an amplitude modulation of Gamma rhythms by the phase of a Delta wave whose coupling strength directly correlates with the number of correct responses in a motion discrimination task (Händel and Haarmeier, 2009). This phenomenon has been as well reported in other contexts involving visual perception such as short memory tasks (Demiralp et al., 2007), intracranial recordings during a visual matching task (Bruns and Eckhorn, 2004), selective attention rhythmic entrainment in monkeys (Lakatos et al., 2008) and even in a working memory task (Lee et al., 2005).

By taking into account that oscillatory activity in the brain might be taken as organized patterns of activity that represent encoding of motion information processing in the cortex, and this processing is actually characterized by prominent rhythms (i.e. Alpha and Gamma), how could one influence and/or modulate such precise brain oscillatory signatures in order to induce a modulation of motion perception? In the upcoming section of the introduction, we propose a non-invasive stimulation technique that might be the key factor helping with this endeavor.

1.4. Transcranial Alternating Current Stimulation

Non-invasive brain stimulation techniques are used with the aim of driving brain electrical activity through the elicitation of different electrophysiological mechanisms that might be associated to changes in cortical excitability, brain plasticity and specific behavioral outputs (for review see Hummel and Cohen, 2006). Taking into account specifically brain oscillations as a meaningful electrophysiologcal correlate of behavior (Singer, 2018), two main transcranial techniques have been used to tackle their modulation : Repetitive transcranial magnetic stimulation (rTMS) or transcranial alternating current stimulation (tACS). In the case of rTMS, it has been proven that it is possible to generate pulsed activity that resembles brain oscillations and thus, drive the endogenous oscillatory activity of the brain achieving an improved synchronization over time. One important factor in this regard is to take into account the phase of the endogenous frequency-specific signal that is being modulated (Thut et al. 2011).

In the case of tACS, it bases its operation in the output of low-power sinusoidal signals of a certain frequency, that aims at mimicking the endogenous brain activity. The main advantages of tACS and our main motivations behind its use are the relative low-cost of its implementation compared to other techniques such as rTMS, its portability and its versatility to adjust its parameters, such as frequency, intensity and location of stimulation. Therefore, in the upcoming sections we will provide more information about the tACS known effects, its properties and some examples of its use related to motion perception.

1.4.1 Principle of action of tACS

tACS has been reported safe to use (Antal et al., 2017) and it has been extensively applied especially in the last decade with the aim of boosting ongoing oscillatory activity through the principle of online neural “entrainment” that ultimately might lead to plasticity (Bola et al., 2014; Schutter and Hortensius, 2011). Its normal range of spatial resolution is in the centimeter range, although recent electrical field modeling optimization techniques have been proposing better montages to place the stimulation electrodes that might improve this resolution (Saturnino et al., 2019).

The entrainment associated to the tACS refers to the imposition of a rhythm to an interconnected system of oscillators and its occurrence depends on both amplitude and phase from an mastering external source (Strogatz, 2003). This is possible because these specific frequencies, with defined phase characteristics, applied through tACS, imply an online synchronization of neuronal clusters that behave as grouped oscillators adhering up to the flow from the externally applied electrical signal (Herrmann et al., 2013). This might generate a long-term potentiation (or depression, depending on the network) in neuronal connections (Deperrois and Graupner, 2020), mainly motivated by the quantity and the moment in which neuronal spikes are generated in time. This is associated with the variation of the cellular sensitivity to fire reinforcing the adaptation to novel connections and configurations (Markram et al., 1997). As an example of this online effect, an augmentation in the perception of retinal phosphenes was associated to the use of tACS when it was set to the predominant frequency of the occipital cortex (Kanai et al., 2008).

This modification of firing sensitivity refers to the modulation of intrinsic properties from neurons because the oscillatory activity from the tACS makes fluctuate their membrane potential threshold (Bergmann et al., 2009) (See figure 8), probably also generating this way a transient offline effect that might remain over a period of time (Kasten et al., 2016). This fact has been proven with pure electrophysiological studies where for example occipital alpha band activity was enhanced 3 minutes after the use of tACS (Zaehle et al., 2010), and from a behavioral point of view, with for instance, an enhanced behavioral performance in a mental rotation task, 50 minutes after tACS stimulation, associated to an augmentation in alpha coherence and power (Kasten and Herrmann, 2017).

Nevertheless, the effects of tACS have been controversial, because it seems to exist a relevant heterogenity in electrophysiological and behavioral results. This might be due to the anatomical and physiological differences among subjects suggesting that the intensity of the electrical field is not enough to reach the cortex (Vöröslakos et al., 2018) (See figure 9), plus the fact that it has not been possible to effectively look at the online consequences of its function especially in the same frequency without reliably removing brain endogenous activity, given the presence of the artifact associated to the stimulation (Barban et al., 2019).

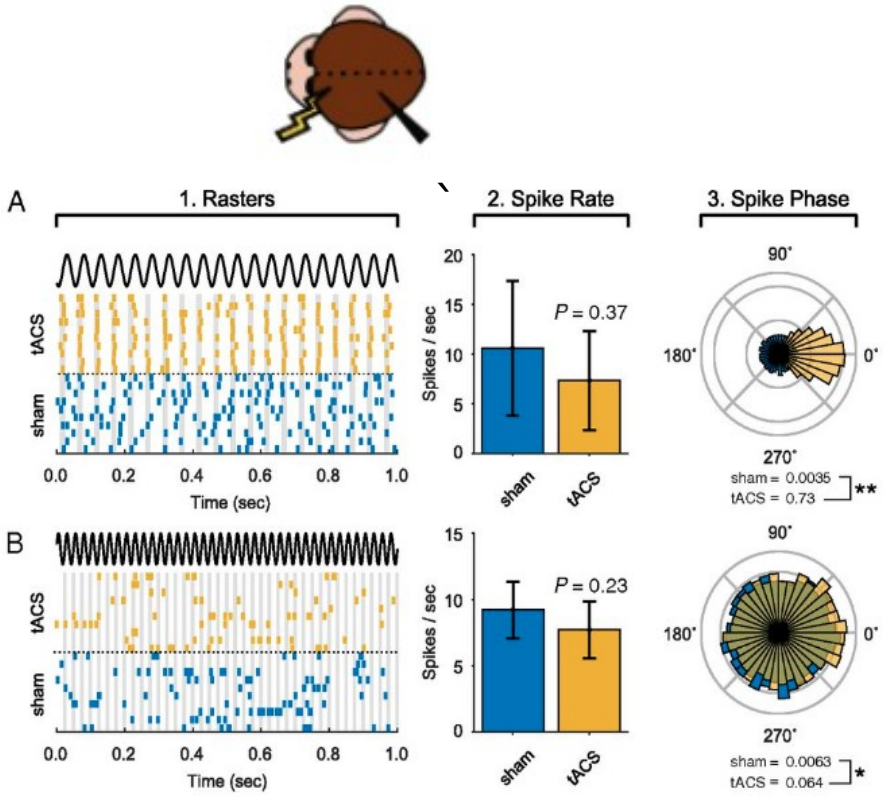

Figure 8. Example of intracortical evidence from the tACS entrainment in the posterior neuronal activity of a monkey. The tACS entrainment imply a concentration in the phase distribution compared to a Sham condition. This occurs for both low and high frequencies of stimulation. Adapted from (Krause et al., 2019).

However, given that it has been suggested that tACS might be capable of modulating cortical excitability (Schutter and Hortensius, 2011) by modifying the connections between the areas where it is applied (Neuling et al., 2015), this is a great technique to be implemented in the studies composing this thesis given that we intend to modulate non-invasively the inter-areal interactions between V1 and V5. Besides, although there is no accepted implementation of an artifact removal tool that permits to evaluate the online effects of its use, tACS has been proven to effectively have offline electrophysiological consequences after using it for more that ~70 minutes (Kasten et al., 2016) fact that facilitates our evaluation of its consequences in our protocols.

Furthermore, we decided to make use of tuning it to the most prominent personalized oscillatory signature related to motion perception by knowing that the efficacy of this intervention is dependent on the modulation of endogenous frequencies of the network and thus, on the individualization of the peak frequencies from the subject (Neuling et al., 2013a). This builds on top of the paper of Koninck and colleagues which supported the idea that the accurate parametrization of the tACS based on the predominant natural characteristics of the network is ideal permitting the modulation of the characteristic frequencies in the cortex (De Koninck et al., 2021).

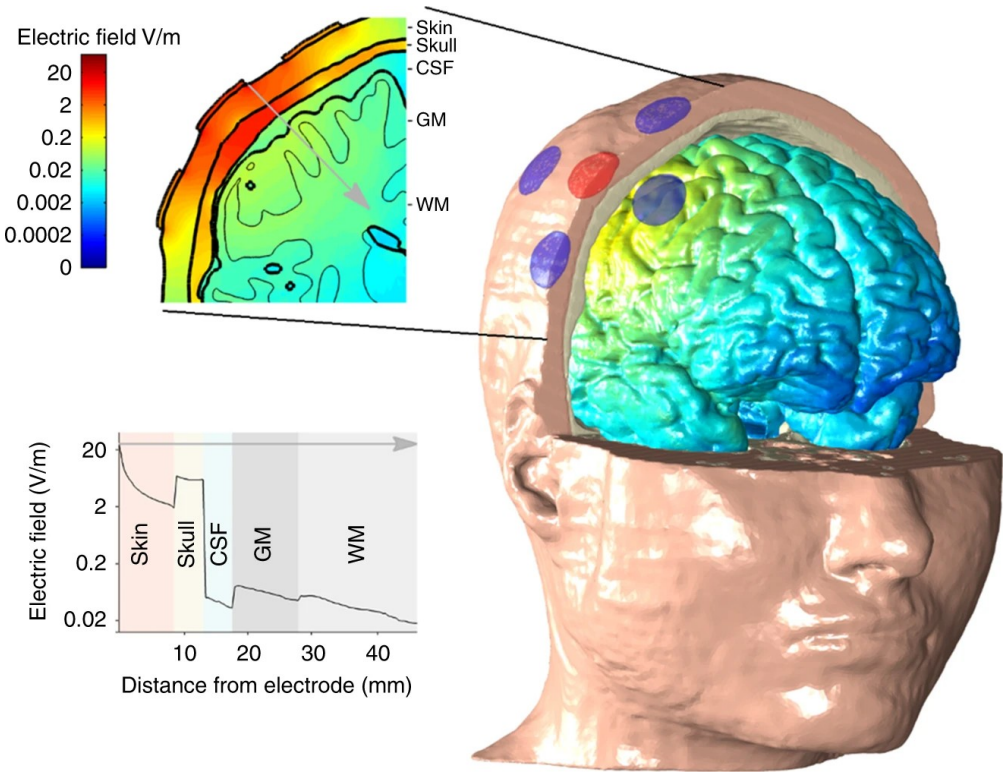

Figure 9. Example of electrical field modeling of tACS with a high-definition montage composed of 5 electrodes (Red and blue dots). The colors in the brain represent the intensity of the electrical field in the different layers between the scalp, the gray matter (GM) and the white matter (WM). Taken from (Asamoah et al., 2019).

1.4.2 tACS influencing visual perception

Examples of the use of tACS affecting visual perception achieved mixed results in different behavioral applications. For example, during a two flash fusion task, alpha tACS applied over extrastriate areas, was linked to a temporal resolution diminishment, meaning that the subjects were more likely to think of the two flashes as a single stimulus, highlighting that the perception of visual stimulus could be effectively modulated by means of tACS (Battaglini et al., 2020). In a similar vein, an increase in visual working memory performance was achieved through the application of a contralateral 4Hz tACS of the parietal cortex and not of the prefrontal cortex (Bender et al., 2019).

Contrary to these positive results, during a gabor detection task where several frequencies of posterior tACS were contrasted, the results showed that tACS over the occiput-parietal area, at 10 and 6 Hz disrupted the capacity of detection compared to a sham control (Brignani et al., 2013). Similarly, in a segregation and integration task, individualized alpha tACS over the parietal cortex, did not influence the accuracy of participants in the task. These examples complement the remark that an accurate montage placed directly over the cortical region that is in charge of the visual feature

to be processed, either at the striate and/or extra striate areas, or other spots of the network, is essential when aiming at boosting visual capacities.

The closest example of tACS to our objective in the visual system due to its aim of modulating the perception of motion is the experiment from Helfrich and colleagues where the tACS stimulation was applied bilaterally over the occipital cortex, contrasting two conditions of inter-hemispheric synchrony: In-Phase (90) and Anti-Phase (180°). They found that an In-Phase stimulation paradigm was able to increase the interhemispheric connectivity and to modulate the perception of motion. Besides, this was complemented by their electrophysiological results where Alpha oscillations were decreased in presence of a boosted Gamma pattern (Helfrich et al., 2014a).

Another close reference to our motion perception application demonstrated that 10 Hz tACS over hMT+/V5 produced a significantly increased motion direction sensitivity and reduced the subjects adaptation to motion when used during the presentation of the stimulus (Kar and Krekelberg, 2014), proving the role of the hMT+/V5 complex in motion perception and the possibility of achieving the modulation of its associated behavior. A complementary example demonstrated that 60 Hz Gamma tACS over the primary visual cortex, was able to influence covert attention expressed in a contrast-discrimination task, suggesting that there are indeed specific frequencies associated to particular processes and they could be boosted if they are targeted accurately (Laczó et al., 2012). In a similar manner, 180° bihemispheric gamma tACS over the occipital-parietal cortex, and not the 0° condition, was capable of disrupting the perception of bistable apparent motion compared to the effects of the sham condition. Additionally, the after effect of 180° gamma tACS was an augmented interhemispheric gamma coherence (Strüber et al., 2014).

These reports grouped together set a good basis to consider that tACS might be capable of modulating the ongoing brain oscillatory activity and thus, visual-related behavioral performance. We believe that the accurate set of stimulation parameters must take into account a precise targeting of areas (e.g., Bender et al., 2019), specific frequencies (Laczó et al., 2012) and phase inter-areal relationships (Helfrich et al., 2014a; Strüber et al., 2014), in order to not only influence the mechanisms represented in the electrophysiological measurements during and after intervention, but through it, modify beneficially visual perception and probably generate beneficial plastic changes (Wischnewski et al., 2019). In addition, more recent literature has suggested that another variable might be of relevance to optimally tune the tACS, the timing associated to the stimulation, meaning its duration and the moment of its application in regard of the task or ongoing brain activity. This might play a fundamental role for the modulation effects on interregional interactions and behavior, because it takes into account the engagement of the brain in a specific behavioral task (Thut et al., 2017), circumscribed in precise physiological circumstances (Zrenner et al., 2016).

In this order of ideas, tACS appears to be a good instrumental candidate through which an external stimulation of the V1-V5 pathway might drive the oscillatory activity associated to the processing of moving stimuli. Nevertheless, the tuning of several parameters of bifocal tACS remain an open question. For instance, what is the optimal inter-areal phase relationship (e.g. no phase shift, 180°, 270°, individualized phase

shift, etc.) between V1 and V5 to improve motion perception? What are the most accurate frequencies that the bifocal tACS might output to support the conveying information in the V1-V5 pathway? Or what is the precise moment and duration of the tACS to modulate behavior in a motion discrimination task?

In the upcoming chapters, based on the literature presented above, I will present the studies that reflect how we tried to experimentally address some of these questions within three different configurations of bifocal tACS targeting the motion sensing pathway, explicitly V1 and hMTt+/V5. These configurations were evaluated while healthy subjects undertake a motion discrimination task and EEG was recorded. The first configuration evaluated two different phase-shifts (0° vs. 180°) between both areas (i.e. V1 and V5), the second one evaluated a cross-frequency montages (V1 Alpha – V5 Gamma and vice versa), and the third one evaluated behavior-triggered tACS in two different phase shifts (0° vs. 180°).

1.5 This Thesis

1.5.1. General context

Current research trends have evolved towards improving the anatomical and functional knowledge of highly specific brain functions, and towards controlling and interfering in a really precise manner the neuronal basis that supports such a function. In this regard, the visual system has received immense attention given the great progress at understanding its underlying pathways. There is a large interest in systems neuroscience in finding ways to modulate neuronal activity and its respective functions by means of invasive or (even more important) non-invasive methods, determining its associated physiological and behavioral effects and understanding the underlying mechanisms that could be translated into healthy subjects or patient applications. Though there are some first promising results, there are still several important open questions which I planned to address in the current thesis within the visual domain and specifically associated to motion perception.

The choice of a motion discrimination task as experimental task was motivated by the fact that motion discrimination is a skill essential for daily life activities such as walking, driving, reading or navigating into space, and constitutes one of the most studied visual functions that provides a clear and measurable behavioral output. Besides, contemplating future translation into clinical settings, it is important to remark that patients with a cortically-generated visual field defects have shown to retain certain degree of ability at motion discrimination making this task very suitable for testing novel treatment strategies that support brain reorganization and recovery.

In this line of thought, our results might help with future developments of bio-inspired, non-invasive, electrical stimulation protocols that benefits both healthy subjects and pave the way towards helping patients, all this basing our ideas on the concept that neural electrical activity sensed as cortical oscillations and proven to be associated

with behavioral modulation, could be externally manipulated by means of tACS given that it is a neuromodulation tool that permits to apply an oscillatory electrical brain orchestration in the most similar way to endogenously generated oscillatory brain rhythms.

1.5.2. Main scope

The main research questions addressed in the present thesis are :

- Can the application of tACS applied at the main hubs of the motion detection cortical network (i.e. V1 and V5) modify behavior and interregional interactions determined by EEG-based measures?
- Is phase-shifted inter-areal Alpha stimulation (i.e. 180°) be able to increase motion discrimination performance by influencing the phase synchronization between V1-V5 ?
- Can α-ɣ inter-areal coupling through cross frequency tACS be modulated and in turn modulate motion discrimination ?
- Are task-locked bursts of inter-areal tACS be able to enhance motion discrimination capacity?

Therefore, in the current thesis, we had as a general objective to evaluate how different configurations of bifocal transcranial alternating current stimulation (tACS) modulate neuronal communication by interfering with patterns of oscillatory rhythmic activity between two key nodes of the motion discrimination network: V1 and hMT+/V5 (respectively, primary visual cortex – human medial temporal complex) and determine its impact on a motion integration and discrimination task. We hypothesized that modulating inter-areal coupling via the tACS between V1 and V5, would promote improved motion perception in healthy subjects.

1.5.3. Overview of the main methods

In this sub section, before going to the detailed research projects, a brief overview of the methods used in the present thesis will be provided, detailed methodological considerations could be found in the respective research project section.

For neuromodulation, we proposed on the current thesis the use of a bifocal configuration of ring tACS electrodes, placed over V1 and V5. The concentric ring electrodes were placed according to the 10-20 EEG systems coordinates, taking into account landmarks used in literature (Hülsdünker et al., 2019; Kar and Krekelberg, 2014). Specifically, the simulation ring aiming to stimulate V1 was placed in the vicinity of electrode P2, whereas the ring targeting V5 was placed over P6. This shape of electrodes was used due to modeling studies where it has been proven a greater

focal dispersion of the electrical field over the cortex, in the order of magnitude of some units of centimeters (Saturnino et al., 2017).

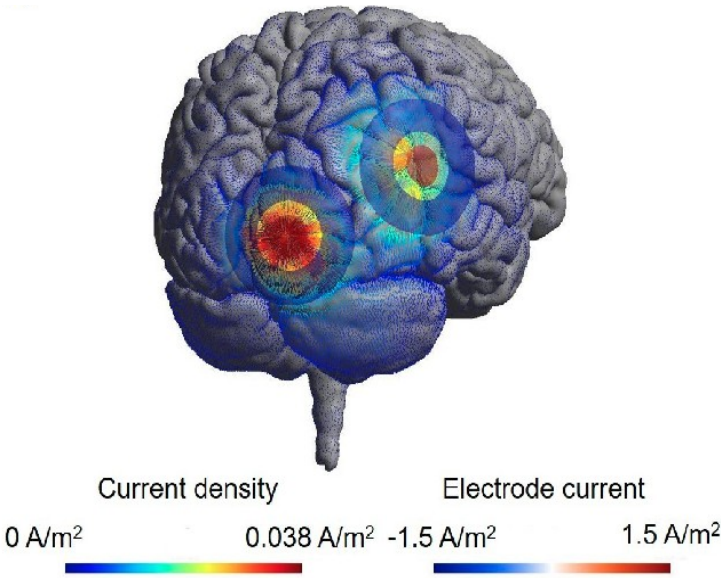

Figure 10. Electrical Field modeling of the Bifocal tACS montage by means of SimNIBS (Saturnino et al., 2019), targeting V1 and V5.

This was accompanied by the use of a well-stablished motion and integration task in three double-blinded, sham-controlled experiments, used in different studies by our collaborators (Das et al., 2014; Huxlin et al., 2009), comprising representative stimulation cohorts composed by randomly-assigned healthy participants. The task consisted in discriminating the generalized motion direction of a group of tiny black dots, located at the bottom-left of a computer screen, that were either moving to the right or to the left. The movement of the dots was randomly contaminated at each trial with some noise between 0 and 360 degrees affecting the movement. The performance score from the task was calculated from an Individual threshold extracted from the value corresponding to 75% of correct answers within a Weibull function fitted from all trials. This value was normalized to the maximum value of noise (i.e. 360 degrees) that could appear in a trial from the task (Das et al., 2014; Huxlin et al., 2009).

Each participant had electrophysiological recordings that were used to determine the oscillatory connectivity markers (phase-amplitude or phase-phase connectivity) between V1 and V5 that could be associated with changes in performance and/or the functional signatures linked to every group of stimulation. Analyses were performed at the source level through the use of the MNE library (Gramfort et al., 2014). The sources at V1 and V5 were calculated through an optimized covariance matrix. The segmentation from the forward solution was composed by 8196 sources. The inverse solution made use of the MNE-Algorithm (Hämäläinen and Ilmoniemi, 1994) to be computed. The cluster of source points that represented the anatomical landmarks for

V1 and V5, as well as the template brain used for all analyses, were taken from the predefined “SPM” atlas embedded in the MNE-Python datasets (Wakeman and Henson, 2015). From all the dipoles in each area calculated orthogonal to the cortex, we used a Principal Component Analysis with the aim of defining a single electrical signal representing the activity at both V1 and V5. A sign-flip procedure was implemented to assure a correct phase calculation of all sources at the area of interest and ultimately the first component accounting for the highest variance was selected for each case.

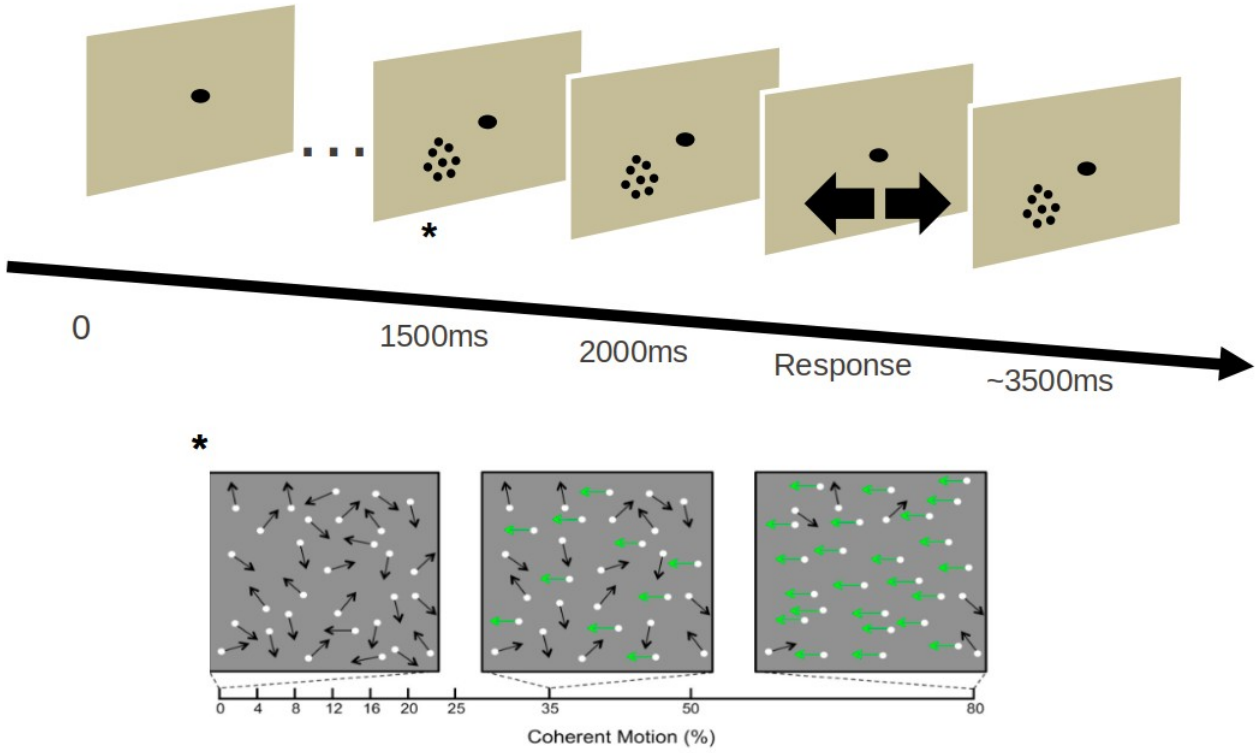

Figure 11. Graphical representation of the motion integration and discrimination task throughout time plus examples of differents levels of noise in the stimulus that could appear at the bottom left part of the computer screen. Adapted from (Romei et al., 2016)

1.5.4. Outline of the chapters

The details of the scientific motivations and the hypothesis pursued in each one of the chapters are outlined below:

Chapter 2 ("Enhancing visual motion discrimination by desynchronizing bifocal oscillatory activity"): In this first experiment we evaluated whether stimulating V1 and V5 with Alpha oscillatory activity, with different phase-shifts (0° In-Phase vs. 180° Anti-Phase) will lead to an improvement in motion discrimination. We hypothesized that In-Phase versus Anti-Phase tACS will have different behavioral impacts on motion discrimination performance.

Chapter 3 ("Cross-frequency tACS modulates EEG coupling during a motion discrimination task"): In the second experiment, we inspired our stimulation protocols on the electrophysiological results from the first study and thus, we asked whether bifocal, cross-frequency stimulation between V1 and V5 (V1αV5ɣ vs. V1ɣV5α), will impact on behavior and respective electrophysiological correlates. We hypothesized that V1αV5ɣ will support beneficial changes in visual motion perception.

Chapter 4 ("Bursts of bifocal α-tACS improve visual motion discrimination"): In this last and third chapter, inspired on the results from the two precedent chapters, we were wondering whether there would be a performance improvement, if we implement not only a phase-shift in the stimulation, proven beneficial on chapter 2, but also controlling the timing of its application as suggested in chapter 3, and its precise occurrence with respect to the task. Therefore, we performed a Sham controlled experiment, with 2 active conditions (0° In-Phase vs. 180° Anti-Phase) of Alpha, bifocal, bursts of tACS, applied over V1 and V5, time-locked to the visual stimuli onset. We hypothesized that as seen in the firs study, Anti-Phase vs In-Phase burst will have different behavioral outputs in a motion perception task.

2

Enhancing visual motion discrimination by desynchronizing bifocal oscillatory activity

Roberto F. SALAMANCA-GIRON[1,2], Estelle RAFFIN[1,2], Sarah B. Zandvliet[1,2], Martin SEEBER[3], Christoph M. MICHEL[3,7], Paul Sauseng[4], Krystel R. HUXLIN[5], Friedhelm C. HUMMEL[1,2,6]

1 Defitech Chair in Clinical Neuroengineering, Center for Neuroprosthetics and Brain Mind Institute, EPFL, Geneva, Switzerland.

2 Defitech Chair in Clinical Neuroengineering, Center for Neuroprosthetics and Brain Mind Institute, Clinique Romande de Readaptation (CRR), EPFL Valais, Sion, Switzerland.

3 Functional Brain Mapping Lab, Department of Fundamental Neurosciences, University of Geneva, Campus Biotech, Chemin des Mines 9, 1202 Geneva, Switzerland

4 Department of Psychology, LMU Munich, Leopoldstr. 13, 80802, Germany

5 The Flaum Eye Institute and Center for Visual Science, University of Rochester, Rochester, NY, USA

6 Clinical Neuroscience, University of Geneva Medical School, Geneva, Switzerland

7 Lemanic Biomedical Imaging Centre (CIBM), Lausanne, Geneva, Switzerland

Status:

Published

Contributions:

F.C.H. and E.R. provided the funding and the original idea and F.C.H., R.S.G., E.R., K.H. the experimental design. R.S.G. and E.R. were in charge of the data acquisition and data analyses. S.Z., M.S. added to the analyses. R.S.G. drafted first version of the manuscript. All authors revised the manuscript significantly.

2.1 Introduction

Interactions among brain areas are assumed to be essential to most brain functions. Previous studies of inter-areal interactions have described the spiking activity of neurons in distant areas (Chouinard and Ivanowich, 2014; Nowak et al., 2008; Roe and Ts'o, 1999; Ruff and Cohen, 2016) under different contexts (Jia et al., 2013; Nowak et al., 2008; Oemisch et al., 2015; Pooresmaeili et al., 2014; Semedo et al., 2019). Neuroimaging studies in humans have also related specific connectivity patterns to behavioral profiles (Schipul et al., 2011; Wen et al., 2018), providing insight into how inter-regional interaction strength, directionality or spectral features are shaped by attentional state (Bosman et al., 2012; Oemisch et al., 2015; Ruff and Cohen, 2016), decision making (Gangopadhyay et al., 2021), stimulus drive (Jia et al., 2013; Roberts et al., 2013), or task demands (Pooresmaeili et al., 2014; Salazar et al., 2012).

The visual system is the archetype of a complex model that arises from the interplay among multiple brain regions that are hierarchically organized into a coarse, but richly interconnected network (Dosher and Lu, 1998; Gilbert et al., 2001; Gilbert and Sigman, 2007). For motion discrimination, research in humans (Blakemore and Campbell, 1969) and primates (Simoncelli and Heeger, 1998) has established that the primary visual cortex (V1) and medio-temporal areas (MT/V5, labeled henceforth as V5) are co-activated in complementary feedforward and feedback sweeps (Lamme and Roelfsema, 2000; Newsome and Pare, 1988), sweeps that are tuned to the characteristics of the stimulus (e.g., orientation) and to the anatomical pathways that are recruited. Moreover, this channel is endowed with specific patterning of electrical signals. Recent evidence suggests that communication between these two regions may be established by orchestrated phase synchronization of oscillations at lower frequencies (i.e., at Alpha-Beta frequencies, <25 Hz), acting as a temporal reference frame for information conveyed by high-frequency activity (at Gamma frequencies >40 Hz) (Bastos et al., 2015; Bonnefond et al., 2017; Fries, 2009; Seymour et al., 2019). In fact, the orchestrated interactions between Alpha and Gamma oscillations may serve as a framework supporting the feedforward and feedback loops of inter-regional brain communication within the visual system (Kerkoerle et al., 2014; Michalareas et al., 2016). Specifically, top-down Alpha appears to control the timing and elicitation of higher frequency rhythms, thus optimizing communication in the visual cortex (Fries, 2015; Michalareas et al., 2016).

More generally, phase synchronization is a key neuronal mechanism that drives spontaneous communication among dynamical nodes (Gollo et al., 2014), implying that this mechanism supports attentional, executive, and contextual functions (Doesburg et al., 2009; Freunberger et al., 2007; Palva and Palva, 2011). The two simplest phase synchronization patterns are *in-phase synchronization* (i.e., zero phase lag between the two regions) and *anti-phase synchronization* (i.e., 180° phase lag between the two regions). In-phase synchronization between two distant neuronal populations is thought to serve the integration of separated functions that are performed in these different regions (Engel et al., 1991; Roelfsema et al., 1997; Wang et al., 2010). Conversely, anti-phase patterns reflect more dynamical reciprocity, where certain areas of the brain increase their activity while others decrease their own activity. Such anti-phase patterns have been reported during sleep (Horovitz et al.,

2009), or during visual attentional tasks (Yaple and Vakhrushev, 2018). It has been proposed that these anti-phase oscillation patterns reflect time-delays in functional coupling between two connected regions (Petkoski and Jirsa, 2019). Since communication between neurons is achieved by propagation of action potentials throughout axons, with conduction times defined by some regional specificities, such as myelination density, number of synaptic relays, inhibitory couplings etc., an optimal phase delay relationship between two interconnected regions could be a key driver of successful brain communication.

In this article, we set out to determine whether motion discrimination performance can be enhanced when ‘artificially’ entraining/manipulating the phase relationship between V1 and V5. This is based on the idea that inter-areal synchronization plays a significant role in V1-V5 communication, as demonstrated previously (Lewis et al., 2016; Siegel et al., 2008). We used individually adjusted, Alpha transcranial alternating current stimulation (tACS) to entrain endogenous oscillations (Helfrich et al., 2014) and enhance inter-areal information flow (Zhang et al., 2019). The modulation consisted in applying approximately 15 minutes of concurrent, bifocal (over V1 and V5), individualized Alpha-tACS. We assessed two conditions of stimulation: In-Phase (zero phase lag) stimulation and Anti-Phase stimulation (180° phase lag); and a Sham tACS group was evaluated to control for non-specific, placebo-like effects.

Furthermore, the entire experiment was conducted while recording multi-channel electroencephalography (EEG). Electrophysiological analyses were computed with the objective of determining EEG markers of inter-areal modulation between the two target areas. We paid special attention to connectivity metrics in the Alpha band, as well as in the Gamma band because of their role in visual feature binding (Elliott and Müller, 1998; Gray and Singer, 1989; Zhang et al., 2019) and inter-areal communication in the visual cortex (Fries, 2015; Michalareas et al., 2016). Taken together, we hypothesize that the best inter-areal Alpha phase relationship for optimal oscillatory entrainment leading to respective behavioral enhancement is associated with changes in Alpha-Gamma coupling within the V1-V5 pathway.

2.2 Methods

Subjects

50 healthy subjects were recruited (range age: 18 to 40 years old, 24 females). All individuals were right-handed with normal or corrected to normal vision, and had no history of neurological diseases or cognitive disability. A written consent form was obtained from all participants prior the experiment. The study was performed according to the guidelines of the Declaration of Helsinki and approved by the local Swiss Ethics Committee (2017-01761).

Study design

Individual testing started with a familiarization phase followed by the actual experiment. During the familiarization phase, we ensured that the subject understood the visual discrimination task and reached stable performance. After EEG acquisition was prepared, a baseline block, which consisted of a task-related EEG recording without tACS was started. After a few minutes of rest, electrodes were placed over the occipital and temporal cortex, and electrical stimulation was started, remaining on for the entire duration of the block. Immediately after the start of stimulation, the second timepoint (TP0) was recorded with concurrently-measured EEG. Thereafter, the stimulation electrodes were removed and after a few minutes of rest, two succeeding evaluation points (TP10: 10 minutes after stimulation, TP30: 30 minutes after stimulation) were measured using the same task-related EEG setup, without tACS (see **Figure 1A**).

Visual discrimination task

The visual task used is a well-established 2-alternatives, forced-choice, left-right, global direction discrimination and integration task (150 trials per time point) (Das et al., 2014; Huxlin et al., 2009). The stimulus consisted of a group of black dots moving globally left- or rightwards on a mid-grey background LCD projector (1024 x 768 Hz, 144 Hz) at a density of 2.6 dots per degree and in a 5˚ diameter circular aperture centered at Cartesian coordinates [-5°, 5°] (i.e., the bottom left quadrant of the visual field, relative to central fixation) (see Figure 1B and 1C). This stimulus location was used to optimized V5 activation strength based on previous literature (e.g., Albright, 1989; Levy et al., 2001). Direction range of the dots was varied between 0˚ (total coherence) and 360° (complete random motion). The degree of difficulty was increased with improving task performance by increasing the range of dot directions within the stimulus. A 3:1 staircase design was implemented to allow us to compute a threshold level of performance for direction integration at the end of each timepoint (Das et al., 2014; Huxlin et al., 2009). For every 3 consecutive correct trials, direction range increased by 40˚, while for every incorrect response, it decreased by 40˚. The black dots making up the stimulus were 0.06° in diameter and moved at a speed of 10° per second over a time lapse of 250ms for a stimulus lifespan of 500ms. At every stimulus onset, an auditory beep was played for the subject. After each trial, auditory feedback indicated whether the response was correct or incorrect. Correct trials were followed by two beeps at 800 Hz and 1000 Hz. Incorrect trials were followed by two beeps at 500 Hz and 400 Hz.

Transcranial Electrical Stimulation

Subjects were randomly assigned into 3 groups: In the first experimental group (n=17, 10 females), In-Phase (0° phase lag) bifocal tACS was applied over the right V1 and V5 areas. The second experimental group (n=18, 8 females), received Anti-Phase (180° phase lag) bifocal tACS over V1 and V5 areas, also in the right hemisphere (see Figure 1E). The control group (n=15, 6 females) received Sham (i.e., ramp up and subsequent ramp down lasting in total one individually defined alpha cycle) bifocal stimulation over identical V1 and V5 locations as the first two groups. The electrode placement on V1 and V5 were determined according to the 10-20 EEG system, based on previous literature investigating motion processing (Kar and Krekelberg, 2014; Hülsdünker et al., 2019; Zito et al., 2015) i.e., covering the Oz-O2 and P08-P6 electrodes, respectively. Figure 1D gives an overview on the stimulating electrodes' positions for the three groups.

Prior to the baseline recording, the Alpha peak frequency of each individual was determined over a 180s-long EEG resting-state recording with the eyes open, used thereafter as the individualized frequency for the tACS in time point TP0. The individualization of the Alpha rhythm is justified by the idea that Alpha rhythms appear to be in charge of bottom-up and top-down inter areal sweeps, that ultimately gate and time the information flow in cortical networks (Sauseng et al., 2009; von Stein et al., 2000). Moreover, there have been several examples of non-invasive stimulation studies showing that tailoring the oscillatory traces to the endogenous Alpha rhythms, effectively modulates the ongoing activity (Neuling et al., 2013; Vosskuhl et al., 2016; Zaehle et al., 2010). Mean Alpha stimulation frequency for the In-Phase group was 9 Hz (range 7-11 Hz), for the Anti-Phase group:10 Hz (range 7-12 Hz) and for the Sham group: 10 Hz (range 7-11 Hz).

Apparatus and devices

All experiments took place inside the same, shielded Faraday cage designed for EEG recordings, and under the same light conditions. Participants' heads were placed over a chin-rest at a distance of 60 cm from the presentation screen, assuring a fixed position across all trials. The task ran on a Windows OS machine, based on a custom Matlab (The MathWorks Inc., USA) script, using the Psychophysics Toolbox.

Gaze and pupils' movements were controlled in real time with an EyeLink 1000 Plus Eye Tracking System (SR Research Ltd., Canada) sampling at a frequency of 1000 Hz. The task required the subject to fixate a target at the center of the screen for every trial, with a maximal tolerance for eye deviation from this fixation target of about 1°. If the participant broke fixation during stimulus presentation, the moving stimulus froze and then disappeared; the trial was discontinued, and an auditory tone (at 400 Hz) was presented. Once the participant repositioned their gaze correctly, a novel trial was started.

Bifocal tACS was delivered by means of two Neuroconn DC Plus stimulators (Neurocare group) triggered every cycle repeatedly to assure the chosen phase synchronization between the two stimulation sites. Custom-made, concentric, rubber electrodes of external diameter 5 cm, internal diameter of 1.5 cm and 2.5 cm of hole diameter were

used to deliver stimulation. The intensity was fixed to 3mA corresponding to a current density of 0.18 mA per cm². The electrodes were held by placing the EEG cap over them. The period of continuous stimulation, although it was slightly different for every participant, took on average ~13 ± 2 minutes (SEM), i.e., the time to complete 150 trials of the motion discrimination task described above. The inter-individual variability in the stimulation duration is explained by the fact that participants were told to be as accurate as possible without having any time pressure, resulting in a relatively large inter-individual variability in reaction times, hence durations to complete the 150 trials.

EEG was recorded from a 64 channels passive system (Brain Products GMBH) at a sampling frequency of 5 kHz.

- Please insert Figure 1 approximately here -

Data Analysis

Behavioral data: For each subject and time point, we extracted direction range thresholds using all trials, by fitting a Weibull function, which defined the direction range level at which performance reached 75% correct. These direction range thresholds were then normalized to the maximum possible range of motion (360°), resulting in a normalized direction range threshold (NDR), a procedure previously described (Das et al., 2014; Huxlin et al., 2009).

$$NDRthreshold(\%) = \left[\frac{(360° - WeibullfittedDR)}{360} ° \right] * 100$$

Finally, NDR thresholds were corrected for inter-individual variability in baseline performances by dividing all data by the individual baseline performances (referred as baseline-corrected NDR throughout the manuscript).

EEG data: All analyses on EEG data were performed on periods without tACS (at Baseline, TP10 and TP30) using MNE-Python (Gramfort et al., 2013) and customized scripts.

For the preprocessing, data were re-referenced to the average of signals, filtered through a Finite Response Filter of order 1, between 0.5 and 45Hz, epoched in 3s blocks, corresponding to -1.5 s before and +1.5 s after the stimulus onset. Every epoch corresponded to the time interval of a trial from the behavioral task. They were visually inspected to clear up noisy channels or unreadable trials. Bad channels were interpolated, data was re-sampled to 250Hz. Independent component analysis was used to remove physiological artifacts (i.e., eyeblinks, muscle torches).

For analyses in the frequency domain, Morlet wavelets convolution changing as a function of frequency was applied to 40 frequency bins, between 2 and 42Hz, increasing logarithmically.

For the source reconstruction analyses, data was re-referenced to the average of signals, noise covariance matrix was calculated to enhance the source approximation,

a template brain and segmentation was used to compute the forward solution for 4098 sources per hemisphere. The inverse solution was calculated by means of MNE algorithm (Hämäläinen and Ilmoniemi, 1994). The source estimates were computed with dipole orientations perpendicular to the cortical surface (Lin et al., 2006). The source points belonging to specific areas of interest (i.e. V1 and V5), were defined using the templates provided in the "SPM" open access database included in the MNE library (Wakeman and Henson, 2015). In order to extract one time-series per area of interest, we computed the first principal component from all source dipoles within each area. This first principal component is representing the source estimates associated with these pre-defined areas. Subsequently, a sign-flip was applied with the objective of avoiding sign ambiguities in the phase of different source estimates within the same area (Gramfort et al., 2012).

From the preprocessed EEG signals, we extracted a series of markers to depict the global features of the signal in the temporal, spectral and spatial domains with a specific focus on the activity over V1 and V5 and the coupling between the two areas, in the two frequency bands of interest: Alpha and Gamma rhythms. Specifically, the EEG metrics of interest computed were: Power Spectral Density (PSD) in the Alpha and Gamma band, both computed in the sensors' space, Coherence and Imaginary Coherence in the Alpha and Gamma Band, V1 Alpha Phase to V5 Gamma Amplitude coupling (ZPAC-V1pV5a) and, V5 Alpha Phase to V1 Gamma Amplitude coupling (ZPAC-V5pV1a), computed in the sources' space. Given that the sensor signals have passed through a source reconstruction method prior the calculation of the connectivity metrics, the problem of volume conduction is reduced (Hoechstetter et al., 2004). All these variables were baseline-normalized. Moreover, the Phase Amplitude coupling (i.e. PAC) was standardized to avoid confounders by creating a non-parametrized distribution of values to which to compare the observations through a Z-score transformation (i.e. ZPAC) (Canolty et al., 2006; Cohen, 2014).

Thus, PSD (Φ) was calculated taking an average of all electrodes through the Welch's estimator (Welch, 1967), that considers averaging PSDs from different windows, according to the formula:

$$\Phi(f)=\frac{1}{K}\sum_{i=1}^{K} \square \frac{1}{W}\left|X_K(v)\right|^2, where W=\sum_{m=1}^{M} \square w^2[m]$$

Where K corresponds to the number of segments where a windowed Discret Fourier Transform is computed, X is the segment where it is computed at some frequency v and w is the window segment

(Magnitude-square) Coherence (Carter, 1987) was calculated through:

$$C_{xy}(f)=\frac{\left|\Phi_{xy}(f)\right|^2}{\Phi_{xx}(f)\cdot\Phi_{yy}(f)}$$

V1-V5 coherence analyses are used to investigate frequency-specific phase coupling between these source areas. Although coherence values might be biased due to source leakage effects (Palva et al., 2018), we included this metric because it is of

relevance given our brain stimulation approach. Specifically, we expect that tACS will modulate the amplitude of the endogenous the Alpha, fact that will have direct repercussions in the weighting of the (Magnitude Square) Coherence metric.

Imaginary Coherence (Nolte et al. 2014), followed the formula:

$$IC_{xy}(f) = \frac{I\left[\Phi_{xy}(f)\right]}{\sqrt{\Phi_{xx}(f) \cdot \Phi_{yy}(f)}}$$

Where I denotes the imaginary part of the numerator. Although we do not expect this metric to directly catch changes in the Alpha amplitude modulated by the tACS, the Imaginary Coherence was chosen as a connectivity metric that is not influenced by volume conductance

Phase Amplitude coupling (PAC) (Canolty et al., 2006) was obtained through:

$$PAC = n^{-1} \sum_{t=1}^{n} \text{❑} a_t(f) \cdot e^{i\theta t} \text{ ∨}$$

Where *t* corresponds to a certain time point, *a* denotes the power at a certain specific frequency for this specific time point, *i* is the imaginary variable, θ the phase angle and *n* the number of time points. PAC values were Z-transformed (i.e., ZPAC) by means of a non-parametric permutation test. This was carried out by shuffling repeatedly the power values (maintaining the phase array) with the aim of drawing a distribution allowing null hypothesis testing. This distribution was then used to make a comparison with every observation. Ultimately, this procedure avoids problems of circular normality, power fluctuations and scaling (Cohen, 2014). In the manuscript, we will refer to ZPAC V1 Alpha phase – V5 Gamma amplitude (ZPAC-$V1p_{Alpha}V5a_{Gamma}$) as a bottom-up modulation and PAC V1 Gamma amplitude – V5 Alpha phase (ZPAC-$V1a_{Gamma}V5p_{Alpha}$) as a top-down modulation (see (Nandi et al., 2019)). We have chosen a priori these two bands of interest, Alpha and Gamma, because the oscillatory traces that have been widely reported in literature of the visual system rather correspond to these two frequency bands (Michalareas et al., 2016; van Kerkoerle et al., 2014; Doesburg et al., 2009; Fries, 2015; Gray and Singer, 1989; Hanslmayr et al., 2011; Jensen and Mazaheri, 2010; Michalareas et al., 2016; Tu et al., 2016). Moreover, our hypothesis is built under the premise that if we stimulate in the Alpha band, that is the frequency that is going to be modulated by the stimulation. In order to verify the lack of influence concerning the signal leakage problem in the calculation of the Phase Amplitude Coupling, computations showing the modulation of the phase and amplitude within the same areas of source estimates were computed (See supplementary figure 2).

Statistical Analyses

Behavior: Statistical analyses were carried out using mixed-effect linear models. The evolution of the baseline-corrected NDR was investigated as a dependent variable, with stimulation group and time points as the main fixed effects.

EEG metrics: PSD (Gamma and Alpha components across time) significance within subjects was tested through a sliding FDR-corrected T-test. Significance within subjects in the Coherence and Phase-Amplitude coupling spectrums were evaluated

through non-parametric permutation tests and clusters-based corrected for multiple comparisons. Differences were considered significant when $p < 0.05$.
A mixed linear model was performed in order to evaluate the variability of the chosen EEG metric (dependent variable) over time, among stimulation groups.

Best EEG metric: In order to determine the EEG metric that had the highest impact on the behavioral scores and then reduce the model space of the baseline-corrected NDR mixed linear model, an embedded regularization method (i.e., least absolute shrinkage and selection operator - Lasso) was applied (Tibshirani, 1996) following the Langragian version of the formula:

$$argmin_{\beta} \| y - F \cdot \beta \|^2 + \lambda_s \| \beta \|$$

Where β corresponds to the unknown vector of weighted coefficients estimated for every metric (regression coefficient), y is the matrix with all the labeled metrics, λ is in charge of the variable selection and F correspond to the acquired data points. Lasso was selected due to the fact that it provides a preferred solution with the highest sparsity given the shrink provided by the penalty term. The vector of λ chosen consisted in 30 testing points spaced between 0 and 1. The number of iterations was set to 1000.

Behavior + EEG: As a second step, covariates that could explain variance in NDR outcome and a possible interaction effect with stimulation group were added to the first mixed linear model. A random intercept per subject was used to correct for the dependency between time points for all models. Given that we implement a single mixed linear model with several factors accounting for the variance of the same variable (i.e., NDR), there is no need to correct for multiple comparisons. All contrasts were obtained by changing the labels at the intercept. The residuals of each statistical model were tested for normality by inspecting histograms and through the omnibus normality test (D'Agostino and Pearson, 1973).

2.3 Results

All participants tolerated the stimulation well and did not report any adverse effects, such as peripheral sensory or phosphene perception. Five participants could not be included in the analyses: One participant discontinued the experiment without stating the reason for it and four participants were discarded, due to poor performance (60% correct responses or less). Poor task performance prevented reliable curve-fitting procedures to extract our primary output, the direction range thresholds. Therefore, 45 full sets of data were analyzed, forming homogeneous groups of 15 participants/group. For the EEG metrics of interest (ZPAC), three data points (i.e., 2 from the In-Phase group, 1 from the Anti-Phase group) were found by Cook's Distance algorithm (Cook, 1977) to be more than two standard deviations from the mean of the distribution, and were thus not included in the analyses.

Motion direction performance throughout groups and time

Figure 2A displays the mean baseline-corrected NDR thresholds across participants, reflecting the normalized motion direction value corresponding to 75% correct performance (see Method section) across groups and time. There was no statistically significant difference between groups at baseline (Anti Phase vs. In Phase b = 1.670, P = 0.809, CI = -11.835 15.175, Sham vs. In Phase b = 3.260, P = 0.624, CI = -9.770 16.290, Sham vs Anti Phase b = 1.590, P = 0.815, CI = -11.696 14.876; see also Supplementary Table 1 providing the raw NDR values), as the baseline values showed large variability, we applied a baseline correction procedure to account for this variability. When considering all the groups together, the change in baseline-corrected NDR was not significant between TP0 and TP10 (b = -0.05, P = 0.189, CI = -0.124 0.024) nor between TP0 and TP30 (b = -0.067, P = 0.079, CI = -0.141 0.008), neither between TP10 and TP30 (b = -0.017, P = 0.657, CI = -0.091 0.057). However, there was a significant difference at TP0, TP10 and TP30 between the In-Phase and the Anti-Phase group (b = 0.257, P = 0.015, CI = 0.05 0.464). There was no difference for other group comparisons for all time points (b = 0.16, P = 0.118, CI = -0.04 0.36 Sham and In-Phase; b = -0.097, P = 0.349, CI = -0.301 0.107 Sham and Anti-Phase).

- Please insert Figure 2 approximately here –

EEG Results

In all participants, the visual discrimination task led to an amplitude increase in the Theta/Low Alpha band, right after the onset of the stimulus, followed by a phasic decrease in power in the High Alpha/Low Beta bands ~200 ms thereafter (**Figure 2B**). Additionally, in frequencies above 30 Hz, there was a constant decrease in magnitude during stimulus presentation, as previously described in the literature for this type of visual task (e.g., (Siegel et al., 2007; Townsend et al., 2017)).

The Lasso model, defined for each time point, showed that a single EEG marker, namely ZPAC-V1p_{Alpha}V5a_{Gamma} had the largest explanatory value for the variance of NDR at TP10 (R^2=0.1081, λ=0.0516) and TP30 (R^2=0.0731, λ=0.1114), irrespective of the stimulation group.

Since the ZPAC-V1p_{Alpha}V5a_{Gamma} values best explained changes in the performance after stimulation, the rest of the manuscript focuses on this metric in order to further explore stimulation and time effects. The opposite direction, ZPAC-V1a_{Gamma}V5p_{Alpha} was used as a control analysis to test for the directional specificity of the present results.

Changes in bottom-up V1 Alpha phase (V1p_{Alpha}) - V5 Gamma amplitude (V5a_{Gamma}) coupling

Figure 3A shows the mean baseline-corrected ZPAC-V1p_{Alpha}V5a_{Gamma} values for the three groups across time. As a pre-requisite, we ensured that there was no significant difference at baseline between the In Phase group and the Anti Phase group (b = -0.506, P = 0.486, CI = -1.93 0.918) nor between the In Phase and the Sham group (b = -1.052, P = 0.121, CI = -2.382 0.279). Likewise, there was no significant difference between the Anti Phase and the Sham group (b = -0.545, P = 0.422, CI = -1.878 0.787). These values were extracted from the significant modulation of interest between the Alpha/High Theta and the Low Gamma bands shown in Figure 3B. It reveals a significant diminishment in the Alpha/High Theta (5-12 Hz) – Low Gamma (30-42 Hz) phase amplitude coupling at TP10 for the Anti-Phase and the Sham group and a significant augmentation in coupling for the In-Phase group. At TP30, there is overall a more prominent augmentation of the coupling for the In-Phase group, a more pronounced diminishment for the Anti-Phase and rather a stable response for the Sham group. To statistically analyze the descriptive differences between the three conditions, we computed a mixed linear model on the ZPAC-V1p_{Alpha}V5a_{Gamma}values. The model returned a marginally significant change over time between the interval TP10 and TP30 (b = -0.769, P = 0.055, CI = -1.556, 0.018), but no significant differences between the Anti-Phase and the In-Phase groups (b = 0.836, P = 0.35, CI =-0.916, 2.588). This held true also when comparing the Anti-Phase and Sham groups (b = 1.009, P = 0.249, CI = -0.708 2.726), and the In-Phase and Sham groups (b = 0.173, P = 0.84, CI = -1.51 1.856).

When ZPAC-V1p_{Alpha}V5a_{Gamma}values were entered as a single confounder into the baseline-corrected NDR model, it did not significantly account for the overall variance for all the stimulation groups at all time points (b = 0.015, P = 0.196, CI = -0.008, 0.039). However, ZPAC-V1pV5a from the Anti-Phase group as compared to the In-Phase group, did significantly account for the variability of the NDR as a fixed effect over time at both TP10 and TP30 (b = 0.071, P = 0.048, CI = 0.001, 0.142). This was not the case when comparing the ZPAC-V1pV5a values from the In-Phase group *versus* those from Sham (b = -0.023, P = 0.44, CI = 0.081, 0.035), nor when comparing those from Anti-Phase and Sham groups (b = 0.048, P = 0.095, CI = -0.008, 0.105) at any of the two time points (all other comparisons are shown in the Supplementary Table 2).

- Please insert Figure 3 approximately here -

Changes in top-down V1 Gamma amplitude ($V1a_{Gamma}$) - V5 Alpha phase ($V5p_{Alpha}$) coupling

To test the eventual directional specificity of the present results, we examined the opposite phase-amplitude coupling between V1 and V5. **Figure 4A** provides the descriptive data for the ZPAC-$V1a_{Gamma}V5p_{Alpha}$ for all 3 experimental groups over time. To statistically analyze these data, we applied a comparable approach as in the previous section. Baseline comparison revealed no overall baseline difference group versus Anti-Phase group (b = -0.587, P = 0.457, CI = -2.136 0.962), In-Phase group versus Sham group (b = 0.141, P = 0.85, CI = -1.318 1.599) and Anti Phase group versus Sham group (b = 0.728, P = 0.324, CI = -0.718 2.175). **Figure 4B** shows the results for the ZPAC-$V1a_{Gamma}V5p_{Alpha}$, which appeared to have a significant Alpha/Theta – Low Gamma phase amplitude cluster at both TP10 and TP30. Diminished coupling is evident for the three stimulation groups when V5 Alpha/ High Theta (6-10 Hz) modulated Low V1 Low Gamma (30–37 Hz) amplitude. We then built a similar mixed linear model using the ZPAC-$V1a_{Gamma}V5p_{Alpha}$ values. These analyses showed no significant change in time between TP10 and TP30 (b = 0.409, P = 0.286, CI = -0.343, 1.161). Neither at TP10 nor at TP30 was a significant difference between the Anti-Phase and Sham group (b = -0.718, P = 0.484, CI = -2.727, 1.292), between the Anti-Phase and In-Phase group (b = 0.695, P = 0.506, CI = -1.353, 2.744) or between the In-Phase and Sham group (b = -1.413, P = 0.161, CI = -3.39, 0.564). Unsurprisingly, when ZPAC-$V1a_{Gamma}V5p_{Alpha}$ was entered as a confounder into the NDR model, it did not significantly account for the variance in NDR scores for all the stimulation groups together at all time points (b = -0.007, P = 0.53, CI = -0.029, 0.015). Additionally, there was an absence of a significant interaction between ZPAC-$V1a_{Gamma}V5p_{Alpha}$ and each stimulation group, suggesting that the ZPAC-$V1a_{Gamma}V5p_{Alpha}$ group values did not explain the group differences in the NDR values at all timepoints (In-Phase vs. Anti-Phase: b = -0.055, P = 0.432, CI = -0.191, 0.082, In-Phase vs. Sham: b = 0.006, P = 0.908, CI = -0.09, 0.101, Anti-Phase vs. Sham: b = 0.06, P = 0.234, CI = -0.039, 0.16) (all other comparisons are shown in the Supplementary Table 3).

- Please insert Figure 4 approximately here -

2.4 Discussion

By applying multisite tACS in the Alpha range to V1 and V5 with a phase difference of 180 degrees (Anti-Phase) with respect to zero degree (In-Phase), we were able to improve motion direction discrimination and integration in young healthy individuals, by modulating inter-regional oscillatory coupling between the two stimulated areas (see Figure 5). More specifically, the three main findings can be summarized as follows: 1) *Anti-Phase* $V1_{Alpha}$-$V5_{Alpha}$ tACS stimulation leads to an improvement in visual performance shortly after stimulation compared to *In-Phase* $V1_{Alpha}$-$V5_{Alpha}$, which appears rather detrimental to motion discrimination and integration, 2) improved performance with *Anti-Phase* $V1_{Alpha}$-$V5_{Alpha}$ tACS can best be explained by reduced bottom-up V1 Alpha phase - V5 Gamma amplitude coupling (*ZPAC-*$V1p_{Alpha}V5a_{Gamma}$), and 3) the opposite, top-down modulation (*ZPAC-*$V5p_{Alpha}V1a_{Gamma}$) did not influence performance in the current paradigm.

- Please insert Figure 5 approximately here -

Anti-Phase $V1A_{lpha}$-$V5_{Alpha}$ tACS and In-Phase $V1_{Alpha}$-$V5_{Alpha}$ tACS drive opposite effects on motion discrimination and integration

In-Phase tACS between two distant regions is motivated by the idea of increasing interregional synchronization and connectivity within a network (Polanía et al., 2012; Schwab et al., 2019; Vieira et al., 2020), under the hypothesis that a reduced phase-lag (~0°) between sites would promote an optimal inter-areal coupling and thus, optimal communication (Fries, 2005)). There is empirical evidence supporting this hypothesis. For instance, In-Phase stimulation has been associated with increased performance in visuo-attentional and memory tasks (Alagapan et al., 2019; Polanía et al., 2012; Violante et al., 2017), together with increased phase synchronization in the stimulated frequency band. In contrast to these data however, the present results showed opposite effects, i.e., the In-Phase condition rather impaired visual discrimination capacity during the stimulation period of 13±2 minutes, and performance did not improve, but rather decreased 10 and even 30 minutes after applying it.

Visual discrimination is associated with local Alpha desynchronization right after stimulus presentation (Dijk et al., 2008; Erickson et al., 2019; Hillyard et al., 1998; Sauseng et al., 2009; Zammit et al., 2018). Subsequently, it has been shown in several perceptual experimental modalities that a decrease in the Alpha-Beta band is linked to better stimulus perception (Griffiths et al., 2019). Thus, a high amplitude and zero-phase lag condition seems not to be optimal in this case because, as shown in the present data, focal increases in V1 Alpha phase - V5 Gamma amplitude coupling post stimulation (co-modulograms) are rather associated with poor performance. Instead, the underlying oscillatory mechanisms would most likely involve an intricate orchestration of oscillatory signatures that travels throughout the clusters of the neural network, controlled by stimuli properties (Muller et al., 2018). This oscillatory orchestration could be modeled as a multi-level interacting dynamical system (Alexander et al., 2019). Ultimately, cognition relies on feedback and feedforward

dynamics. These processes are only possible through complex, well-orchestrated phase and amplitude interactions (Siegel et al., 2012).

From a more integrative perspective, the inhibition timing hypothesis (Klimesch, 2012) states that the optimal electrophysiological scenario that promotes perception relies on an inter-regional interplay of Alpha inhibition and Alpha disinhibition among areas belonging to the same network, as shown in the visual cortex (Shen et al., 2011). When this precise timing of activation/deactivation is disrupted by enforced Alpha In-Phase rhythms, it might generate a subsequent flood of massively synchronized signals, creating an artificial source of noise that may prevent accurate perception of stimulus features (Faisal et al., 2008; Voytek and Knight, 2015). The neuronal oscillatory system might require some time to come back to its basal processing state, as pointing to for the performance at 10 min and 30 min after stimulation of the In-Phase group.

In conclusion, though based on a straight forward assumption, positive behavioral effects are not always necessarily associated with an In-Phase synchronized magnification of the Alpha occipital rhythms, but under certain circumstances visual processing is driven through an ordered gating of oscillations that the Anti-Phase condition might promote. As a matter of fact, the improved offline performance reported in the present study is in accordance with a body of literature showing that inter-areal Anti-Phase stimulation might boost behavior in several contexts. For instance, Beta band Anti-Phase bi-hemispheric stimulation has been shown to increase visual attentional capacity (Yaple and Vakhrushev, 2018). In the same vein, Theta band Anti-Phase stimulation over the prefrontal and perysilvian area has been found to improve controlled memory retrieval (Marko et al., 2019), while Gamma band Anti-Phase stimulation between the cerebellum and M1 enhances visuomotor control (Miyaguchi et al., 2019). Here, we found that Anti-Phase $V1_{Alpha}$-$V5_{Alpha}$ tACS applied on average for 13±2 minutes during a motion discrimination task significantly supported motion direction discrimination and integration 10 minutes after the end of the stimulation and the effects continued to strengthen even 30 minutes later when compared to In-Phase.

Alekseichuk and colleagues compared intracranial recordings in the temporal area of macaques undergoing frontoparietal 10Hz Anti-Phase or In-Phase stimulation, as well as, the voltage and electric field distribution associated with the two stimulation modes (Alekseichuk et al., 2019). Results showed a higher electric field magnitude, plus an unidirectional concentration of field lines for the Anti-Phase condition, whereas for the In-Phase condition there was a reduced magnitude and a bidirectional flow of electric field lines. The present electrical field simulation globally revealed similar spatial patterns suggesting that Anti-Phase stimulation generates more dynamical changes in electrical field distribution, with specific dynamics across time, which might be related to signal propagation speed.

After-effects of tACS are under debate in the field (Strüber et al., 2015), we think that the improved performance measured in the Anti-Phase group, which persists over time, are not only explained by an offline effect of the stimulation per se. Instead, we argue that it is the repeated practice of the task combined with the Anti-Phase tACS condition that promotes a “learning-like after-effect”. These after-effects might indeed

find a justification in the accumulation of offline effects that lead to a carry-over of the achieved behavioral improvement (Heise et al., 2019). These offline effects might then generate favorable plastic changes in the visual cortex due to the learning associated with the task, as it has been shown in non-human primates (Yang and Maunsell, 2004).

Anti-Phase tACS might exert its beneficial behavioural effects through bottom-up phase-amplitude decoupling

The present positive behavioral effects were associated with a bottom-up V1-Alpha phase V5-Gamma amplitude decoupling. This measure reflects the idea that the feedforward direction between V1 and V5 is regulated by a controlled amplitude modulation of Alpha-V1 over the phase of Gamma-V5, which scales with improved motion discrimination in the Anti-Phase group. Using EEG-derived phase amplitude coupling, it is possible to infer directionality of signal flow (Nandi et al., 2019). The direction of the coupling is assumed to be bottom-up if the modulating signal (Alpha band) is recorded in a primary functional neuronal population, located in lower anatomical areas (V1), whereas the carrier signal (Gamma band) is rather on higher cognitive and anatomical areas (MT/V5), receiving inputs mainly from other regions of the cortex (Jiang et al., 2015). Otherwise, the interaction ought to be top-down. This idea could be supported at some extent from a signal processing point of view, where it is presumed that in order to achieve modulation, the low frequency Alpha wave holding the information must travel and be imposed over the amplitude of the local high frequency Gamma that turns into the carrier wave (Roder, 1931). This superimposition of Alpha V1 into Gamma V5, provides a framework of direction and thus, an orientation of information flow. Furthermore, this idea is also fed by electrophysiological studies in primates, where it have been shown that high-frequency Gamma oscillatory activity (e.g., amplitude modulation coefficients almost equal to 1, meaning that the amplitude of the modulating signal equals the maximum peak amplitude of the carrier without modulation) preferably seems to travel in a feedforward manner in the visual cortex, whereas low-frequency Alpha (e.g., amplitude modulation coefficient almost equals to 0) appears to flow in a feedback direction (Michalareas et al., 2016; van Kerkoerle et al., 2014).

Visual stimulus onset has been shown to trigger propagating rhythms in the primary and secondary visual cortices of monkeys, leading to a specific phase relationship between the oscillations at both sites (Muller et al., 2014). In humans, propagation of feedforward flows has been reported during visual motion discrimination, with latencies modulated by characteristics of the stimulus (Sato et al., 2012; Seriès et al., 2002). Then, this suggests the idea that there is an optimal range of Alpha rhythm magnitude that is more favorable to generate trains of local Gamma bursts, which might convey the most relevant information of the visual stimulus' features to promote motion discrimination (Nelli et al., 2017; Tu et al., 2016).

This bottom-up Alpha-Gamma interaction is in line with the theory of cross-frequency nested oscillations (Bonnefond et al., 2017). Accordingly, the organization of tasks in the visual system is done through the timed gating of information encoded in local Gamma bursts, happening every 10-30 ms and that are regulated through the Alpha inhibitory role (Jensen et al., 2014). Additionally, our finding that changes in phase

amplitude coupling between Alpha-V1 and Gamma-V5 predict behavioural improvements in the Anti-Phase group is congruent with the fact that motion discrimination has been shown to occur as a feedforward oscillatory phenomenon (Seriès et al., 2002), and that these oscillations in the occipital cortex do not only belong to a single frequency band, but rather to a modulation of Alpha and Gamma rhythms (Bahramisharif et al., 2013).

Finally, we did not find any significant changes in the opposite top-down V5-Alpha phase - V1-Gamma Amplitude coupling and the values measured 10 minutes and 30 minutes after stimulation did not account for changes in motion discrimination performance or their variance. Although recordings in monkeys' visual cortex have shown a top-down Alpha-Beta that granger-causes a bottom-up Gamma rhythm (Richter et al., 2017), it does not necessarily contradict our findings since what we report reflect bottom-up coupled nested oscillations from one neuronal cluster to another, rather than a causal generation of oscillatory activity from one site to another. These markers indeed imply two different processes of interaction, in most of the circumstances, not mutually exclusive. Then, there might be different cross-frequency mechanisms that sustain visual discrimination that are revealed by these different electrophysiological markers. Exploring this variety of markers might lead to a better understanding of neural communication supporting visual discrimination.

CONCLUSIONS

The present experiments revealed that generating Anti-Phase oscillation patterns between V1 and V5 during motion discrimination using bi-focal tACS might enhance performance persisting even after the stimulation period. These after-effects were mechanistically partially explained by changes in bottom-up V1-Alpha V5-Gamma Phase-Amplitude coupling. We believe that these results might illustrate enhanced signal propagation from V1 to higher visual areas, under a precise phase-timing relationship. One can speculate that an optimal phase-lag between stimulation sites, induced by Anti-Phase tACS aftereffects, did promote neuronal communication because of the inherent speed of wave propagation. Furthermore, one could infer that Alpha Anti-Phase tACS might act as a controller of the Alpha disinhibition-gating capacities and as such, might modulate bottom-up trains of Gamma bursts in the V1-V5 pathway. The precise characteristics of the Gamma bursts (e.g., phase, time) might play a significant role in improving the performance in motion discrimination.

The present findings might point towards the exciting potential of the current approach to be extended towards an ameliorated stimulation orchestration with cross-frequency montages targeting the motion discrimination pathway. Furthermore, it potentially opens a novel direction of non-invasive interventions to treat patients with deficits in the visual domain, such as after a stroke.

2.5 References

Alagapan, S., Riddle, J., Huang, W.A., Hadar, E., Shin, H.W., Fröhlich, F., 2019. Network-Targeted, Multi-site Direct Cortical Stimulation Enhances Working Memory by Modulating Phase Lag of Low-Frequency Oscillations. Cell Rep. 29, 2590-2598.e4. https://doi.org/10.1016/j.celrep.2019.10.072

Alekseichuk, I., Falchier, A.Y., Linn, G., Xu, T., Milham, M.P., Schroeder, C.E., Opitz, A., 2019. Electric field dynamics in the brain during multi-electrode transcranial electric stimulation. Nat. Commun. 10, 2573. https://doi.org/10.1038/s41467-019-10581-7

Alexander, D.M., Ball, T., Schulze-Bonhage, A., Leeuwen, C. van, 2019. Large-scale cortical travelling waves predict localized future cortical signals. PLOS Comput. Biol. 15, e1007316. https://doi.org/10.1371/journal.pcbi.1007316

Bahramisharif, A., Gerven, M.A.J. van, Aarnoutse, E.J., Mercier, M.R., Schwartz, T.H., Foxe, J.J., Ramsey, N.F., Jensen, O., 2013. Propagating Neocortical Gamma Bursts Are Coordinated by Traveling Alpha Waves. J. Neurosci. 33, 18849–18854. https://doi.org/10.1523/JNEUROSCI.2455-13.2013

Bastos, A.M., Vezoli, J., Bosman, C.A., Schoffelen, J.-M., Oostenveld, R., Dowdall, J.R., De Weerd, P., Kennedy, H., Fries, P., 2015. Visual areas exert feedforward and feedback influences through distinct frequency channels. Neuron 85, 390–401. https://doi.org/10.1016/j.neuron.2014.12.018

Blakemore, C., Campbell, F.W., 1969. On the existence of neurones in the human visual system selectively sensitive to the orientation and size of retinal images. J. Physiol. 203, 237-260.1.

Bonnefond, M., Kastner, S., Jensen, O., 2017. Communication between Brain Areas Based on Nested Oscillations. eNeuro 4. https://doi.org/10.1523/ENEURO.0153-16.2017

Bosman, C.A., Schoffelen, J.-M., Brunet, N., Oostenveld, R., Bastos, A.M., Womelsdorf, T., Rubehn, B., Stieglitz, T., De Weerd, P., Fries, P., 2012. Attentional stimulus selection through selective synchronization between monkey visual areas. Neuron 75, 875–888. https://doi.org/10.1016/j.neuron.2012.06.037

Canolty, R.T., Edwards, E., Dalal, S.S., Soltani, M., Nagarajan, S.S., Kirsch, H.E., Berger, M.S., Barbaro, N.M., Knight, R.T., 2006. High Gamma Power Is Phase-Locked to Theta Oscillations in Human Neocortex. Science 313, 1626–1628. https://doi.org/10.1126/science.1128115

Carter, G.C., 1987. Coherence and time delay estimation. Proc. IEEE 75, 236–255. https://doi.org/10.1109/PROC.1987.13723

Chouinard, P.A., Ivanowich, M., 2014. Is the Primary Visual Cortex a Center Stage for the Visual Phenomenology of Object Size? J. Neurosci. 34, 2013–2014. https://doi.org/10.1523/JNEUROSCI.4902-13.2014

Cohen, M.X., 2014. Analyzing Neural Time Series Data: Theory and Practice. MIT Press.

Cook, R.D., 1977. Detection of Influential Observation in Linear Regression. Technometrics 19, 15–18. https://doi.org/10.2307/1268249

D'Agostino, R., Pearson, E.S., 1973. Tests for Departure from Normality. Empirical Results for the Distributions of b2 and √ b1. Biometrika 60, 613–622. https://doi.org/10.2307/2335012

Das, A., Tadin, D., Huxlin, K.R., 2014. Beyond Blindsight: Properties of Visual Relearning in Cortically Blind Fields. J. Neurosci. 34, 11652–11664. https://doi.org/10.1523/JNEUROSCI.1076-14.2014

Dijk, H. van, Schoffelen, J.-M., Oostenveld, R., Jensen, O., 2008. Prestimulus Oscillatory Activity in the Alpha Band Predicts Visual Discrimination Ability. J. Neurosci. 28, 1816–1823. https://doi.org/10.1523/JNEUROSCI.1853-07.2008

Doesburg, S.M., Green, J.J., McDonald, J.J., Ward, L.M., 2009. From local inhibition to long-range integration: a functional dissociation of alpha-band synchronization across cortical scales in visuospatial attention. Brain Res. 1303, 97–110. https://doi.org/10.1016/j.brainres.2009.09.069

Elliott, M.A., Müller, H.J., 1998. Synchronous Information Presented in 40-HZ Flicker Enhances Visual Feature Binding. Psychol. Sci. 9, 277–283. https://doi.org/10.1111/1467-9280.00055

Engel, A.K., Kreiter, A.K., Konig, P., Singer, W., 1991. Synchronization of oscillatory neuronal responses between striate and extrastriate visual cortical areas of the cat. Proc. Natl. Acad. Sci. 88, 6048–6052. https://doi.org/10.1073/pnas.88.14.6048

Erickson, M.A., Smith, D., Albrecht, M.A., Silverstein, S., 2019. Alpha-band desynchronization reflects memory-specific processes during visual change detection. Psychophysiology 56, e13442. https://doi.org/10.1111/psyp.13442

Faisal, A.A., Selen, L.P.J., Wolpert, D.M., 2008. Noise in the nervous system. Nat. Rev. Neurosci. 9, 292–303. https://doi.org/10.1038/nrn2258

Freunberger, R., Klimesch, W., Sauseng, P., Griesmayr, B., Höller, Y., Pecherstorfer, T., Hanslmayr, S., 2007. Gamma oscillatory activity in a visual discrimination task. Brain Res. Bull. 71, 593–600. https://doi.org/10.1016/j.brainresbull.2006.11.014

Fries, P., 2015. Rhythms For Cognition: Communication Through Coherence. Neuron 88, 220–235. https://doi.org/10.1016/j.neuron.2015.09.034

Fries, P., 2009. Neuronal Gamma-Band Synchronization as a Fundamental Process in Cortical Computation. Annu. Rev. Neurosci. 32, 209–224. https://doi.org/10.1146/annurev.neuro.051508.135603

Gangopadhyay, P., Chawla, M., Dal Monte, O., Chang, S.W.C., 2021. Prefrontal–amygdala circuits in social decision-making. Nat. Neurosci. 24, 5–18. https://doi.org/10.1038/s41593-020-00738-9

Gollo, L.L., Mirasso, C., Sporns, O., Breakspear, M., 2014. Mechanisms of Zero-Lag Synchronization in Cortical Motifs. PLoS Comput. Biol. 10, e1003548. https://doi.org/10.1371/journal.pcbi.1003548

Gramfort, A., Kowalski, M., Hämäläinen, M., 2012. Mixed-norm estimates for the M/EEG inverse problem using accelerated gradient methods. Phys. Med. Biol. 57, 1937–1961. https://doi.org/10.1088/0031-9155/57/7/1937

Gramfort, A., Luessi, M., Larson, E., Engemann, D.A., Strohmeier, D., Brodbeck, C., Goj, R., Jas, M., Brooks, T., Parkkonen, L., Hämäläinen, M., 2013. MEG and EEG data analysis with MNE-Python. Front. Neurosci. 7. https://doi.org/10.3389/fnins.2013.00267

Gray, C.M., Singer, W., 1989. Stimulus-specific neuronal oscillations in orientation columns of cat visual cortex. Proc. Natl. Acad. Sci. U. S. A. 86, 1698–1702.

Griffiths, B.J., Mayhew, S.D., Mullinger, K.J., Jorge, J., Charest, I., Wimber, M., Hanslmayr, S., 2019. Alpha/beta power decreases track the fidelity of stimulus-specific information. eLife 8, e49562. https://doi.org/10.7554/eLife.49562

Hämäläinen, M.S., Ilmoniemi, R.J., 1994. Interpreting magnetic fields of the brain: minimum norm estimates. Med. Biol. Eng. Comput. 32, 35–42. https://doi.org/10.1007/BF02512476

Heise, K.-F., Monteiro, T.S., Leunissen, I., Mantini, D., Swinnen, S.P., 2019. Distinct online and offline effects of alpha and beta transcranial alternating current stimulation (tACS) on continuous bimanual performance and task-set switching. Sci. Rep. 9, 3144. https://doi.org/10.1038/s41598-019-39900-0

Helfrich, R.F., Knepper, H., Nolte, G., Strüber, D., Rach, S., Herrmann, C.S., Schneider, T.R., Engel, A.K., 2014. Selective modulation of interhemispheric functional connectivity by HD-tACS shapes perception. PLoS Biol. 12, e1002031. https://doi.org/10.1371/journal.pbio.1002031

Hillyard, S.A., Teder-Sälejärvi, W.A., Münte, T.F., 1998. Temporal dynamics of early perceptual processing. Curr. Opin. Neurobiol. 8, 202–210. https://doi.org/10.1016/S0959-4388(98)80141-4

Horovitz, S.G., Braun, A.R., Carr, W.S., Picchioni, D., Balkin, T.J., Fukunaga, M., Duyn, J.H., 2009. Decoupling of the brain's default mode network during deep sleep. Proc. Natl. Acad. Sci. U. S. A. 106, 11376–11381. https://doi.org/10.1073/pnas.0901435106

Huxlin, K.R., Martin, T., Kelly, K., Riley, M., Friedman, D.I., Burgin, W.S., Hayhoe, M., 2009. Perceptual Relearning of Complex Visual Motion after V1 Damage in Humans. J. Neurosci. 29, 3981–3991. https://doi.org/10.1523/JNEUROSCI.4882-08.2009

Jensen, O., Gips, B., Bergmann, T.O., Bonnefond, M., 2014. Temporal coding organized by coupled alpha and gamma oscillations prioritize visual processing. Trends Neurosci. 37, 357–369. https://doi.org/10.1016/j.tins.2014.04.001

Jia, X., Tanabe, S., Kohn, A., 2013. Gamma and the Coordination of Spiking Activity in Early Visual Cortex. Neuron 77, 762–774. https://doi.org/10.1016/j.neuron.2012.12.036

Jiang, H., Bahramisharif, A., van Gerven, M.A.J., Jensen, O., 2015. Measuring directionality between neuronal oscillations of different frequencies. NeuroImage 118, 359–367. https://doi.org/10.1016/j.neuroimage.2015.05.044

Klimesch, W., 2012. Alpha-band oscillations, attention, and controlled access to stored information. Trends Cogn. Sci. 16, 606–617. https://doi.org/10.1016/j.tics.2012.10.007

Lamme, V.A.F., Roelfsema, P.R., 2000. The distinct modes of vision offered by feedforward and recurrent processing. Trends Neurosci. 23, 571–579. https://doi.org/10.1016/S0166-2236(00)01657-X

Lewis, C.M., Bosman, C.A., Womelsdorf, T., Fries, P., 2016. Stimulus-induced visual cortical networks are recapitulated by spontaneous local and interareal synchronization. Proc. Natl. Acad. Sci. U. S. A. 113, E606-615. https://doi.org/10.1073/pnas.1513773113

Lin, F.-H., Belliveau, J.W., Dale, A.M., Hämäläinen, M.S., 2006. Distributed current estimates using cortical orientation constraints. Hum. Brain Mapp. 27, 1–13. https://doi.org/10.1002/hbm.20155

Marko, M., Cimrová, B., Riečanský, I., 2019. Neural theta oscillations support semantic memory retrieval. Sci. Rep. 9, 17667. https://doi.org/10.1038/s41598-019-53813-y

Michalareas, G., Vezoli, J., van Pelt, S., Schoffelen, J.-M., Kennedy, H., Fries, P., 2016. Alpha-Beta and Gamma Rhythms Subserve Feedback and Feedforward Influences among Human Visual Cortical Areas. Neuron 89, 384–397. https://doi.org/10.1016/j.neuron.2015.12.018

Miyaguchi, S., Otsuru, N., Kojima, S., Yokota, H., Saito, K., Inukai, Y., Onishi, H., 2019. Gamma tACS over M1 and cerebellar hemisphere improves motor performance in a phase-specific manner. Neurosci. Lett. 694, 64–68. https://doi.org/10.1016/j.neulet.2018.11.015

Muller, L., Chavane, F., Reynolds, J., Sejnowski, T.J., 2018. Cortical travelling waves: mechanisms and computational principles. Nat. Rev. Neurosci. 19, 255–268. https://doi.org/10.1038/nrn.2018.20

Muller, L., Reynaud, A., Chavane, F., Destexhe, A., 2014. The stimulus-evoked population response in visual cortex of awake monkey is a propagating wave. Nat. Commun. 5. https://doi.org/10.1038/ncomms4675

Nandi, B., Swiatek, P., Kocsis, B., Ding, M., 2019. Inferring the direction of rhythmic neural transmission via inter-regional phase-amplitude coupling (ir-PAC). Sci. Rep. 9, 6933. https://doi.org/10.1038/s41598-019-43272-w

Nelli, S., Itthipuripat, S., Srinivasan, R., Serences, J.T., 2017. Fluctuations in instantaneous frequency predict alpha amplitude during visual perception. Nat. Commun. 8, 2071. https://doi.org/10.1038/s41467-017-02176-x

Newsome, W., Pare, E., 1988. A selective impairment of motion perception following lesions of the middle temporal visual area (MT). J. Neurosci. 8, 2201–2211. https://doi.org/10.1523/JNEUROSCI.08-06-02201.1988

Nowak, L.G., Sanchez-Vives, M.V., McCormick, D.A., 2008. Lack of Orientation and Direction Selectivity in a Subgroup of Fast-Spiking Inhibitory Interneurons: Cellular

and Synaptic Mechanisms and Comparison with Other Electrophysiological Cell Types. Cereb. Cortex N. Y. N 1991 18, 1058–1078. https://doi.org/10.1093/cercor/bhm137

Oemisch, M., Westendorff, S., Everling, S., Womelsdorf, T., 2015. Interareal Spike-Train Correlations of Anterior Cingulate and Dorsal Prefrontal Cortex during Attention Shifts. J. Neurosci. 35, 13076–13089. https://doi.org/10.1523/JNEUROSCI.1262-15.2015

Palva, J.M., Wang, S.H., Palva, S., Zhigalov, A., Monto, S., Brookes, M.J., Schoffelen, J.-M., Jerbi, K., 2018. Ghost interactions in MEG/EEG source space: A note of caution on inter-areal coupling measures. NeuroImage 173, 632–643. https://doi.org/10.1016/j.neuroimage.2018.02.032

Palva, S., Palva, J.M., 2011. Functional Roles of Alpha-Band Phase Synchronization in Local and Large-Scale Cortical Networks. Front. Psychol. 2. https://doi.org/10.3389/fpsyg.2011.00204

Petkoski, S., Jirsa, V.K., 2019. Transmission time delays organize the brain network synchronization. Philos. Transact. A Math. Phys. Eng. Sci. 377. https://doi.org/10.1098/rsta.2018.0132

Polanía, R., Nitsche, M.A., Korman, C., Batsikadze, G., Paulus, W., 2012. The Importance of Timing in Segregated Theta Phase-Coupling for Cognitive Performance. Curr. Biol. 22, 1314–1318. https://doi.org/10.1016/j.cub.2012.05.021

Pooresmaeili, A., Poort, J., Roelfsema, P.R., 2014. Simultaneous selection by object-based attention in visual and frontal cortex. Proc. Natl. Acad. Sci. 111, 6467–6472. https://doi.org/10.1073/pnas.1316181111

Richter, C.G., Thompson, W.H., Bosman, C.A., Fries, P., 2017. Top-Down Beta Enhances Bottom-Up Gamma. J. Neurosci. Off. J. Soc. Neurosci. 37, 6698–6711. https://doi.org/10.1523/JNEUROSCI.3771-16.2017

Roberts, M.J., Lowet, E., Brunet, N.M., Ter Wal, M., Tiesinga, P., Fries, P., De Weerd, P., 2013. Robust gamma coherence between macaque V1 and V2 by dynamic frequency matching. Neuron 78, 523–536. https://doi.org/10.1016/j.neuron.2013.03.003

Roe, A.W., Ts'o, D.Y., 1999. Specificity of color connectivity between primate V1 and V2. J. Neurophysiol. 82, 2719–2730. https://doi.org/10.1152/jn.1999.82.5.2719

Roelfsema, P.R., Engel, A.K., König, P., Singer, W., 1997. Visuomotor integration is associated with zero time-lag synchronization among cortical areas. Nature 385, 157–161. https://doi.org/10.1038/385157a0

Ruff, D.A., Cohen, M.R., 2016. Attention Increases Spike Count Correlations between Visual Cortical Areas. J. Neurosci. 36, 7523–7534. https://doi.org/10.1523/JNEUROSCI.0610-16.2016

Salazar, R., Dotson, N., Bressler, S., Gray, C., 2012. Content Specific Fronto-Parietal Synchronization during Visual Working Memory. Science 338, 1097–1100. https://doi.org/10.1126/science.1224000

Sato, T.K., Nauhaus, I., Carandini, M., 2012. Traveling Waves in Visual Cortex. Neuron 75, 218–229. https://doi.org/10.1016/j.neuron.2012.06.029

Saturnino, G.B., Madsen, K.H., Siebner, H.R., Thielscher, A., 2017. How to target inter-regional phase synchronization with dual-site Transcranial Alternating Current Stimulation. NeuroImage 163, 68–80. https://doi.org/10.1016/j.neuroimage.2017.09.024

Sauseng, P., Klimesch, W., Heise, K.F., Gruber, W.R., Holz, E., Karim, A.A., Glennon, M., Gerloff, C., Birbaumer, N., Hummel, F.C., 2009. Brain oscillatory substrates of visual short-term memory capacity. Curr. Biol. CB 19, 1846–1852. https://doi.org/10.1016/j.cub.2009.08.062

Schipul, S.E., Keller, T.A., Just, M.A., 2011. Inter-regional brain communication and its disturbance in autism. Front. Syst. Neurosci. 5, 10. https://doi.org/10.3389/fnsys.2011.00010

Schwab, B.C., Misselhorn, J., Engel, A.K., 2019. Modulation of large-scale cortical coupling by transcranial alternating current stimulation. Brain Stimul. Basic Transl. Clin. Res. Neuromodulation 12, 1187–1196. https://doi.org/10.1016/j.brs.2019.04.013

Semedo, J.D., Zandvakili, A., Machens, C.K., Yu, B.M., Kohn, A., 2019. Cortical Areas Interact through a Communication Subspace. Neuron 102, 249-259.e4. https://doi.org/10.1016/j.neuron.2019.01.026

Seriès, P., Georges, S., Lorenceau, J., Frégnac, Y., 2002. Orientation dependent modulation of apparent speed: a model based on the dynamics of feed-forward and horizontal connectivity in V1 cortex. Vision Res. 42, 2781–2797. https://doi.org/10.1016/s0042-6989(02)00302-4

Seymour, R.A., Rippon, G., Gooding-Williams, G., Schoffelen, J.M., Kessler, K., 2019. Dysregulated oscillatory connectivity in the visual system in autism spectrum disorder. Brain 142, 3294–3305. https://doi.org/10.1093/brain/awz214

Shen, W., McKeown, C.R., Demas, J.A., Cline, H.T., 2011. Inhibition to excitation ratio regulates visual system responses and behavior in vivo. J. Neurophysiol. 106, 2285–2302. https://doi.org/10.1152/jn.00641.2011

Siegel, M., Donner, T.H., Engel, A.K., 2012. Spectral fingerprints of large-scale neuronal interactions. Nat. Rev. Neurosci. 13, 121–134. https://doi.org/10.1038/nrn3137

Siegel, M., Donner, T.H., Oostenveld, R., Fries, P., Engel, A.K., 2008. Neuronal synchronization along the dorsal visual pathway reflects the focus of spatial attention. Neuron 60, 709–719. https://doi.org/10.1016/j.neuron.2008.09.010

Siegel, M., Donner, T.H., Oostenveld, R., Fries, P., Engel, A.K., 2007. High-Frequency Activity in Human Visual Cortex Is Modulated by Visual Motion Strength. Cereb. Cortex 17, 732–741. https://doi.org/10.1093/cercor/bhk025

Simoncelli, E.P., Heeger, D.J., 1998. A model of neuronal responses in visual area MT. Vision Res. 38, 743–761. https://doi.org/10.1016/s0042-6989(97)00183-1

Strüber, D., Rach, S., Neuling, T., Herrmann, C.S., 2015. On the possible role of stimulation duration for after-effects of transcranial alternating current stimulation. Front. Cell. Neurosci. 9. https://doi.org/10.3389/fncel.2015.00311

Thielscher, A., Antunes, A., Saturnino, G.B., 2015. Field modeling for transcranial magnetic stimulation: A useful tool to understand the physiological effects of TMS?, in: 2015 37th Annual International Conference of the IEEE Engineering in Medicine and Biology Society (EMBC). Presented at the 2015 37th Annual International Conference of the IEEE Engineering in Medicine and Biology Society (EMBC), IEEE, Milan, pp. 222–225. https://doi.org/10.1109/EMBC.2015.7318340

Tibshirani, R., 1996. Regression Shrinkage and Selection via the Lasso. J. R. Stat. Soc. Ser. B Methodol. 58, 267–288.

Townsend, R.G., Solomon, S.S., Martin, P.R., Solomon, S.G., Gong, P., 2017. Visual Motion Discrimination by Propagating Patterns in Primate Cerebral Cortex. J. Neurosci. 37, 10074–10084. https://doi.org/10.1523/JNEUROSCI.1538-17.2017

Tu, Y., Zhang, Z., Tan, A., Peng, W., Hung, Y.S., Moayedi, M., Iannetti, G.D., Hu, L., 2016. Alpha and gamma oscillation amplitudes synergistically predict the perception of forthcoming nociceptive stimuli. Hum. Brain Mapp. 37, 501–514. https://doi.org/10.1002/hbm.23048

Vieira, P.G., Krause, M.R., Pack, C.C., 2020. tACS entrains neural activity while somatosensory input is blocked. PLOS Biol. 18, e3000834. https://doi.org/10.1371/journal.pbio.3000834

Violante, I.R., Li, L.M., Carmichael, D.W., Lorenz, R., Leech, R., Hampshire, A., Rothwell, J.C., Sharp, D.J., 2017. Externally induced frontoparietal synchronization modulates network dynamics and enhances working memory performance. eLife 6, e22001. https://doi.org/10.7554/eLife.22001

von Stein, A., Chiang, C., König, P., 2000. Top-down processing mediated by interareal synchronization. Proc. Natl. Acad. Sci. U. S. A. 97, 14748–14753.

Voytek, B., Knight, R.T., 2015. Dynamic network communication as a unifying neural basis for cognition, development, aging, and disease. Biol. Psychiatry 77, 1089–1097. https://doi.org/10.1016/j.biopsych.2015.04.016

Wakeman, D.G., Henson, R.N., 2015. A multi-subject, multi-modal human neuroimaging dataset. Sci. Data 2, 150001. https://doi.org/10.1038/sdata.2015.1

Wang, J., Brown, R., Dobkins, K.R., McDowell, J.E., Clementz, B.A., 2010. Diminished Parietal Cortex Activity Associated with Poor Motion Direction Discrimination Performance in Schizophrenia. Cereb. Cortex 20, 1749–1755. https://doi.org/10.1093/cercor/bhp243

Welch, P., 1967. The use of fast Fourier transform for the estimation of power spectra: A method based on time averaging over short, modified periodograms. IEEE Trans. Audio Electroacoustics 15, 70–73. https://doi.org/10.1109/TAU.1967.1161901

Wen, T., Liu, D.-C., Hsieh, S., 2018. Connectivity patterns in cognitive control networks predict naturalistic multitasking ability. Neuropsychologia 114, 195–202. https://doi.org/10.1016/j.neuropsychologia.2018.05.002

Yang, T., Maunsell, J.H.R., 2004. The effect of perceptual learning on neuronal responses in monkey visual area V4. J. Neurosci. Off. J. Soc. Neurosci. 24, 1617–1626. https://doi.org/10.1523/JNEUROSCI.4442-03.2004

Yaple, Z., Vakhrushev, R., 2018. Modulation of the frontal-parietal network by low intensity anti-phase 20 Hz transcranial electrical stimulation boosts performance in the attentional blink task. Int. J. Psychophysiol. Off. J. Int. Organ. Psychophysiol. 127, 11–16. https://doi.org/10.1016/j.ijpsycho.2018.02.014

Zammit, N., Falzon, O., Camilleri, K., Muscat, R., 2018. Working memory alpha-beta band oscillatory signatures in adolescents and young adults. Eur. J. Neurosci. 48, 2527–2536. https://doi.org/10.1111/ejn.13897

Zhang, H., Morrone, M.C., Alais, D., 2019. Behavioural oscillations in visual orientation discrimination reveal distinct modulation rates for both sensitivity and response bias. Sci. Rep. 9, 1115. https://doi.org/10.1038/s41598-018-37918-4

2.6 Figures

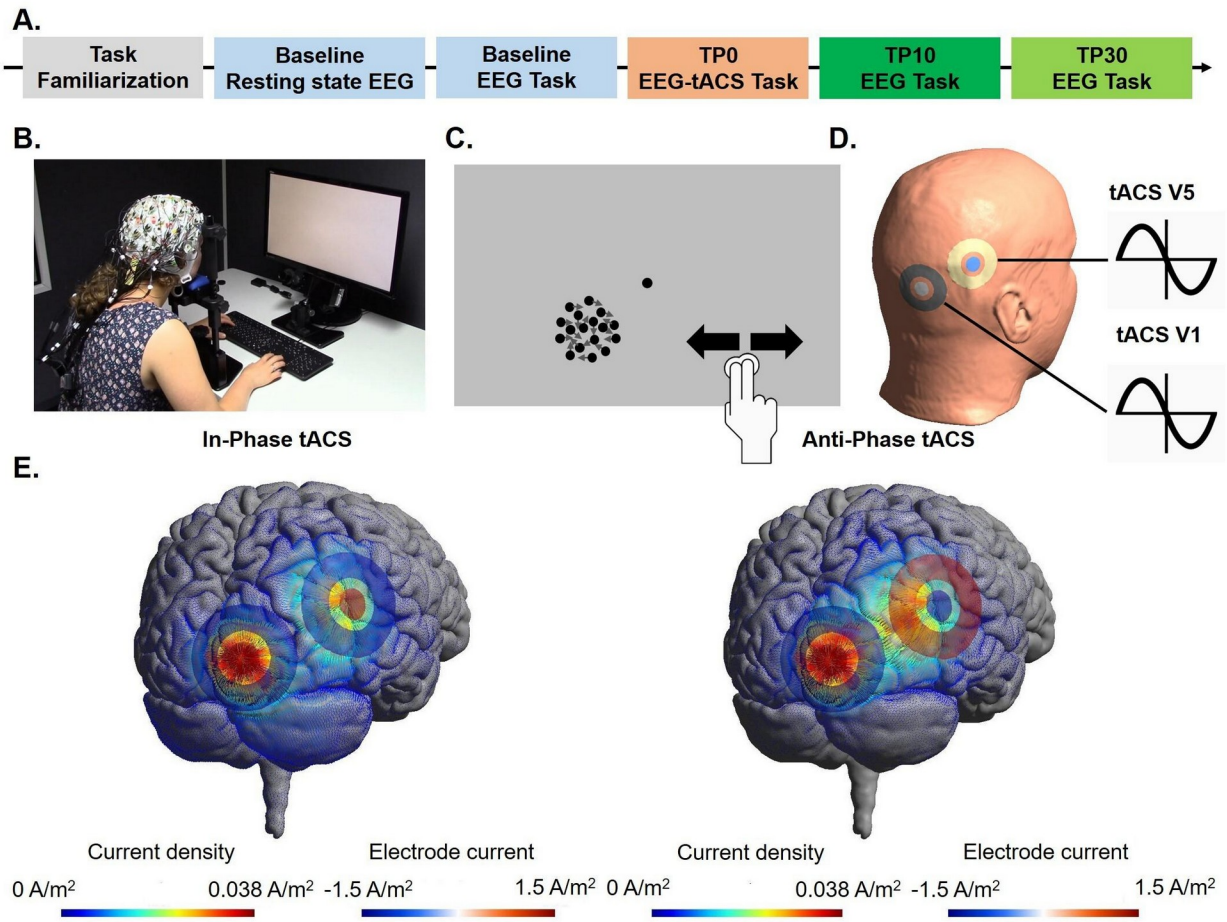

Figure 1. General features of the study (A) Experimental design. The total duration of the experiment was around 3hrs. **(B) Real example** of the experimental setup inside the Faraday's cage. The EEG system and an ongoing visual task are shown. **(B) Schematic example of the motion discrimination task**. **(C) Schematic of the bifocal tACS** applied with concentric electrodes over P6 and O2 while subject performs the global direction discrimination visual task. (**D) Electrical field 3D representation of bifocal tACS** at the two different phase differences (Thielscher et al., 2015). The dispersion of the field does not change over time in the two conditions, but rather the magnitude of the electrical field lines (Saturnino et al., 2017).

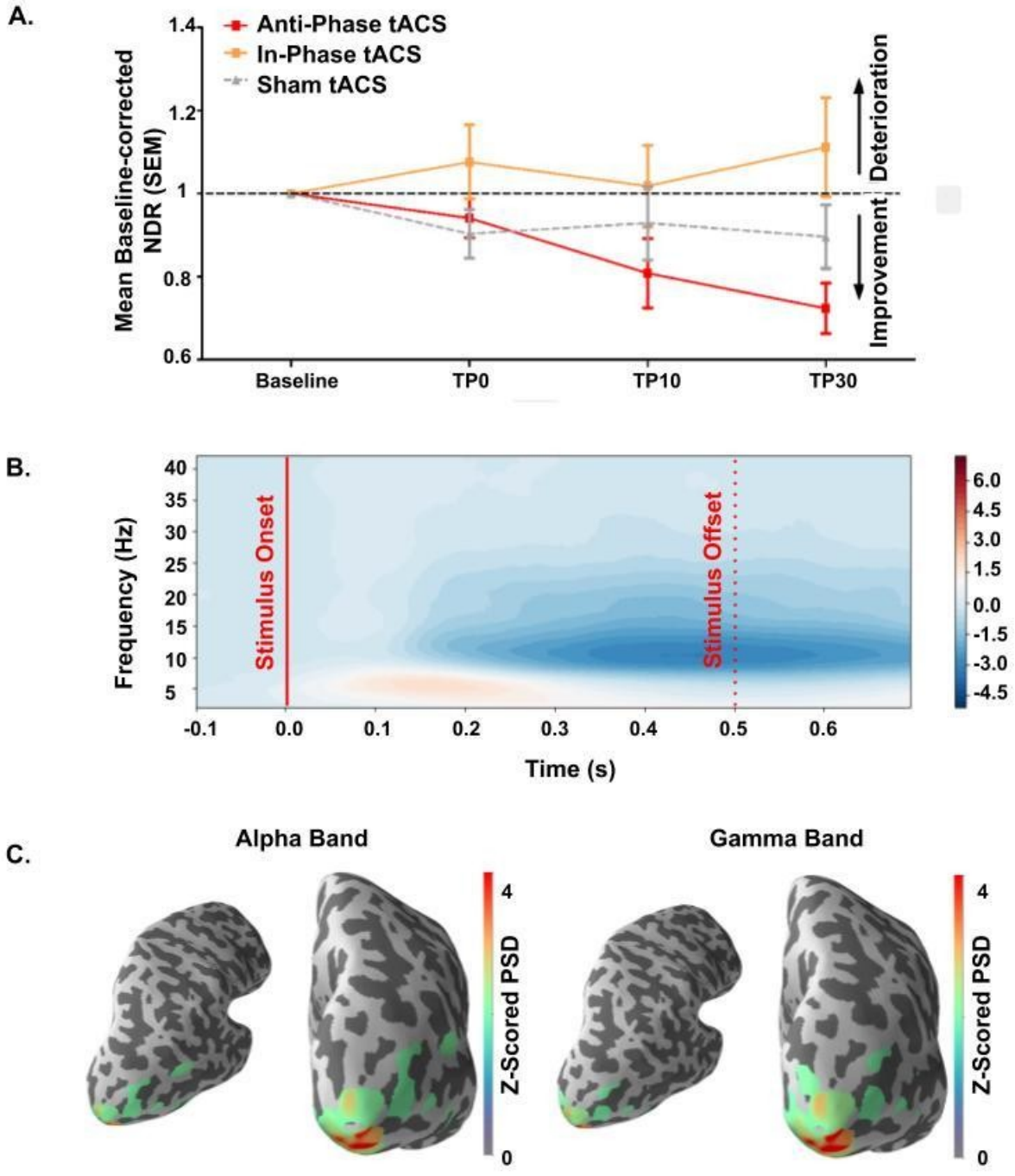

Figure 2. Main behavioral results and their main EEG associated traces. (A) Baseline-corrected NDR (Normalized Direction Range) threshold evolution across time-points for the three stimulation conditions. Bars correspond to Standard Errors of the Mean (SEM). Anti-Phase stimulation induced an increased performance translating into a significantly pronounced behavioral improvement over time at the group level. The behavioral performance of the Anti-Phase group was significantly enhanced compared to the In-Phase group. **(B) Time-frequency representation** of the averaged response during a trial at the baseline period, before the stimulation. It shows a typical Event Related Synchronization at (ERS) the Theta/Alpha band, followed by an Event Related Desynchronization (ERD) in the Beta band (in z-scores). **(C)** 3D plot representation of the normalized activation of sources V1 and V5 of interest defined using the templates provided in the “SPM” open access database included in

the MNE library (Wakeman and Henson, 2015) for the Alpha and Gamma band during the stimulus presentation

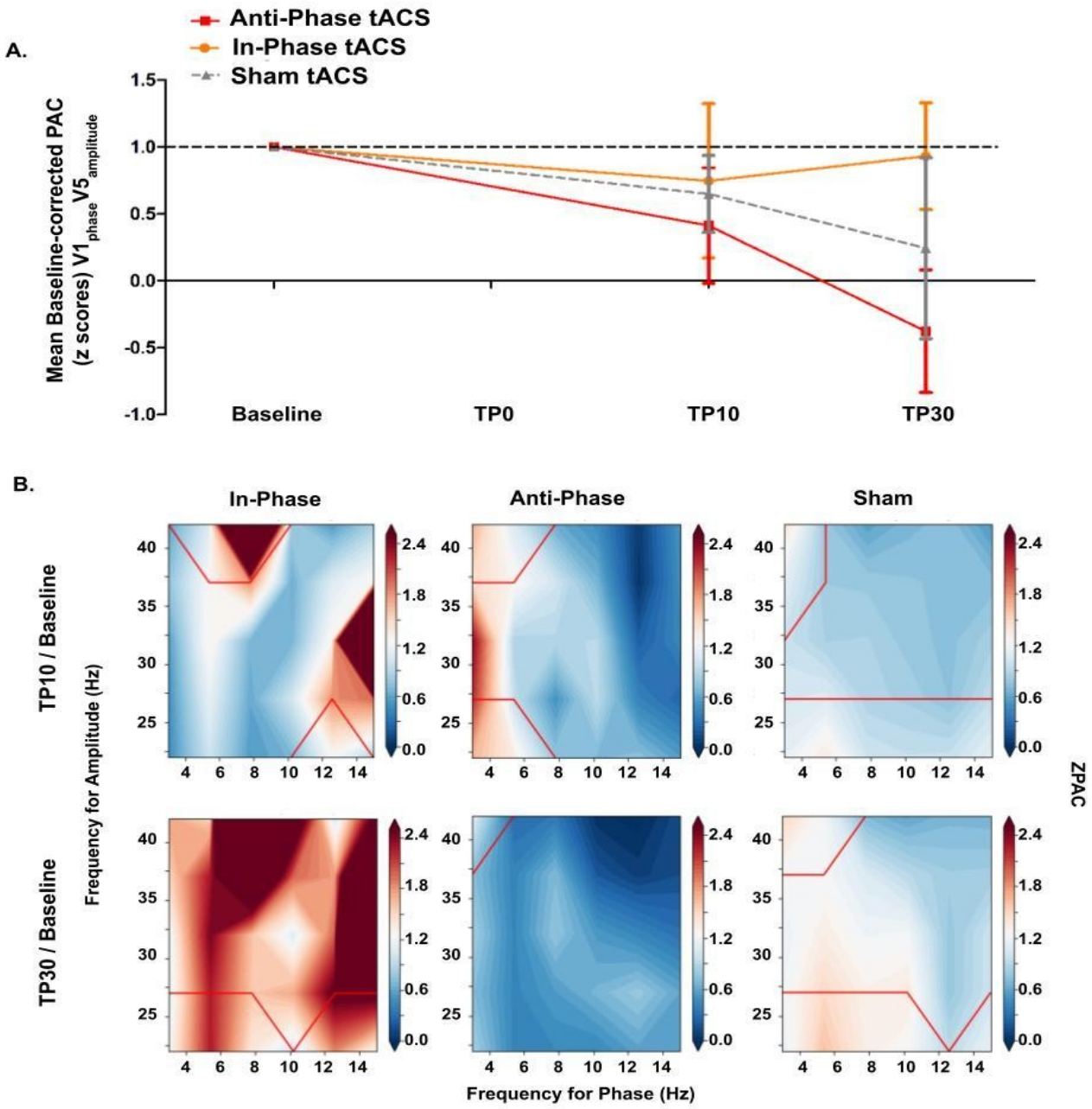

Figure 3. V1-Alpha phase V5-Gamma Amplitude PAC (A) Baseline-corrected, bottom-up V1-Alpha phase V5-Gamma Amplitude coupling across time-points. Bars correspond to Standard Errors of the Mean (SEM). Please note the strong decrease for the In-Phase group towards TP30. (**B) Averaged, baseline-corrected, V1-Gamma amplitude V5-Alpha phase coupling spectrums** for the three stimulation groups and for the two time points after stimulation averaged during the stimulus presentation interval. Significant clusters are highlighted in red ($p<0.05$, corrected for multiple comparisons).

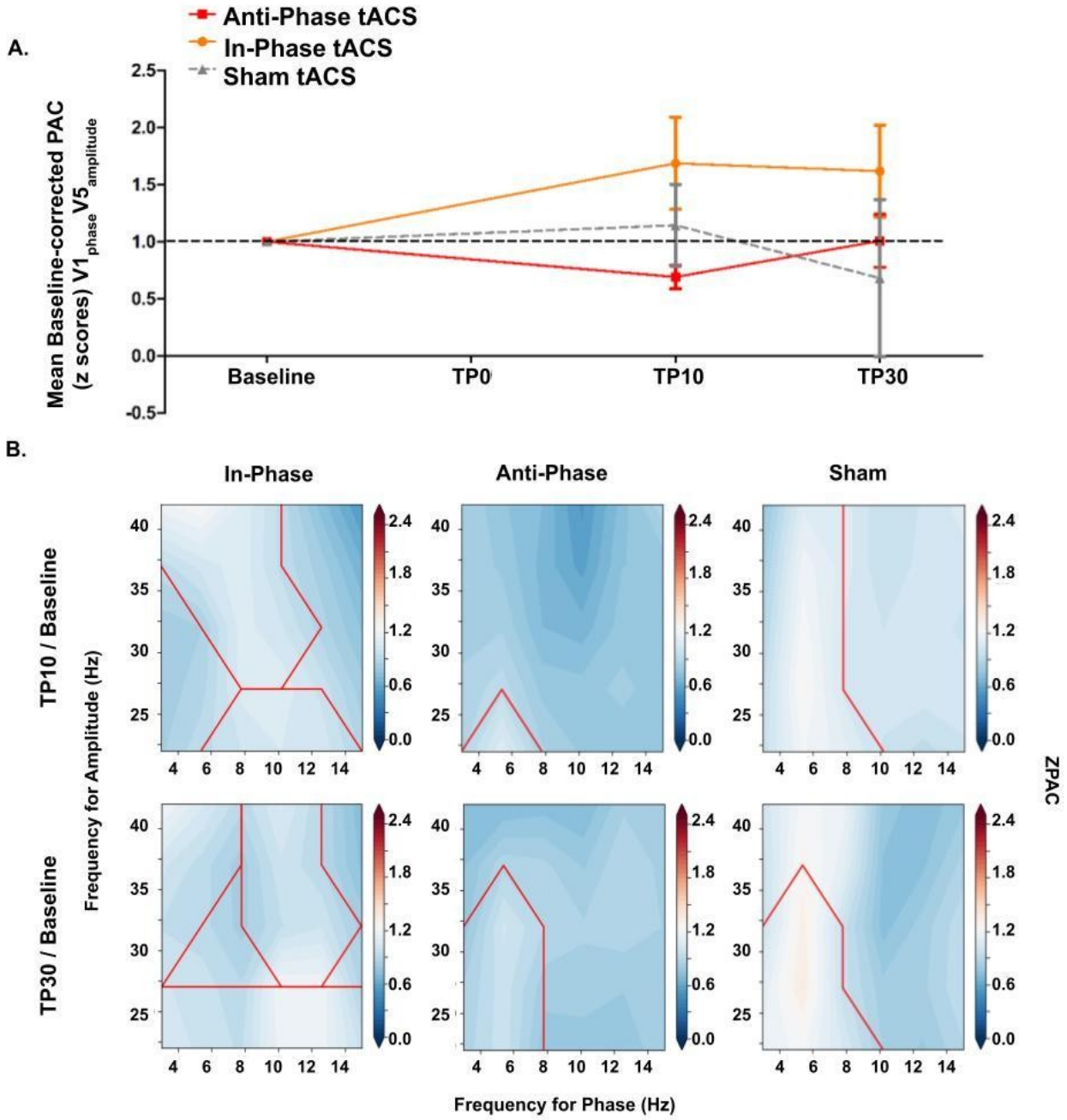

Figure 4. V1-Gamma amplitude V5-Alpha phase PAC (A) Baseline-corrected, top-down V1-Gamma amplitude V5-Alpha phase coupling across time-points. Bars correspond to Standard Errors of the Mean (SEM). **(B) Averaged, baseline-corrected, V1-Gamma amplitude V5-Alpha phase coupling spectrums** for the three stimulation groups and for the two time points after stimulation averaged during the stimulus presentation interval. Significant clusters are highlighted in red ($p<0.05$, corrected for multiple comparisons).

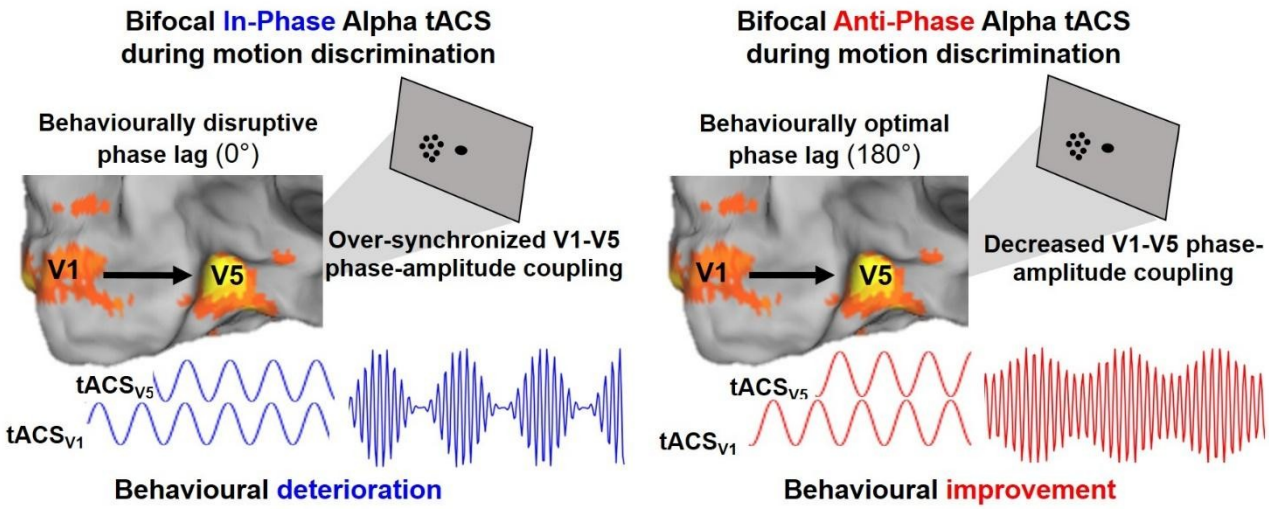

Figure 5. Summary and mechanistic interpretation of the effects of bifocal In-Phase tACS (left part) and the Anti-Phase tACS (right part).

2.7 Supplementary Materials

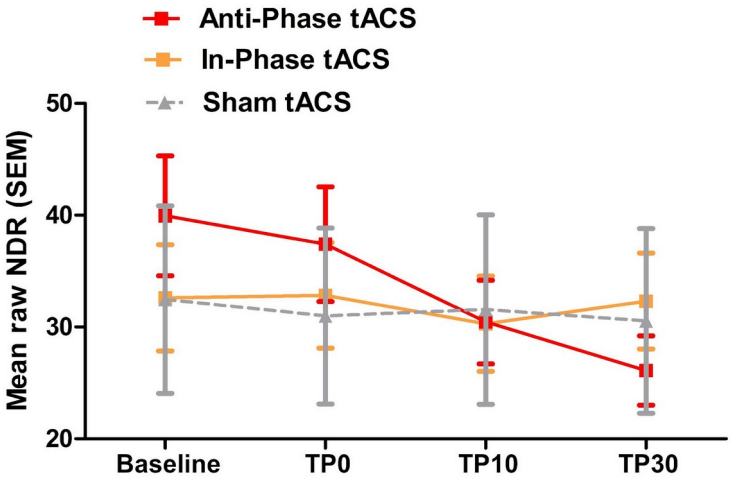

Supplementary Figure 1. NDR (Normalized Direction Range) threshold evolution across time-points for the three stimulation conditions. Bars correspond to Standard Errors of the Mean (SEM).

	Baseline	TP0	TP10	TP30
In-Phase	32.61 (4.75)	32.84 (4.73)	30.30 (4.27)	32.32 (4.29)
Anti-Phase	39.95 (5.36)	37.42 (5.13)	30.45 (3.73)	26.11 (3.11)
Sham	32.45 (8.39)	30.99 (7.87)	31.56 (8.48)	30.55 (8.27)

Supplementary Table 1. Mean raw NDR (Normalized Direction Ratio) values (SEM) for the three groups and four timepoints (TP). The group differences, although not significant (see the Results section) at baseline and the large overall inter-individual variability prompted us to perform a baseline-correction procedure by normalizing (dividing) all performances by the individual baseline value (see the Methods section).

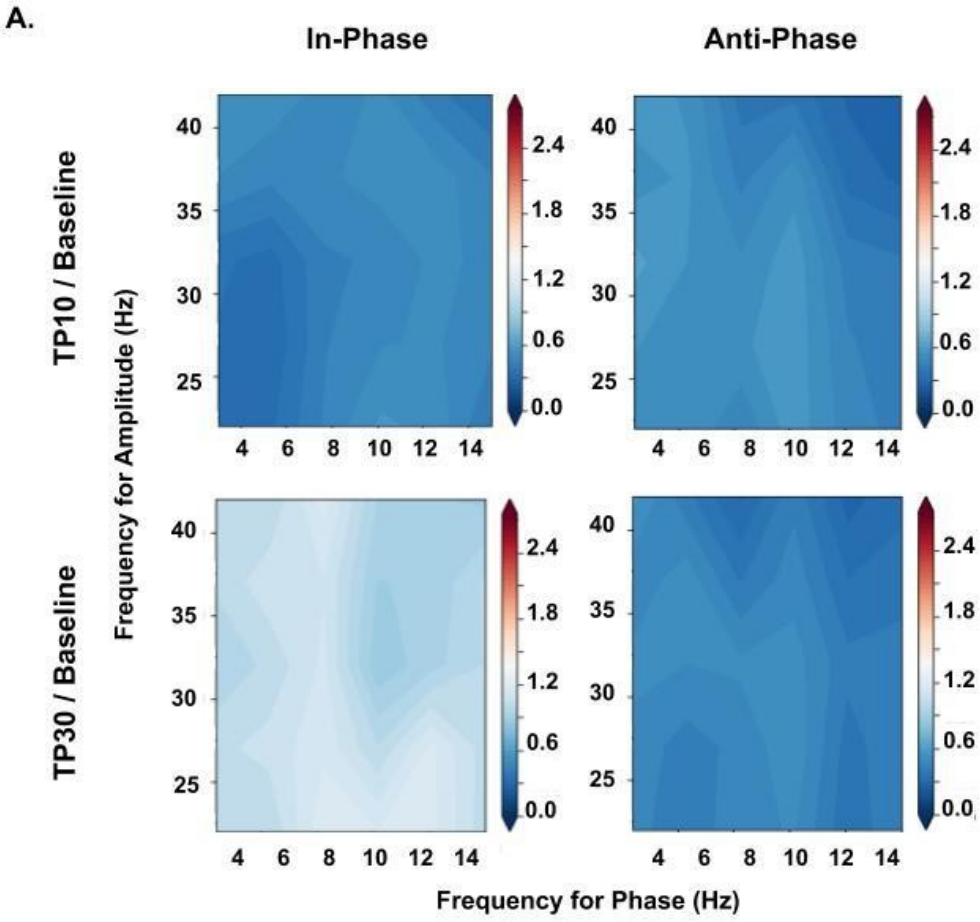
A.
In-Phase
Anti-Phase
TP10 / Baseline
TP30 / Baseline
Frequency for Amplitude (Hz)
Frequency for Phase (Hz)
40
35
30
25
4 6 8 10 12 14
2.4
1.8
1.2
0.6
0.0

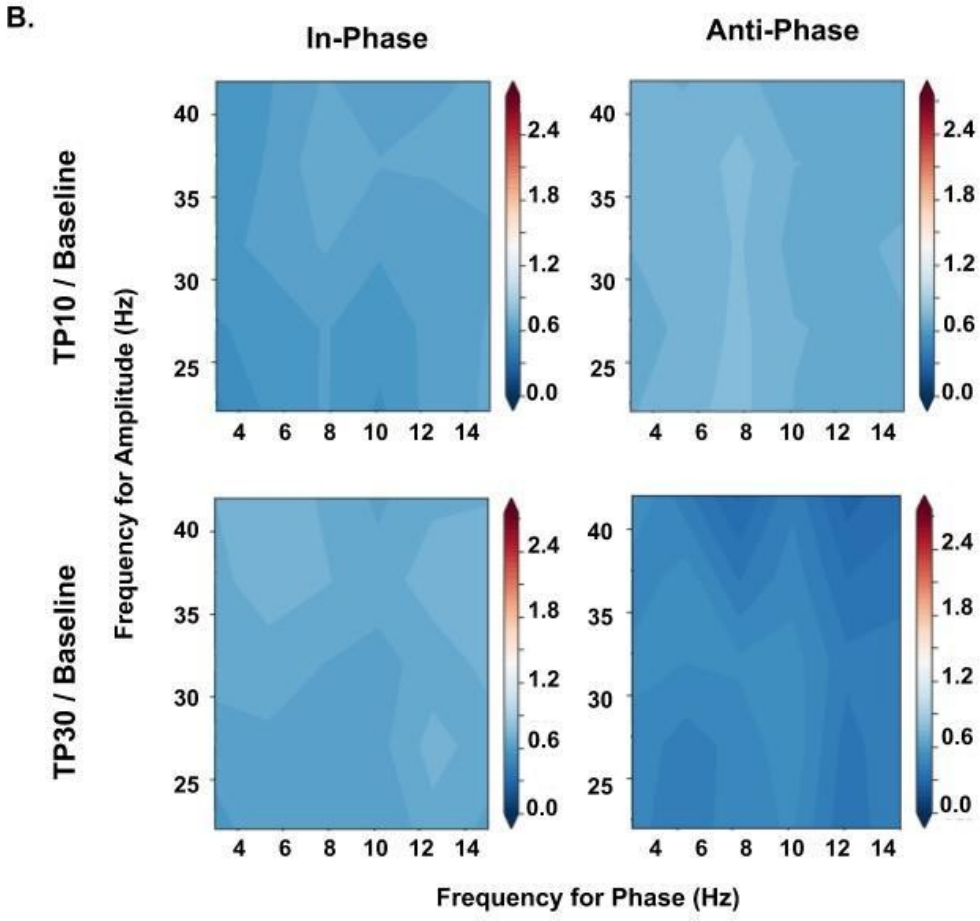
B.
In-Phase
Anti-Phase
TP10 / Baseline
TP30 / Baseline
Frequency for Amplitude (Hz)
Frequency for Phase (Hz)
40
35
30
25
4 6 8 10 12 14
2.4
1.8
1.2
0.6
0.0

Supplementary Figure 2. Alpha Phase -Gamma Amplitude cross frequency spectrums evaluated within the same brain area for the two conditions shown to be significantly different from each other (i.e. In-Phase vs. Anti-Phase). There is no Alpha-Gamma modulation of interest within the areas. **A. V1 Alpha Phase – V1 Gamma Amplitude B. V5 Alpha Phase – V5 Gamma Amplitude**

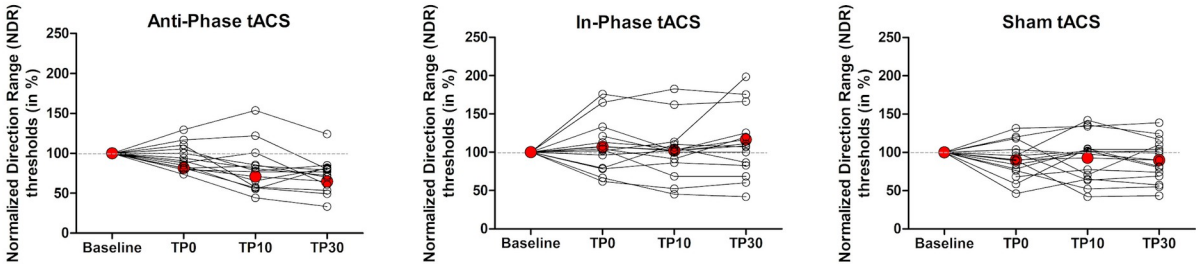

Supplementary Figure 3: Individual baseline-corrected normalized direction range (NDR) values for the three groups throughout the four time points (TP). The red overlay represents the group average.

Stimulation Group		Coef.	P>|z|	[0.025	0.975]
Anti-Phase	Baseline-TP0	-2.865	0.31	-8.401	2.671
	Baseline-TP10	-9.655	0.001	-15.19	-4.119
	Baseline-TP30	-14.519	0.001	-20.054	-8.983
	TP0-TP10	-6.79	0.016	-12.325	-1.254
	TP0-TP30	-11.653	0.001	-17.189	-6.118
	TP10-TP30	-4.864	0.085	-10.4	0.672
In-Phase	Baseline-TP0	0.23	0.93	-4.881	5.342
	Baseline-TP10	-2.309	0.376	-7.42	2.802
	Baseline-TP30	-0.291	0.911	-5.403	4.82
	TP0-TP10	-2.539	0.33	-7.65	2.572
	TP0-TP30	-0.522	0.841	-5.633	4.59
	TP10-TP30	2.017	0.439	-3.094	7.129
	Baseline-TP0	-5.802	0.04	-11.339	-0.265
	Baseline-TP10	-4.577	0.105	-10.114	0.96
	Baseline-TP30	-6.311	0.025	-11.849	-0.774
	TP0-TP10	1.225	0.665	-4.312	6.762
	TP0-TP30	-0.509	0.857	-6.047	5.028
	TP10-TP30	1.734	0.539,	-7.272	3.803

Supplementary Table 2 - NDR Mixed Linear Model Discriminated by singular group. Beta coefficients, P-values and Confidence intervals for each stimulation group individually across timepoints.

	Coef.	Std.Err.	z	P>|z|	[0.025	0.975]
TP10-TP0	-0.05	0.038	-1.314	0.189	-0.124	0.024
TP30-TP0	-0.067	0.038	-1.758	0.079	-0.141	0.008
TP30-TP10	-0.017	0.038	-0.443	0.657	-0.091	0.057
Anti-Phase-In-Phase (TP0)	-0.257	0.106	-2.43	0.015	-0.464	-0.05
Sham-In-Phase (TP0)	-0.16	0.102	-1.564	0.118	-0.36	0.04
Sham-Anti-Phase (TP0)	0.097	0.104	0.936	0.349	-0.107	0.301
Anti-Phase-In-Phase (TP10)	-0.257	0.106	-2.43	0.015	-0.464	-0.05
Sham-In-Phase (TP10)	-0.16	0.102	-1.564	0.118	-0.36	0.04
Sham-Anti-Phase (TP10)	0.097	0.104	0.936	0.349	-0.107	0.301
Anti-Phase-In-Phase (TP30)	-0.257	0.106	-2.43	0.015	-0.464	-0.05
Sham-In-Phase (TP30)	-0.16	0.102	-1.564	0.118	-0.36	0.04

Sham-Anti-Phase (TP30)	0.097	0.104	0.936	0.349	-0.107	0.301
ZPAC_V1pV5a	0.015	0.012	1.292	0.196	-0.008	0.039
ZPAC_V1pV5a : Anti-Phase (In-Phase + TP10)	-0.071	0.036	-1.975	0.048	-0.142	-0.001
ZPAC_V1pV5a : Sham (In-Phase + TP10)	-0.023	0.03	-0.771	0.44	-0.081	0.035
ZPAC_V1pV5a : Sham (Anti-Phase + TP10)	0.048	0.029	1.667	0.095	-0.008	0.105
ZPAC_V1pV5a : Anti-Phase (In-Phase + TP30)	-0.071	0.036	-1.975	0.048	-0.142	-0.001
ZPAC_V1pV5a : Sham (In-Phase + TP30)	-0.023	0.03	-0.771	0.44	-0.081	0.035
ZPAC_V1pV5a : Sham (Anti-Phase + TP30)	0.048	0.029	1.667	0.095	-0.008	0.105
ZPAC_V5pV1a	-0.007	0.011	-0.629	0.53	-0.029	0.015
ZPAC_V5pV1a : Anti-Phase (In-Phase + TP10)	-0.055	0.069	-0.786	0.432	-0.191	0.082
ZPAC_V5pV1a : Sham (In-Phase + TP10)	0.006	0.049	0.115	0.908	-0.09	0.101
ZPAC_V5pV1a : Sham (Anti-Phase + TP10)	0.06	0.051	1.189	0.234	-0.039	0.16
ZPAC_V5pV1a : Anti-Phase (In-Phase + TP30)	-0.055	0.069	-0.786	0.432	-0.191	0.082
ZPAC_V5pV1a : Sham (In-Phase + TP30)	0.006	0.049	0.115	0.908	-0.09	0.101
ZPAC_V5pV1a : Sham (Anti-Phase + TP30)	0.06	0.051	1.189	0.234	-0.039	0.16

Supplementary Table 3 - NDR Mixed Linear Model with all the independent variable contributions. Beta coefficients, P-values and Confidence intervals are presented for all the comparisons and interactions among time points, stimulation groups and the EEG markers: V1 Alpha Phase V5 Gamma Amplitude coupling (ZPAC_V1pV5a) and V1 Gamma Amplitude V5 Alpha Phase coupling (ZPAC_V5pV1a).

	Coef.	Std.Err.	z	P>|z|	[0.025	0.975]
TP30-TP10	-0.769	0.402	-1.915	0.055	-1.556	0.018
Anti-Phase-In-Phase (TP10)	-0.836	0.894	-0.935	0.35	-2.588	0.916
Sham-In-Phase (TP10)	0.173	0.859	0.202	0.84	-1.51	1.856
Sham-Anti-Phase (TP10)	1.009	0.876	1.152	0.249	-0.708	2.726
Anti-Phase-In-Phase (TP30)	-0.836	0.894	-0.935	0.35	-2.588	0.916
Sham-In-Phase (TP30)	0.173	0.859	0.202	0.84	-1.51	1.856
Sham-Anti-Phase (TP30)	1.009	0.876	1.152	0.249	-0.708	2.726

Supplementary Table 4 - ZPAC_V1pV5a Mixed Linear Model. Beta coefficients, P-values and Confidence intervals are presented for all the comparisons and interactions among time points and stimulation groups

	Coef.	Std.Err.	z	P>|z|	[0.025	0.975]
TP30-TP10	0.409	0.383	1.066	0.286	-0.343	1.161
Anti-Phase-In-Phase (TP10)	-0.695	1.045	-0.665	0.506	-2.744	1.353
Sham-In-Phase (TP10)	-1.413	1.009	-1.401	0.161	-3.39	0.564
Sham-Anti-Phase (TP10)	-0.718	1.025	-0.7	0.484	-2.727	1.292
Anti-Phase-In-Phase (TP30)	-0.695	1.045	-0.665	0.506	-2.744	1.353
Sham-In-Phase (TP30)	-1.413	1.009	-1.401	0.161	-3.39	0.564
Sham-Anti-Phase (TP30)	-0.718	1.025	-0.7	0.484	-2.727	1.292

Supplementary Table 5 - ZPAC_V5pV1a Mixed Linear Model. Beta coefficients, P-values and Confidence intervals are presented for all the comparisons and interactions among time points and stimulation groups

3

Cross-frequency tACS modulates EEG coupling during a motion discrimination task

Roberto F. SALAMANCA-GIRON[1,2], Martin SEEBER[3], Christoph M. MICHEL[3,6], Krystel R. HUXLIN[4], Estelle RAFFIN[1,2]*, Friedhelm C. HUMMEL[1,2,5]*

1 Defitech Chair in Clinical Neuroengineering, Center for Neuroprosthetics and Brain Mind Institute, EPFL, Geneva, Switzerland.

2 Defitech Chair in Clinical Neuroengineering, Center for Neuroprosthetics and Brain Mind Institute, Clinique Romande de Readaptation (CRR), EPFL Valais, Sion, Switzerland.

3 Functional Brain Mapping Lab, Department of Fundamental Neurosciences, University of Geneva, Campus Biotech, Chemin des Mines 9, 1202 Geneva, Switzerland

4 The Flaum Eye Institute and Center for Visual Science, University of Rochester, Rochester, NY, USA

5 Clinical Neuroscience, University of Geneva Medical School, Geneva, Switzerland

6 Lemanic Biomedical Imaging Centre (CIBM), Lausanne, Geneva, Switzerland

* co last authors

Status:

In preparation

Contributions:

R.S.G., E.R., F.C.H., K.H. developed the experimental design. R.S.G. was in charge of the data acquisition, data analyses and drafted the entire manuscript. M.S. added to the analyses. C.M. aided at interpreting the results. All authors revised the manuscript significantly. F.C.H. and E.R provided the funding.

3.1 Introduction

The V1-V5 network in humans has been widely reported as the pathway in charge of processing sensory information from moving stimuli (Hubel and Wiesel, 1969; Zeki, 2015, 1993; Zeki et al., 1991). It possesses characteristic oscillatory rhythms that are linked to the transfer of specific stimulus features within the pathway and that enable the mental interpretation of the attended stimuli (Händel et al., 2011; Thut et al., 2006).

For instance, Alpha oscillations have shown to control the activation of the visual cortex by continuously scanning for incoming stimulus (Shevelev et al., 1991), probably through a role of inhibition and desinhibition of brain areas, leading to the determination of the contextual state of a brain network (Klimesch et al., 2007). Supporting this idea, Alpha oscillations in the visual cortex have been correlated with visuo-attentional cues (Foxe et al., 1998), and behavioral changes in visual detection tasks (Thut et al., 2006). In turn, Gamma is elicited through the presentation of moving stimuli, encoding the stimulus' features in early parts from the visual cortex, i.e. Broadmann Area 17, V1 (Swettenham et al., 2009). Besides, it has been shown that Gamma oscillations respond to moving stimulus and they are modulated by surrounding areal inhibition (Orekhova et al., 2020). Ultimately, these two different frequency bands and their interactions have been shown to be crucially involved in neuronal integration and long-range cortical synchronization (von Stein and Sarnthein, 2000).

This neuronal integration might be the basis of processing visual discrimination tasks (Shadlen and Newsome, 1996). As a matter of fact, the integration and binding of information, has been described as one of the main roles of ɣ activity (Gray and Singer, 1989; Tallon-Baudry and Bertrand, 1999). Furthermore, when it comes to inter-areal, long-range synchronization, α has been also shown to play a significant role in integrating information (Zhang et al., 2019). Supporting the idea that both rhythms and probably their interplay, are essentially involved in coding and processing sensory inputs that in the end, contribute to convey visual information to the system.

This cross-frequency interplay across regions has been framed as inter-areal connections, communicating with each other through a phenomenon of nested oscillations. This implies cross-frequency modulations where the low-frequency establishes the framework and route of communication, and thus, the high-frequency ciphers the information as representational bursts (Bonnefond et al., 2017). The diverse modulation patterns occurring back and forth from V1 to V5 describe both linear and non-linear processes necessary for visual features encoding in the visual network (Rust et al., 2006; Simoncelli and Heeger, 1998). For instance, α-ɣ coupling in V1-V5 has been described as a trace of task-related stimuli processing (Pagnotta et al., 2020), while α-ɣ phase amplitude coupling might be a marker of visual information gating (Bonnefond and Jensen, 2015).

In a precedent study, we have demonstrated that bifocal Anti-Phase (and In-Phase) stimulation was associated to the modulation of V1-V5 α-ɣ Phase-amplitude coupling after stimulation (Salamanca-Giron et al., 2021). Hence, under this premise, we tested whether we can modulate this α-ɣ coupling by means of bifocal cross-frequency tACS.

This cross-frequency stimulation opened up the possibility of understanding whether there might be a preferential direction of applying the tACS over V1 and V5 that ultimately might lead to a boost motion discrimination capacity of healthy individuals. Therefore, in the current experiment, we used the same bifocal V1-V5 tACS montage from our previous study, but we intended to provide a sustained electrical flow of individualized α and ɣ rhythms in two contrasting conditions (i.e. V1α-V5ɣ vs. V1ɣ-V5α) to the V1-V5 network, during a motion discrimination task.

Based on our previous results (Salamanca-Giron et al., 2021), we expected to find, a specific intermingling of low and high frequencies mediating optimized signal transmission along the pathway, represented as an amplitude modulation (i.e., phase-amplitude coupling - ZPAC). Additionally, we further anticipated to find a modulation of the inter-aeerial synchronization along the pathway reflecting an unbiased proxy of the degree of connectivity (i.e. phase-phase coupling – WPLI) in a single frequency band.

From a behavioral point of view, we contemplated the idea that boosting the inter-areal cross-frequency interactions with bifocal tACS would lead to a modulation of behavior, given the predominance of the α-ɣ bands during the processing of visual information in the V1-V5 network. Moreover, motivated by our previous ZPAC results (Salamanca-Giron et al., 2021), we thought that the V1α-V5ɣ tACS direction was going to preferentially help with the interpretation of incoming moving stimuli and thus, improve performances.

3.2 Methods

Study design

The experiment was composed of 6 different blocks. It started with a familiarization block, where all participants got familiarized to the behavioral task, reaching a sustained level of accuracy (i.e. 75%). In due course, a baseline block (i.e. Bsl) took place in order to determine the individual basaline performance. Subsequently, a block with tACS for a complete run of the behavioral task was applied (i.e., TP0). Afterwards, the fourth and fifth block were respectively post evaluation points at 10 (i.e., TP10) and 30 (i.e., TP30) minutes after the block with brain stimulation. In all blocks, but the familiarization phase, EEG was constantly monitored and recorded. For an illustration of the experimental design, please see Fig. 1.

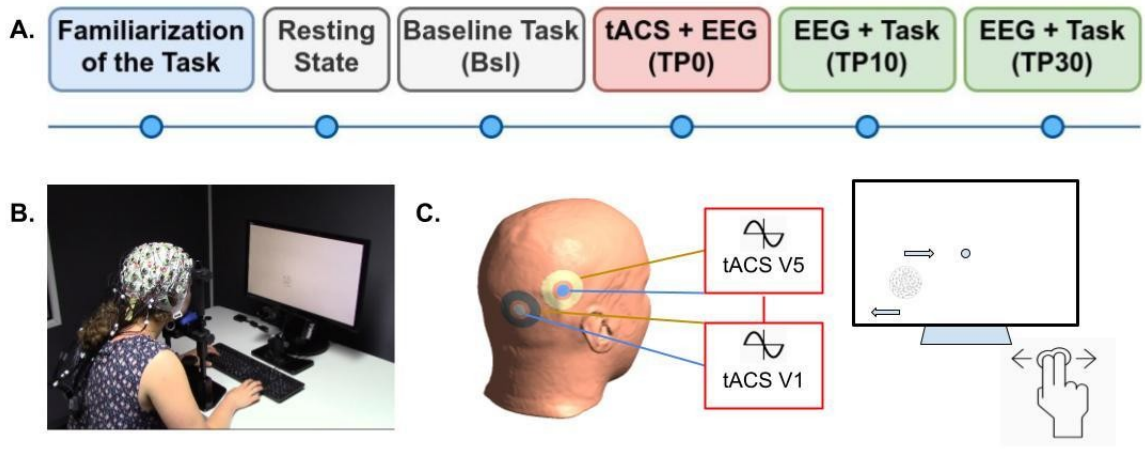

Figure 1. A. Study design consisting of 6 blocks. **B.** Experimental setup showing the EEG headset and the montage for performing the visual task **C.** Scheme representing the location of the concentric tACS electrodes over P6 and O2 and an indication of the way the motion takes places in the task.

Subjects

A total of 45 participants were part of the study (18 to 40 years old, 25 females). None of the individuals reported cognitive or neurological dysfunction. Moreover, they were all right-handed and had normal or corrected to normal vision. Participants provided signed informed consent within the framework of the guidelines of the Declaration of Helsinki based on the approval of the local Swiss Ethics Committee (2017-01761).

Behavioral Task

A well-established direction discrimination and integration task (Salamanca et al. 2021, Cavanaugh and Huxlin, 2017) was used as a behavioral measurement for all

blocks. The task consisted in a two-options, forced-choice, visual exercise, where the participant was supposed to perceive the global movement of tiny black dots going either to the right or to the left. The stimulus was always placed in the same part of a LCD (coordinates: [-5, -5] ~ lower right quadrant of the visual field) screen running a gray background (1024 x 768 Hz at 144 Hz). The dots composing the visual stimulus had a diameter of 0.06° and a velocity of 10°/s. The whole stimulus was organized in a circular shape with a diameter of 5° and a density of 2.6 dots/°. Its duration on the screen was set to 500ms. The difficulty of the task was set through a 3:1 staircase design as used before (Salamanca et al. 2021, Cavanaugh and Huxlin, 2017), implying that for every 3 positive responses the direction of the movement was disturbed by variations of 40°, in a scale between 0° and 360°, likewise, for every incorrect response the difficulty was reduced at the same rate. Besides, at every onset of the stimulus, a beep was played, as well as a feedback discriminating between a correct and incorrect response.

Transcranial Electrical Stimulation

Subjects were divided randomly and evenly into two Verum groups and they were compared to a Sham cohort previously used in an equivalent experimental design. This Sham dataset was previously used in another publication (Salamanca-Giron et al., 2021). The first verum group corresponded to Alpha stimulation over V1 and Gamma stimulation over V5 (i.e. V1α-V5ɣ). The second one was the opposite condition, meaning Gamma band stimulation over V1 and Alpha over V5 (i.e. V1ɣ-V5α). The Sham stimulation corresponded to a ramp up and ramp down stimulation lasting in total the equivalent of an individualized Alpha cycle. Electrodes were placed for the three groups by means of the P6 and O2 from the 10-20 EEG system representing V1 and V5 in the right hemisphere. Individual Alpha and Gamma frequency peaks were calculated before the Baseline block during an EEG Resting State recording for personalization of the stimulation.

Electrical Stimulation Devices

The multisite transcranial stimulation was applied using two Neuroconn DC Plus stimulators (Neurocare, Germany) triggered repetitively and at the same time to assure no time lag between them. The stimulators were connected to customized concentric rubber electrodes that were delivering a current density of 0.18 mA/cm2 at a constant current intensity of 3 mA. The outer and inner diameters of the electrodes were 5 and 1.5 cm respectively. The hole diameter was 2.5 cm. The stimulation lasted for the entire duration of the task at TP0 (13 +/- 2 min).

The experiments were performed inside a shielded EEG room equipped with a Windows machine running Matlab (Mathworks Inc., USA) and Psychtoolbox, an EyeLink 1000 Plus Eye Tracking System (SR Research Ltd., Canada) and a chin rest. All individuals sat at 60 cm from the computer’s screen supporting their heads with the chin rest, while all the trials were controlled with the eye tracker system. If the gaze fixation was lost for more than 1°, the trial was interrupted and discarded, until the person would re center his eyes at the fixation dot.

EEG was recorded using a passive system with 64 electrodes (Brain Products GMBH, Germany) sampling at 5 kHz.

Data Analyses

Behavior: Based on methods described in previous work from us and others (Salamanca et al. 2021, Cavanaugh and Huxlin, 2017), the maximum tolerated noise for every participant at each block was calculated through the use of a Weibull function. The individualized threshold was set to 75% of accuracy and it was given as a percentage of the maximum range of motion (i.e. 360°) through the formula below.

$$NDR(\%) = \left[\frac{360° - WeibullThreshold}{360} ° \right] \cdot 100$$

The values coming from this formula were then computed as a ratio expressing the change between the block of interest (e.g., TP0, TP10, TP30) and the Baseline.

EEG: The analyses were performed by means of customized algorithms and MNE-Python (Gramfort et al., 2013) and applied to all data sets (Bsl, TP10 and TP30) except TP0, due to the limitations of reliably removing the tACS artifact.

The preprocessing of all EEG datasets passed through the same procedure: Reference to the average of all channels, band-passed filtered between 0.5 Hz and 45 Hz, and divided in epochs of 3s length. Visual inspection was used to remove explicit artifacts among channels and trials, followed by the reconstruction of dropped channels and epochs. Ultimately, an Independent Component Analysis was applied to down-sample data (250 Hz) to remove electrophysiological interferences, such as eyeblinks or muscle artifacts.

Analyses at the source level were done through the use of the MNE algorithm (Gramfort et al., 2014). The sources at V1 and V5 were calculated through an optimized covariance matrix and the template brain and anatomical segmentations were taken from the sample dataset “SPM” provided by MNE-Python. Dipoles were estimated orthogonal to the cortex and a Signed-flipped, Principal Component Analysis was used to determine the most likely signal from the location of interest.

All metrics involving a frequency domain decomposition were calculated through Morlet wavelets between 2 and 40 Hz.

Thus, the EEG markers computed were:

- Weighted Phase Locking Value (WPLI) between V1 and V5 in the source space.

$$WPLI(f)=\frac{\left|\sum_{k=1}^{K} \square I\left(\Phi_{xy}(f)\right)\right|}{\sum_{k=1}^{K} \square \left|I\left(\Phi_{xy}(f)\right)\right|}$$

WPLI was chosen as an unbiased estimator of the connectivity accounting for possible biases associated with source leakage effects.

- Phase Amplitude Coupling (PAC) between V1 and V5 at the source space.

$$PAC(f)=n^{-1}\sum_{t=1}^{n} \square a_t(f)\cdot e^{i\theta t}$$

Where a corresponds to the amplitude of the instant t among n intervals multiplied by the imaginary component of the phase angle θ.

Cross-frequency interactions were computed from the EEG data recorded before and after tACS in phase-amplitude coupling of α-ɣ between V1 and V5. Complementary, given that the inclusion of amplitude in the phase-amplitude coupling measurement might be biased by widespread network augmentations (Darvas et al., 2009), we have complemented it with a robust phase-phase coupling measurement between neuronal populations (i.e. WPLI), expressed independently of amplitude fluctuations (Palva and Palva, 2011)

Statistical Analyses

Behavior: NDR ratios were entered into a Mixed Linear Model (i.e. MLM) that included as independent factors (i.e., fixed effects) the stimulation groups and all timepoints. The random effects were defined as the variability coming from subjects. The regression model followed the equation below:

$$NDR=TIMEP+GROUP+\left(\frac{1}{SUBJECT}\right)$$

Since we were interested in comparing the learning dynamics across groups, we performed planned group comparisons.

EEG: WPLI and PAC significance was evaluated within subjects through a non-parametric, cluster-based corrected, permutation testing. Significance was defined as a p value of less than 5%.

Behavior and EEG: An interaction factor composed by the EEG marker and the stimulation groups was added to the first Mixed Linear Model in order to evaluate the mechanistic (i.e electrophysiological) differences that each group could bring along.

$$NDR=TIMEP+GROUP*EEG+\left(\frac{1}{SUBJECT}\right)$$

3.3 Results

None of the healthy subjects reported any type of sensory perception (e.g., tactile, visual) during the stimulation. One dataset was not included in the analyses due to the incapacity of fitting a Weibull function, the other 44 datasets were included in the entire analyses.

EEG spectral differences between Verum and Sham

The two EEG markers of interest were the Z-scored PAC (ZPAC), which reflects cross-frequency coupling between V1 and V5 in Alpha and Gamma, and WPLI values estimating EEG functional connectivity between V1 and V5 in Alpha and Gamma as well. They were extracted at the sources level during stimulus presentation in the Alpha and Gamma band for every subject and all timepoints (i.e. Bsl, TP10 and TP30). All values were normalized to Baseline (Supplementary Table 2).

The only significant difference in ZPAC co-modulograms occurred between Sham and the V1ɣ-V5α group, showing a strong negative modulation of ZPAC-$V1a_{Gamma}V5p_{Alpha}$ at TP30 indicating a strong increase in $V1a_{Gamma}V5p_{Alpha}$ coupling in this group. The V1α-V5ɣ group showed a similar trend at TP10 and TP30. ZPAC-$V1p_{Alpha}V5a_{Gamma}$ co-modulograms of both Sham versus V1ɣ-V5α and Sham versus V1α-V5ɣ showed a non-significant positive low Gamma-Alpha modulation at TP10 and TP30 reflecting a decrease in Gamma-Alpha coupling for the two Verum groups compared to Sham (Figure 2A).

The WPLIα spectrums suggested a sustained elevated Alpha connectivity for the Sham group compared to the V1α-V5ɣ group 50-500 ms after stimulus onset at TP10 as indicated by significant positive clusters in the Alpha band. In contrast, at TP30, the V1α-V5ɣ group showed significantly more alpha connectivity in the late period of the stimulus presentation as indicated by the negative clusters, 350-500 ms after stimulus onset. The comparison of Sham against V1ɣ-V5α at TP10 showed significantly more Alpha connectivity for the Sham group between 400 and 500 ms while it occurred for a longer period (100-500 ms after stimulus onset) at TP30, indicating a pronounced decrease in Alpha connectivity for the V1ɣ-V5α group (Figure 2B).

The WPLI spectrums in the Gamma band showed significant positive clusters at TP10 between 50-250 ms after the stimulus onset between Sham and V1α-V5ɣ, which turned into decreased connectivity clusters in the interval 250-500 ms, indicating decreased and then increased Gamma connectivity for the V1α-V5ɣ group. At TP30, significant positive clusters between 50-500 ms became more prominent suggesting a strong decrease in gamma connectivity for V1α-V5ɣ compared to Sham and linked with strong rhythmic Beta modulations throughout stimulus presentation. The comparison of Sham versus V1ɣ-V5α revealed significant clusters of increased Gamma - decreased rhythmic low Gamma/Beta connectivity at TP10 and TP30. Similar to V1α-V5ɣ, V1ɣ-V5α tACS induced a significant and sustained decreased Gamma connectivity together with rhythmic bursts of Beta activity (Figure 2B).

Changes in EEG coupling as predictors of behavioural performance

In a first MLM, we entered the ZPAC-V1a$_{Gamma}$V5p$_{Alpha}$ values as an interacting factor with groups and time-points to explain NDR variability (Figure 3A). An ANOVA evaluating the factors from the MLM revealed significant time effect ($F(2,6) = 12.932$, $p < 0.0001$) and group effect ($F(2,6) = 3.585$, $p = 0.033$) as well as a significant group by ZPAC-V1a$_{Gamma}$V5p$_{Alpha}$ interaction ($F(2,6) = 4.141$, $p = 0.018$). This last interaction was mainly driven by the strong association between ZPAC-V1a$_{Gamma}$V5p$_{Alpha}$ and NDR changes in the V1ɣ-V5α group compared to the two other groups as shown in Figure 3A and as further suggested by the pairwise comparisons showing a trend between V1ɣ-V5α and Sham ($b = 0.065$, $p = 0.058$, CI = 0.0002 0.130), and between V1ɣ-V5α and V1α -V5ɣ ($b = 0.062$, $p = 0.118$, CI = -0.013 0.138). All the other comparisons were not significant (see supplementary Table 3 for all the other comparisons in this section).

In a second MLM including the other ZPAC-V1p$_{Alpha}$V5a$_{Gamma}$ values, the ANOVA from the MLM showed that there was only an effect over time ($F(2,6) = 10.393$, $p = 0.000114$), but not within the groups ($F(2,6) = 0.381$, $p = 0.684$), neither a group by ZPAC-V1p$_{Alpha}$V5a$_{Gamma}$ interaction ($F(2,6) = 0.670$, $p = 0.514$ and see Figure 3B).

A third MLM with the WPLIα values was evaluated under the same procedure. The ANOVA applied to the model showed a significant time effect ($F(2,6) = 8.813$, $p = 0.0003$) but no group effect ($F(2,6) = 1.444$, $p = 0.240$) and no WPLIα by group interaction was not significant ($F(2,6) = 1.230$, $p = 0.296$ and Figure 3C).

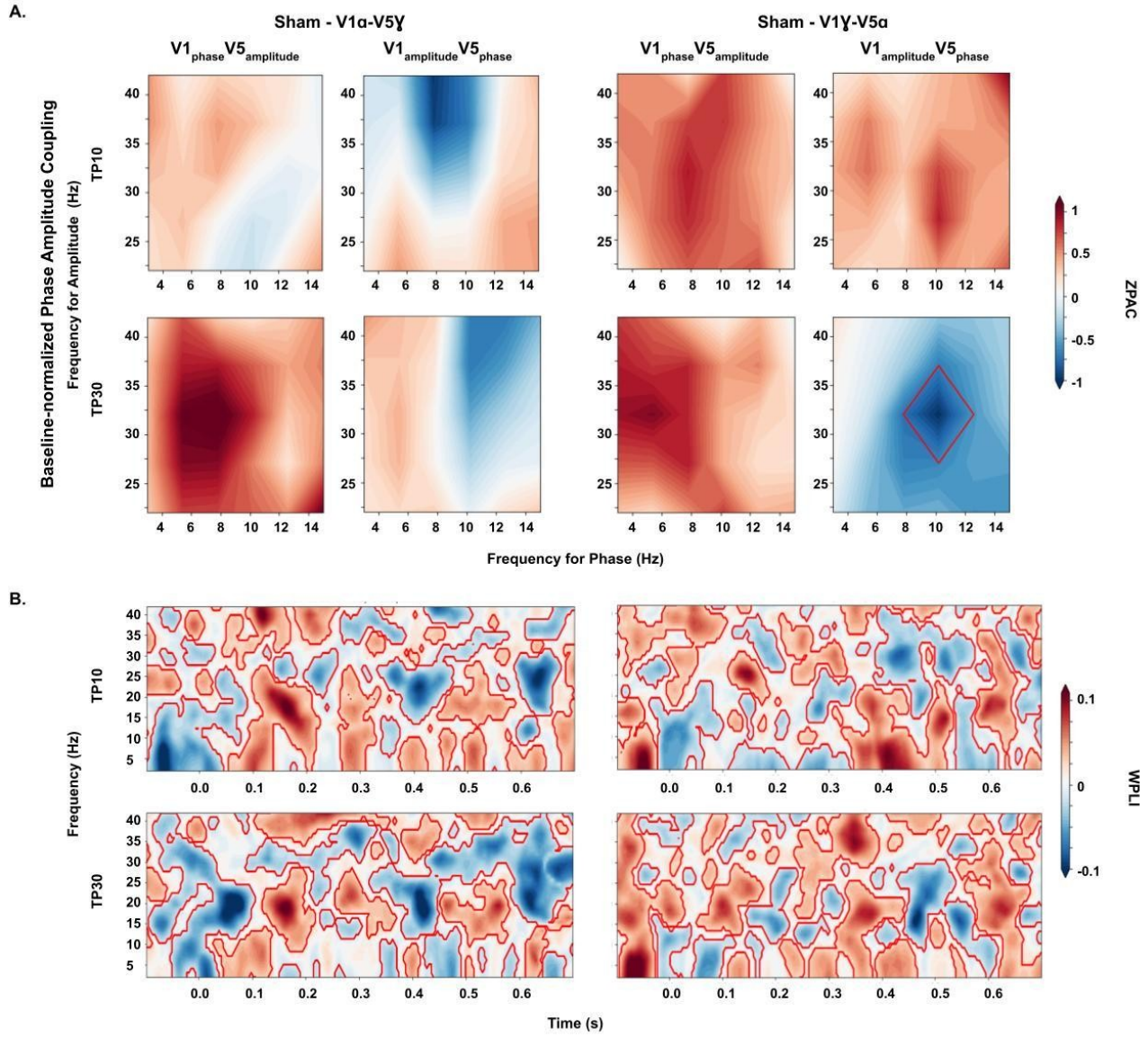

Figure 2. A. Differential comodulograms for both time points after tACS (i.e. TP10, TP30) contrasting each verum condition against Sham, averaged during the stimulus presentation. Only one significant cluster ($p<0.05$), highlighted in red, was found among all contrasts. It corresponds to the V1 amplitude V5 phase ZPAC orientation at TP30, suggesting an augmentation in phase-amplitude modulation for the V1ɣ-V5α group **B.** Differential WPLI time-frequency spectrums contrasting each one of the verum groups against Sham. Time zero (i.e. 0.0) corresponds to the stimulus onset. Clusters surrounded in red are significant ($p<0.05$). Patches of increased connectivity in red and decreased connectivity in blue between V1 and V5 might reflect a phasic coupling between both regions, highlithing the interplay between the two frequeny bands of interest.

Finally, a last MLM including WPLIɣ as an interacting factor with the stimulation groups and time points was performed. The ANOVA on the model revealed a main effect of time ($F(2,6) = 7.689$, $p = 0.0009$) and group ($F(2,6) = 7.552$, $p = 0.0008$). More importantly, the interaction between group and WPLIɣ appeared also significant ($F(2,6) = 6.7$, $p = 0.0018$).

In details, WPLIɣ could differently explain behavioral performances in the V1α-V5ɣ group and the Sham group (b = 0.742, p = 0.003, CI = 0.262 1.228) for all time-points. The same applies to the comparison between the V1ɣ-V5α group and the Sham group (b = 0.893, p = 0.006, CI = 0.282 1.507). Finally, as shown in Figure 4D, the difference between the two Verum groups could not be explained by their interaction with WPLIɣ (b = 0.150, p = 0.675, CI = -0.538 0.834) at all time-points. Of note, the MLM revealed a significant effect of WPLIɣ as a single variable into the model (b = -0.391 p = 0.003, CI = -0.645 -0.140), suggesting that WPLIɣ is an unspecific marker of performance changes.

Our results indicated that the Verum and Sham conditions can be dissociated through the role of V1-V5 phase-phase WPLI coupling in Gamma, in improving performances. In the next section, we directly contrasted the two Verum groups against each other, to provide a better mechanistic understanding of the condition-specific stimulation effects and explore the main electrophysiological drivers of performance changes.

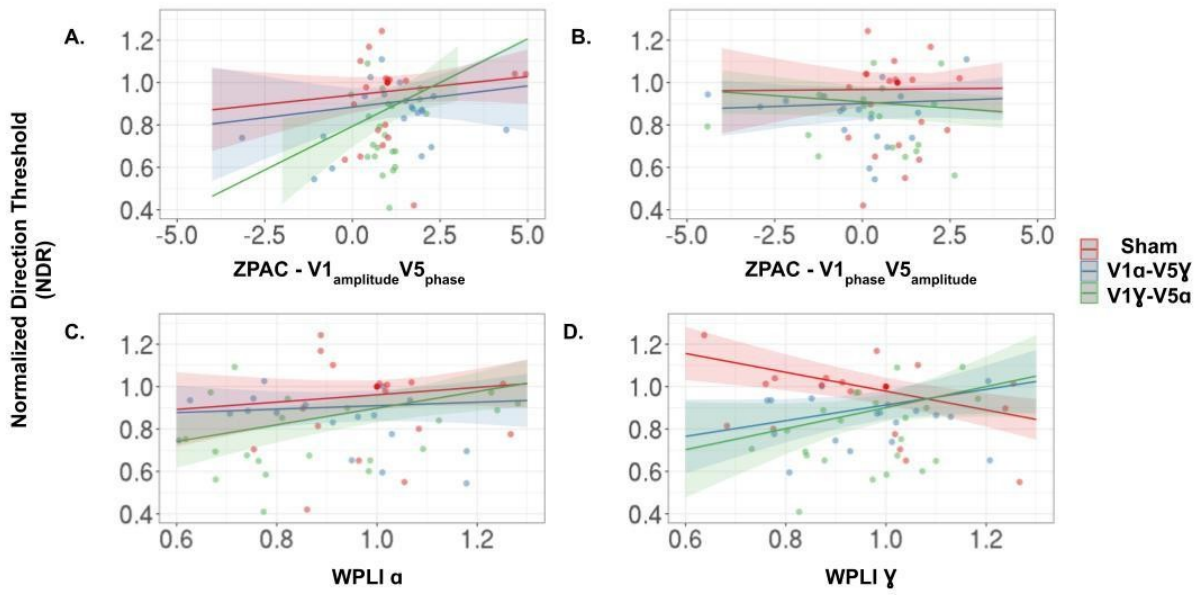

Figure 3. Regression lines for the three groups together fitted from the NDR datapoints distribution against: **A.** ZPAC-V1a$_{Gamma}$V5p$_{Alpha}$ **B.** ZPAC-V1p$_{Alpha}$V5a$_{Gamma}$ **C.** WPLI α **D.** WPLI ɣ.

EEG coupling distinction between the two Verum groups

The difference between the ZPAC comodulograms of the two Verum groups revealed a significant increase in ZPAC-V1a$_{Gamma}$V5p$_{Alpha}$ for the V1α-V5ɣ group at TP10 only (Figure 4A and 4C left panel). These ZPAC values differently explained NDR changes of the two Verum groups as shown by the MLM (b = 0.065, p = 0.047, CI = 0.003 0.127, see also Figure 4C left panel). In contrast, the difference in ZPAC-V1p$_{Alpha}$V5a$_{Gamma}$ was not significant (Figure 4A right panel) and was not differently related to performance in the two groups (ZPAC-V1p$_{Gamma}$V5a$_{Alpha}$: b = -0.016, p = 0.139, CI = -0.037 0.004) (See Supplementary Table 4).

Significant clustered differences in WPLI in Alpha (WPLIα) were found at TP10 suggesting an increased V1-V5 phase-phase coupling between ~200 and ~500 ms after the stimulus onset for the V1ɣ-V5α group. At TP30, the same observation was made in the last part of the stimulus presentation (350 to ~500 ms) (Figure 3B). The MLM further revealed that WPLIa contributes differently to changes in behavioural performances in the two groups (b = 0.338, p = 0.047, CI = 0.018 0.662, see also Figure 3C right panel). Complementary, significant WPLI clusters in Gamma (WPLIɣ) showed a decreased connectivity between ~100 to ~500 ms after the stimulus onset for V1ɣ-V5α at both TP10 and TP30, without contributing differently to performance changes in the two groups (b = 0.057, p = 0.856, CI = -0.547 0.659).

Behavioral results

Figure 4D shows the NDR values that were normalized to Baseline after ensuring that Baseline values were not different in the three groups (V1α-V5ɣ vs V1ɣ-V5α: t = 1.475, p = 0.160, p cor = 1.0, V1α-V5ɣ vs Sham: t = 1.225, p = 0.232, p cor = 1.0, V1ɣ-V5α vs Sham: t = -0.057, p = 0.954, p cor = 1.0).

A first MLM was designed to test the effects of timepoints and groups on the baseline-corrected NDR variability. An ANOVA evaluating the MLM revealed a significant effect of timepoint (F(3,6) = 5.65, p = 0.001) reflecting a general improvement in task performance. In details the MLM considering all groups together revealed that there was a significant change in NDR between Baseline and TP0 (b = 0.109, p = 0.002, CI = 0.038 0.180), between Baseline and TP10 (b = 0.132, p = 0.0005, CI = 0.059 0.205) and between Baseline and TP30 (b = 0.150, p = 0.0001, CI = 0.078 0.223). However, it was not the case between TP0 - TP10 (b = 0.023, p = 0.535, CI = -0.050 0.096), TP0 - TP30 (b = 0.041, p = 0.261, CI = -0.031 0.114) or between TP10 - TP30 (b = 0.018, p = 0.627, CI = -0.056 0.093).The ANOVA did not show a group effect when considering all timepoints together (F(2,6) = 1.09, p = 0.346) nor a significant group by time interaction (F(6,6), = 0.744, p = 0.615), hence the comparisons are not displayed here (See Table 1 in the Supplementary Materials).

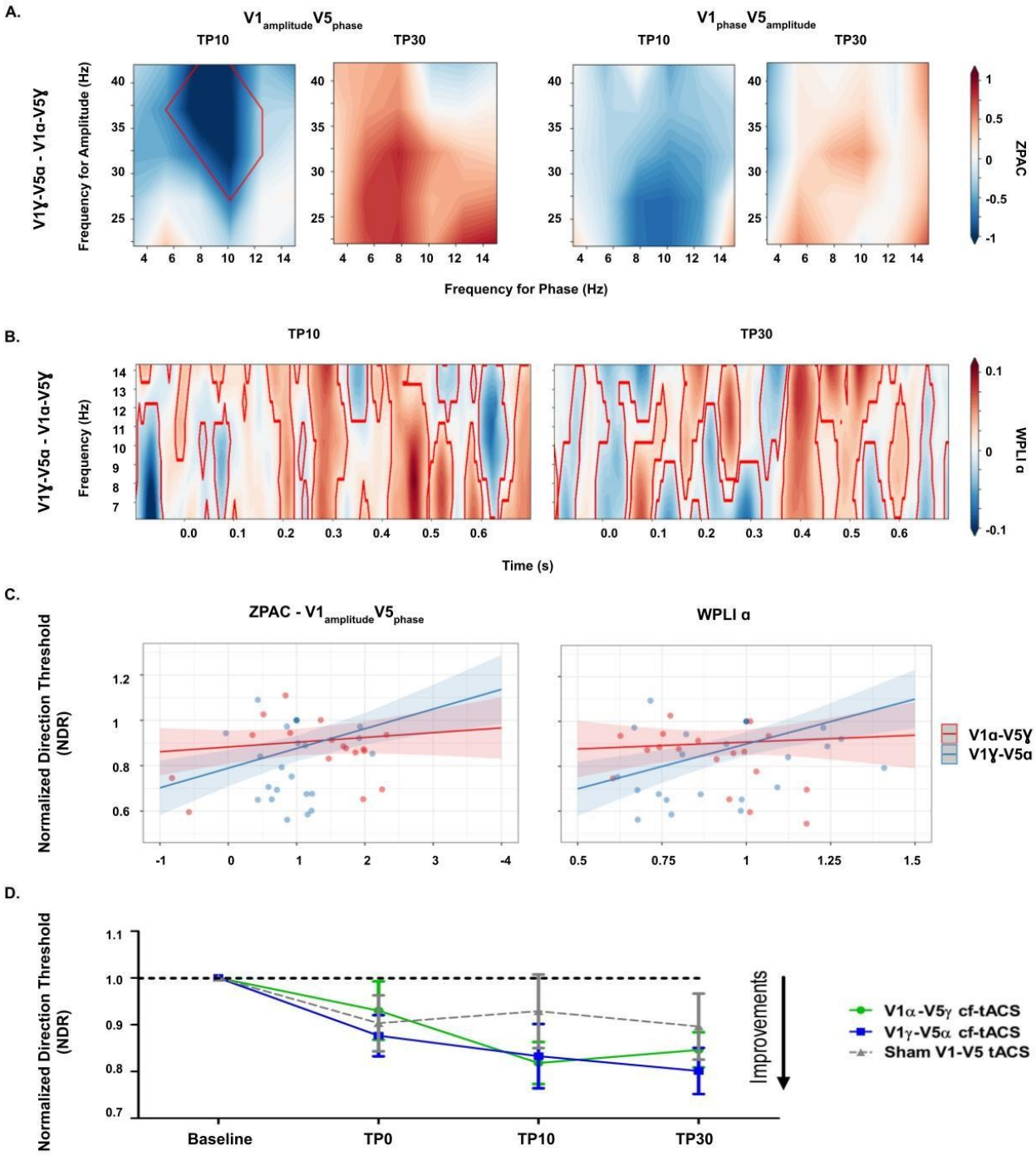

Figure 4. A. Differential comodulograms for both time points after the stimulation (i.e. TP10, TP30) contrasting both verum conditions averaged during the stimulus presentation. Significant clusters ($p<0.05$) are highlighted in red **B.** Differential WPLI time-frequency spectrums contrasting once more both verum groups. Time zero (i.e. 0.0) corresponds to the stimulus onset. Clusters surrounded in red are significant ($p<0.05$) **C.** Regression lines fitted from the NDR datapoints distribution against the two markers, ZPAC-V1a$_{Gamma}$V5p$_{Alpha}$ and WPLIα, that interact significantly with both verum groups and thus, explain the NDR differences between them. **D.** Averaged evolution of the normalized NDR across all time points and comparison among groups.

3.4 Discussion

The current manuscript examined the effects of two cross frequency (i.e. V1α-V5ɣ vs. V1ɣ-V5α) tACS conditions and a Sham condition applied to healthy subjects undertaking a visual motion discrimination and integration task. The analyses focused on the changes in inter-areal coupling between V1 and V5 in the two frequency bands of interest (i.e. Alpha and Gamma), 10 minutes and 30 minutes after the stimulation period (i.e. TP10 and TP30), induced by cross-frequency tACS. The oscillatory activity along the V1-V5 pathway at the source level was described through phase-amplitude coupling (i.e. ZPAC) and phase-phase coupling (i.e. WPLI). We then assessed, how these connectivity metrics relate to behavioral performance in the visual task.

In summary, we found that 1) Different WPLI functional connectivity profiles in Gamma explained the learning performances in the two Verum groups versus the Sham condition. 2) WPLIα and ZPAC-V1a_{Gamma}V5p_{Alpha} helped distinguishing performance changes between the two Verum groups 3) The tACS induced electrophysiological changes did not translate into behavioural differences as the Verum and the Sham group showed comparable behavioural profiles.

Shared neural effects between the two cross-frequency V1-V5 tACS

The ZPAC comparison against Sham showed that both Verum groups increased ZPAC-V1a_{Gamma}V5p_{Alpha} and diminished ZPAC-V1p_{Alpha}V5a_{Gamma}. Although these traces did not survive corrections for multiple comparisons, these dynamics suggest the elicitation of an amplitude modulated mechanism in V1-V5, which might be equivalently triggered by any of the two cross-frequency sustained stimulation. This finding might be associated with the fact that there is a tACS-induced bottom-up facilitation plus a top-down, long-range integrative processing that engages lower frequency bands (<30 Hz), such as alpha controlling local networks in the gamma-band (>30 Hz).

Additionally, both Verum groups showed a common decrease in WPLI ɣ during stimulus presentation inversely proportional to performances. This relationship was opposite for Sham for which WPLI ɣ and NDR were negatively correlated. This could be explained by enhanced post-stimulation motion sensitivity in the V1-V5 network after tACS (Kar and Krekelberg, 2014), due to the proliferation of ɣ oscillations that permits better processing of moving features such as velocity (Orekhova et al., 2015). This sensitivity might be complemented by the idea that the Verum stimulation actually makes reverberate the features integration mechanism in the occipital areas, given the incidence of α oscillations in either V1 or V5, that might help blossoming ɣ traces (Ferro et al., 2021; Sokolov et al., 1999). These ɣ traces appear to enable signalling in this pathway and have been shown to be linked to short-term plasticity (Carver et al., 2008; Ramcharitar et al., 2006).

Importantly, in our study, the most favorable communication bonding, associated with better performances seems to occur at a specific reduced WPLI coupling ratio for the two Verum groups compared to Sham. In support of this, previous studies have shown

that transient suppression of gamma activity or coupling are correlated with task complexity or subject performance (Lachaux et al., 2012).

Distinct effects induced by each cross-frequency V1-V5 tACS condition

While the two Verum conditions share some neuronal substrates, the direct comparison between them also revealed significant differences in the comodulogram of ZPAC-V1a$_{Gamma}$V5p$_{Alpha}$ at TP10 reflecting a decreased coupling in the V1ɣ-V5α group compared to the V1α-V5ɣ group. Moreover, the relationship between these ZPAC values and the performance changes (i.e. NDR) was significantly different in the two Verum groups. Weaker ZPAC values were associated with better performances in the V1ɣ-V5α group.

This decoupling suggests bottom-up demodulation after stimulating with V1ɣ-V5α, which might be compensated by top-down signals as main mechanism of action explaining behavioral improvement in young healthy participants. This phenomenon might be transient since at TP30, V1ɣ-V5α showed increased ZPAC-V1a$_{Gamma}$V5p$_{Alpha}$ compared to sham and the difference was not significant anymore with the other Verum Group.

In this order of ideas, our data might suggest that V1ɣ-V5α tACS provides a temporary suitable biological substrate to support the reception of newer visual information from the environment, and this in turn generates a more accurate representation from outer visually dynamic experiences through top-down signalling (Rao and Ballard, 1999).

This result is in line with the proposed imbalance between feedforward and feedback connections stated in the predictive coding theory (Friston, 2009, 2008). The theory justifies the imbalance through a mechanism of constant comparison between an expected, top-down signal and a novel and a bottom-up sensory input that produces an error factor. This error acts out as an update to the expectation and thus, permits to refine the upcoming predictions (Bastos et al., 2012; Friston, 2008; Michalareas et al., 2016). Then, V1ɣ-V5α tACS might trigger offline and sustained enhancement of a preferential long range, inter-areal communication channel that could support the transmission of top-down oscillatory activity in lower areas (Kasten et al., 2016). This pattern of oscillatory activity that is essential to enable the accumulation of error and thus, would in turn permit the interpretation of non-linear patterns of electrical activity, usually associated with the activation of higher frequencies (Kang et al., 2010; Márton et al., 2019; Völker et al., 2018).

Encoding has been indeed described as a non-linear integration associated with feedforward processing of complex moving features (Mineault et al., 2012). To achieve a complete encoding process there must be regulation imposed by feedback projections (Briggs, 2020) that have been proven to be a fundamental stage for the understanding of moving stimuli (Marquardt et al., 2020). Furthermore, temporal encoding of moving stimuli is promoted by the neuronal hierarchy that shapes its information transfer (Singer et al., 2019), and this anatomical hierarchy is linked to the weight and organization of both feedback and feedforward fibers between V1 and V5 (Markov et al., 2013). Paying especial attention to the feedback connections that rule

the activation of neuronal clusters in charge of the motion-related direction maps (Galuske et al., 2002).

Due to the highly nonlinear nature of the V1-V5 interactions, WPLI might be a more relevant and accurate metric of linear and non-linear connectivity (David et al., 2004). These non-linear dynamics imply time asymmetries and predictive relationships between signals in V1 and V5 (Stam, 2005). The WPLI results presented here, showed with this in mind, lower values in Gamma that were linked to better performance. This is nurtured by the significant differential clusters in WPLIα, especially between 100ms to 300ms of the stimulus presentation suggesting a decreased Alpha connectivity for the group V1ɣ-V5α. All together, we have a better understanding of the stimulation mechanisms and the link with motion discrimination performances in the V1ɣ-V5α condition. This stimulation condition seems to be mediated by a decreased feedback top-down communication as demonstrated via lowered phase-phase coupling plus a feeble ZPAC-V1a_{Gamma}V5p_{Alpha} (Park et al., 2016).

Furthermore, there is a preferred way in the endogenous circuits to elicit bi-focal activity according to the structural hierarchy (Tschechne and Neumann, 2014). For instance, it could be that Alpha oscillations sets up the V1-V5 path for later evoking and gating more local Gamma activity, through a selective attentional process of the characteristics from the stimuli (Fries et al., 2001; Gruber et al., 1999). This process when elicited, appears to follow precise timings because it is linked to the binding capacity of Gamma oscillations that lead to the stimulus's features processing (Foxe and Snyder, 2011; Singer, 1993). This feature encoding has been suggested to occur around the N1 visual evoked potential that correspond quite well to the timings were there is a decrease in WPLIα for group V1ɣ-V5α (Brandt and Jansen, 1991) and that matches as well with the earliest traces of feedback in apparent motion perception around ~100ms (Wibral et al., 2009).

In the end, the linear fits between the electrophysiology and the behavior permits us to hypothesize that a precise timing of the V1ɣ-V5α might lead to a significant change in the capacity of discriminating motion. This precise dosage might lead to an optimal inter-areal synchronization of Alpha waves (i.e. WPLIα), plus a precise modulation of ascending Gamma rhythms in V1 through Alpha V5 gating (i.e. ZPAC-V1a_{Gamma}V5p_{Alpha}), enabling the network to better process incoming sensory inputs. This being said, further investigation is needed in order to retrieve markers that similarly expresses the mechanisms underneath the opposite tACS condition, V1α-V5ɣ.

Cross-frequency V1-V5 tACS did not provide a strong behavioral benefit in young healthy participants

All the young healthy participants start from their best level of performance above chance and therefore, an induction of further behavioral improvement is challenging. Besides, the intervention phase is short and thus, enormous brain changes are not expected. This being said, the three groups showed a well-reported gradual improvement through practice at motion discrimination (Gibson, 1963; Sagi, 2011). However, there was no evidence for an additional significant behavioural benefit induced by one of the Verum conditions in this young healthy population.

An interpretation of this result is that both Verum stimulation regimes when applied continuously in healthy participants (i.e. during the entire visual task), although inducing the refinement of retinotopic motion-related-maps, they might also restrain them due to the duration of the stimulation (Fu et al., 2004; Philips and Chakravarthy, 2015). This hold in the maps-refinement could come from the fact that the continous Verum stimulation does not give the time for the optimal synaptic asymmetries to flourish precisely. In other words, the long-lasting electrical stimulation, constantly bumping into the V1- V5 areas, might might generate a spatial organization but it prevents it to be optimal to process information between the two areas (Gundavarapu et al., 2019).

Complementary, given that direction selectivity occurs mostly in V1 (Miikkulainen et al., 2005) and it is later nourished by pattern selectivity in V5 (Simoncelli and Heeger, 1998), these different stages of the same process highlight that there is a precise timed processing around ~130-150 ms for the ascending stimulus to travel throughout the pathway and thus, permit the correct understanding of the movement (Ahlfors et al., 1999). Hence, if the asynchronous timing from the tACS stimulation is constantly active, after a certain moment it does not permit the neuronal population to fully process motion at a latency of 5°/s and thus taking at least 100 ms to move feed-forward after arriving to V1 (Heller et al., 1995).

In the same line of thought, it is possible that the stimulation generates an overpass of the preferred transmission rate of information that is compatible with the architecture of this visual network, and its primordial to achieve Hebbian-like learning of the movement (Frégnac, 2010; Zhang et al., 1998). This saturation of the natural thresholds of firing and connection among synapses might hinder an further improvement in motion discrimination after a certain dosage of stimulation either in the feedforward and/or feedback projections (Romei, 2016; Zhang et al., 1998). Besides, given that the tACS stimulation is unlocked from the onset of the movement, it is completely unstuck from the kinetogram dynamics that conditions the information flow within the visual pathway (ffytche et al., 1995; Sack et al., 2006).

Additionally, the V1-V5 circuit has shown precise time relationships and roles for their two most relevant endogenous rhythms, α and ɣ (Klimesch et al., 2011; Michalareas et al., 2016; Rohenkohl et al., 2018). When these two rhythms are constantly exogenously modulated because of a long-lasting stimulation that lead to an atemporal non-optimal elicitation of the tACS, they might try to go back to the optimal gating process of local ɣ information ruled by its α inhibition (Fries, 2015; Klimesch et al., 2007; Richter et al., 2017; Singer and Gray, 1995). This implies that there is still room for optimization of stimulation timing and dose in order to enhance motion discrimination capacities.

In summary, the present work points towards the fact that bifocal cross-frequency tACS allows to modulate the interregional interactions between the target areas. The stimulation led to distinguishable signatures in phase-amplitude (ZPAC) and phase-phase (WPLI) coupling for both Verum groups that contributed to differentiate it from the electrophysiological effects of a Sham stimulation. The differences in connectivity between the two Verum groups suggest that the V1ɣ-V5α group might find a physiological substrate on the primordial feedback connections plus the non-linear links given the precise timings at which visual features get processed in the V1-V5

network, when compared to V1α-V5ɣ. It is of note that the induced electrophysiological changes did not translate into significant behaviroal effects in this healthy young subjects. There might be several reasons for this, ranging from pontetial ceiling effects to the quantity and timeing of the electrical stimulation in association with the respective task. Moreover, the direction of the electrical flow play fundamental roles in the efficacy of the stimulation when combined with a visual motion discrimination task (Salamanca-Giron et al., 2021). In this order of ideas, further experiments systematically varying the timing and dose of cross-frequency tACS are required to better effectively modulate motion discrimination in healthy participants.

3.5 Supplementary Materials

Power Calculation

Taking into account that we expect a small effect size (Cohen's d ~=0.3) due to the fact that our experiments are performed in healthy subjects, and by knowing that our number of participants per group was 15, the power of our statistics is around ~75%. An additional subjects wouldn't increase the power as seen in the graph below.

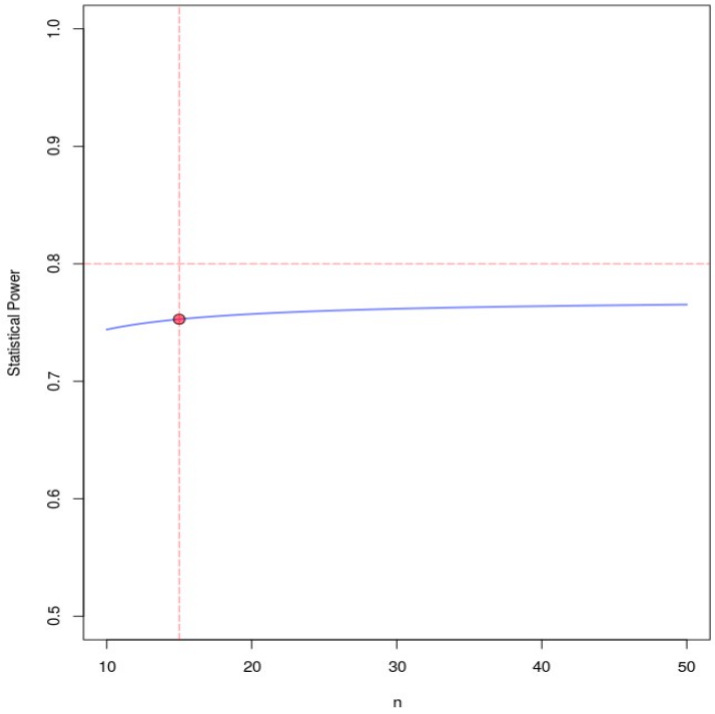

Table 1

Within Groups Comparison

V1α-V5ɣ	**b**	**p**	**CI**
Bsl - TP0	-0.1075	0.0941	-0.228 0.013
Bsl - TP10	-0.1914	0.0056	-0.318 -0.065
Bsl - TP30	-0.1537	0.0188	-0.274 -0.032
V1ɣ-V5α	**b**	**p**	**CI**
Bsl - TP0	-0.1235	0.0482	-0.240 -0.006
Bsl - TP10	-0.1687	0.0093	-0.288 -0.049

Bsl - TP30	-0.2100	0.0019	-0.332 -0.087
Sham	**b**	**p**	**CI**
Bsl - TP0	-0.0969	0.142	-0.222 0.028
Bsl - TP10	-0.0502	0.452	-0.177 0.077
Bsl - TP30	-0.0927	0.168	-0.220 0.035

Table 2

Baseline Comparison

WPLIA	**t**	**p**	**P corrected**
V1α-V5ɣ vs. V1ɣ-V5α	0.806	0.427	1.0
V1α-V5ɣ vs. Sham	1.725	0.098	0.88
V1ɣ-V5α vs. Sham	0.945	0.352	1.0
WPLIG	**t**	**p**	**P corrected**
V1α-V5ɣ vs. V1ɣ-V5α	1.475	0.160	1.0
V1α-V5ɣ vs. Sham	1.225	0.232	1.0
V1ɣ-V5α vs. Sham	-0.057	0.954	1.0
ZPAC-$V1p_{Alpha}V5a_{Gamma}$	**t**	**p**	**P corrected**
V1α-V5ɣ vs. V1ɣ-V5α	-1.243	0.224	1.0
V1α-V5ɣ vs. Sham	-2.802	0.009	0.088
V1ɣ-V5α vs. Sham	-1.812	0.08	0.725
ZPAC-$V1a_{Gamma}V5p_{Alpha}$	**t**	**p**	**P corrected**
V1α-V5ɣ vs. V1ɣ-V5α	-0.481	0.517	1.0
V1α-V5ɣ vs. Sham	0.157	0.634	1.0
V1ɣ-V5α vs. Sham	1.996	0.875	1.0

Table 3

MLM Group*EEG Interactions - Verum vs. Sham

WPLIA	**b**	**p**	**CI**
WPLIA	0.1736	0.3474	-0.182 0.523
V1α-V5ɣ vs. V1ɣ-V5α	0.3114	0.1305	-0.076 0.704
V1α-V5ɣ vs. Sham	-0.0918	0.7039	-0.549 0.371
V1ɣ-V5α vs. Sham	0.2196	0.3465	-0.222 0.672
WPLIG	**b**	**p**	**CI**
WPLIG	-0.3910	0.0037	-0.645 -0.140
V1α-V5ɣ vs. V1ɣ-V5α	0.1506	0.6755	-0.538 0.834
V1α-V5ɣ vs. Sham	0.7426	0.0039	0.262 1.228
V1ɣ-V5α vs. Sham	0.8932	0.0063	0.282 1.507
ZPAC-$\mathbf{V1p_{Alpha}V5a_{Gamma}}$	**b**	**p**	**CI**
ZPAC-$V1p_{Alpha}V5a_{Gamma}$	0.0056	0.6093	-0.015 0.026
V1α-V5ɣ vs. V1ɣ-V5α	-0.0173	0.1822	-0.042 0.007
V1α-V5ɣ vs. Sham	0.0042	0.8424	-0.036 0.044
V1ɣ-V5α vs. Sham	-0.0131	0.4987	-0.050 0.023
ZPAC-$\mathbf{V1a_{Gamma}V5p_{Alpha}}$	**b**	**p**	**CI**
ZPAC-$V1a_{Gamma}V5p_{Alpha}$	0.0174	0.2905	-0.013 0.048
V1α-V5ɣ vs. V1ɣ-V5α	0.0625	0.1188	-0.013 0.138
V1α-V5ɣ vs. Sham	0.0025	0.9334	-0.055 0.060
V1ɣ-V5α vs. Sham	0.0651	0.0589	0.0002 0.130

Table 4

MLM Group*EEG Interactions - V1α-V5ɣ vs. V1ɣ-V5α

WPLIA	**b**	**p**	**CI**
V1α-V5ɣ vs. V1ɣ-V5α	0.3387	0.0479	0.018 0.662
WPLIG	**b**	**p**	**CI**
V1α-V5ɣ vs. V1ɣ-V5α	0.0573	0.8566	-0.547 0.659
ZPAC-$V1p_{Alpha}V5a_{Gamma}$	**b**	**p**	**CI**
V1α-V5ɣ vs. V1ɣ-V5α	-0.0163	0.1394	-0.037 0.004
ZPAC-$V1a_{Gamma}V5p_{Alpha}$	**b**	**p**	**CI**
V1α-V5ɣ vs. V1ɣ-V5α	0.0657	0.0473	0.003 0.127

3.6 References

Ahlfors, S.P., Simpson, G.V., Dale, A.M., Belliveau, J.W., Liu, A.K., Korvenoja, A., Virtanen, J., Huotilainen, M., Tootell, R. b. h., Aronen, H.J., Ilmoniemi, R.J., 1999. Spatiotemporal Activity of a Cortical Network for Processing Visual Motion Revealed by MEG and fMRI. J. Neurophysiol. 82, 2545–2555. https://doi.org/10.1152/jn.1999.82.5.2545

Bastos, A.M., Usrey, W.M., Adams, R.A., Mangun, G.R., Fries, P., Friston, K.J., 2012. Canonical microcircuits for predictive coding. Neuron 76, 695–711. https://doi.org/10.1016/j.neuron.2012.10.038

Bonnefond, M., Jensen, O., 2015. Gamma Activity Coupled to Alpha Phase as a Mechanism for Top-Down Controlled Gating. PLOS ONE 10, e0128667. https://doi.org/10.1371/journal.pone.0128667

Bonnefond, M., Kastner, S., Jensen, O., 2017. Communication between Brain Areas Based on Nested Oscillations. eNeuro 4. https://doi.org/10.1523/ENEURO.0153-16.2017

Brandt, M.E., Jansen, B.H., 1991. The Relationship Between Prestimulus Alpha Amplitude and Visual Evoked Potential Amplitude. Int. J. Neurosci. 61, 261–268. https://doi.org/10.3109/00207459108990744

Briggs, F., 2020. Role of Feedback Connections in Central Visual Processing. Annu. Rev. Vis. Sci. 6, 313–334. https://doi.org/10.1146/annurev-vision-121219-081716

Carver, S., Roth, E., Cowan, N.J., Fortune, E.S., 2008. Synaptic Plasticity Can Produce and Enhance Direction Selectivity. PLoS Comput. Biol. 4. https://doi.org/10.1371/journal.pcbi.0040032

Cavanaugh, M.R., Huxlin, K.R., 2017. Visual discrimination training improves Humphrey perimetry in chronic cortically induced blindness. Neurology 88, 1856–1864. https://doi.org/10.1212/WNL.0000000000003921

Darvas, F., Miller, K.J., Rao, R.P.N., Ojemann, J.G., 2009. Nonlinear Phase–Phase Cross-Frequency Coupling Mediates Communication between Distant Sites in Human Neocortex. J. Neurosci. 29, 426–435. https://doi.org/10.1523/JNEUROSCI.3688-08.2009

David, O., Cosmelli, D., Friston, K.J., 2004. Evaluation of different measures of functional connectivity using a neural mass model. NeuroImage 21, 659–673. https://doi.org/10.1016/j.neuroimage.2003.10.006

Ferro, D., van Kempen, J., Boyd, M., Panzeri, S., Thiele, A., 2021. Directed information exchange between cortical layers in macaque V1 and V4 and its modulation by selective attention. Proc. Natl. Acad. Sci. U. S. A. 118. https://doi.org/10.1073/pnas.2022097118

ffytche, D.H., Guy, C.N., Zeki, S., 1995. The parallel visual motion inputs into areas V1 and V5 of human cerebral cortex. Brain 118, 1375–1394. https://doi.org/10.1093/brain/118.6.1375

Foxe, J.J., Snyder, A.C., 2011. The Role of Alpha-Band Brain Oscillations as a Sensory Suppression Mechanism during Selective Attention. Front. Psychol. 2. https://doi.org/10.3389/fpsyg.2011.00154

Frégnac, Y., 2010. A Re-Examination of Hebbian-Covariance Rules and Spike Timing-Dependent Plasticity in Cat Visual Cortex in vivo. Front. Synaptic Neurosci. 2. https://doi.org/10.3389/fnsyn.2010.00147

Fries, P., 2015. Rhythms For Cognition: Communication Through Coherence. Neuron 88, 220–235. https://doi.org/10.1016/j.neuron.2015.09.034

Fries, P., Reynolds, J.H., Rorie, A.E., Desimone, R., 2001. Modulation of oscillatory neuronal synchronization by selective visual attention. Science 291, 1560–1563. https://doi.org/10.1126/science.291.5508.1560

Friston, K., 2009. The free-energy principle: a rough guide to the brain? Trends Cogn. Sci. 13, 293–301. https://doi.org/10.1016/j.tics.2009.04.005

Friston, K., 2008. Hierarchical models in the brain. PLoS Comput. Biol. 4, e1000211. https://doi.org/10.1371/journal.pcbi.1000211

Fu, Y.-X., Shen, Y., Gao, H., Dan, Y., 2004. Asymmetry in Visual Cortical Circuits Underlying Motion-Induced Perceptual Mislocalization. J. Neurosci. 24, 2165–2171. https://doi.org/10.1523/JNEUROSCI.5145-03.2004

Galuske, R.A.W., Schmidt, K.E., Goebel, R., Lomber, S.G., Payne, B.R., 2002. The role of feedback in shaping neural representations in cat visual cortex. Proc. Natl. Acad. Sci. 99, 17083–17088. https://doi.org/10.1073/pnas.242399199

Gibson, E.J., 1963. Perceptual Learning. Annu. Rev. Psychol. 14, 29–56. https://doi.org/10.1146/annurev.ps.14.020163.000333

Gramfort, A., Luessi, M., Larson, E., Engemann, D.A., Strohmeier, D., Brodbeck, C., Goj, R., Jas, M., Brooks, T., Parkkonen, L., Hämäläinen, M., 2013. MEG and EEG data analysis with MNE-Python. Front. Neurosci. 7. https://doi.org/10.3389/fnins.2013.00267

Gramfort, A., Luessi, M., Larson, E., Engemann, D.A., Strohmeier, D., Brodbeck, C., Parkkonen, L., Hämäläinen, M.S., 2014. MNE software for processing MEG and EEG data. NeuroImage 86, 446–460. https://doi.org/10.1016/j.neuroimage.2013.10.027

Gray, C.M., Singer, W., 1989. Stimulus-specific neuronal oscillations in orientation columns of cat visual cortex. Proc. Natl. Acad. Sci. U. S. A. 86, 1698–1702.

Gruber, T., Müller, M.M., Keil, A., Elbert, T., 1999. Selective visual-spatial attention alters induced gamma band responses in the human EEG. Clin. Neurophysiol. 110, 2074–2085. https://doi.org/10.1016/S1388-2457(99)00176-5

Gundavarapu, A., Chakravarthy, V.S., Soman, K., 2019. A Model of Motion Processing in the Visual Cortex Using Neural Field With Asymmetric Hebbian Learning. Front. Neurosci. 13. https://doi.org/10.3389/fnins.2019.00067

Haegens, S., Händel, B.F., Jensen, O., 2011. Top-Down Controlled Alpha Band Activity in Somatosensory Areas Determines Behavioral Performance in a Discrimination Task. J. Neurosci. 31, 5197–5204. https://doi.org/10.1523/JNEUROSCI.5199-10.2011

Händel, B.F., Haarmeier, T., Jensen, O., 2011. Alpha Oscillations Correlate with the Successful Inhibition of Unattended Stimuli. J. Cogn. Neurosci. 23, 2494–2502. https://doi.org/10.1162/jocn.2010.21557

Heller, J., Hertz, J.A., Kjær, T.W., Richmond, B.J., 1995. Information flow and temporal coding in primate pattern vision. J. Comput. Neurosci. 2, 175–193. https://doi.org/10.1007/BF00961433

Hubel, D.H., Wiesel, T.N., 1969. Visual area of the lateral suprasylvian gyrus (Clare-Bishop area) of the cat. J. Physiol. 202, 251–260. https://doi.org/10.1113/jphysiol.1969.sp008808

Kang, K., Shelley, M., Henrie, J.A., Shapley, R., 2010. LFP spectral peaks in V1 cortex: network resonance and cortico-cortical feedback. J. Comput. Neurosci. 29, 495–507. https://doi.org/10.1007/s10827-009-0190-2

Kar, K., Krekelberg, B., 2014. Transcranial Alternating Current Stimulation Attenuates Visual Motion Adaptation. J. Neurosci. 34, 7334–7340. https://doi.org/10.1523/JNEUROSCI.5248-13.2014

Kasten, F.H., Dowsett, J., Herrmann, C.S., 2016. Sustained Aftereffect of α-tACS Lasts Up to 70 min after Stimulation. Front. Hum. Neurosci. 10. https://doi.org/10.3389/fnhum.2016.00245

Klimesch, W., Fellinger, R., Freunberger, R., 2011. Alpha oscillations and early stages of visual encoding. Front. Psychol. 2, 118. https://doi.org/10.3389/fpsyg.2011.00118

Klimesch, W., Sauseng, P., Hanslmayr, S., 2007. EEG alpha oscillations: the inhibition-timing hypothesis. Brain Res. Rev. 53, 63–88. https://doi.org/10.1016/j.brainresrev.2006.06.003

Lachaux, J.-P., Axmacher, N., Mormann, F., Halgren, E., Crone, N.E., 2012. High-frequency neural activity and human cognition: past, present and possible future of intracranial EEG research. Prog. Neurobiol. 98, 279–301. https://doi.org/10.1016/j.pneurobio.2012.06.008

Markov, N.T., Vezoli, J., Chameau, P., Falchier, A., Quilodran, R., Huissoud, C., Lamy, C., Misery, P., Giroud, P., Ullman, S., Barone, P., Dehay, C., Knoblauch, K., Kennedy, H., 2013. Anatomy of hierarchy: Feedforward and feedback pathways in macaque visual cortex. J. Comp. Neurol. 522, 225–259. https://doi.org/10.1002/cne.23458

Marquardt, I., De Weerd, P., Schneider, M., Gulban, O.F., Ivanov, D., Wang, Y., Uludağ, K., 2020. Feedback contribution to surface motion perception in the human early visual cortex. eLife 9, e50933. https://doi.org/10.7554/eLife.50933

Márton, C.D., Fukushima, M., Camalier, C.R., Schultz, S.R., Averbeck, B.B., 2019. Signature Patterns for Top-Down and Bottom-Up Information Processing via Cross-Frequency Coupling in Macaque Auditory Cortex. eNeuro 6. https://doi.org/10.1523/ENEURO.0467-18.2019

Michalareas, G., Vezoli, J., van Pelt, S., Schoffelen, J.-M., Kennedy, H., Fries, P., 2016. Alpha-Beta and Gamma Rhythms Subserve Feedback and Feedforward Influences among Human Visual Cortical Areas. Neuron 89, 384–397. https://doi.org/10.1016/j.neuron.2015.12.018

Miikkulainen, R., Bednar, J., Choe, Y., Sirosh, J., 2005. Computational Maps in the Visual Cortex. Comput. Maps Vis. Cortex. https://doi.org/10.1007/0-387-28806-6

Mineault, P.J., Khawaja, F.A., Butts, D.A., Pack, C.C., 2012. Hierarchical processing of complex motion along the primate dorsal visual pathway. Proc. Natl. Acad. Sci. 109, E972–E980. https://doi.org/10.1073/pnas.1115685109

Orekhova, E.V., Butorina, A.V., Sysoeva, O.V., Prokofyev, A.O., Nikolaeva, A.Yu., Stroganova, T.A., 2015. Frequency of gamma oscillations in humans is modulated by velocity of visual motion. J. Neurophysiol. 114, 244–255. https://doi.org/10.1152/jn.00232.2015

Pagnotta, M.F., Pascucci, D., Plomp, G., 2020. Nested oscillations and brain connectivity during sequential stages of feature-based attention. bioRxiv 2020.02.28.969253. https://doi.org/10.1101/2020.02.28.969253

Palva, S., Palva, J.M., 2011. Functional Roles of Alpha-Band Phase Synchronization in Local and Large-Scale Cortical Networks. Front. Psychol. 2. https://doi.org/10.3389/fpsyg.2011.00204

Park, H., Lee, D.S., Kang, E., Kang, H., Hahm, J., Kim, J.S., Chung, C.K., Jiang, H., Gross, J., Jensen, O., 2016. Formation of visual memories controlled by gamma power

phase-locked to alpha oscillations. Sci. Rep. 6, 28092. https://doi.org/10.1038/srep28092
Philips, R.T., Chakravarthy, V.S., 2015. The mapping of eccentricity and meridional angle onto orthogonal axes in the primary visual cortex: an activity-dependent developmental model. Front. Comput. Neurosci. 9. https://doi.org/10.3389/fncom.2015.00003
Ramcharitar, J.U., Tan, E.W., Fortune, E.S., 2006. Global electrosensory oscillations enhance directional responses of midbrain neurons in eigenmannia. J. Neurophysiol. 96, 2319–2326. https://doi.org/10.1152/jn.00311.2006
Rao, R.P.N., Ballard, D.H., 1999. Predictive coding in the visual cortex: a functional interpretation of some extra-classical receptive-field effects. Nat. Neurosci. 2, 79–87. https://doi.org/10.1038/4580
Richter, C.G., Thompson, W.H., Bosman, C.A., Fries, P., 2017. Top-down beta enhances bottom-up gamma. J. Neurosci. 3771–16. https://doi.org/10.1523/JNEUROSCI.3771-16.2017
Rohenkohl, G., Bosman, C.A., Fries, P., 2018. Gamma Synchronization between V1 and V4 Improves Behavioral Performance. Neuron 100, 953-963.e3. https://doi.org/10.1016/j.neuron.2018.09.019
Romei, V., 2016. Empowering Reentrant Projections from V5 to V1 Boosts Sensitivity to Motion. Curr. Biol. 26, 2155–2160.
Rust, N.C., Mante, V., Simoncelli, E.P., Movshon, J.A., 2006. How MT cells analyze the motion of visual patterns. Nat. Neurosci. 9, 1421–1431. https://doi.org/10.1038/nn1786
Sack, A.T., Kohler, A., Linden, D.E.J., Goebel, R., Muckli, L., 2006. The temporal characteristics of motion processing in hMT/V5+: Combining fMRI and neuronavigated TMS. NeuroImage 29, 1326–1335. https://doi.org/10.1016/j.neuroimage.2005.08.027
Sagi, D., 2011. Perceptual learning in Vision Research. Vision Res. 51, 1552–1566. https://doi.org/10.1016/j.visres.2010.10.019
Salamanca-Giron, R.F., Raffin, E., Zandvliet, S.B., Seeber, M., Michel, C.M., Sauseng, P., Huxlin, K.R., Hummel, F.C., 2021. Enhancing visual motion discrimination by desynchronizing bifocal oscillatory activity. NeuroImage 240, 118299. https://doi.org/10.1016/j.neuroimage.2021.118299
Shadlen, M.N., Newsome, W.T., 1996. Motion perception: seeing and deciding. Proc. Natl. Acad. Sci. 93, 628–633. https://doi.org/10.1073/pnas.93.2.628
Simoncelli, E.P., Heeger, D.J., 1998. A model of neuronal responses in visual area MT. Vision Res. 38, 743–761. https://doi.org/10.1016/s0042-6989(97)00183-1
Singer, W., 1993. Synchronization of Cortical Activity and its Putative Role in Information Processing and Learning. Annu. Rev. Physiol. 55, 349–374. https://doi.org/10.1146/annurev.ph.55.030193.002025
Singer, W., Gray, C.M., 1995. Visual feature integration and the temporal correlation hypothesis. Annu. Rev. Neurosci. 18, 555–586. https://doi.org/10.1146/annurev.ne.18.030195.003011
Sokolov, A., Lutzenberger, W., Pavlova, M., Preissl, H., Braun, C., Birbaumer, N., 1999. Gamma-band MEG activity to coherent motion depends on task-driven attention. NeuroReport 10, 1997–2000.
Stam, C.J., 2005. Nonlinear dynamical analysis of EEG and MEG: Review of an emerging field. Clin. Neurophysiol. 116, 2266–2301. https://doi.org/10.1016/j.clinph.2005.06.011

Swettenham, J.B., Muthukumaraswamy, S.D., Singh, K.D., 2009. Spectral Properties of Induced and Evoked Gamma Oscillations in Human Early Visual Cortex to Moving and Stationary Stimuli. J. Neurophysiol. 102, 1241–1253. https://doi.org/10.1152/jn.91044.2008

Tallon-Baudry, C., Bertrand, O., 1999. Oscillatory gamma activity in humans and its role in object representation. Trends Cogn. Sci. 3, 151–162. https://doi.org/10.1016/S1364-6613(99)01299-1

Thut, G., Nietzel, A., Brandt, S.A., Pascual-Leone, A., 2006. α-Band Electroencephalographic Activity over Occipital Cortex Indexes Visuospatial Attention Bias and Predicts Visual Target Detection. J. Neurosci. 26, 9494–9502. https://doi.org/10.1523/JNEUROSCI.0875-06.2006

Tschechne, S., Neumann, H., 2014. Hierarchical representation of shapes in visual cortex—from localized features to figural shape segregation. Front. Comput. Neurosci. 8. https://doi.org/10.3389/fncom.2014.00093

Völker, M., Fiederer, L.D.J., Berberich, S., Hammer, J., Behncke, J., Kršek, P., Tomášek, M., Marusič, P., Reinacher, P.C., Coenen, V.A., Helias, M., Schulze-Bonhage, A., Burgard, W., Ball, T., 2018. The dynamics of error processing in the human brain as reflected by high-gamma activity in noninvasive and intracranial EEG. NeuroImage 173, 564–579. https://doi.org/10.1016/j.neuroimage.2018.01.059

von Stein, A., Sarnthein, J., 2000. Different frequencies for different scales of cortical integration: from local gamma to long range alpha/theta synchronization. Int. J. Psychophysiol. 38, 301–313. https://doi.org/10.1016/S0167-8760(00)00172-0

Wibral, M., Bledowski, C., Kohler, A., Singer, W., Muckli, L., 2009. The Timing of Feedback to Early Visual Cortex in the Perception of Long-Range Apparent Motion. Cereb. Cortex N. Y. NY 19, 1567–1582. https://doi.org/10.1093/cercor/bhn192

Zeki, S., 2015. Area V5—a microcosm of the visual brain. Front. Integr. Neurosci. 9. https://doi.org/10.3389/fnint.2015.00021

Zeki, S., 1993. A vision of the brain, A vision of the brain. Blackwell Scientific Publications, Cambridge, MA, US.

Zeki, S., Watson, J.D., Lueck, C.J., Friston, K.J., Kennard, C., Frackowiak, R.S., 1991. A direct demonstration of functional specialization in human visual cortex. J. Neurosci. Off. J. Soc. Neurosci. 11, 641–649.

Zhang, L.I., Tao, H.W., Holt, C.E., Harris, W.A., Poo, M., 1998. A critical window for cooperation and competition among developing retinotectal synapses. Nature 395, 37–44. https://doi.org/10.1038/25665

Zhang, Yanyu, Zhang, Yifei, Cai, P., Luo, H., Fang, F., 2019. The causal role of α-oscillations in feature binding. Proc. Natl. Acad. Sci. 116, 17023–17028. https://doi.org/10.1073/pnas.1904160116

4

Bursts of bifocal α-tACS improve visual motion discrimination

Roberto F. SALAMANCA-GIRON[1,2], Martin SEEBER[3], Christoph M. MICHEL[3,6],Krystel R. HUXLIN[4], Friedhelm C. HUMMEL[1,2,5*], Estelle RAFFIN[1,2*]

1 Defitech Chair in Clinical Neuroengineering, Center for Neuroprosthetics and Brain Mind Institute, EPFL, Geneva, Switzerland.

2 Defitech Chair in Clinical Neuroengineering, Center for Neuroprosthetics and Brain Mind Institute, Clinique Romande de Readaptation (CRR), EPFL Valais, Sion, Switzerland.

3 Functional Brain Mapping Lab, Department of Fundamental Neurosciences, University of Geneva, Campus Biotech, Chemin des Mines 9, 1202 Geneva, Switzerland

4 The Flaum Eye Institute and Center for Visual Science, University of Rochester, Rochester, NY, USA

5 Clinical Neuroscience, University of Geneva Medical School, Geneva, Switzerland

6 Lemanic Biomedical Imaging Centre (CIBM), Lausanne, Geneva, Switzerland

* Co last authors

Status:

In preparation

Contributions:

R.S.G. performed the measurements, processed the experimental data, performed the analysis and calculations, drafted the manuscript and designed the figures E.R. and F.C.H. were involved in the experimental design, supervising the work and securing the funding, M.S. C.M. K.H. aided in interpreting the results. All authors discussed the results and commented on the manuscript.

4.1 Introduction

A demand for effectively targeted non-invasive brain stimulation protocols and more individualized approaches is on the raise in neuroscience research. This with the aim of tackling inter-individual variabilityreducing heterogeneity of intervention effects and thinking in terms of clinical translation, paving the way towards patient-tailored precision-medicine approaches. Reasons for the development of such novel targeted approaches is that previous concepts such as long-term brute-force stimulation through time-sustained DC/AC currents or trains of magnetic pulses reached their limitations with significant heterogeneity of response and limited interventional effect. Thus, both novel, innovative concepts of stimulation that resembleneuronal electrophysiology or that take ongoing brain activity to tailor stimulation are gaining terrain (Thut et al. 2017). For instance, considering the natural brain oscillatory activity, protocols using transcranial Alternating Current Stimulation (tACS) have been customized with event-locking procedures (e.g. (Braun et al., 2017; Chander et al., 2016; Mansouri et al., 2019, 2018)) or state-dependent setups (e.g. (Brittain et al., 2013; Ketz et al., 2018; Lustenberger et al., 2016)). Moreover, traditional ideas of applying electricity over a single path, with big electrodes (e.g., 4 cm^2) that cover several functional areas at the same time, are instead being replaced by multi-focal montages (e.g. (Saturnino et al., 2017; Salamanca et al. 2021; Plewnia et al. 2008)) that take into account several cortical nodes within a network and the physical interaction of the information signals between them (e.g. (Turi et al., 2020)).

Among these parameters, two that are easy to modify are the time that lasts the stimulation and the time point when it is applied in relation to a task or ongoing brain activity. The rationale to adjust those two parameters are based on the idea of reducing stimulation intervals and heading towards more similar timings to those from physiological brain signals and normal cognitive processes. This over passes the assumption of a static brain state supposed to last unchanged for several tens of seconds to minutes, as widely assumed before, and it takes into account a more physiological way of approaching cognitive load and whereby attention and engagement, as the mutable and switching processes that they are (Mathewson et al., 2011; Wutz et al., 2020).

Hence, some researchers have been exploring such an idea with some mixed results. For instance, Vossen and colleagues revealed that there was traceable Alpha power enhancement after-effects after 8s α-tACS bursts, while it was not the case for the 3s bursts. Besides, there was no sign of long-lasting entrainment independently of the frequency or phase configuration of stimulation used (Vossen et al., 2015). In line with these results, Struber and colleagues did not find any amplitude or phase modification after intermittent 1s α-tACS during a vigilance task (Strüber et al., 2015), where it was previously shown that a continuous 20 minutes stimulation had as a consequence an enhancement of the Alpha power for 30 minutes (Neuling et al., 2013). In a similar fashion, Braun et al. reported null results after using β-tACS time-locked to speech-task trials lasting 2s (Braun et al., 2017).

On the contrary, Castellano *et al.* showed that 5s α-tACS improved Alpha and Gamma power, Gamma Phase Locking Value and LZW complexity (i.e., a metric of repetitive

patterns in the data) during a change-of-speed visual task (Castellano et al., 2020). Similarly, in the context of evoked steady state visual responses, Fiene and colleagues demonstrated that 6-8s α-tACS modulated the amplitude of the responses depending on the phase between a flicker that is presented and its evoked activity (Fiene et al., 2020). Lastly, Zarubin and colleagues, went one step ahead and implemented an adaptive closed-loop tACS that was stimulating for a duration of 1s, discovering that this duration was modulating the ongoing Alpha activity, depending on the phase difference between the external stimulation and the endogenous rhythms (Zarubin et al., 2020).

Although these studies suggest that tACS can modulate oscillatory activity with short stimulation bursts, it is likely that the effects depend on several variables such as the frequency of stimulation, the characteristics of the task, the brain-state of the subject (i.e. resting state vs. task), etc. In the context of visual perception, earlier studies have demonstrated that alpha oscillations might be the naturally preferred method of processing dynamic, broadband visual inputs, via the implementation of a series of "echoes" of the input sequence throughout the visual pathways (Alamia and VanRullen, 2019; Hillyard et al., 1998; VanRullen and Macdonald, 2012).

This literature adds up to our previous published results showing that Anti-Phase bifocal (V1-V5) α-tACS applied continuously for ~15min has beneficial effects on motion direction discrimination when compared to an In-Phase condition (Salamanca-Giron et al., 2021). Moreover, we also found out that these phase-shifted stimulation conditions had repercussions in the cross-frequency electrophysiological coupling between V1-V5 and these connectivity traces were associated to changes in visual performance. Besides, in a follow up bifocal (V1-V5) cross-frequency tACS study (Salamanca-Giron et al., 2021a, In preparation), we sensed that in order to achieve a significant change in behavior by means of the tACS, a precise time and duration of stimulation must be respected, suggesting the implementation of an event-locked stimulation. In this order of ideas, in the current study we applied short bursts of half a second of Anti-phase versus In-Phase α-tACS, time-locked to the visual stimulus presentation.

Furthermore, most studies examined the after-effects (i.e. offline) of tACS, and not the online effects of short intermittent tACS, most probably because of the difficulties to remove the tACS-induced artifacts, entangled with the endogenous EEG signals and the difficulty to account for them in the EEG data analyses. Importantly, these phenomena mostly become explicit with long stimulation periods, things that we avoid in the present work with the short tACS bursts and that permitted the proposition of our artifact-rejection algorithm.

In sum, based on our previous results and the current literature, we hypothesize that bursts of Alpha Anti-Phase tACS will induce different immediate, "online" electrophysiological and behavioral effects compared to the In-Phase and the Sham condition leading to behavioral improvement. Precisely, we hypothesize that it the phase-shifted, event-locked stimulation between V1 and V5 might be associated with improved visual motion processing and thus, to an improved capacity of a perceiving the direction of a moving stimulus.

4.2 Methods

Study design

The experiment consisted of a single session, participants were assigned to one of two active conditions (In-Phase α-tACS or Anti-Phase α-tACS) where either sham tACS bursts or active tACS bursts were applied time-locked to the motion stimulus onset. All trials were randomized within the 300 trials composing the motion discrimination task. The active conditions applied were double-blinded, implying that the experimenter and the participant where not aware of the conditions nor the order of the trials used. Multi-channel EEG was continuously recorded during the task. All participants performed a familiarization session before starting the experiments, in order to assure a stable degree of performance in the task. Furthermore, resting state EEG activity was recorded before the task, with the aim of extracting the individualized Alpha band peak for personalized tACS.

Subjects

30 young, right-handed, subjects participated in the experiment (18 to 40 years old, 18 females). All participants were in perfect health and there were no reports of any neurological conditions that might have interfered with the task. Signed informed consent was achieved form all participant according to the ethical approval by the Swiss Ethics Committee (2017-01761) and performed under the specification of the Declaration of Helsinki.

Behavioral Task

Changes in behavior were evaluated through a visual motion discrimination and integration task, where the objective was to determine the generalized movement of a visual stimulus always placed at the bottom right (coordinates: [5, -5]) of an LCD screen (1024 x 768 Hz at 144 Hz) displaying a gray background. Trials could not be skipped, meaning that a response was always expected, and the only two possible answers for each one of them were either right or left. Every trial, at the stimulus onset and immediately after the response was given, two different beeps were played (onset: Hz, correct response: Hz, incorrect response: Hz). The circle-shaped stimulus (diameter: 5°) was composed by grouped and moving black dots (diameter: 0.06°, density: 2.6 dots/°, speed: 10°/s) lasting for 500 ms on the screen. Besides, the quantity of noise of every trial was ruled through a 3:1 design, meaning that 3 correct answers in a row, would increment in steps of 40° the quantity of noise in to the movement, whereas than a single incorrect answer, would lead to a decrease in noise at the same rate. Noise was fluctuating in a scale from 0° to 360°. A total of 300 randomized trials were performed, where half corresponded to the active condition and the other half to the Sham stimulation (Figure 1A).

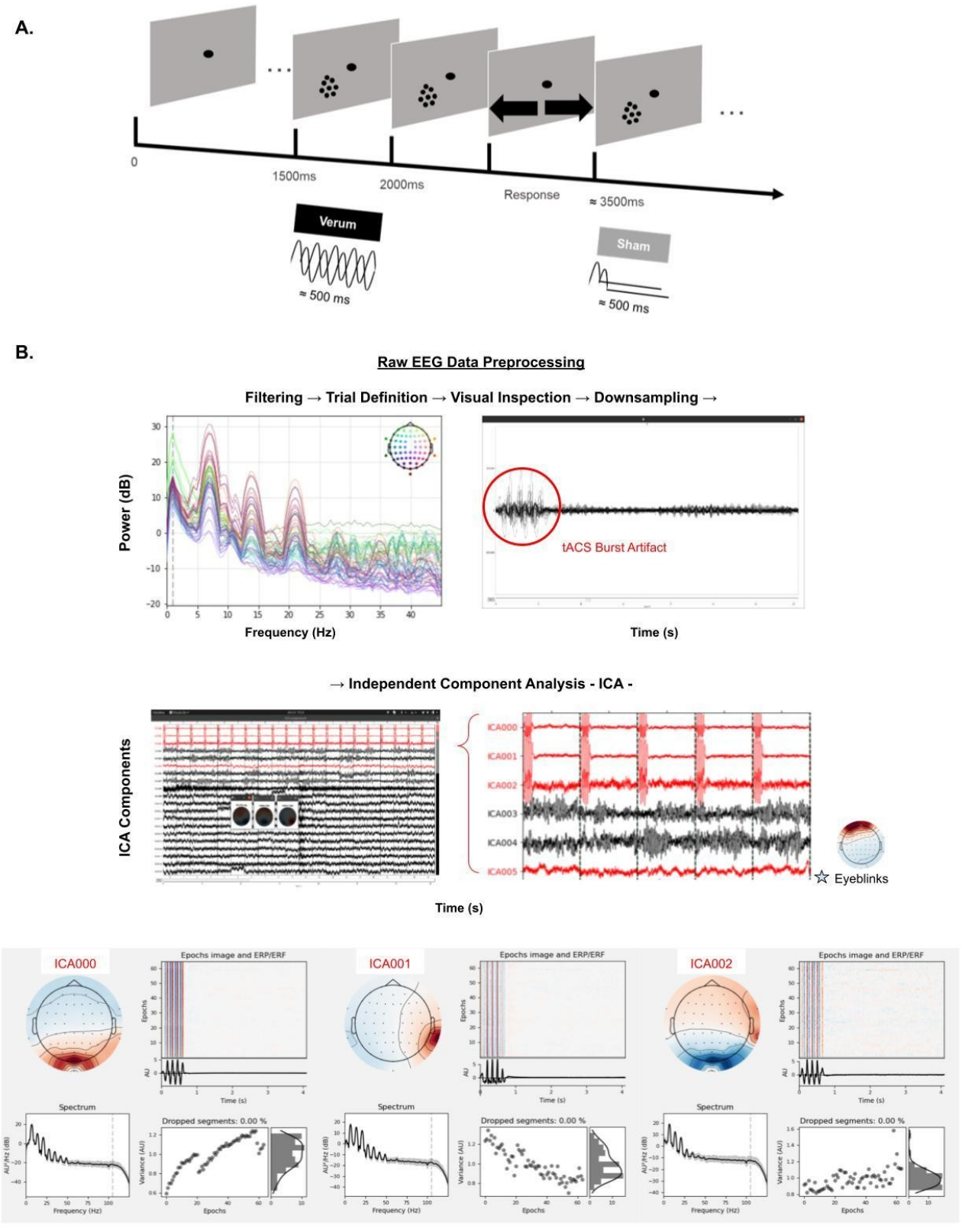

Figure 1. A. Diagram of the experimental protocol showing when the tACS/Sham bursts were triggered at the onset of the visual stimulus. The conditions were symmetrically randomized within the same session **B.** Workflow of the artifact-removal procedure (refs) implemented for every dataset during the preprocessing steps

Transcranial Electrical Stimulation

Participants were randomly assigned to one of two groups: In-Phase or Anti-Phase tACS bursts. The stimulation consisted of applying 5 cycles of individualized Alpha tACS placed over P6 and O2 (according to the 10-20 EEG system) at every randomized trial that demanded it. The stimulation was time-locked to and triggered at every visual stimulus onset and it could have either a 0° phase shift (i.e. In-Phase) or a 180° shift (Anti-Phase) between the two places of stimulation. Sham consisted on a ramp-up, ramp-down stimulation lasting the equivalent of a single cycle of the individual Alpha frequency (Figure 1A).

Device

Two Neuroconn DC Plus stimulators (Neurocare, Germany) were used to deliver the bifocal tACS. They were triggered at the same time directly from the script running the behavioral task in Matlab (Mathworks Inc., USA) and making use of Psychtoolbox. The same script was also in charge of controlling an EyeLink 1000 Plus Eye Tracking System (SR Research Ltd., Canada), assuring that participants were always looking at the center of the screen while they were seating at 60 cm and placing their head over a chin-rest. If there was a deviation of the gaze greater than 1°, the task was stopping and waiting for the eyes fixation to occur to restart the trial.

The electrodes used were concentric and customized (Diameters, Outer: 5 cm, Inner: 1.5 cm, Hole: 2.5 cm) made out of rubber, assuring a current density of 0.18 mA/cm2 at a current intensity of 3 mA. The duration of the 5 individualized-alpha depended on every person's endogenous peak.

The EEG systems used was composed of 64 active electrodes (Brain Products GMBH, Germany) sampling at 5 kHz and used inside a Faraday's cage where the computer and the stimulators were also placed.

Data Analyses

Behavior: A Weibull function was fitted to every subject's performance in order to extract the value corresponding to the 75% of accuracy. This value implied the maximum level of variation in the movement endured and it was expressed as a percentage of the higher amount of degrees that one could bear.

$$NDR(\%) = \left[\frac{360° - WeibullThreshold}{360}°\right] 100$$

EEG: All analyses were performed through customized scripts and MNE-Python routines.

The pre-processing steps consisted on referencing to the channels average, filtering between 0.5 Hz and 45 Hz, and creating 3 s epochs. Artifacts within trials and noisy channels were removed through a visual inspection process. Discarded channels were reconstructed later. The high temporal resolution data was down-sampled to 250 Hz to remove electrophysiological interference and then it was used to calculate an Independent Component Analyses (ICA).

The removal of the tACS-related artifact was performed as explained on Figure 1B. After the first basic steps of preprocessing of every individual dataset and within the ICA calculation, we looked for the components that aside from the eyeblinks, were showing a topography of concentrated electrical activity in the right parieto-occipital areas, and that had an event related potential that resemble explicitly to the tACS bursts.

In order to pass from the sensors level to the sources space, a template brain and the associated regional segmentation were taken from the MNE-Python datasets (i.e. SPM). These data was used to calculate the forward solution and inverse solutions and thus, get the signals from V1 and V5 clusters through the MNE algorithm. The dipoles used to calculate activity at the sources space were programmed orthogonal to the brain surface and a signed-flipped, Principal Component Analysis was performed to get the most representative signal from the clusters of interest.

Morlet Wavelets decomposition between 2 and 45 Hz were used to find the components in the frequency domain.

The EEG metrics used for analysis between V1 and V5 at the source space were:

- Phase Amplitude Coupling (PAC)

$$PAC(f) = n^{-1} \sum_{t=1}^{n} \left| a_t(f) \cdot e^{i\theta t} \right|$$

Where a corresponds to the amplitude of the instant t among n intervals multiplied by the imaginary component of the phase angle θ. The metric was used to remain consistent with our previous published analyses and results, intending to see a similar amplitude modulation exerted from a low frequency to a high frequency oscillation.

5 Phase Slope Index (PSI)

$$PSI(f) = I\left(\sum_{f}^{F} \left| \Phi \right|_{xy}(f) + \Phi_{xy}(f + \delta f) \right)$$

Where the slope from the Cross Spectrum Φ describes a causal and directional relationship between points x and y, over a set of frequencies F. PSI was chosen as a metric of causality that mainly depends on phase links between regions of interest and thus, could express the directional effects that might be cause by the tACS phase-shifts.

Statistical Analyses

Behavior: A Mixed Linear Model (MLM) explaining the variability from the NDR in terms of the stimulation conditions as fixed effects was calculated. Each one of the subjects were added as random effects. The model was expressed by the equation below:

$$NDR = GROUP + \left(\frac{1}{SUBJECT} \right)$$

EEG: The within-subjects significance ($p < 0.05$) from the PAC and PSI spectrum made use of a non-parametric, cluster-based corrected, permutation testing.

Behavior and EEG: Several Mixed Models were evaluated for every EEG marker computed. Thus, the NDR was evaluated in terms of not only the group of stimulation, but in terms of the interaction that each group could have with each one of the EEG metrics of interest. Besides, the random effect coming from the inter-subject variability was always kept.

$$NDR = GROUP * EEG + \left(\frac{1}{SUBJECT} \right)$$

4.3 Results

None of the 30 participant reported concurrent sensory (e.g. tactile, visual) effects induced by the stimulation. Three data sets had to be discarded because of poor performances (<75% accuracy) preventing a reliable fit of the Weibull function, hence 27 dataset were included in the analysis.

The upcoming sections describe the behavioral results for all groups and how these might be associated to specific EEG findings.

Behavioral results

Figure 2A shows the behavioral performances measured with normalized direction ration (NDR). A first Mixed Linear Model was used to evaluate the differences among the stimulation groups. In details, the difference between Anti-Phase and In-Phase was not significant (b = 3.384, p = 0.47, CI = -6.094 12.863), as well as between Anti-Phase and Sham (b = -1.975 p = 0.259 CI = -5.507 1.557). There was a trend between In-Phase and Sham (b = -3.669, p = 0.068, CI = -7.644 0.304). Furthermore, a global stimulation effect was found when the two Verum groups were grouped together as a single active condition against Sham. The MLM revealed a significant difference between Verum and Sham stimulation (b = 2.731, p = 0.040, CI = 0.128 5.334).

Online EEG data

We performed a thorough inspection of the individual data to ensure that the tACS-artifact was effectively removed. In Figure 2C, a representative example belonging to the Anti-Phase group is shown allowing to discriminate the effects of the tACS bursts on the magnitude and the phase of the Alpha band. In the left panel it is possible to appreciate the noteworthy augmentation of the Alpha magnitude accompanied by the non-mutable time shift phase-synchronization during the stimulus presentation. These two characteristics traces of the tACS Bursts are completely removed after applying the artifact-removal procedure, as it is shown in the right panel. Besides, when comparing the results from the Verum condition against to those from Sham, a similar magnitude-phase dynamics is evident for both groups, encouraging the idea that only the external-Alpha activity is removed, whereas the endogenous activity is kept.

Complementary Figure 2B, permits to disentangle at the group level how the procedure works after applying it to all the subjects and averaging the response. The absence of an immense power elicitation after the stimulus onset, plus the resemblance of the Verum evoked power (irrespective of the Verum groups) to the Sham dynamics enables to validate the procedure. Furthermore, the power profile over time corresponds to what we have previously reported in this type of visual discrimination tasks (Salamanca-Giron et al., 2021). In details the dynamics show an augmentation of the low frequencies Alpha/Low Beta right after the stimulus onset, followed by a decreased activity in this bands after ~150 ms. This is complemented by a generalized attenuation of higher Gamma frequencies (<30 Hz) when the moving stimulus appears (Siegel et al., 2007; Townsend et al., 2017)).

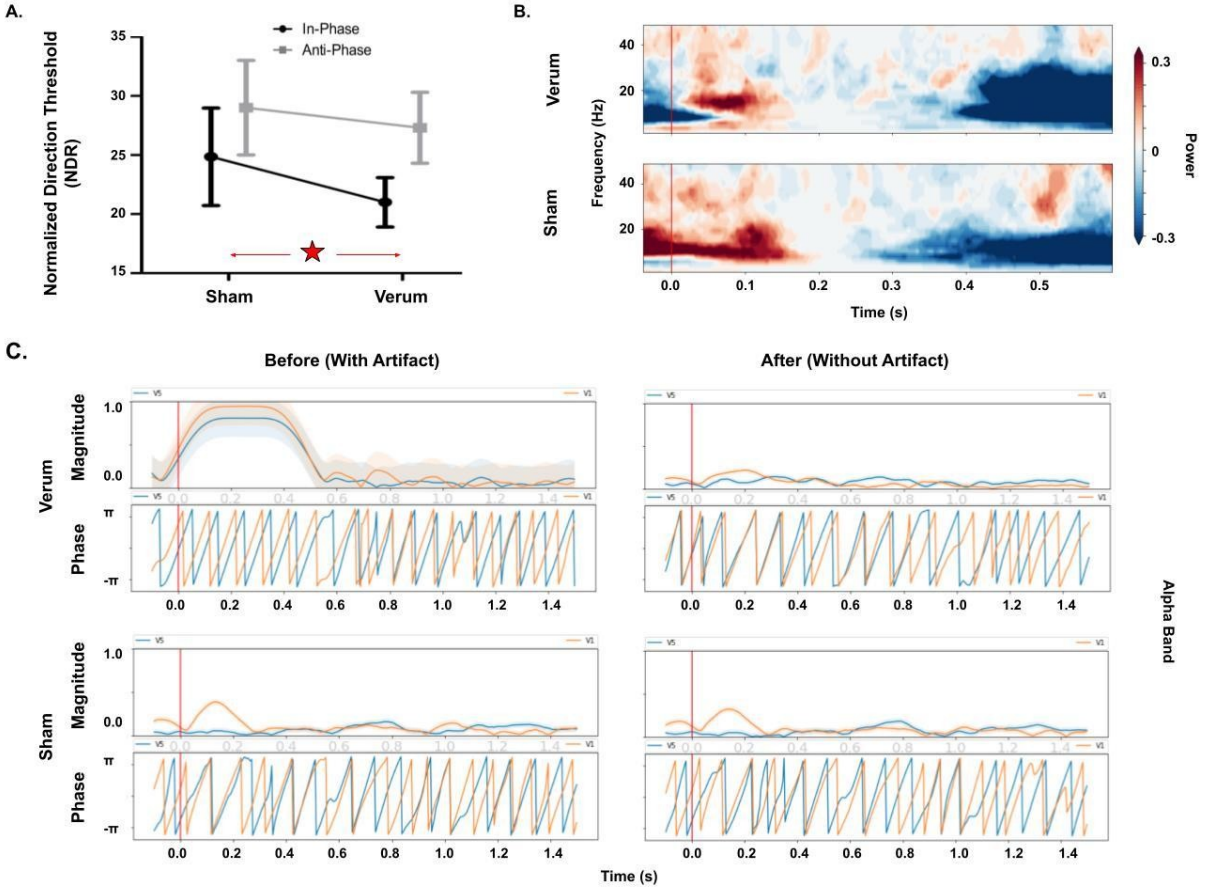

Figure 2. A. Averaged behavioral performance (i.e. NDR) for all groups discriminating between In-Phase and Anti-Phase conditions. The graphs shows the significance of the Verum groups grouped together against the Sham condition **B.** Group Time-Frequency representation of power. Stimulus onset at 0.0, represented by the red line. No traces of an augmented Alpha activity during the stimulus presentation **C.** Real example of the data in the Alpha Band with and without having applied the artifact removal method. Stimulus onset at 0.0, represented by the red line. The Verum condition is contrasted against a Sham condition to show the efficacy of the proposed method.

EEG Spectrum Differences between Verum and Sham

Because the behavioral results rather suggest a non-specific effect of bifocal stimulation where the phase relationship between the two stimulation sites does not seem to play a major role, we first merged the data from the two Verum groups together to investigate whether common EEG features could be extracted.

The Z-scored PAC (ZPAC) comodulograms depicting the difference between both Verum stimulation groups and Sham showed significant general increases in Theta-

Gamma and Alpha-Gamma coupling for the Verum condition compared to the Sham condition regardless for both orientations of the ZPAC (Figure 3A).

PSI spectrums on the other hand comparing Verum and Sham, showed causal feedforward flows between V1 and V5 within the Gamma / High-Beta, every 150 ms, intercalated with feedback flows in the same frequency bands. However, these changes are not significant between groups when corrected for multiple comparisons (Figure 3B).

Behavior differences explained by EEG between Verum and Sham

To test whether the ZPAC values extracted from the significant clusters could actually be used to explain the differences in performance (NDR) between groups, MLM were built for each direction of ZPAC. In details, for the direction ZPAC-$V1_{Phase}V5_{Amplitude}$ the model revealed that there was no significant difference in the way the ZPAC values predicted performances between Anti-Phase and Sham (b = 7.085, p = 0.118, CI = -1.027 15.300), nor between In-Phase and Sham (b = 5.384, p = 0.181, CI = -1.820 12.607), neither between Anti-Phase and In-Phase (b = 0.274, p = 0.919, CI = -5.257 5.804). In a similar manner, for the direction ZPAC-$V1_{Amplitude}V5_{Phase,}$ none of the contrasts appeared significant: Anti-Phase-Sham (b = 1.407, p = 0.760, CI = -7.010 9.863), In-Phase – Sham (b = -1.475, p = 0.715, CI = -8.894 5.918), Anti-Phase – In-Phase (b = 10.106, p = 0.798, CI = -3.844 7.179).

Given that Verum and Sham could not be dissociated using cross-frequency phase-amplitude coupling, we performed the same analysis using phase-phase coupling in using the frequency interactions found in the ZPAC comparisons. To this end, we estimated the interaction between the PSI values in the frequency bands which showed significant modulations when contrasting Verum versus Sham (i.e Theta, Alpha, Beta and Gamma) and the cofactor groups in a big MLM, to explain changes in NDR.

Thus, an ANOVA applied to the model revealed that there was a significant Group by PSI_{Gamma} interaction (F(1,6) = 11.267, p = 0.004), and a trend for significant for the interactions: Group by PSI_{Theta} and by PSI_{Gamma} (F(1,6) = 5.598, p = 0.083), Group by PSI_{Alpha} and by PSI_{Gamma} (F(1,6) = 4.736, p = 0.057) and Group by PSI_{Beta} and by PSI_{Gamma} (F(1,6) = 9.327, p = 0.064).

Therefore, we ran 4 different models taking into account each one of these interactions to see if any of them was able to help making the difference between Verum and Sham at the behavioral level.

The first MLM accounting for the Group by PSI_{Gamma}, revealed a general effect of $PSI_{Gamma,}$ explaining NDR irrespective of the group (b = 680.766, p = 0.018, CI = 157.692 1225.843, see Figure 3C). Nonetheless, the interaction Verum by PSI_{Gamma} versus Sham by PSI_{Gamma} did not reach significance (b = -645.857, p = 0.147, CI = -1511.152 191.185).

The second MLM revealed a significant triple interaction Group by PSI_{Theta} and by PSI_{Gamma} (Verum:PSI_{Theta}:PSI_{Gamma} and Sham:PSI_{Theta}:PSI_{Gamma}: b = 7.636e5, p = 0.0015, CI = 3.487e5 1.149e6, see Figure 3D). Besides, the interaction PSI_{Theta}:PSI_{Gamma} also significantly explained the changes in behavior (b = -4.587e5, p = 0.012, CI = -7.587e5 -1.415e5).

The third MLM for Group by PSI_{Alpha} and by PSI_{Gamma} and the fourth MLM, for the interaction Group by PSI_{Beta} and by PSI_{Gamma} are presented in the Supplementary Table 1, given that they not account signficantly for the variability of the NDR.

EEG Spectrum Differences between In-Phase and Anti-Phase

Next, we tried to find a mechanistic correlate that would distinguishes to the two Verum groups by contrasting their EEG signature (not confounded by different levels of performances) and examining whether these EEG markers contribute differently to performances in the two Verum groups. We first compared the ZPAC comodulograms of both Verum groups. Our results showed two significant differential clusters (Theta-Beta & Alpha-Gamma) for the ZPAC-$V1_{Phase}V5_{Amplitude}$ orientation. They, imply a higher modulation for the Anti-Phase condition. No statistical difference was found for the other ZPAC direction (Figure 4A).

In terms of PSI-causality, there were significant phasic, bottom-up clusters in the High-Beta/Low Gamma occurring every ~100ms, suggesting ascending flows between V1 and V5, complemented by frail phasic, top-down activity from V5 to V1 taking place more or less every two ascending waves. These clusters originate respectively in a phasic bottom-up activity from the Anti-Phase condition every 100 ms, contrasted with a phasic, although much weaker, top-down activity in the In-Phase condition also every 100ms. It is important to remark an important top-down at 200ms after the stimulus onset, right after the first ascending flow at 100ms (Figure 4B).

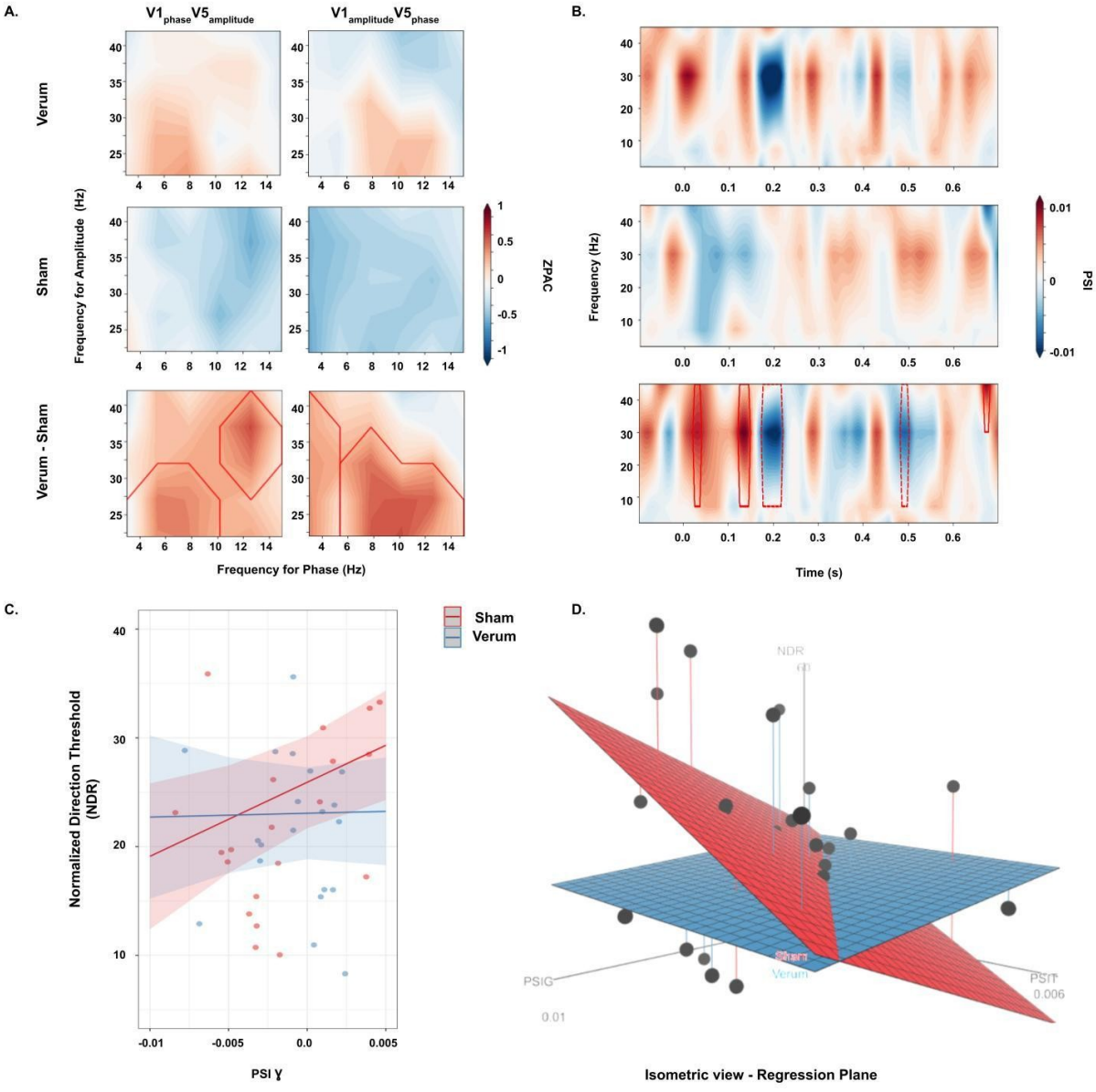

Figure 3. A. Z-scored Phase Amplitude coupling comodulograms in both directions, averaged over the period of presentation of the visual stimulus for Verum groups together against Sham. Clusters in red are significant between groups ($p<0.05$) **B.** Time-Frequency representations of the Phase-Slope Index between V1-V5 across the period of presentation of the visual stimulus for Verum, Sham and their differences. Red clusters imply a feedforward causal link, whereas blue imply feedback causal connections. Time 0.0 corresponds to the stimulus onset. Clusters in red are significant between groups ($p<0.05$) **C.** Fitted regression line of Verum and Sham groups contrasting their NDR performance against their values PSI_{Gamma} **D.** Planar 3D fit of Verum and Sham groups contrasting their NDR performance against their interaction PSI_{Theta}:PSI_{Beta}

Behavior differences explained by EEG between In-Phase and Anti-Phase

Based on the ZPAC results, we performed a first MLM using the ZPAC-$V1_{Phase}V5_{Amplitude}$ was created in order to see whether individual $ZPAC_{Theta\text{-}Beta}$ values differently contributed to performance changes between both Verum groups. It was not the case as revealed by the absence of a significant Group by ZPAC-$V1_{Phase}V5_{Amplitude}$ $\{_{Theta\text{-}Beta}\}$ interaction (b = -4.757, p = 0.353, CI = -15.161 5.647). Likewise, the second cluster corresponding to $ZPAC_{Alpha\text{-}Gamma}$ did not reveal a siginificant Group by ZPAC-$V1_{Phase}V5_{Amplitude}$ $\{_{Alpha\text{-}Gamma}\}$ (b = 1.089, p = 0.884, CI = -14.272 16.451).

Therefore, we used the PSI values with the idea that Verum conditions can be distinguished by a phase-causality relationship. Two MLM were created, testing the two significant pairs of frequency bands revealed by the ZPAC comodulograms.

The first MLM revealed that Beta PSI-causality differently explained performance changes in the two Verum groups as shown by the significant Group by PSI_{Beta} interaction (b = -2.422e3, p = 0.011, CI = -4.240e3 -604.097, and see Figure 4C). The triple interaction Group by PSI_{Theta} by PSI_{Beta} was not significant (b = 9.357e+05, p = 0.170, CI = -4.423e5 2313770.387) neither all the other comparisons (PSI_{Theta}:PSI_{Beta}: b = -7.057e5, p = 0.290, CI = -2.066e6 655436.665; Anti-Phase:PSI_{Theta} - In-Phase: PSI_{Theta}: b = 7.927e1, p = 0.979, CI = -6.188e3 6347.312).

Given the lack of significant results in the second MLM, corresponding to Group by PSI_{Alpha} by PSI_{Gamma}, the results can be found in the Supplementary Table 2.

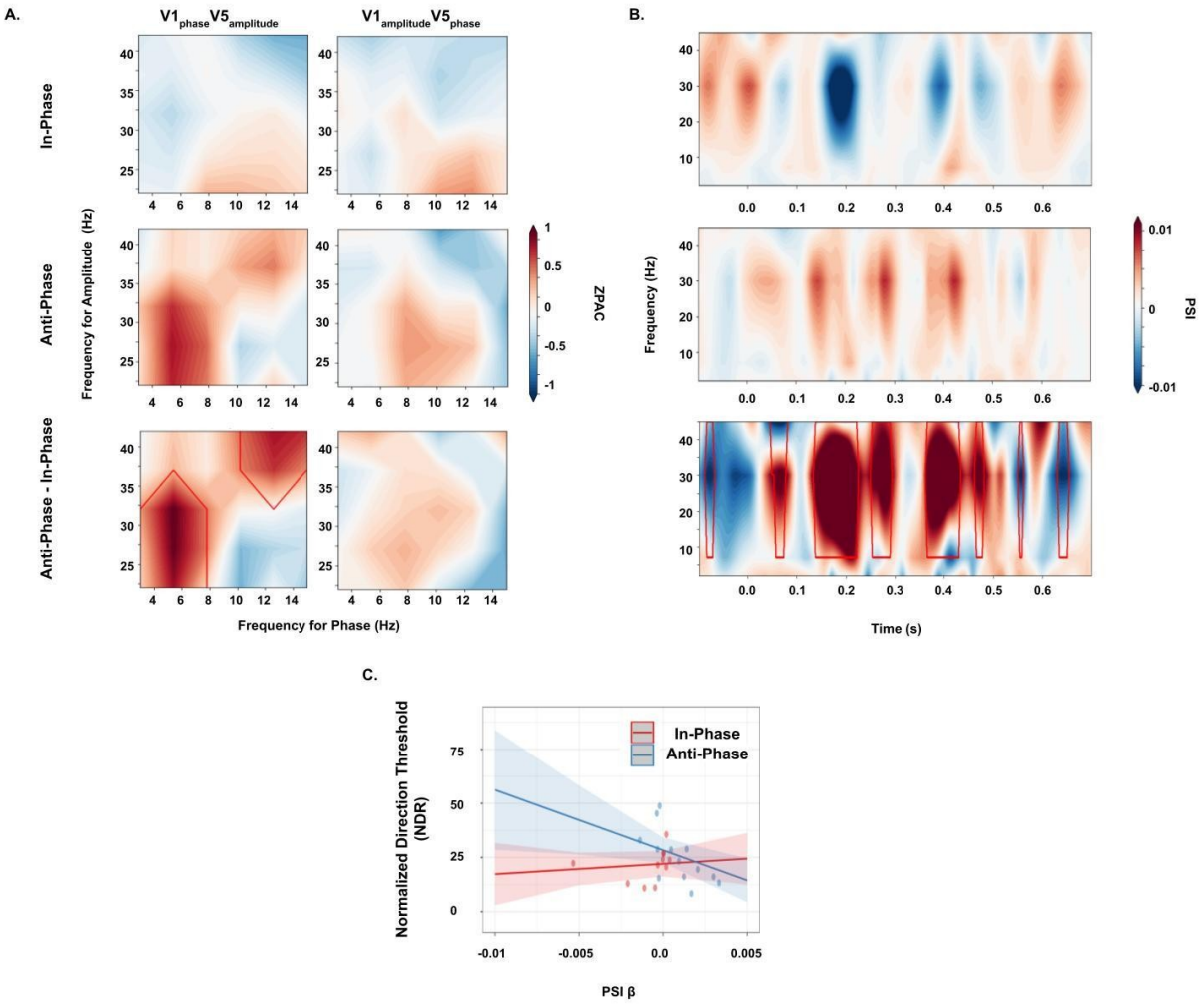

Figure 4. A. Differential Z-scored Phase Amplitude coupling comodulograms in both directions, averaged over the period of presentation of the visual stimulus contrasting Anti-Phase against In-Phase. Clusters in red are significant between groups ($p<0.05$) **B.** Time-Frequency representations of the Phase-Slope Index between V1-V5 across the period of presentation of the visual stimulus for the In-Phase, Anti-Phase and their differences. Red clusters imply a feedforward causal link, whereas blue imply feedback causal connections. Time 0.0 corresponds to the stimulus onset. Clusters in red are significant between groups ($p<0.05$) **C.** Fitted regression line of In-Phase and Anti-Phase groups contrasting their NDR performance against their values PSI_{Beta}

4.4. Discussion

In the current study we demonstrated that short bursts of bifocal V1-V5 tACS, time-locked to the presentation of a moving stimulus, improves the “online” capacity of healthy subjects to discriminate its movement compared to a Sham stimulation condition. This occurs when grouping together both phase-shifted stimulation conditions (i.e., either 0° for In-Phase or 180° for Anti-Phase). Verum conditions were associated with increased V1-V5 cross-frequency coupling. Moreover, performance changes were differently associated with changes in PSI-causal Theta-Gamma coupling compared to Sham. Additionally, our results showed a clear electro-physiological distinction between the two Verum groups. Anti-Phase tACS mostly affected bottom-up Beta inputs while In-Phase tACS mainly acted on the top-down Beta inputs, both predicting performance changes.

Bifocal α-tACS bursts enhance performance by modulating PSI-causal Theta-Gamma coupling

The few reports looking at the after-effects of short tACS bursts have not found clear electro-physiological traces of the tACS bursts (Sliva et al., 2018; Strüber et al., 2015; Vossen et al., 2015). Instead, our results show that it is possible to modulate online EEG activity and induce behavioral improvements in a motion discrimination task with two bifocal synchronized bursts of +/- 500ms. As suggested by Zarubin and colleagues (Zarubin et al., 2020), our results are not explained by neural oscillatory entrainment, given that the effect was independent of the phase-relationship between the two sites of stimulation (Vossen et al., 2015). Usually entrainment is considered as the main mechanism underlying tACS effects. It implies the synchronization of endogenous oscillations with extrinsic, rhythmic stimuli (Helfrich et al., 2014; Vieira et al., 2020). It manifests as an increase in spectral power in the stimulated frequency band (Guerra et al., 2016; Huang et al., 2021; Thut et al., 2011). In fact, entrainment, as an electromagnetic physical phenomenon, describes how an oscillator gets tuned to the period of another oscillator in the vicinity through the transfer of energy that makes them result in synchrony. This synchronization might be represented by any stable phase relationship and it depends upon the level of coupling between the oscillators. Hence, in our experimental case, the lack of entrainment could be due to the fact that in such a short period of time the V1-V5 network is not able to transition to a steady oscillatory state, with a specific phase delay between spots (Villegas et al., 2014; Ferrari et al., 2015; Hagos et al., 2019), but rather just a high external fuzzy injection of ascending and descending power that is utilized by the system as accelerated paths to transmit incoming sensory information (Wu et al., 2018).

Moreover, several studies have shown that online tACS effects cannot be mediated by an entrainment echo (Zaehle et al., 2010). Instead, one potential online mechanism might involve spike-timing dependent plasticity (STDP) in relationship with the stimulus presentation. This idea of short term STDP modulation is in line with the results from Zaehle and colleagues, where they argued that occipital individualized α-tACS was influencing STDP by resonating with different synaptic networks (Zaehle et al., 2010). Here associative plasticity might have occurred following the repeated

pairing of short Alpha bursts triggering local network dynamics, and visual cortex activation induced by the visual stimulus (Galuske et al., 2019), reinforced by the interaction between the cognitive and attentional load involved in the task and tACS effects (Feurra et al., 2013).

This concept of short-term plastic changes associated with task practice and enhanced by short α-tACS bursts, is congruent with the idea of an optimal timing for feedforward and feedback flows of information within the visual system (Bastos et al., 2015; Kafaligonul et al., 2015; Lamme et al., 1998; Michalareas et al., 2016). These information flows are evoked at precise moments in the visual system, for instance for motion discrimination, a first peak occurs at around ~100 ms when the visual signals reaches the visual cortex and this is accompanied by a trough occurring ~100ms later when the information reaches V5 (Buzzell et al., 2013; Kuba et al., 2007). This timing happens to match quite well with STDP firing rates outside the Long-Term Potention or Depression ranges, reflecting the molecular properties of postsynaptic NMDA receptors, circumscribed in frequencies of around 10 Hz (Feldman, 2012).

Accordingly, we found an online enhanced cross-frequency V1-V5 amplitude modulation (i.e. ZPAC) in Theta/Alpha – Gamma modulation after both Verum tACS conditions regardless the phase relationship between the two stimulation sites, in both directions. This reflects an increase in bottom up and top-down signal transmission (Salamanca-Giron et al., 2021). In a previous paper, we showed that continuous bifocal tACS induced opposite after-effects in cross-frequency V1-V5 amplitude modulation with a decreased bottom-up V1-Alpha phase - V5-Gamma amplitude coupling especially after Anti-Phase stimulation (Salamanca-Giron et al., 2021). This implies that there is an immediate boost of a cross-frequency inter-areal communication probably associated with the injection of individualized-alpha power in the cortical system as reported earlier (Helfrich et al., 2014; Vossen et al., 2015; Zaehle et al., 2010), followed by an offline compensatory ZPAC decrease, as a homeostatic regulatory mechanism in order to maintain the V1-V5 pathway into a specific coupling state.

Importantly, this strong increase in coupling was not linked to enhanced performance, as a matter of fact, ZPAC does not explain Sham versus Verum behavioral variability. This could simply be because of the fact that the tACS bursts duration (~500ms) was not long enough to achieve the optimal and stable amplitude modulation as mentioned before, but instead it imposes a transition state of Alpha activity that is bothersome for the pulsed-inhibition necessary for visuo-attentional control and thus, for visual processing (Mathewson et al., 2011). Specifically, the brain might receive the burst of electricity and react immediately to it, in such way that the local endogenous Gamma rhythm gets suddenly shaped by the external Alpha burst, but probably not in the range of modulation index that is ideal to convey the information (Womelsdorf and Fries, 2007). This generates a fuzzy neuronal demodulation, likely because the neuronal cluster in charge of interpreting the ciphered amplitude modulated signal gets confused by the excessive power from the spectral content (i.e. side-bands) that distorts the message that intend to be encoded in this specific type of oscillatory modulation (Abbas Elserougi et al., 2013; Li and Atlas, 2004).

This problem of a highly complex signal, hard to interpret because of the richness of its frequency composition, a constant amplitude and a polynomial phase, ultimately

leads to a poor signal to noise ratio that limits the capacity of the neuronal oscillators to function properly (Peleg and Porat, 1991). Nevertheless, these sudden changes in electrophysiology could be captured by phase-locked associations that are less sensitive to noise and more efficient to broadcast information quicker (i.e. more content per unit time) and with a fairly decent fidelity in shorter distances, when compared to amplitude modulation (Buehlmann and Deco, 2010; Eckhorn et al., 1990; Engel et al., 1999). This explains our significant effects in the phase slope index (PSI), which assess interareal directed phase synchronization. As a matter of fact, there seems to be phase-locked modulations that might contribute to an effective inter-areal communication (e.g. Theta-Gamma, Beta-Gamma) as seen in our PSI results. Importantly, phase-phase coupling in Gamma within the V1-V5 pathway seems to be influenced by the stimulation and explains improvements between Sham and Verum stimulation.

Gamma has been indeed vastly reported as the main information coder in visual processes and thus, an essential part of local synchronization and information conveying (Fries, 2009; Fries et al., 2007). Therefore, it is not surprising that activity changes in this rhythm differentiates Sham versus Verum stimulation and that it explains the visual performance enhancement induced by Verum stimulation. Moreover, it has been shown that different phases of Gamma synchronize with different clusters of neural oscillators engaged in visuo-attentional tasks, and thus, inter-areal time-lags between clusters are ruled in a deterministic manner by the elicitation of this rhythm (Vinck et al., 2013). Then improvement in motion discrimination might rely on a specific and timed gating of Gamma bursts (Barardi et al., 2014). But what is the precise temporal structure coding the Gamma bursts elicitation, optimizing information transfer within the V1-V5 pathway?

Our results suggest that the Theta-Gamma coupling might be the response to this question. As a matter of fact, there is evidence showing that the Theta oscillations seems to be a marker of visuo-attention sampling and thus, responsible of resetting local Gamma power (Bosman et al., 2012; Fries, 2015), acting like a pulsed door that opens and closes rhythmically to the high speed coding from the visual representation. Moreover, in accordance with our results, it seems that the simple augmentation of the PSI Gamma synchronization is not enough to make a difference at the behavioral level between groups, but it is rather a complex interaction between Theta-Gamma rhythms that seems to be proportional to performances. Nevertheless, a question to be further explored in upcoming studies is whether there is an inflection point that best describes the interaction between NDR and the PSI Theta-Gamma, in other words, whether there might be an inferior or superior threshold that determines behavioral improvements versus deterioration.

It is also important to highlight that the regression plane is just a predictive model that provide more information about the tendencies in a grouped behavior as a function of EEG variables. Given that the Sham group, a priori does not induce electrical modulation of the brain activity, the shown trends are not determined by the tACS influence over the EEG, but rather what would happen if endogenously an individual would demonstrate more or less magnitude of a certain marker. Nonetheless, in the case of the Verum intervention, given that there is a significant association between

the EEG markers and the tACS, we can actually make assumptions about the impact in behavior of the electrophysiology.

Considering the 3D regression plot, we could drive the following conclusions: 1. In the Sham condition an increased performance might be achieved when there is a V1→V5 increased Gamma flow plus a low Theta flow in the same direction, that read in the light of our ZPAC results, this might imply a really low value of V1 phase (Theta) - V5 amplitude (Gamma) coupling. In the opposite scenario, a V5→V1 Gamma flow with and augmented Theta connectivity imply a decreased performance and thus, a high value of ZPAC V1 amplitude (Gamma) - V5 phase (Theta) coupling. 2. In the Verum group, it seems that the stimulation generates a precise amplitude modulation index of Theta and Gamma that leads to a maximum value of reached enhancement in performance, regardless of the directions of the flow (i.e., V1→V5 or V5→V1). Fact that suggests that the room for improvement in healthy subjects has an upper threshold.

These results convey to several questions, for instance: Is there an experimental variable that would modulate the V5→V1 Gamma flow and thus the NDR, without the use of tACS (i.e. Sham condition)? Would another set of Verum parameters (e.g., phase individualization, duration of stimulation, etc.) induce a better modulation scheme between Theta and Gamma to provide even higher values of performance or is it rather a biological constraint the limited room for improvement? What would happen if the stimulation would rather be in the Gamma band?

Importantly, Theta-Gamma coupling has not only been associated to the process of visual purposeful exploration and attention (Landau et al., 2015; Landau and Fries, 2012), but it has also been associated with working memory (Colgin et al., 2009; Lisman, 2005; Lopes-dos-Santos et al., 2018; Sauseng et al., 2019; Schomburg et al., 2014; Vivekananda et al., 2021). For instance, cross-frequency Theta-Gamma tACS has been shown to successfully modulate working memory, by reactivating frontoparietal connections that boost the synchrony in the network and thus, encourage the topological interactions between spots (Alekseichuk et al., 2016; Reinhart and Nguyen, 2019). We suggest, that our bifocal Alpha-tACS bursts intervention might have as well boosted working memory through Theta and Gamma modulation, given that it functions as an important neural mechanism that might contribute to set up individual exploratory strategies to easily detect the movement within the noisy trials of the kinetogram. Moreover, given the auditory feedback provided after every trial of the task, it might also help with the learning-like associated with every repetition that permits a more efficient motion discrimination and thus, minimal plastic changes.

Besides, from a mechanistic point of view, the effects of Alpha-tACS bursts in Theta/Gamma activity might be justified in the fact that in this short period of stimulation time, the oscillations being transmitted through all the different anatomical layers between the scalp and the visual cortex lose power and thus, frequency is reduced, leaving rather a lower frequency wave to interact with the ascending Gamma signals elicited by the visual stimulation. A complementary idea could be that when the Alpha waves enter and touch the neuronal non-linear active clusters, instead of entraining the ongoing local processing, they actually pass through

a neuronal electrical mixer that ends up generating heterodyne frequencies because of the trigonometric identity it follows (Rowe, 2020(Rowe, 2020)).

The two Verum groups act on distinct top-down and bottom-up channels

The contrast between In-Phase and Anti-Phase showed significant clusters in ZPAC-$V1_{Phase}V5_{Amplitude}$ in the same frequency bands than previously reported (Salamanca-Giron et al., 2021), although these ZPAC clusters did not contribute to explain the variance of the performance in the two groups .

More interestingly, the PSI spectrums clearly show distinct direction of information flow in the two Verum groups, especially in the early stage of the stimulus processing. The results show stronger top-down inputs for the In-Phase group and stronger bottom-up inputs in the Anti-Phase group. The fitted regression lines further revealed that a strengthened V1 PSI-causing V5 Beta oscillations in the Anti-Phase condition is associated with better performances, whereas, V5-V1 top-down Beta bursts from the In-Phase condition doesn't seem to be beneficial for motion discrimination performances.

Beta oscillations have been associated with attentional top-down controller of visual information that provides contextual information (Richter et al., 2018, 2017). These top-down Beta oscillations might be reflected in the In-Phase α-tACS group, nonetheless we propose that the PSI-causal bottom-up beta enhanced by Anti-Phase α-tACS might actually trigger a different complementary mechanism. One potential explanation is the involvement of mechanisms that are not relying of the normal visual pathway as shown in V1 lesion studies, in which increased bottom-up Beta activity in response to moving stimuli occurs in the absence of V1 inputs (Aissani et al., 2014; Schmiedt et al., 2014). This might allow the interpretation of motion directly and locally in V5 a few milliseconds after the stimulus onset, as shown in the PSI spectrums. Another explanation could be that the Anti-Phase bifocal α-tACS is interpreted by the network as a Beta stimulation given the short period of time to achieve a steady Anti-Phase Alpha entrainment plus the fact that the phase-shift between the V1 and V5 signals lead to consecutive peaks and troughs, "artificially doubling" the Alpha frequency. This might generate a beneficial bottom-up activity in V5 that acts as a filtering mechanism to the non-coherent noise that crowds the kinetogram at every trial (Battaglini et al., 2020).

Ultimately, the apparition of these tACS associated PSI-causal traces in Beta, both bottom-up and top-down could be due to the fact that they are essential for the perceptual integration of incoming motion information. As a matter of fact, given that they appear in really early traces after the stimulus onset, this might be a representation of end-stopping inhibition, meaning the hindrance of the neurons preference to respond to short stimuli, that allows the processing of the global coherent movement within the stimulus (Aissani et al., 2014). Nevertheless, further experiments with other tACS configurations (e.g. monofocal Alpha/Beta tACS) could help to better understand the exact oscillatory orchestration and the the physiological origin of these oscillations.

Conclusive remarks

It is worthwhile highlightigh that the use of the In-Phase conditions responded mainly to the idea of having an active tACS control, besides of a Sham, for the Verum condition that showed the clearest behavioral effect throughout the first two studies (i.e. Anti-Phase) (Salamanca-Giron et al., 2021). The characteristics of the tACS protocol differ very much between our previous results and the current ones. It is not surprising to see different results given that the duration of the stimulation on our previous study (Salamanca-Giron et al., 2021) was ~15 sustained minutes, whereas for the current one we used bursts of ~500ms each, applied over a period of ~30 minutes (given the fact that verum trials were intermingled with sham trials), therefore it is expected to have distinct electro-physiological mechanisms elicited. Moreover, as literature has shown and we could infer from our studies, the consequences of the tACS when it is time-locked to an event, might contribute to the priming of the neural network involved (Thut et al., 2017, Zrenner et al., 2016; Neuling et al., 2013), whereas than continuous tACS signals interfere without any ordered electrical pattern to the motion perception process at every trial, leading probably to an habituated state of the visual network that augments or decreases sensitivity as seen on (Salamanca-Giron et al., 2021), depending on the timings between the areas of interest. Furthermore, on (Salamanca-Giron et al., 2021) study took mainly into account the offline effects of the stimulation at two post-evaluation time points (i.e. TP10, TP30), whereas on the current paper we focused on the online effects of the intervention.

Therefore, given that there was no significant difference between Sham, Anti-Phase nor In-Phase, but there were some shallow trends between both Verum groups against Sham, we speculated that the changes might actually correspond to the fact of having stimulation versus not having it. Plus the fact that grouping together the groups would imply increasing the number of subjects in the statistical test and thus, possibly have a stronger effect to conclude from. As highlighted in the results section, this was indeed the case when we compared Verum vs. Sham.

Based on the previously presented ideas, we hypothesize that the most likely reason why both phase-shifted tACS conditions have a similar positive but not significant effect in behavior when separated and significant when grouped together, is that they both are associated to the same causality routing mechanism between V1 and V5. Specifically, given that the short bursts do not lead to phase entrainment, what the dosed, event-locked stimulation does is to facilitate the interpretation of the moving features from the visual stimulus, through an optimized V1-V5 transmission ciphered in the weak power and frequency, inter-aerial Theta that modulates local, features-encoded Gamma waves representation directional coupling. The differences between both Verum stimulation conditions, although having similar behavioral output, might rely on the direction of these elicited Beta waves that serve as flow keepers of visual perception. Either in the top-down direction for the In-Phase condition or in the bottom-up for the Anti-Phase, but in the end leading to this end-stopping inhibition that opens up the possibility of comprehending the generalized motion.

Another important point is that it seems that there is an effect of PSI before stimulus (and stimulation) onset. These traces of activity represent either a bottom-up, V1→V5 interaction, or a top-down, V5→V1, connective flow. With this in mind, it is likely that there are prestimulus oscillations flowing between the two areas of interest as a preparation of the upcoming trial. This might be due to the activation of a beep that serves as feedback (correct vs. incorrect response) after every trial, priming the response of the upcoming one (Shams et al., 2000). As it has been shown in literature where multi-modal sensory inputs are associated with changes in electro-physiology prior to the presentation of a visual stimulus (Keil & Senkowski, 2018), and this changes in turn are also associated with accuracy of visual perception (Kaiser et al., 2019). In our case, the research question of whether this prestimulus activity serve as predictors of behavioral performance is outside the scope of the current paper as we want to evaluate the online effects of the tACS intervention, however it would be an interesting point to raise with other analyses that respond to this interesting question.

Finally, we are well aware that our electro-physiological results rest on the proposed artifact-removal method. Nonetheless, the use of phase dynamics metrics instead of changes in power for instance as the main EEG marker, provides solid grounds for comparison in this type of short bursts stimulation, since these measures are less vulnerable to tACS artifact (Kasten et al., 2018; Vossen et al., 2015). However, to validate and further develop the used ICA-based approach, a few semi-automatic procedures could be considered to ensure the homogeneity of the ICA components despite the heterogeneous cohort of individuals presenting different anatomical characteristics, and to ensure that the components always account for the same amount of variability, given the different statistical distributions of events. Nevertheless, it is reassuring to see at the individual and group level, that there is no presence of an enormous amplitude coming from the tACS. Have we removed some endogenous EEG activity by it? The response is probably yes, but in our context of defining how signal transmission was tuned by the bifocal bursts, this might not have relevantly impacted on our results as we rely on several complex EEG metrics that take into account linear and non-linear interactions.

Similar attempts support this method because they have been proven effective on other Non-Invasive Brain Stimulation techniques (Roy et al., 2014; Rogasch et al., 2017), taking into account they are not strictly comparable because of the rich frequency content of the tACS that lead to non-linearities and high-order artifacts. This complex nature of the artifact coming from the dynamic changes in impedance and the electrical properties of the machine’s circuitry have been successfully overcome with a similar attempt from Helfrich and colleagues based on Principal Component Analysis applied to longer periods of stimulation (Helfrich et al., 2014). This enables us to think that for these really short bursts, the present ICA approach makes way more sense to capture less intermingled and more separate and noticeable bursts of tACS. With this in mind, we aim to explore further ideas such as spatial filters (Jonmohamadi and Muthukumaraswamy, 2018) and machine learning (Kohli and Casson, 2020) approaches, potentially combined together for creating a better set of artifact-removal tools.

Nevertheless, despite the new questions and experimental possibilities arising, it is worth highlighting above all that the inclusion of PSI-causality analyses have permitted

to have a notion of the electrophysiological causal links between V1 and V5 and thus, their statistical association with the Verum stimulation conditions and how those actually explain the enhanced performance. This open up new possibilities to set up more bio-inspired stimulation protocols that support the pathway dynamics (i.e. bottom-up, top-down flows) in a more precise manner, with the goal of improving one’s capacities and hopefully establishing the basis of beneficial therapeutic initiatives.

4.5 Supplementary materials

Table 1

Group : PSI_{Alpha} : PSI_{Gamma}	**b**	**p**	**CI**
PSI_{Gamma}	765.746	0.014	2.257e2 1.269e3
Verum:PSI_{Alpha}:PSI_{Gamma} - Sham:PSI_{Alpha}:PSI_{Gamma}	47461.019	0.8	-2.762e5 3.956e5
PSI_{Alpha}:PSI_{Gamma}	57568.746	0.682	-2.014e5 3e5
Group : PSI_{Beta} : PSI_{Gamma}	**b**	**p**	**CI**
Bsl - TP0	757.753	0.029	1.449e2 1.337e3
Verum:PSI_{Beta}:PSI_{Gamma} - Sham:PSI_{Beta}:PSI_{Gamma}	-19353.523	0.751	-1.257e5 8.942e4
PSI_{Beta}:PSI_{Gamma}	-6406.779	0.911	-1.081e5 9.433e4

Table 2

Group : PSI_{Alpha} : PSI_{Gamma}	**b**	**p**	**CI**
Anti-Phase:PSI_{Alpha} - In-Phase: PSI_{Alpha}	-1.139e3	0.350	-2.066e6 655436.665
Anti-Phase:PSI_{Gamma} - In-Phase: PSI_{Gamma}	-5.312e1	0.966	-2.616e3 2.510e3
Anti-Phase:PSI_{Alpha}:PSI_{Gamma} - In-Phase:PSI_{Alpha}:PSI_{Gamma}	5.324e5	0.215	-3.377e5 1.402e6
PSI_{Alpha}:PSI_{Gamma}	-4.351e5	0.266	-1.231e6 3.610e5

4.6 References

Abbas Elserougi, A., Abdel-Khalik, A.S., Massoud, A., Ahmed, S., 2013. Studying the effect of over-modulation on the output voltage of three-phase single-stage grid-connected boost inverter. Alex. Eng. J. 52, 347–358. https://doi.org/10.1016/j.aej.2013.05.006

Aissani, C., Martinerie, J., Yahia-Cherif, L., Paradis, A.-L., Lorenceau, J., 2014. Beta, but Not Gamma, Band Oscillations Index Visual Form-Motion Integration. PLOS ONE 9, e95541. https://doi.org/10.1371/journal.pone.0095541

Alamia, A., VanRullen, R., 2019. Alpha oscillations and traveling waves: Signatures of predictive coding? PLOS Biol. 17, e3000487. https://doi.org/10.1371/journal.pbio.3000487

Alekseichuk, I., Turi, Z., Amador de Lara, G., Antal, A., Paulus, W., 2016. Spatial Working Memory in Humans Depends on Theta and High Gamma Synchronization in the Prefrontal Cortex. Curr. Biol. CB 26, 1513–1521. https://doi.org/10.1016/j.cub.2016.04.035

Barardi, A., Sancristóbal, B., Garcia-Ojalvo, J., 2014. Phase-Coherence Transitions and Communication in the Gamma Range between Delay-Coupled Neuronal Populations. PLOS Comput. Biol. 10, e1003723. https://doi.org/10.1371/journal.pcbi.1003723

Bastos, A.M., Vezoli, J., Bosman, C.A., Schoffelen, J.-M., Oostenveld, R., Dowdall, J.R., De Weerd, P., Kennedy, H., Fries, P., 2015. Visual areas exert feedforward and feedback influences through distinct frequency channels. Neuron 85, 390–401. https://doi.org/10.1016/j.neuron.2014.12.018

Battaglini, L., Mena, F., Ghiani, A., Casco, C., Melcher, D., Ronconi, L., 2020. The Effect of Alpha tACS on the Temporal Resolution of Visual Perception. Front. Psychol. 11. https://doi.org/10.3389/fpsyg.2020.01765

Bosman, C.A., Schoffelen, J.-M., Brunet, N., Oostenveld, R., Bastos, A.M., Womelsdorf, T., Rubehn, B., Stieglitz, T., De Weerd, P., Fries, P., 2012. Attentional stimulus selection through selective synchronization between monkey visual areas. Neuron 75, 875–888. https://doi.org/10.1016/j.neuron.2012.06.037

Braun, V., Sokoliuk, R., Hanslmayr, S., 2017. On the effectiveness of event-related beta tACS on episodic memory formation and motor cortex excitability. Brain Stimulat. 10, 910–918. https://doi.org/10.1016/j.brs.2017.04.129

Brittain, J.-S., Probert-Smith, P., Aziz, T.Z., Brown, P., 2013. Tremor Suppression by Rhythmic Transcranial Current Stimulation. Curr. Biol. 23, 436–440. https://doi.org/10.1016/j.cub.2013.01.068

Buehlmann, A., Deco, G., 2010. Optimal Information Transfer in the Cortex through Synchronization. PLOS Comput. Biol. 6, e1000934. https://doi.org/10.1371/journal.pcbi.1000934

Buzzell, G., Chubb, L., Safford, A.S., Thompson, J.C., McDonald, C.G., 2013. Speed of Human Biological Form and Motion Processing. PLOS ONE 8, e69396. https://doi.org/10.1371/journal.pone.0069396

Castellano, M., Ibañez-Soria, D., Kroupi, E., Acedo, J., Campolo, M., Soria-Frisch, A., Valls-Sole, J., Verma, A., Ruffini, G., 2020. Intermittent tACS during a visual task

impacts neural oscillations and LZW complexity. Exp. Brain Res. 238, 1411–1422. https://doi.org/10.1007/s00221-020-05820-z

Chander, B.S., Witkowski, M., Braun, C., Robinson, S.E., Born, J., Cohen, L.G., Birbaumer, N., Soekadar, S.R., 2016. tACS Phase Locking of Frontal Midline Theta Oscillations Disrupts Working Memory Performance. Front. Cell. Neurosci. 0. https://doi.org/10.3389/fncel.2016.00120

Colgin, L.L., Denninger, T., Fyhn, M., Hafting, T., Bonnevie, T., Jensen, O., Moser, M.-B., Moser, E.I., 2009. Frequency of gamma oscillations routes flow of information in the hippocampus. Nature 462, 353–357. https://doi.org/10.1038/nature08573

Eckhorn, R., Reitboeck, H.J., Arndt, M., Dicke, P., 1990. Feature Linking via Synchronization among Distributed Assemblies: Simulations of Results from Cat Visual Cortex. Neural Comput. 2, 293–307. https://doi.org/10.1162/neco.1990.2.3.293

Engel, A.K., Fries, P., König, P., Brecht, M., Singer, W., 1999. Temporal Binding, Binocular Rivalry, and Consciousness. Conscious. Cogn. 8, 128–151. https://doi.org/10.1006/ccog.1999.0389

Feldman, D.E., 2012. The spike timing dependence of plasticity. Neuron 75, 556–571. https://doi.org/10.1016/j.neuron.2012.08.001

Ferrari, F. a. S., Viana, R.L., Lopes, S.R., Stoop, R., 2015. Phase synchronization of coupled bursting neurons and the generalized Kuramoto model. Neural Netw. Off. J. Int. Neural Netw. Soc. 66, 107–118. https://doi.org/10.1016/j.neunet.2015.03.003

Feurra, M., Pasqualetti, P., Bianco, G., Santarnecchi, E., Rossi, A., Rossi, S., 2013. State-Dependent Effects of Transcranial Oscillatory Currents on the Motor System: What You Think Matters. J. Neurosci. 33, 17483–17489. https://doi.org/10.1523/JNEUROSCI.1414-13.2013

Fiene, M., Schwab, B.C., Misselhorn, J., Herrmann, C.S., Schneider, T.R., Engel, A.K., 2020. Phase-specific manipulation of rhythmic brain activity by transcranial alternating current stimulation. Brain Stimulat. 13, 1254–1262. https://doi.org/10.1016/j.brs.2020.06.008

Fries, P., 2015. Rhythms For Cognition: Communication Through Coherence. Neuron 88, 220–235. https://doi.org/10.1016/j.neuron.2015.09.034

Fries, P., 2009. Neuronal Gamma-Band Synchronization as a Fundamental Process in Cortical Computation. Annu. Rev. Neurosci. 32, 209–224. https://doi.org/10.1146/annurev.neuro.051508.135603

Fries, P., Nikolić, D., Singer, W., 2007. The gamma cycle. Trends Neurosci. 30, 309–316. https://doi.org/10.1016/j.tins.2007.05.005

Galuske, R.A.W., Munk, M.H.J., Singer, W., 2019. Relation between gamma oscillations and neuronal plasticity in the visual cortex. Proc. Natl. Acad. Sci. 116, 23317–23325. https://doi.org/10.1073/pnas.1901277116

Guerra, A., Pogosyan, A., Nowak, M., Tan, H., Ferreri, F., Di Lazzaro, V., Brown, P., 2016. Phase Dependency of the Human Primary Motor Cortex and Cholinergic Inhibition Cancelation During Beta tACS. Cereb. Cortex 26, 3977–3990. https://doi.org/10.1093/cercor/bhw245

Hagos, Z., Stankovski, T., Newman, J., Pereira, T., McClintock, P.V.E., Stefanovska, A., 2019. Synchronization transitions caused by time-varying coupling functions. Philos. Trans. R. Soc. Math. Phys. Eng. Sci. 377, 20190275. https://doi.org/10.1098/rsta.2019.0275

Helfrich, R.F., Schneider, T.R., Rach, S., Trautmann-Lengsfeld, S.A., Engel, A.K., Herrmann, C.S., 2014. Entrainment of Brain Oscillations by Transcranial Alternating Current Stimulation. Curr. Biol. 24, 333–339. https://doi.org/10.1016/j.cub.2013.12.041

Hillyard, S.A., Teder-Sälejärvi, W.A., Münte, T.F., 1998. Temporal dynamics of early perceptual processing. Curr. Opin. Neurobiol. 8, 202–210. https://doi.org/10.1016/s0959-4388(98)80141-4

Huang, W.A., Stitt, I.M., Negahbani, E., Passey, D.J., Ahn, S., Davey, M., Dannhauer, M., Doan, T.T., Hoover, A.C., Peterchev, A.V., Radtke-Schuller, S., Fröhlich, F., 2021. Transcranial alternating current stimulation entrains alpha oscillations by preferential phase synchronization of fast-spiking cortical neurons to stimulation waveform. Nat. Commun. 12, 3151. https://doi.org/10.1038/s41467-021-23021-2

Jonmohamadi, Y., Muthukumaraswamy, S.D., 2018. Multi-band component analysis for EEG artifact removal and source reconstruction with application to gamma-band activity. Biomed. Phys. Eng. Express 4, 035007. https://doi.org/10.1088/2057-1976/aab0ce

Kafaligonul, H., Breitmeyer, B.G., Öğmen, H., 2015. Feedforward and feedback processes in vision. Front. Psychol. 6. https://doi.org/10.3389/fpsyg.2015.00279

Kasten, F.H., Negahbani, E., Fröhlich, F., Herrmann, C.S., 2018. Non-linear transfer characteristics of stimulation and recording hardware account for spurious low-frequency artifacts during amplitude modulated transcranial alternating current stimulation (AM-tACS). NeuroImage 179, 134–143. https://doi.org/10.1016/j.neuroimage.2018.05.068

Ketz, N., Jones, A., Bryant, N., Clark, V.P., Pilly, P.K., 2018. Closed-loop slow-wave tACS improves sleep dependent long-term memory generalization by modulating endogenous oscillations. J. Neurosci. 0273–18. https://doi.org/10.1523/JNEUROSCI.0273-18.2018

Kohli, S., Casson, A.J., 2020. Machine learning validation of EEG+tACS artefact removal. J. Neural Eng. 17, 016034. https://doi.org/10.1088/1741-2552/ab58a3

Kohli, S., Casson, A.J., 2019. Removal of Gross Artifacts of Transcranial Alternating Current Stimulation in Simultaneous EEG Monitoring. Sensors 19, 190. https://doi.org/10.3390/s19010190

Kuba, M., Kubová, Z., Kremláček, J., Langrová, J., 2007. Motion-onset VEPs: Characteristics, methods, and diagnostic use. Vision Res. 47, 189–202. https://doi.org/10.1016/j.visres.2006.09.020

Lamme, V.A., Supèr, H., Spekreijse, H., 1998. Feedforward, horizontal, and feedback processing in the visual cortex. Curr. Opin. Neurobiol. 8, 529–535. https://doi.org/10.1016/S0959-4388(98)80042-1

Landau, A.N., Fries, P., 2012. Attention Samples Stimuli Rhythmically. Curr. Biol. 22, 1000–1004. https://doi.org/10.1016/j.cub.2012.03.054

Landau, A.N., Schreyer, H.M., van Pelt, S., Fries, P., 2015. Distributed Attention Is Implemented through Theta-Rhythmic Gamma Modulation. Curr. Biol. 25, 2332–2337. https://doi.org/10.1016/j.cub.2015.07.048

Li, Q., Atlas, L.E., 2004. Over-modulated AM-FM decomposition, in: Advanced Signal Processing Algorithms, Architectures, and Implementations XIV. Presented at the Advanced Signal Processing Algorithms, Architectures, and Implementations XIV, International Society for Optics and Photonics, pp. 172–183. https://doi.org/10.1117/12.564245

Lisman, J., 2005. The theta/gamma discrete phase code occuring during the hippocampal phase precession may be a more general brain coding scheme. Hippocampus 15, 913–922. https://doi.org/10.1002/hipo.20121

Lopes-dos-Santos, V., van de Ven, G.M., Morley, A., Trouche, S., Campo-Urriza, N., Dupret, D., 2018. Parsing Hippocampal Theta Oscillations by Nested Spectral Components during Spatial Exploration and Memory-Guided Behavior. Neuron 100, 940-952.e7. https://doi.org/10.1016/j.neuron.2018.09.031

Lustenberger, C., Boyle, M.R., Alagapan, S., Mellin, J.M., Vaughn, B.V., Fröhlich, F., 2016. Feedback-Controlled Transcranial Alternating Current Stimulation Reveals a Functional Role of Sleep Spindles in Motor Memory Consolidation. Curr. Biol. CB 26, 2127–2136. https://doi.org/10.1016/j.cub.2016.06.044

Mansouri, F., Fettes, P., Schulze, L., Giacobbe, P., Zariffa, J., Downar, J., 2018. A Real-Time Phase-Locking System for Non-invasive Brain Stimulation. Front. Neurosci. 0. https://doi.org/10.3389/fnins.2018.00877

Mansouri, F., Shanbour, A., Mazza, F., Fettes, P., Zariffa, J., Downar, J., 2019. Effect of Theta Transcranial Alternating Current Stimulation and Phase-Locked Transcranial Pulsed Current Stimulation on Learning and Cognitive Control. Front. Neurosci. 0. https://doi.org/10.3389/fnins.2019.01181

Mathewson, K.E., Lleras, A., Beck, D.M., Fabiani, M., Ro, T., Gratton, G., 2011. Pulsed Out of Awareness: EEG Alpha Oscillations Represent a Pulsed-Inhibition of Ongoing Cortical Processing. Front. Psychol. 2. https://doi.org/10.3389/fpsyg.2011.00099

Michalareas, G., Vezoli, J., van Pelt, S., Schoffelen, J.-M., Kennedy, H., Fries, P., 2016. Alpha-Beta and Gamma Rhythms Subserve Feedback and Feedforward Influences among Human Visual Cortical Areas. Neuron 89, 384–397. https://doi.org/10.1016/j.neuron.2015.12.018

Neuling, T., Rach, S., Herrmann, C.S., 2013. Orchestrating neuronal networks: sustained after-effects of transcranial alternating current stimulation depend upon brain states. Front. Hum. Neurosci. 7, 161. https://doi.org/10.3389/fnhum.2013.00161

Peleg, S., Porat, B., 1991. The Cramer-Rao lower bound for signals with constant amplitude and polynomial phase. IEEE Trans. Signal Process. 39, 749–752. https://doi.org/10.1109/78.80864

Reinhart, R.M.G., Nguyen, J.A., 2019. Working memory revived in older adults by synchronizing rhythmic brain circuits. Nat. Neurosci. 22, 820–827. https://doi.org/10.1038/s41593-019-0371-x

Richter, C.G., Coppola, R., Bressler, S.L., 2018. Top-down beta oscillatory signaling conveys behavioral context in early visual cortex. Sci. Rep. 8, 6991. https://doi.org/10.1038/s41598-018-25267-1

Richter, C.G., Thompson, W.H., Bosman, C.A., Fries, P., 2017. Top-down beta enhances bottom-up gamma. J. Neurosci. 3771–16. https://doi.org/10.1523/JNEUROSCI.3771-16.2017

Rogasch, N.C., Sullivan, C., Thomson, R.H., Rose, N.S., Bailey, N.W., Fitzgerald, P.B., Farzan, F., Hernandez-Pavon, J.C., 2017. Analysing concurrent transcranial magnetic stimulation and electroencephalographic data: A review and introduction to the open-source TESA software. NeuroImage 147, 934–951. https://doi.org/10.1016/j.neuroimage.2016.10.031

Roy, A., Baxter, B., He, B., 2014. High-definition transcranial direct current stimulation induces both acute and persistent changes in broadband cortical

synchronization: a simultaneous tDCS-EEG study. IEEE Trans. Biomed. Eng. 61, 1967–1978. https://doi.org/10.1109/TBME.2014.2311071

Salamanca-Giron, R.F., Raffin, E., Zandvliet, S.B., Seeber, M., Michel, C.M., Sauseng, P., Huxlin, K.R., Hummel, F.C., 2021. Enhancing visual motion discrimination by desynchronizing bifocal oscillatory activity. NeuroImage 240, 118299. https://doi.org/10.1016/j.neuroimage.2021.118299

Saturnino, G.B., Madsen, K.H., Siebner, H.R., Thielscher, A., 2017. How to target inter-regional phase synchronization with dual-site Transcranial Alternating Current Stimulation. NeuroImage 163, 68–80. https://doi.org/10.1016/j.neuroimage.2017.09.024

Sauseng, P., Peylo, C., Biel, A.L., Friedrich, E.V.C., Romberg-Taylor, C., 2019. Does cross-frequency phase coupling of oscillatory brain activity contribute to a better understanding of visual working memory? Br. J. Psychol. Lond. Engl. 1953 110, 245–255. https://doi.org/10.1111/bjop.12340

Schmiedt, J.T., Maier, A., Fries, P., Saunders, R.C., Leopold, D.A., Schmid, M.C., 2014. Beta Oscillation Dynamics in Extrastriate Cortex after Removal of Primary Visual Cortex. J. Neurosci. 34, 11857–11864. https://doi.org/10.1523/JNEUROSCI.0509-14.2014

Schomburg, E.W., Fernández-Ruiz, A., Mizuseki, K., Berényi, A., Anastassiou, C.A., Koch, C., Buzsáki, G., 2014. Theta phase segregation of input-specific gamma patterns in entorhinal-hippocampal networks. Neuron 84, 470–485. https://doi.org/10.1016/j.neuron.2014.08.051

Siegel, M., Donner, T.H., Oostenveld, R., Fries, P., Engel, A.K., 2007. High-Frequency Activity in Human Visual Cortex Is Modulated by Visual Motion Strength. Cereb. Cortex 17, 732–741. https://doi.org/10.1093/cercor/bhk025

Sliva, D.D., Black, C.J., Bowary, P., Agrawal, U., Santoyo, J.F., Philip, N.S., Greenberg, B.D., Moore, C.I., Jones, S.R., 2018. A Prospective Study of the Impact of Transcranial Alternating Current Stimulation on EEG Correlates of Somatosensory Perception. Front. Psychol. 9. https://doi.org/10.3389/fpsyg.2018.02117

Strüber, D., Rach, S., Neuling, T., Herrmann, C.S., 2015. On the possible role of stimulation duration for after-effects of transcranial alternating current stimulation. Front. Cell. Neurosci. 9. https://doi.org/10.3389/fncel.2015.00311

Thut, G., Schyns, P., Gross, J., 2011. Entrainment of Perceptually Relevant Brain Oscillations by Non-Invasive Rhythmic Stimulation of the Human Brain. Front. Psychol. 0. https://doi.org/10.3389/fpsyg.2011.00170

Thut, G., Bergmann, T.O., Fröhlich, F., Soekadar, S.R., Brittain, J.-S., Valero-Cabré, A., Sack, A., Miniussi, C., Antal, A., Siebner, H.R., Ziemann, U., Herrmann, C.S., 2017. Guiding transcranial brain stimulation by EEG/MEG to interact with ongoing brain activity and associated functions: A position paper. Clin. Neurophysiol. Off. J. Int. Fed. Clin. Neurophysiol. 128, 843–857. https://doi.org/10.1016/j.clinph.2017.01.003

Townsend, R.G., Solomon, S.S., Martin, P.R., Solomon, S.G., Gong, P., 2017. Visual Motion Discrimination by Propagating Patterns in Primate Cerebral Cortex. J. Neurosci. 37, 10074–10084. https://doi.org/10.1523/JNEUROSCI.1538-17.2017

Turi, Z., Mittner, M., Lehr, A., Bürger, H., Antal, A., Paulus, W., 2020. θ-γ Cross-Frequency Transcranial Alternating Current Stimulation over the Trough Impairs Cognitive Control. eneuro 7, ENEURO.0126-20.2020. https://doi.org/10.1523/ENEURO.0126-20.2020

VanRullen, R., Macdonald, J.S.P., 2012. Perceptual Echoes at 10 Hz in the Human Brain. Curr. Biol. 22, 995–999. https://doi.org/10.1016/j.cub.2012.03.050

Vieira, P.G., Krause, M.R., Pack, C.C., 2020. tACS entrains neural activity while somatosensory input is blocked. PLOS Biol. 18, e3000834. https://doi.org/10.1371/journal.pbio.3000834

Villegas, P., Moretti, P., Muñoz, M.A., 2014. Frustrated hierarchical synchronization and emergent complexity in the human connectome network. Sci. Rep. 4, 5990. https://doi.org/10.1038/srep05990

Vinck, M., Womelsdorf, T., Buffalo, E.A., Desimone, R., Fries, P., 2013. Attentional Modulation of Cell-Class-Specific Gamma-Band Synchronization in Awake Monkey Area V4. Neuron 80, 1077–1089. https://doi.org/10.1016/j.neuron.2013.08.019

Vivekananda, U., Bush, D., Bisby, J.A., Baxendale, S., Rodionov, R., Diehl, B., Chowdhury, F.A., McEvoy, A.W., Miserocchi, A., Walker, M.C., Burgess, N., 2021. Theta power and theta-gamma coupling support long-term spatial memory retrieval. Hippocampus 31, 213–220. https://doi.org/10.1002/hipo.23284

Vossen, A., Gross, J., Thut, G., 2015. Alpha Power Increase After Transcranial Alternating Current Stimulation at Alpha Frequency (α-tACS) Reflects Plastic Changes Rather Than Entrainment. Brain Stimulat. 8, 499–508. https://doi.org/10.1016/j.brs.2014.12.004

Witkowski, M., Garcia-Cossio, E., Chander, B.S., Braun, C., Birbaumer, N., Robinson, S.E., Soekadar, S.R., 2016. Mapping entrained brain oscillations during transcranial alternating current stimulation (tACS). NeuroImage, Transcranial electric stimulation (tES) and Neuroimaging 140, 89–98. https://doi.org/10.1016/j.neuroimage.2015.10.024

Womelsdorf, T., Fries, P., 2007. The role of neuronal synchronization in selective attention. Curr. Opin. Neurobiol., Cognitive neuroscience 17, 154–160. https://doi.org/10.1016/j.conb.2007.02.002

Wu, H., Kang, L., Liu, Z., Dhamala, M., 2018. Exact explosive synchronization transitions in Kuramoto oscillators with time-delayed coupling. Sci. Rep. 8, 15521. https://doi.org/10.1038/s41598-018-33845-6

Wutz, A., Zazio, A., Weisz, N., 2020. Oscillatory Bursts in Parietal Cortex Reflect Dynamic Attention between Multiple Objects and Ensembles. J. Neurosci. 40, 6927–6937. https://doi.org/10.1523/JNEUROSCI.0231-20.2020

Zaehle, T., Rach, S., Herrmann, C.S., 2010. Transcranial Alternating Current Stimulation Enhances Individual Alpha Activity in Human EEG. PLOS ONE 5, e13766. https://doi.org/10.1371/journal.pone.0013766

Zarubin, G., Gundlach, C., Nikulin, V., Villringer, A., Bogdan, M., 2020. Transient Amplitude Modulation of Alpha-Band Oscillations by Short-Time Intermittent Closed-Loop tACS. Front. Hum. Neurosci. 14. https://doi.org/10.3389/fnhum.2020.00366

6 General Discussion

6.1 Summary and discussion of results

- Main outputs, interpretations and discussion

1st Paper: We revealed that Anti-Phase (180° shift) α-tACS after-effects over V1 and V5 lead to an increased performance in a motion discrimination task, compared to an In-Phase (0° shift) condition that showed to rather impair this performance. These changes in behavior were associated with traces in Phase Amplitude coupling, expressed through the ZPAC - V1 alpha V5 gamma. Specifically, a decrease in coupling on the comodulograms of the Anti-Phase group contrasted an increased coupling for the In-Phase group, modulatory traces that were significantly associated to the changes in behavior.

An explanation of the findings might be that the time delay imposed between the two α waves in Anti-Phase resemble to the endogenous timing that normally a moving stimulus take to travel from V1 to V5. This natural delay seems to promote a gating-like mechanism that is attainable by the shift in phase from the Anti-Phase condition, and represented in the ɣ-α modulation. Instead in the In-Phase, the excessive synchronization of rhythms in the network might not allow an information flow.

Although the use of tACS was constant throughout the task, the fact of having a phase-shift between the two spots implied a periodicity that permitted different windows of action, meaning a window for motion features decomposition and a window for integration of features (Jensen and Mazaheri, 2010). This was not really considered when we first posed our hypothesis, given that we were thinking that a change in amplitude, as seen in the In-Phase condition due to constructive interference, was going to be of more relevance than a change in phase, as seen in the Anti-Phase condition.

These results led us to the questions: Could we modulate cross-frequency interactions that are associated to these behavioral changes? According to the theory of nested oscillations, optimal brain communication and sensory perception are achieved through an ordered interplay between low and high frequency oscillations (Bonnefond et al., 2017). This question was tackled in the 2nd study.

Furthermore, we wondered whether time-locking the Anti-phase stimulation to the task would be beneficial for augmenting the behavioral effects? In order to do so, we tested in the 3rd study short bursts of tACS (Georgy Zarubin et al., 2020) triggered at the stimulus onset (Thut et al., 2017a), as it has been suggested beneficial for an improved response to the tACS.

2nd Paper: Based on the electrophysiological results of the 1st Paper, we performed a similar experiment with the same experimental protocol, but we modified the stimulation parameters by taking into account the rhythms from the ZPAC modulation found previously. This meant that we contrasted two active tACS conditions: V1α-V5ɣ vs. V1ɣ-V5α, and we controlled their performance with a Sham group. However, in this case, there were no significant group differences in performance. Nonetheless, we found out that the phase-phase coupling, expressed through WPLI ɣ permitted to explain differently the performance from the verum groups against the sham. Distinct neural signatures were also found between the two verum groups, WPLI α plus the phase-amplitude coupling, expressed through ZPAC - V1 gamma V5 alpha.

We propose that the lack of significant differences in behavior among groups could be due to the continuous application of the cross-frequency tACS as a constant flow of energy, instead of modulating it according to the task needs, as we have found that occurred with the phase-amplitude coupling in our first study whose modulation was short and time-locked to the visual stimulus presentation. This would not allow the network to switch between the gating regimes essential to convey information (e.g. inhibition and disinhibition) that define precise times for feedforward and feedback flows. Nevertheless, we found that V1ɣ-V5α condition promoted the transferring and interpreting of incoming information through elicitation of feedback signalling from V5 and specific oscillatory interactions unlike the V1α-V5ɣ group. Fact that was contrary to our expectations, given that we thought that a clearer output was going to be associated to Alpha activity in more specific parts of the network (i.e. V1) and Gamma activity, most prominent and local in V5, due to its integrative properties (Zeki, 2015).

3rd Paper: We took into account the positive effects found from the 1st Paper, but in this case, we aimed at not only using a bifocal Anti-Phase and In-Phase continuous stimulation, but rather time-locked it to the stimulus onset and thus, limit the time of the stimulation to the duration of the visual stimulation. Our results revealed that the main comparison between Anti-Phase and In-Phase was no significantly different. However, regardless of the tACS phase-shift between the V1-V5 stimulation, there is a significant amelioration of performance when the two verum groups are put together and compared to a sham, although there was no significant difference between each verum group separately and sham. Besides, changes in PSI-caused ɣ flows explain the differences in behavior and when this ɣ rhythm is modulated by Θ, it is actually able to significantly differentiate the task performance associated to verum and sham. Besides, a feedforward PSI-caused β from the Anti-Phase condition establishes a mechanistic difference from the top-down PSI-caused β from the In-Phase condition.

We believe that the effects of timed verum tACS elicits beneficial changes in the V1-V5 path and these changes translate to an enhanced visual motion perception. The specific inter-areal communication that is induced by the verum conditions combined with the task is ruled by the degree of ɣ-Θ modulation. The signals' ideal framework imply a long-range Θ sampling of traveling ɣ sensory information. Besides, the PSI-caused β differences between In-phase and Anti-Phase might respond to 2 different processes: Respectively, top-down attentional β control for the In-Phase or a nourished β input from V1 to V5 to better index/filter the visual inputs. The fact that the phase-shift was not of relevance to distinguish a behavioral modulation, was contrary to our expectations based on our results from the 1st study. However, we believe that this might be associated to the fact that the duration of the presentation of the visual

stimulus (~500ms) is a really short time-window for the network to profit from the tACS inter-areal phase-shift due to the slow period and long wavelength characteristic of the Alpha band, a different case would have been if stimulation would have been in the Gamma band (Vinck et al., 2010).

Moreover, it is necessary to make the distinction between the effects of time-locking the stimulation to the task stimulus onset versus the duration of the tACS bursts stimulation. We propose that time-locking the stimulation to the task played a relevant role in defining a specific brain oscillatory alignment linked to the characteristics of the well-established task plus the controlled experimental circumstances. This defined alignment is primed by the psyco-physical design of the stimulus motion and might elicit specific precise oscillatory phenomena, such as a phase reset with every new stimulus similar to what occurs in other brain processes (Kleen et al., 2016). We hypothesize that triggering the stimulation at other moments of the task and not at the stimulus onset, would have rather disturbed the interpretation of motion, although further tests are needed in this regard.

The duration of the tACS bursts, although of importance because they might activate other quicker underlying mechanisms in the V1-V5 network different to online entrainment from a constant stimulation, it must be necessarily defined time-locked to the behavioral task or to a certain specific event from the associated electrophysiology (e.g. phase-lock) in order to be able to perceive and maximize its impact (Zrenner et al., 2016). Taken together, several open questions emerged from the present results, which have to be addressed in upcoming studies.

- Commonalities of the three studies

Merging these oscillatory results together, our studies allow us to confirm that there are mainly evoked low frequency activity (Alpha/Theta) interacting with high frequency activity (Gamma) that seem to play a fundamental role in the process of encoding and interpreting incoming sensory information in the V1-V5 pathway (Busch et al., 2009; Fries, 2005). Hence, the accurate modulation of these rhythms might lead to an improved processing of motion in healthy subjects. However, it is important to remark, that their elicitation does not necessarily mean imposing these rhythms through tACS, as it was seen in our 2nd study. Further in depth understanding of this cross-frequency interactions is needed, because it seems that the elicitation of rhythms rather respond to a nested oscillations phenomenon (Bonnefond et al., 2017).

In order to achieve so, from one side we have identified that the fluctuant power of low frequency rhythms (>13Hz) seems beneficial to set up the adequate path, probably through the modification of the neuronal firing sensitivity (Klimesch et al., 2007). This biological conditioning plus the favourable long wavelength of the low frequencies ends up promoting the inter-areal connection between V1 and V5 and thus, lead to a fluid convey of the sensory inputs (Palva and Palva, 2011). From the other side, high frequency waves (>30 Hz), are likely to encode in their phase by their quick oscillating speed, the features that compose these inputs (Park and Lee, 2007). Therefore, they ought to be transmitted and processed in the nodes of the pathway through different modulation schemes encompassed by the low inter-areal frequencies (Bonnefond et al., 2017; Köster et al., 2018).

Besides, we have shown that the direction of these modulation schemes is primordial to achieve beneficial oscillatory scenarios. As highlighted in non-human primates experiments, we found that it is not only a matter of promoting the ascension of the sensory inputs, but also how the system sends down signals that reinforce the interpretation process (Bastos et al., 2015). In fact, our results also suggest that the directions of the flows follow precise time dynamics and must be respected in order to see an accumulated behavioral improvement as it has been in other visual tasks (e.g., there is a delay of ~100ms between a top-down Beta that elicits bottom-up Gamma in a visuo-attentional task) (Richter et al., 2017). Nevertheless, these studies (Michalareas et al. 2016, van Kerkoerle et al., 2014, Bastos et al. 2015, Richter et al., 2017) do not take into account cross-frequency interactions and more complex modulation schemes, as we showed in our results, and that have been proposed as a mechanism that serves to integrate inter-areally, locally processed features in different time scales (Canolty and Knight, 2010). In this regard, our analyses on phase-amplitud coupling and phase-slope index permit to hypothesize about amplitude modulated, bi-directional, cross-frequency mechanisms that resemble electrical motifs recorded from endogenous activity and that seem to support a modulation of behavior (e.g. Theta-Gamma phase-amplitude coupled waves are associated to the behavior changes in our 3rd study), and that are also congruent with the theory of nested oscillations (Bonnefond et al., 2017).

As one conceptual framework, traveling waves seem to be the phenomenon that might describe the induced feedforward and feedback inter-areal electrical flow of activations among nodes of the network (Muller et al., 2018), suggesting the elicitation of waves that carry information throughout different locations of the cortex and that might serve as predictors of the local behavior in lower biological scales (Alamia and VanRullen, 2019).

As a matter of fact, these traveling waves have been shown to accurately describe the hierarchical organization and timed electrical activity in the visual cortex (Alamia and VanRullen, 2019; Klimesch et al., 2007), especially suggested as the framework through which incoming moving stimuli travel from V1 to V5 demonstrating a specific oscillatory time-dynamics in the cortex (Townsend et al., 2017), influencing the inhibition and disinhibition time patterns that are endogenous to visual perception (Heitmann and Ermentrout, 2020). Therefore, further analyses should be directed towards this idea.

As a limiting factor for the analysis of these traveling waves and in general, any other online analysis of the tACS effects, is the lack of a tACS artifact removal method in order to have a more detailed idea of the online/concurrent effects from the stimulation and its signatures. Despite the fact that there have been several efforts in the community to set up a golden standard to get rid of the tACS traces that are evident in the EEG, there is still a case-by-case evaluation required because the characteristics of the artifacts highly depend on the parameters of the experimental protocol. Nevertheless, for our specific application, several ideas have been encountered in literature that might be worth exploring, for example Signal Space projection (Uusitalo and Ilmoniemi, 1997), Spatial filtering (Blankertz et al., 2008; Ille et al., 2002) or machine learning algorithms (Kohli and Casson, 2019).

From a behavioral point of view, first it is worth mentioning that the chosen sham tACS stimulation seemed to work for the 3 studies, given that the individual reports of participants after the experiments reassured us that it was not possible to make a clear distinction between a verum and sham condition from a sensation point of view (e.g., phosphenes, skin disturbances). Besides, the distribution of performance scores for all experiments did not capture any clustered behavior that could represent a bias between conditions in the measurements. Second, the blinding procedure was optimal, given that the person analyzing and conducting the experiments did not introduce any personal preference or bias in the results and as a clear example of this, some of our original hypothesis were discarded, given that our results showed a different trend compared to our initial ideas.

Third, the condition that seems to have clearer positive effects among all studies is Anti-Phase stimulation. Surprisingly, when applied time-locked to the behavioral task, the effects were not as clear as expected, even though we thought it was going to maximize the behavioral effects. Nonetheless, a bifocal Alpha tACS between V1 and V5 seem to effectively differentiate from a sham intervention. These results lead to two ideas: From one side, it might be that when applying a continuous tACS, in order to have a pronounced and significant effect against sham on behavior, a personalization of the phase-shift is needed. From the other side, this idea would also be interesting to apply it to the short bursts intervention in order to determine whether phase-shifts in the alpha band matter in such a short period of time. More importantly, it would be important to test if the frequency of these time-locked bursts might actually play a role.

Additionally, we could intuitively say that as a lesson learned from our 2nd study, although we might have found precise electrophysiological correlates associated to a modulation of a behavioral output on our 1st experiment, this does not imply that stimulating with the frequencies from those oscillatory correlates will produce an augmented improvement in behavior. It might be that in order to ahieve a significant behavioral output from a cross-frequency bifocal tACS, a strict tracing of the time of presentation of the visual stimulus must be kept, leading to the idea ot time-locked stimulation (Thut et al., 2017), as we implemented on our 3rd study. Another complementary idea might be that locally placed cross-frequency stimulation (one tACS electrode over V1 and another over V5, with two different frequencies) is not enough to achieve a significant change in performance because it must take into account also the inter-areal communication. This means that it might be necessary to implement cross-frequency modulated stimulation schemes (Alpha-Gamma amplitude modulated tACS), that could mimick in a more natural way the oscillatory patterns found on EEG analyses and associated to an improved behavioral score (Kasten et al., 2018). Advances in this regard are now being proposed in literature (Negahbani et al., 2018, Witkowski et al., 2016).

As a last point worth mentioning regarding behavior is that the increment of the sample size, would in principle not augment the effects of the experiments (See supplementary materials from chapter 3), Therefore, in order to maximize the behavioral effects, it would be interesting to test other parameters of stimulation as suggested above, but also other metrics that evaluate changes in the same behavior, trying to better handle the inter-individual variability in the task performance.

- tACS mechanism influencing brain activity

In this line, tACS was used with the underlying expectation of promoting, boosting or accelerating plastic changes that might have been triggered due to the psychophysical design of the task (Antal and Paulus, 2012). Even though the mechanisms through which tACS act might relate to one or a combination of physical phenomena (e.g., entrainment, stochastic resonance, etc.), what we can take for granted from our results is that the duration and moment of activation of the tACS, the location of the stimulation (i.e. placement of the electrodes over V1-V5) over spots of interest, the electrical field generated, among other stimulation variables we adjusted were indeed associated with functional changes of the brain. Nevertheless, we are fully aware that these functional findings have been also influenced by cognitive-associated components (e.g. perceptual learning, environmental context, etc.) as well as by the task-dependent effects that definitely play a role in the process of mastering a skill.

tACS has been proposed to act under the principle of regulating the neural firing of population of neurons (Schutter and Hortensius, 2011), given that these neurons might act as coupled oscillators that synchronize to stronger physical phenomena (Roelfsema et al., 1997), such as the fluctuating electrical field from the tACS. Due to the oscillatory output from the stimulation, it has been shown that there are moments of augmented or diminished sensitivity that have led to the idea that this type of intervention might entrain the neural firing (Krause et al., 2019). At the same time, depending on the variables that are measured, an additional mechanism has been proposed, stochastic resonance (Lefebvre et al., 2017), implying that the frequency of oscillations that is applied non-invasively might help augmenting the energy of neural clusters that are physically tuned (natural oscillatory frequency) to that specific rhythm and thus, their electrical firing might maximize. Nonetheless, independently of the mechanisms behind the stimulation, it has been proven that tACS influences neural systems and it might rely on the correct setup of its characteristics to achieve a beneficial behavioral output.

For our first two studies where a sustained ~15 minutes bifocal tACS was applied, we propose that a combination of both mechanisms takes place, given that we stimulate for a long period of time permitting to the neuronal clusters that act as coupled oscillators to synchonize completely to the pattern of the tACS, and moreover, this occurs in a smooth and efficient manner, given that the natural resonant frequency of the brain network is maximized due to the fact that we have previously set up the stimulation to the individualized frequency peaks in each frequency band of interest. For our third study, we rather suggest that due to the short period of time of the stimulation, entrainment might not be achieved, but a strong and transient resonance might trigger an optimal activation of the brain spots of interest through a quick cascade of electrophysiological events.

From the present results emerges the open question, whether a mono-focal alpha α-tACS as a common denominator of the studies might be able to achieve comparable behavioral effects as the behavioural results showing that continuous α-tACS in Anti-Phase improves performance (compared to In-Phase) and V1α-V5ɣ has a positive

tendency to achieve the same. Though that Anti-Phase and In-Phase α-tACS achived differential effects in study 1 speaks rather against this hypothesis. Comparing this idea to current results in literature, we find that from an electrophysiological point of view, occipital α-tACS indeed entrains endogenous activity in an eyes-open resting condition (Ruhnau et al., 2016), it also has been proven to induce phosphenes in dark spaces (Kanai et al., 2008) and as an after-effect it decreases brain blood oxygenation in parieto-occipital areas (Alekseichuk et al., 2016), but would occipital α-tACS have a consequence at the behavioural level?

Results are not encouraging because it has been shown that occipital α-tACS leads to blindness due to the lack of attention (i.e. inattentional blindness), suggesting that it impairs visual perception (Hutchinson et al., 2020). In support of this and closer to our experiments, it has been suggested that occipital α-tACS also affect negatively the spread of Gamma waves, which in turn ends up hindering visual detection and associated to an increase in Alpha-Gamma Phase-amplitude coupling (Herring et al., 2019). Further examples of parietal α-tACS, show rather poor results in the visual domain, for instance, it seems not to affect visuospatial attention (Coldea et al., 2021; Schuhmann et al., 2019), gabor detection (Brignani et al., 2013) and it inconsistently modulates visual integration accuracy (Ronconi et al., 2020). In sum, monofocal α-tACS in the view of the published scientific articles, does not seem to be an appropriate alternative to explain the beneficial effects in motion discrimination described here.

In the light of this, if all our connectivity markers and literature (e.g. (Fries, 2009)) show that a modulation of Gamma rhythms is fundamental for having a beneficial electrophysiological effect, what about stimulating mono-focally with ɣ-tACS? Motion perception has been modulated when stimulating with ɣ-tACS over the entire (i.e. bilateral) occipital cortex (Helfrich et al., 2014a) and additionally, it helps covert-attention in a discrimination task when placed over V1 (Laczó et al., 2012). These control conditions might help make a more detailed distinction between the effects induced by the bifocal V1-V5 phase-shifts or the cross-frequency interactions. Besides, if that is the case for continuous stimulation, would the effect be higher if we rather apply it in a pulsed manner, phase-locked to the stimulus onset? Supporting these monofocal propositions and our views in a phase-locked stimulation, a phase-dependent, occipital, α-tACS example from Helfrich and colleagues was able to modulate visual perception in an oddball paradigm (Helfrich et al., 2014b).

Another additional point to consider would be the inclusion of further hubs of stimulation in the motion perception pathway, in order to control in a more precise manner the electrophysiological communication and by it, the interpretation of an incoming stimulus, given that vision has been shown to be a distributed system (Corbetta, 1998).

- Behavioral task specificity

The selection of this motion and integration discrimination task was made a priori given its widespread use and validation in neuro-ophtalmology research (Das et al., 2014; Huxlin et al., 2009), with the main idea of enhancing a really precise sensory function that might translate to different daily life activities. Modifying the task by

adding some extra experimental variables to take into account (e.g. increased cognitive load, attentional control, etc.) could be an attractive idea but would definitely respond to other research questions and therefore, the tACS would have been necessarily characterized differently.

We set the “orchestration” of oscillatory activity by characterizing this exact type of motion discrimination task. For instance, we chose carefully the location of the ring electrodes, the synchronization pattern between tACS spots, the time of stimulations and the frequencies used so we could elicit a response that would be close to the electro-physiological effects triggered by the task. Are these effects translatable to other type of visual functions? A priori, we would not see the same behavioral effects because they are highly correlated to the experimental motion-related task and design. However, we know from literature that motion processing in the brain might contribute to the correct performance of other visual functions (e.g. (Goodale and Milner, 1992; Markov et al., 2013; Ungerleider and Mishkin, 1979)), so it is worth considering further testing to prove such a statement. In summary, it has been addressed in upcoming studies whether the present interventional strategy, such as anti-phase a-tACS to V1 and V5 will also impact on other visual function for which the interplay between these areas play a relevant role.

- Relevance of this research in a clinical context

As a last point to take into account is that given that all the protocols were applied to healthy participants with no neurological diseases or impairments, the expected effects of our protocols are rather moderate to small because the room for improvement is quite limited, as it has been shown also in other domains and interventional approaches (Zimmerman et al., 2013). Nonetheless, the brain has been deranged due to a lesion, age-related degeneration, accidents, etc. there might be bigger potential opportunities to see significant behavioral changes (McGough and Faraone, 2009). Therefore, as explained in the future directions section, protocols in patients might help validating several of our concepts.

As suggested on our published review (Raffin et al., 2020) we believe that the combination of tACS over V1 and V5, given the fundamental roles of these areas in motion perception as detailed in the introduction, and the psycho-physics behind the behavioral task, might constitute an optimal experimental framework to achieve an enhancement in the capacity of discriminating motion in visually impaired patients (Huxlin et al., 2009). We highlight the use of tACS because we hypothesize that it could modulate the inter-areal connectivity between regions through the reactivation of perilesional tissue surrounding an injury and thus, facilitate the convey of visual information due to the resonant energy that is enhanced (Herpich et al., 2019). This induced electrical field from the tACS might accelerate beneficial changes that assure a good behavioral output, being the departing point of plastic events that are assimilated by the neural system and that eventually might become permanent (Antal and Paulus, 2013). These plastic events might serve to tackle visual challenges in real life, given that the may translate in a quicker and perhaps most pronounced elongation of the healthy visual field of visually impaired patients that in the end, provides them the possibility of regaining more independence in daily life.

6.2 Conclusions

In the present thesis, I have addressed the question whether visual motion processing and underlying electrophysiological mechanisms can be influenced by physiology-inspired, orchestrated application of non-invasive electrical oscillatory stimulation applied to two key areas of the motion perception network by means of tACS. As alpha and gamma oscillatory activity plays a key role in visual processing, tACS was focused on this frequency ranges within the three projects.

The projects within the thesis provided presented first evidence that such an approach can modulate visual processing leading to an improvement of e.g., motion perception in healthy young, however it also pointed out different challenges of this concept and the complexity of underlying mechanisms as discussed above, which will have to be addressed in upcoming studies based on the present findings.

The key conclusions of my thesis can be summarized as follows:

1) Multifocal physiology-inspired orchestrated tACS applied to key areas of the motion perception network, i.e. V1 and V5, has the potential of modulation visual motion perception behavior.

2) The effects of the stimulation in regard of underlying electrophysiological parameters are complex representing the nature of the visual perception network with feedforward and feedback interregional interactions within this network.

3) Bilateral orchestrated cross-frequency tACS of V1 and V5 did not lead to clear behavioral results though cross-frequency interactions has been demonstrated to implement visual motion perception. Reasons for this are potentially manyfold ranging from the stimulation parameters, the way of stimulation (state-independent) or the topographic resolution. These points have to be addressed in upcoming studies.

4) A first approach of applying bifocal orchestrated tACS in an event-related fashion only during the course of the motion perception discrimination phase did not lead to clear behavioral improvement as I would have expected.

5) To enhance the effects of the stimulation approach several factors might have to be considered in upcoming studies, personalization to account for interindividual differences, state-dependent application in relation to the ongoing neuronal activity, individual localization of the key areas to be stimulated.

In the following last section I will provide a brief outlook on future directions and developments to be made based on the current findings.

6.3 Outlook and future developments

The present work within the thesis has added to the understanding of how motion perception in the human visual system might be implemented, how we think the information is conveyed and interpreted in the V1-V5 pathway in the view of results of equivalent pathways in animals and how it might be modulated by non-invasive brain stimulation by means of tACS. Although the behavioral effects are rather small here, probably due ceiling effects, limited room for improvement in healthy subjects, plus the known fact of inter-subject variability, we might have provided a set of relevant ideas (e.g. several spots of stimulation, time-locked stimulation, event-triggering stimulation, etc.) that could be extrapolated to other sensory pathways. As explained in the first part of this thesis, the visual system can be considered as a model system that can be used to have a better generalized overview of other sensory processing pathways. Moreover, changing the target population by, for instance, including more homogenous cohorts of elderly adults, could lead to different effect sizes.

A point to take into account with the translation to other brain pathways is the preponderance of certain plastic mechanisms, different cell types and cyto-architecture, types of skills to learn, body cortical representation, reorganization after damage, among other factors. In general terms, the concept of having either anatomical or functional changes that respond to contextual changes, such as learning of a new skill or adaptation after a lesion, is a globally accepted and proven idea that applies throughout all brain sensory systems. Differences might exist for instance, given the inter-individual variability coming from genetics, malleability and specialization properties of every brain area or environmental exposure to different triggers. Nevertheless, further information, research and scientific discussion is needed in order to widen the topic.

As a step beyond the current protocols one would consider state-dependent stimulation protocols (Zrenner et al., 2016) and thus, even closed-loop paradigms (Georgy Zarubin et al., 2020) that take into account the essential variables such as frequency and event-locked case-scenarios, its duration, the rhythms applied, the location where they are applied, the order in which they are applied and the interactions between them (e.g. modulation). All this in the end with the goal of creating an physiology-inspired orchestration that leads idealy to real life behavioral changes. As an example of this, it has been shown in experimental contexts that the stimulation should be tailored to the brain-state of the subject stimulated, not only to counterbalance the inter-individual variability, but also in order to precisely activate/deactivate the neural clusters of interest that control behaviour (Neuling et al., 2013b; Silvanto et al., 2008).

Besides, novel ideas permit the inclusion of both the electrophysiological traces and the behavioral records at the same time, with the ultimate goal of having a holistic and well-informed management of the brain inner and outer activity (Bergmann et al., 2016; Zrenner et al., 2016). In fact, latest suggestions in literature, get closer to the proposals in this thesis and they actually advice to define these brain-states through oscillatory signatures that could mark the dynamics of a brain network and that eventually will lead to an adaptable system that regulates brain activity automatically (Karabanov et al., 2016; Thut et al., 2017b). As an example of these oscillatory adaptable stimulation protocols, Zarubin and company reported that they were able to

modulate transiently (~500ms) the endogenous Alpha oscillations in the occipital cortex by means of a tACS bursts closed-loop setup (Georgy Zarubin et al., 2020).

Despite all the results widely presented across all chapters, several new inquiries and possibilities to address in the future have appeared to expand our knowledge, and towards the idea of implementing an orchestrated stimulation of the motion discrimination network.

A point to take into account would be to leverage the Resting State data that we have consistently acquired throughout all the experiments. These datasets might carry valuable information that could help enlightening the preparatory phases of the brain before being engaged in a visual task, as some sort of predictor of activity (Allaman et al., 2020; Manuel et al., 2018), or they could be used as a reflection of modulatory electrophysiological changes linked to the behavioral evaluation (Webster and Ro, 2020).

Ultimately, this research ought to be circumscribed in the medical context of visual restoration. Therefore, our proofs of concept with brain stimulation help providing therapeutic ideas for patients suffering from visual loss as it has been already done and suggested in clinical literature (Herpich et al., 2019; Sabel et al., 2019). For instance, in patients suffering of homonymous hemianopia, meaning that they have lost a portion (usually a hemi-field) of their visual field due to a cortical impairment, common approaches only tackle compensatory mechanisms such as prisms or lens (Saionz et al., 2021). Nevertheless, the motion discrimination task we extensively used has actually been designed for expanding the healthy visual field of those legally blind patients. This is possible through the activation of the residual retinotopic connections in the border between the healthy visual field and the scotoma due to the psychophysical characteristics of the kinetogram (Cavanaugh and Huxlin, 2017).

Therefore, all the scientific results and discoveries we acquired, have a direct implication in tackling the rehabilitation of patients (Raffin et al., 2020) and hence, our efforts should be always directed to acquiring and refining our knowledge to translate it into a clinical setting. As a matter of fact, we have already started a clinical protocol where a total of 10 visually impaired stroke patients (e.g. hemianopia) have been recruited to make part of it. The clinical protocol is composed of 10 training consecutive sessions combining tACS and the same motion discrimination task we used with healthy participants. Patients' testimonies in the protocol so far encourage us to keep moving forward pursuing these endeavours. We expect results of this clinical trial and hints about the potential of orchestrated multifocal tACS to enhance residual visual functions and recovery in patients suffering from visual field defects after a stroke.

Ultimately, the current thesis presents the first steps towards the idea of an accurate orchestration of oscillatory brain activity that might modulate motion perception. The parameters tested between V1 and V5, meaning phase-shifts, cross-frequency and time-locked stimulation, constitute essential characteristics that further experiments must take into account in order to achieve a modulation of behavior. Besides, the use of these bifocal configurations have precise underlying electrophysiological mechanisms that provide information that could be leveraged towards more precise interventions and protocols.

References (Introduction & General Discussion)

Adelson, E.H., Movshon, J.A., 1982. Phenomenal coherence of moving visual patterns. Nature 300, 523–525. https://doi.org/10.1038/300523a0

Afgoustidis, A., 2015. Orientation Maps in V1 and Non-Euclidean Geometry. J. Math. Neurosci. 5, 12. https://doi.org/10.1186/s13408-015-0024-7

Ajina, S., Bridge, H., 2018a. Blindsight relies on a functional connection between hMT+ and the lateral geniculate nucleus, not the pulvinar. PLOS Biol. 16, e2005769. https://doi.org/10.1371/journal.pbio.2005769

Ajina, S., Bridge, H., 2018b. Subcortical pathways to extrastriate visual cortex underlie residual vision following bilateral damage to V1. Neuropsychologia. https://doi.org/10.1016/j.neuropsychologia.2018.01.007

Ajina, S., Kennard, C., Rees, G., Bridge, H., 2015a. Motion area V5/MT+ response to global motion in the absence of V1 resembles early visual cortex. Brain 138, 164–178. https://doi.org/10.1093/brain/awu328

Ajina, S., Pestilli, F., Rokem, A., Kennard, C., Bridge, H., 2015b. Human blindsight is mediated by an intact geniculo-extrastriate pathway. eLife 4, e08935. https://doi.org/10.7554/eLife.08935

Akao, T., Kurkin, S.A., Fukushima, J., Fukushima, K., 2005. Visual and vergence eye movement-related responses of pursuit neurons in the caudal frontal eye fields to motion-in-depth stimuli. Exp. Brain Res. 164, 92–108. https://doi.org/10.1007/s00221-004-2213-6

Alamia, A., VanRullen, R., 2019. Alpha oscillations and traveling waves: Signatures of predictive coding? PLOS Biol. 17, e3000487. https://doi.org/10.1371/journal.pbio.3000487

Albright, T.D., Stoner, G.R., 1995. Visual motion perception. Proc. Natl. Acad. Sci. U. S. A. 92, 2433–2440.

Alekseichuk, I., Diers, K., Paulus, W., Antal, A., 2016. Transcranial electrical stimulation of the occipital cortex during visual perception modifies the magnitude of BOLD activity: A combined tES-fMRI approach. NeuroImage 140, 110–117. https://doi.org/10.1016/j.neuroimage.2015.11.034

Allaman, L., Mottaz, A., Kleinschmidt, A., Guggisberg, A.G., 2020. Spontaneous Network Coupling Enables Efficient Task Performance without Local Task-Induced Activations. J. Neurosci. 40, 9663–9675. https://doi.org/10.1523/JNEUROSCI.1166-20.2020

Allman, J., Miezin, F., McGuinness, E., 1985. Stimulus specific responses from beyond the classical receptive field: neurophysiological mechanisms for local-global comparisons in visual neurons. Annu. Rev. Neurosci. 8, 407–430. https://doi.org/10.1146/annurev.ne.08.030185.002203

Andersen, R.A., 1997. Neural Mechanisms of Visual Motion Perception in Primates. Neuron 18, 865–872. https://doi.org/10.1016/S0896-6273(00)80326-8

Antal, A., Alekseichuk, I., Bikson, M., Brockmöller, J., Brunoni, A.R., Chen, R., Cohen, L.G., Dowthwaite, G., Ellrich, J., Flöel, A., Fregni, F., George, M.S., Hamilton, R., Haueisen, J., Herrmann, C.S., Hummel, F.C., Lefaucheur, J.P., Liebetanz, D., Loo, C.K., McCaig, C.D., Miniussi, C., Miranda, P.C., Moliadze, V., Nitsche, M.A., Nowak, R., Padberg, F., Pascual-Leone, A., Poppendieck, W., Priori, A., Rossi, S., Rossini, P.M., Rothwell, J., Rueger, M.A., Ruffini, G., Schellhorn, K., Siebner, H.R.,

Ugawa, Y., Wexler, A., Ziemann, U., Hallett, M., Paulus, W., 2017. Low intensity transcranial electric stimulation: Safety, ethical, legal regulatory and application guidelines. Clin. Neurophysiol. Off. J. Int. Fed. Clin. Neurophysiol. 128, 1774–1809. https://doi.org/10.1016/j.clinph.2017.06.001

Antal, A., Paulus, W., 2013. Transcranial alternating current stimulation (tACS) [WWW Document]. URL https://www.ncbi.nlm.nih.gov/pmc/articles/PMC3695369/ (accessed 9.20.17).

Azouz, R., Gray, C.M., 2000. Dynamic spike threshold reveals a mechanism for synaptic coincidence detection in cortical neurons in vivo. Proc. Natl. Acad. Sci. U. S. A. 97, 8110–8115. https://doi.org/10.1073/pnas.130200797

Barban, F., Buccelli, S., Mantini, D., Chiappalone, M., Semprini, M., 2019. Removal of tACS artefact: a simulation study for algorithm comparison, in: 2019 9th International IEEE/EMBS Conference on Neural Engineering (NER). Presented at the 2019 9th International IEEE/EMBS Conference on Neural Engineering (NER), pp. 393–396. https://doi.org/10.1109/NER.2019.8717102

Bastos, A.M., Vezoli, J., Bosman, C.A., Schoffelen, J.-M., Oostenveld, R., Dowdall, J.R., De Weerd, P., Kennedy, H., Fries, P., 2015. Visual areas exert feedforward and feedback influences through distinct frequency channels. Neuron 85, 390–401. https://doi.org/10.1016/j.neuron.2014.12.018

Beckers, G., Zeki, S., 1995. The consequences of inactivating areas V1 and V5 on visual motion perception. Brain J. Neurol. 118 (Pt 1), 49–60. https://doi.org/10.1093/brain/118.1.49

Bender, M., Romei, V., Sauseng, P., 2019. Slow Theta tACS of the Right Parietal Cortex Enhances Contralateral Visual Working Memory Capacity. Brain Topogr. 32, 477–481. https://doi.org/10.1007/s10548-019-00702-2

Bergmann, T.O., Karabanov, A., Hartwigsen, G., Thielscher, A., Siebner, H.R., 2016. Combining non-invasive transcranial brain stimulation with neuroimaging and electrophysiology: Current approaches and future perspectives. NeuroImage 140, 4–19. https://doi.org/10.1016/j.neuroimage.2016.02.012

Bergmann, T.O., Groppa, S., Seeger, M., Mölle, M., Marshall, L., Siebner, H.R., 2009. Acute changes in motor cortical excitability during slow oscillatory and constant anodal transcranial direct current stimulation. J. Neurophysiol. 102, 2303–2311. https://doi.org/10.1152/jn.00437.2009

Blankertz, B., Tomioka, R., Lemm, S., Kawanabe, M., Muller, K., 2008. Optimizing Spatial filters for Robust EEG Single-Trial Analysis. IEEE Signal Process. Mag. 25, 41–56. https://doi.org/10.1109/MSP.2008.4408441

Bola, M., Gall, C., Moewes, C., Fedorov, A., Hinrichs, H., Sabel, B.A., 2014. Brain functional connectivity network breakdown and restoration in blindness. Neurology 83, 542–551. https://doi.org/10.1212/WNL.0000000000000672

Bonnefond, M., Kastner, S., Jensen, O., 2017. Communication between Brain Areas Based on Nested Oscillations. eNeuro 4. https://doi.org/10.1523/ENEURO.0153-16.2017

Braddick, O.J., O'Brien, J.M.D., Wattam-Bell, J., Atkinson, J., Hartley, T., Turner, R., 2001. Brain Areas Sensitive to Coherent Visual Motion. Perception 30, 61–72. https://doi.org/10.1068/p3048

Brignani, D., Ruzzoli, M., Mauri, P., Miniussi, C., 2013. Is Transcranial Alternating Current Stimulation Effective in Modulating Brain Oscillations? PLOS ONE 8, e56589. https://doi.org/10.1371/journal.pone.0056589

Bruns, A., Eckhorn, R., 2004. Task-related coupling from high- to low-frequency signals among visual cortical areas in human subdural recordings. Int. J. Psychophysiol. 51, 97–116. https://doi.org/10.1016/j.ijpsycho.2003.07.001

Bullier, J., Nowak, L.G., 1995. Parallel versus serial processing: new vistas on the distributed organization of the visual system. Curr. Opin. Neurobiol. 5, 497–503. https://doi.org/10.1016/0959-4388(95)80011-5

Burke, W., Cole, A.M., 1978. Extraretinal influences on the lateral geniculate nucleus. Rev. Physiol. Biochem. Pharmacol. 80, 105–166. https://doi.org/10.1007/3540084665_3

Busch, N.A., Dubois, J., VanRullen, R., 2009. The Phase of Ongoing EEG Oscillations Predicts Visual Perception. J. Neurosci. 29, 7869–7876. https://doi.org/10.1523/JNEUROSCI.0113-09.2009

Buzsáki, G., Draguhn, A., 2004. Neuronal oscillations in cortical networks. Science 304, 1926–1929. https://doi.org/10.1126/science.1099745

Cabral-Calderin, Y., Wilke, M., 2019. Probing the Link Between Perception and Oscillations: Lessons from Transcranial Alternating Current Stimulation. The Neuroscientist 107385841982864. https://doi.org/10.1177/1073858419828646

Canolty, R.T., Edwards, E., Dalal, S.S., Soltani, M., Nagarajan, S.S., Kirsch, H.E., Berger, M.S., Barbaro, N.M., Knight, R.T., 2006. High gamma power is phase-locked to theta oscillations in human neocortex. Science 313, 1626–1628. https://doi.org/10.1126/science.1128115

Casagrande, V., Yazar, F., Jones, K., Ding, Y., 2007. The Morphology of the Koniocellular Axon Pathway in the Macaque Monkey. Cereb. Cortex 17, 2334–2345. https://doi.org/10.1093/cercor/bhl142

Cavanaugh, M.R., Huxlin, K.R., 2017. Visual discrimination training improves Humphrey perimetry in chronic cortically induced blindness. Neurology 88, 1856–1864. https://doi.org/10.1212/WNL.0000000000003921

Childers, D.G., Perry, N.W., 1971. Alpha-like activity in vision. Brain Res. 25, 1–20. https://doi.org/10.1016/0006-8993(71)90563-4

Chrobok, L., Palus-Chramiec, K., Jeczmien-Lazur, J.S., Blasiak, T., Lewandowski, M.H., 2018. Gamma and infra-slow oscillations shape neuronal firing in the rat subcortical visual system. J. Physiol. 596, 2229–2250. https://doi.org/10.1113/JP275563

Coldea, A., Morand, S., Veniero, D., Harvey, M., Thut, G., 2021. Parietal alpha tACS shows inconsistent effects on visuospatial attention. PloS One 16, e0255424. https://doi.org/10.1371/journal.pone.0255424

Cowey, A., 1964. Projection of the retina on to striate and prestriate cortex in the squirrel monkey, saimiri sciureus. J. Neurophysiol. 27, 366–393. https://doi.org/10.1152/jn.1964.27.3.366

Das, A., Tadin, D., Huxlin, K.R., 2014. Beyond blindsight: properties of visual relearning in cortically blind fields. J. Neurosci. Off. J. Soc. Neurosci. 34, 11652–11664. https://doi.org/10.1523/JNEUROSCI.1076-14.2014

De Koninck, B.P., Guay, S., Blais, H., De Beaumont, L., 2021. Parametric study of transcranial alternating current stimulation for brain alpha power modulation. Brain Commun. 3. https://doi.org/10.1093/braincomms/fcab010

Demiralp, T., Bayraktaroglu, Z., Lenz, D., Junge, S., Busch, N.A., Maess, B., Ergen, M., Herrmann, C.S., 2007. Gamma amplitudes are coupled to theta phase in human EEG during visual perception. Int. J. Psychophysiol., Brain Oscillations:Cutting Edges 64, 24–30. https://doi.org/10.1016/j.ijpsycho.2006.07.005

Deperrois, N., Graupner, M., 2020. Short-term depression and long-term plasticity together tune sensitive range of synaptic plasticity. PLoS Comput. Biol. 16, e1008265. https://doi.org/10.1371/journal.pcbi.1008265

DeYoe, E.A., Van Essen, D.C., 1988. Concurrent processing streams in monkey visual cortex. Trends Neurosci. 11, 219–226. https://doi.org/10.1016/0166-2236(88)90130-0
Dougherty, K., Schmid, M.C., Maier, A., 2019a. Binocular Response Modulation in the Lateral Geniculate Nucleus. J. Comp. Neurol. 527, 522–534. https://doi.org/10.1002/cne.24417
Dougherty, K., Cox, M.A., Westerberg, J.A., Maier, A., 2019b. Binocular Modulation of Monocular Neurons in the Primary Visual Pathway. J. Vis. 19, 130c. https://doi.org/10.1167/19.10.130c
Dubner, R., Zeki, S.M., 1971. Response properties and receptive fields of cells in an anatomically defined region of the superior temporal sulcus in the monkey. Brain Res. 35, 528–532. https://doi.org/10.1016/0006-8993(71)90494-X
Eckhorn, R., Bauer, R., Jordan, W., Brosch, M., Kruse, W., Munk, M., Reitboeck, H.J., 1988. Coherent oscillations: a mechanism of feature linking in the visual cortex? Multiple electrode and correlation analyses in the cat. Biol. Cybern. 60, 121–130. https://doi.org/10.1007/BF00202899
Ehrenstein, W., 2003. Basics of seeing motion. Arq. Bras. Oftalmol. 66. https://doi.org/10.1590/S0004-27492003000600006
Engel, A.K., Fries, P., Singer, W., 2001. Dynamic predictions: oscillations and synchrony in top-down processing. Nat. Rev. Neurosci. 2, 704–716. https://doi.org/10.1038/35094565
Engel, A.K., König, P., Kreiter, A.K., Schillen, T.B., Singer, W., 1992. Temporal coding in the visual cortex: new vistas on integration in the nervous system. Trends Neurosci. 15, 218–226. https://doi.org/10.1016/0166-2236(92)90039-b
Engel, A.K., Roelfsema, P.R., Fries, P., Brecht, M., Singer, W., 1997. Role of the temporal domain for response selection and perceptual binding. Cereb. Cortex N. Y. N 1991 7, 571–582. https://doi.org/10.1093/cercor/7.6.571
Engel, A.K., Singer, W., 2001. Temporal binding and the neural correlates of sensory awareness. Trends Cogn. Sci. 5, 16–25. https://doi.org/10.1016/s1364-6613(00)01568-0
Felleman, D.J., Van Essen, D.C., 1991. Distributed Hierarchical Processing in the Primate Cerebral Cortex. Cereb. Cortex 1, 1–47. https://doi.org/10.1093/cercor/1.1.1
Fiebelkorn, I.C., Snyder, A.C., Mercier, M.R., Butler, J.S., Molholm, S., Foxe, J.J., 2013. Cortical cross-frequency coupling predicts perceptual outcomes. NeuroImage 69, 126–137. https://doi.org/10.1016/j.neuroimage.2012.11.021
Foster, K.H., Gaska, J.P., Nagler, M., Pollen, D.A., 1985. Spatial and temporal frequency selectivity of neurones in visual cortical areas V1 and V2 of the macaque monkey. J. Physiol. 365, 331–363. https://doi.org/10.1113/jphysiol.1985.sp015776
Freeman, W.J., Rogers, L.J., 2002. Fine Temporal Resolution of Analytic Phase Reveals Episodic Synchronization by State Transitions in Gamma EEGs. J. Neurophysiol. 87, 937–945. https://doi.org/10.1152/jn.00254.2001
Fries, P., 2009. Neuronal Gamma-Band Synchronization as a Fundamental Process in Cortical Computation. Annu. Rev. Neurosci. 32, 209–224. https://doi.org/10.1146/annurev.neuro.051508.135603
Fries, P., 2005. A mechanism for cognitive dynamics: neuronal communication through neuronal coherence. Trends Cogn. Sci. 9, 474–480. https://doi.org/10.1016/j.tics.2005.08.011

Fries, P., Reynolds, J.H., Rorie, A.E., Desimone, R., 2001. Modulation of oscillatory neuronal synchronization by selective visual attention. Science 291, 1560–1563. https://doi.org/10.1126/science.291.5508.1560

Fries, P., Roelfsema, P.R., Engel, A.K., König, P., Singer, W., 1997. Synchronization of oscillatory responses in visual cortex correlates with perception in interocular rivalry. Proc. Natl. Acad. Sci. 94, 12699–12704. https://doi.org/10.1073/pnas.94.23.12699

Friston, K., 2009. The free-energy principle: a rough guide to the brain? Trends Cogn. Sci. 13, 293–301. https://doi.org/10.1016/j.tics.2009.04.005

Gaarder, K., Koresko, R., Kropfl, W., 1966. The phasic relation of a component of alpha rhythm to fixation saccadic eye movements. Electroencephalogr. Clin. Neurophysiol. 21, 544–551. https://doi.org/10.1016/0013-4694(66)90173-8

Gegenfurtner, K.R., Kiper, D.C., Levitt, J.B., 1997. Functional Properties of Neurons in Macaque Area V3. J. Neurophysiol. 77, 1906–1923. https://doi.org/10.1152/jn.1997.77.4.1906

Gilaie-Dotan, S., 2016. Visual motion serves but is not under the purview of the dorsal pathway. Neuropsychologia 89, 378–392. https://doi.org/10.1016/j.neuropsychologia.2016.07.018

Girard, P., Salin, P.A., Bullier, J., 1992. Response selectivity of neurons in area MT of the macaque monkey during reversible inactivation of area V1. J. Neurophysiol. 67, 1437–1446. https://doi.org/10.1152/jn.1992.67.6.1437

Goodale, M.A., Milner, A.D., 1992. Separate visual pathways for perception and action. Trends Neurosci. 15, 20–25. https://doi.org/10.1016/0166-2236(92)90344-8

Gramfort, A., Luessi, M., Larson, E., Engemann, D.A., Strohmeier, D., Brodbeck, C., Parkkonen, L., Hämäläinen, M.S., 2014. MNE software for processing MEG and EEG data. NeuroImage 86, 446–460. https://doi.org/10.1016/j.neuroimage.2013.10.027

Gray, C.M., König, P., Engel, A.K., Singer, W., 1989. Oscillatory responses in cat visual cortex exhibit inter-columnar synchronization which reflects global stimulus properties. Nature 338, 334–337. https://doi.org/10.1038/338334a0

Gray, C.M., Singer, W., 1989. Stimulus-specific neuronal oscillations in orientation columns of cat visual cortex. Proc. Natl. Acad. Sci. 86, 1698–1702. https://doi.org/10.1073/pnas.86.5.1698

Gray, C.M., Viana Di Prisco, G., 1997. Stimulus-dependent neuronal oscillations and local synchronization in striate cortex of the alert cat. J. Neurosci. Off. J. Soc. Neurosci. 17, 3239–3253.

Haken, H., Stadler, M., 2012. Synergetics of Cognition: Proceedings of the International Symposium at Schloß Elmau, Bavaria, June 4–8, 1989. Springer Science & Business Media.

Hämäläinen, M.S., Ilmoniemi, R.J., 1994. Interpreting magnetic fields of the brain: minimum norm estimates. Med. Biol. Eng. Comput. 32, 35–42. https://doi.org/10.1007/BF02512476

Händel, B., Haarmeier, T., 2009. Cross-frequency coupling of brain oscillations indicates the success in visual motion discrimination. NeuroImage 45, 1040–1046. https://doi.org/10.1016/j.neuroimage.2008.12.013

Händel, B., Lutzenberger, W., Thier, P., Haarmeier, T., 2007. Opposite Dependencies on Visual Motion Coherence in Human Area MT+ and Early Visual Cortex. Cereb. Cortex 17, 1542–1549. https://doi.org/10.1093/cercor/bhl063

Hassenstein, B., Reichardt, W., 1956. Systemtheoretische Analyse der Zeit-, Reihenfolgen- und Vorzeichenauswertung bei der Bewegungsperzeption des Rüsselkäfers Chlorophanus. Z. Für Naturforschung B 11, 513–524. https://doi.org/10.1515/znb-1956-9-1004

Hecht, S., Shlaer, S., Pirenne, M.H., 1942. ENERGY, QUANTA, AND VISION. J. Gen. Physiol. 25, 819–840. https://doi.org/10.1085/jgp.25.6.819

Heitmann, S., Ermentrout, G.B., 2020. Direction-selective motion discrimination by traveling waves in visual cortex. PLOS Comput. Biol. 16, e1008164. https://doi.org/10.1371/journal.pcbi.1008164

Helfrich, R.F., Knepper, H., Nolte, G., Strüber, D., Rach, S., Herrmann, C.S., Schneider, T.R., Engel, A.K., 2014a. Selective modulation of interhemispheric functional connectivity by HD-tACS shapes perception. PLoS Biol. 12, e1002031. https://doi.org/10.1371/journal.pbio.1002031

Helfrich, R.F., Schneider, T.R., Rach, S., Trautmann-Lengsfeld, S.A., Engel, A.K., Herrmann, C.S., 2014b. Entrainment of brain oscillations by transcranial alternating current stimulation. Curr. Biol. CB 24, 333–339. https://doi.org/10.1016/j.cub.2013.12.041

Herpich, F., Melnick, M.D., Agosta, S., Huxlin, K.R., Tadin, D., Battelli, L., 2019. Boosting Learning Efficacy with Noninvasive Brain Stimulation in Intact and Brain-Damaged Humans. J. Neurosci. Off. J. Soc. Neurosci. 39, 5551–5561. https://doi.org/10.1523/JNEUROSCI.3248-18.2019

Herring, J.D., Esterer, S., Marshall, T.R., Jensen, O., Bergmann, T.O., 2019. Low-frequency alternating current stimulation rhythmically suppresses gamma-band oscillations and impairs perceptual performance. NeuroImage 184, 440–449. https://doi.org/10.1016/j.neuroimage.2018.09.047

Herrmann, C.S., Rach, S., Neuling, T., Strüber, D., 2013. Transcranial alternating current stimulation: a review of the underlying mechanisms and modulation of cognitive processes. Front. Hum. Neurosci. 7. https://doi.org/10.3389/fnhum.2013.00279

Hotson, J., Braun, D., Herzberg, W., Boman, D., 1994. Transcranial magnetic stimulation of extrastriate cortex degrades human motion direction discrimination. Vision Res. 34, 2115–2123. https://doi.org/10.1016/0042-6989(94)90321-2

Howarth, M., Walmsley, L., Brown, T.M., 2014. Binocular Integration in the Mouse Lateral Geniculate Nuclei. Curr. Biol. 24, 1241–1247. https://doi.org/10.1016/j.cub.2014.04.014

Hubbard, R., Wald, G., 1951. The Mechanism of Rhodopsin Synthesis. Proc. Natl. Acad. Sci. U. S. A. 37, 69–79.

Hubel, D.H., Wiesel, T.N., 1968. Receptive fields and functional architecture of monkey striate cortex. J. Physiol. 195, 215–243. https://doi.org/10.1113/jphysiol.1968.sp008455

Hubel, D.H., Wiesel, T.N., 1965. RECEPTIVE FIELDS AND FUNCTIONAL ARCHITECTURE IN TWO NONSTRIATE VISUAL AREAS (18 AND 19) OF THE CAT. J. Neurophysiol. 28, 229–289. https://doi.org/10.1152/jn.1965.28.2.229

Hubel, D.H., Wiesel, T.N., 1962. Receptive fields, binocular interaction and functional architecture in the cat's visual cortex. J. Physiol. 160, 106-154.2.

Huk, A.C., Dougherty, R.F., Heeger, D.J., 2002. Retinotopy and Functional Subdivision of Human Areas MT and MST. J. Neurosci. 22, 7195–7205. https://doi.org/10.1523/JNEUROSCI.22-16-07195.2002

Hülsdünker, T., Ostermann, M., Mierau, A., 2019. The Speed of Neural Visual Motion Perception and Processing Determines the Visuomotor Reaction Time of Young Elite Table Tennis Athletes. Front. Behav. Neurosci. 13. https://doi.org/10.3389/fnbeh.2019.00165

Hupé, J.M., James, A.C., Girard, P., Lomber, S.G., Payne, B.R., Bullier, J., 2001. Feedback connections act on the early part of the responses in monkey visual cortex. J. Neurophysiol. 85, 134–145. https://doi.org/10.1152/jn.2001.85.1.134

Hutchinson, B.T., Pammer, K., Bandara, K., 2020. tACS Stimulation at Alpha Frequency Selectively Induces Inattentional Blindness. Brain Topogr. 33, 317–326. https://doi.org/10.1007/s10548-020-00762-9

Huxlin, K.R., Martin, T., Kelly, K., Riley, M., Friedman, D.I., Burgin, W.S., Hayhoe, M., 2009. Perceptual Relearning of Complex Visual Motion after V1 Damage in Humans. J. Neurosci. 29, 3981–3991. https://doi.org/10.1523/JNEUROSCI.4882-08.2009

Ille, N., Berg, P., Scherg, M., 2002. Artifact correction of the ongoing EEG using spatial filters based on artifact and brain signal topographies. J. Clin. Neurophysiol. Off. Publ. Am. Electroencephalogr. Soc. 19, 113–124. https://doi.org/10.1097/00004691-200203000-00002

Jensen, O., Mazaheri, A., 2010. Shaping Functional Architecture by Oscillatory Alpha Activity: Gating by Inhibition. Front. Hum. Neurosci. 4. https://doi.org/10.3389/fnhum.2010.00186

Johansson, G., 1975. VISUAL MOTION PERCEPTION. Sci. Am. 232, 76–89.

Jones, H.E., Andolina, I.M., Shipp, S.D., Adams, D.L., Cudeiro, J., Salt, T.E., Sillito, A.M., 2015. Figure-ground modulation in awake primate thalamus. Proc. Natl. Acad. Sci. 112, 7085–7090. https://doi.org/10.1073/pnas.1405162112

Kanai, R., Chaieb, L., Antal, A., Walsh, V., Paulus, W., 2008. Frequency-dependent electrical stimulation of the visual cortex. Curr. Biol. CB 18, 1839–1843. https://doi.org/10.1016/j.cub.2008.10.027

Kandel, E., 2014. Visual Processing and Action, in: Principles of Neural Science. McGraw-Hill Education, New York, NY.

Kar, K., Krekelberg, B., 2014. Transcranial Alternating Current Stimulation Attenuates Visual Motion Adaptation. J. Neurosci. 34, 7334–7340. https://doi.org/10.1523/JNEUROSCI.5248-13.2014

Karabanov, A., Thielscher, A., Siebner, H.R., 2016. Transcranial brain stimulation: closing the loop between brain and stimulation. Curr. Opin. Neurol. 29, 397–404. https://doi.org/10.1097/WCO.0000000000000342

Kasten, F.H., Dowsett, J., Herrmann, C.S., 2016. Sustained Aftereffect of α-tACS Lasts Up to 70 min after Stimulation. Front. Hum. Neurosci. 10. https://doi.org/10.3389/fnhum.2016.00245

Kasten, F.H., Herrmann, C.S., 2017. Transcranial Alternating Current Stimulation (tACS) Enhances Mental Rotation Performance during and after Stimulation. Front. Hum. Neurosci. 11, 2. https://doi.org/10.3389/fnhum.2017.00002

Kasten, F.H., Maess, B., Herrmann, C.S., 2018. Facilitated Event-Related Power Modulations during Transcranial Alternating Current Stimulation (tACS) Revealed by Concurrent tACS-MEG. eNeuro 5. https://doi.org/10.1523/ENEURO.0069-18.2018

Kinchla, R.A., Wolfe, J.M., 1979. The order of visual processing: “Top-down,” “bottom-up,” or “middle-out.” Percept. Psychophys. 25, 225–231. https://doi.org/10.3758/BF03202991

Klimesch, W., Hanslmayr, S., Sauseng, P., Gruber, W.R., Doppelmayr, M., 2007. P1 and Traveling Alpha Waves: Evidence for Evoked Oscillations. J. Neurophysiol. 97, 1311–1318. https://doi.org/10.1152/jn.00876.2006

Kohli, S., Casson, A.J., 2019. Removal of Gross Artifacts of Transcranial Alternating Current Stimulation in Simultaneous EEG Monitoring. Sensors 19, 190. https://doi.org/10.3390/s19010190

Köster, M., Finger, H., Graetz, S., Kater, M., Gruber, T., 2018. Theta-gamma coupling binds visual perceptual features in an associative memory task. Sci. Rep. 8, 17688. https://doi.org/10.1038/s41598-018-35812-7

Krause, M.R., Vieira, P.G., Csorba, B.A., Pilly, P.K., Pack, C.C., 2019. Transcranial alternating current stimulation entrains single-neuron activity in the primate brain. Proc. Natl. Acad. Sci. 116, 5747–5755. https://doi.org/10.1073/pnas.1815958116

Kreiter, A.K., Singer, W., 1996. Stimulus-dependent synchronization of neuronal responses in the visual cortex of the awake macaque monkey. J. Neurosci. Off. J. Soc. Neurosci. 16, 2381–2396.

Laczó, B., Antal, A., Niebergall, R., Treue, S., Paulus, W., 2012. Transcranial alternating stimulation in a high gamma frequency range applied over V1 improves contrast perception but does not modulate spatial attention. Brain Stimulat. 5, 484–491. https://doi.org/10.1016/j.brs.2011.08.008

Lakatos, P., Karmos, G., Mehta, A.D., Ulbert, I., Schroeder, C.E., 2008. Entrainment of Neuronal Oscillations as a Mechanism of Attentional Selection. Science 320, 110–113. https://doi.org/10.1126/science.1154735

Lee, H., Simpson, G.V., Logothetis, N.K., Rainer, G., 2005. Phase Locking of Single Neuron Activity to Theta Oscillations during Working Memory in Monkey Extrastriate Visual Cortex. Neuron 45, 147–156. https://doi.org/10.1016/j.neuron.2004.12.025

Lefebvre, J., Hutt, A., Frohlich, F., 2017. Stochastic resonance mediates the state-dependent effect of periodic stimulation on cortical alpha oscillations. eLife 6, e32054. https://doi.org/10.7554/eLife.32054

Li, B., Chen, Y., Li, B.W., Wang, L.H., Diao, Y.C., 2001. Pattern and component motion selectivity in cortical area PMLS of the cat. Eur. J. Neurosci. 14, 690–700. https://doi.org/10.1046/j.0953-816x.2001.01689.x

Livingstone, M.S., Hubel, D.H., 1988. Do the relative mapping densities of the magno- and parvocellular systems vary with eccentricity? J. Neurosci. Off. J. Soc. Neurosci. 8, 4334–4339.

Livingstone, M.S., Hubel, D.H., 1984. Specificity of intrinsic connections in primate primary visual cortex. J. Neurosci. Off. J. Soc. Neurosci. 4, 2830–2835.

Llinás, R., Yarom, Y., 1986. Oscillatory properties of guinea-pig inferior olivary neurones and their pharmacological modulation: an in vitro study. J. Physiol. 376, 163–182. https://doi.org/10.1113/jphysiol.1986.sp016147

Manuel, A.L., Guggisberg, A.G., Thézé, R., Turri, F., Schnider, A., 2018. Resting-state connectivity predicts visuo-motor skill learning. NeuroImage 176, 446–453. https://doi.org/10.1016/j.neuroimage.2018.05.003

Markov, N.T., Vezoli, J., Chameau, P., Falchier, A., Quilodran, R., Huissoud, C., Lamy, C., Misery, P., Giroud, P., Ullman, S., Barone, P., Dehay, C., Knoblauch, K., Kennedy, H., 2013. Anatomy of hierarchy: Feedforward and feedback pathways in macaque visual cortex. J. Comp. Neurol. 522, 225–259. https://doi.org/10.1002/cne.23458

Markram, H., Lübke, J., Frotscher, M., Sakmann, B., 1997. Regulation of Synaptic Efficacy by Coincidence of Postsynaptic APs and EPSPs. Science 275, 213–215. https://doi.org/10.1126/science.275.5297.213

Maunsell, J.H., Nealey, T.A., DePriest, D.D., 1990. Magnocellular and parvocellular contributions to responses in the middle temporal visual area (MT) of the macaque monkey. J. Neurosci. 10, 3323–3334. https://doi.org/10.1523/JNEUROSCI.10-10-03323.1990

Michalareas, G., Vezoli, J., van Pelt, S., Schoffelen, J.-M., Kennedy, H., Fries, P., 2016. Alpha-Beta and Gamma Rhythms Subserve Feedback and Feedforward Influences among Human Visual Cortical Areas. Neuron 89, 384–397. https://doi.org/10.1016/j.neuron.2015.12.018

Mishkin, M., Ungerleider, L.G., 1982. Contribution of striate inputs to the visuospatial functions of parieto-preoccipital cortex in monkeys. Behav. Brain Res. 6, 57–77. https://doi.org/10.1016/0166-4328(82)90081-X

Movshon, J.A., Newsome, W.T., 1996. Visual Response Properties of Striate Cortical Neurons Projecting to Area MT in Macaque Monkeys. J. Neurosci. 16, 7733–7741. https://doi.org/10.1523/JNEUROSCI.16-23-07733.1996

Muller, L., Chavane, F., Reynolds, J., Sejnowski, T.J., 2018. Cortical travelling waves: mechanisms and computational principles. Nat. Rev. Neurosci. 19, 255–268. https://doi.org/10.1038/nrn.2018.20

Neuling, T., Rach, S., Herrmann, C.S., 2013a. Orchestrating neuronal networks: sustained after-effects of transcranial alternating current stimulation depend upon brain states. Front. Hum. Neurosci. 7, 161. https://doi.org/10.3389/fnhum.2013.00161

Neuling, T., Rach, S., Herrmann, C.S., 2013b. Orchestrating neuronal networks: sustained after-effects of transcranial alternating current stimulation depend upon brain states. Front. Hum. Neurosci. 7, 161. https://doi.org/10.3389/fnhum.2013.00161

Neuling, T., Ruhnau, P., Fuscà, M., Demarchi, G., Herrmann, C.S., Weisz, N., 2015. Friends, not foes: Magnetoencephalography as a tool to uncover brain dynamics during transcranial alternating current stimulation. NeuroImage 118, 406–413. https://doi.org/10.1016/j.neuroimage.2015.06.026

Newsome, W.T., Wurtz, R.H., Dürsteler, M.R., Mikami, A., 1985. Deficits in visual motion processing following ibotenic acid lesions of the middle temporal visual area of the macaque monkey. J. Neurosci. Off. J. Soc. Neurosci. 5, 825–840.

Orban, G.A., Van Essen, D., Vanduffel, W., 2004. Comparative mapping of higher visual areas in monkeys and humans. Trends Cogn. Sci. 8, 315–324. https://doi.org/10.1016/j.tics.2004.05.009

Orekhova, E.V., Butorina, A.V., Sysoeva, O.V., Prokofyev, A.O., Nikolaeva, A.Yu., Stroganova, T.A., 2015. Frequency of gamma oscillations in humans is modulated by velocity of visual motion. J. Neurophysiol. 114, 244–255. https://doi.org/10.1152/jn.00232.2015

Palva, S., Palva, J.M., 2011. Functional Roles of Alpha-Band Phase Synchronization in Local and Large-Scale Cortical Networks. Front. Psychol. 2. https://doi.org/10.3389/fpsyg.2011.00204

Park, S.H., Lee, S.-H., 2007. Feature-specific modulation of Gamma oscillations in visual detection. J. Vis. 7, 1014. https://doi.org/10.1167/7.9.1014

Pasternak, T., Merigan, W.H., 1994. Motion perception following lesions of the superior temporal sulcus in the monkey. Cereb. Cortex N. Y. N 1991 4, 247–259. https://doi.org/10.1093/cercor/4.3.247

Pasternak, T., Schumer, R.A., Gizzi, M.S., Movshon, J.A., 1985. Abolition of visual cortical direction selectivity affects visual behavior in cats. Exp. Brain Res. 61, 214–217. https://doi.org/10.1007/BF00235638

Pitts, W., McCulloch, W.S., 1947. How we know universals; the perception of auditory and visual forms. Bull. Math. Biophys. 9, 127–147. https://doi.org/10.1007/BF02478291

Polanía, R., Nitsche, M.A., Korman, C., Batsikadze, G., Paulus, W., 2012. The Importance of Timing in Segregated Theta Phase-Coupling for Cognitive Performance. Curr. Biol. 22, 1314–1318. https://doi.org/10.1016/j.cub.2012.05.021

Qiu, F.T., von der Heydt, R., 2005. Figure and Ground in the Visual Cortex: V2 Combines Stereoscopic Cues with Gestalt Rules. Neuron 47, 155–166. https://doi.org/10.1016/j.neuron.2005.05.028

Raffin, E., Salamanca-Giron, R.F., Hummel, F.C., 2020. Perspectives: Hemianopia-Toward Novel Treatment Options Based on Oscillatory Activity? Neurorehabil. Neural Repair 34, 13–25. https://doi.org/10.1177/1545968319893286

Rauss, K., Pourtois, G., 2013. What is Bottom-Up and What is Top-Down in Predictive Coding? Front. Psychol. 4. https://doi.org/10.3389/fpsyg.2013.00276

Richter, C.G., Thompson, W.H., Bosman, C.A., Fries, P., 2017. Top-down beta enhances bottom-up gamma. J. Neurosci. 3771–16. https://doi.org/10.1523/JNEUROSCI.3771-16.2017

Roelfsema, P.R., Engel, A.K., König, P., Singer, W., 1997. Visuomotor integration is associated with zero time-lag synchronization among cortical areas. Nature 385, 157–161. https://doi.org/10.1038/385157a0

Rohenkohl, G., Bosman, C.A., Fries, P., 2018. Gamma Synchronization between V1 and V4 Improves Behavioral Performance. Neuron 100, 953-963.e3. https://doi.org/10.1016/j.neuron.2018.09.019

Rokszin, A., Márkus, Z., Braunitzer, G., Berényi, A., Benedek, G., Nagy, A., 2010. Visual Pathways Serving Motion Detection in the Mammalian Brain. Sensors 10, 3218–3242. https://doi.org/10.3390/s100403218

Ronconi, L., Melcher, D., Junghöfer, M., Wolters, C.H., Busch, N.A., 2020. Testing the effect of tACS over parietal cortex in modulating endogenous alpha rhythm and temporal integration windows in visual perception. Eur. J. Neurosci. https://doi.org/10.1111/ejn.15017

Ronconi, L., Oosterhof, N.N., Bonmassar, C., Melcher, D., 2017. Multiple oscillatory rhythms determine the temporal organization of perception. Proc. Natl. Acad. Sci. 114, 13435–13440. https://doi.org/10.1073/pnas.1714522114

Rowe, H.E., 2020. Heterodyne principle. Access Sci. https://doi.org/10.1036/1097-8542.316000

Ruhnau, P., Neuling, T., Fuscá, M., Herrmann, C.S., Demarchi, G., Weisz, N., 2016. Eyes wide shut: Transcranial alternating current stimulation drives alpha rhythm in a state dependent manner. Sci. Rep. 6, 27138. https://doi.org/10.1038/srep27138

Sabel, B.A., Hamid, A.I.A., Borrmann, C., Speck, O., Antal, A., 2019. Transorbital alternating current stimulation modifies BOLD activity in healthy subjects and in a stroke patient with hemianopia: A 7 Tesla fMRI feasibility study. Int. J. Psychophysiol. https://doi.org/10.1016/j.ijpsycho.2019.04.002

Saionz, E.L., Feldon, S.E., Huxlin, K.R., 2021. Rehabilitation of cortically induced visual field loss. Curr. Opin. Neurol. 34, 67–74. https://doi.org/10.1097/WCO.0000000000000884

Sakata, H., Taira, M., Kusunoki, M., Murata, A., Tanaka, Y., 1997. The TINS Lecture. The parietal association cortex in depth perception and visual control of hand action. Trends Neurosci. 20, 350–357. https://doi.org/10.1016/s0166-2236(97)01067-9

Salzman, C.D., Murasugi, C.M., Britten, K.H., Newsome, W.T., 1992. Microstimulation in visual area MT: effects on direction discrimination performance. J. Neurosci. 12, 2331–2355. https://doi.org/10.1523/JNEUROSCI.12-06-02331.1992

Santarnecchi, E., Biasella, A., Tatti, E., Rossi, A., Prattichizzo, D., Rossi, S., 2017. High-gamma oscillations in the motor cortex during visuo-motor coordination: A tACS interferential study. Brain Res. Bull. 131, 47–54. https://doi.org/10.1016/j.brainresbull.2017.03.006

Saturnino, G.B., Madsen, K.H., Siebner, H.R., Thielscher, A., 2017. How to target inter-regional phase synchronization with dual-site Transcranial Alternating Current Stimulation. NeuroImage 163, 68–80. https://doi.org/10.1016/j.neuroimage.2017.09.024

Saturnino, G.B., Siebner, H.R., Thielscher, A., Madsen, K.H., 2019. Accessibility of cortical regions to focal TES: Dependence on spatial position, safety, and practical constraints. NeuroImage 203, 116183. https://doi.org/10.1016/j.neuroimage.2019.116183

Schaerer, S., Neumeyer, C., 1996. Motion detection in goldfish investigated with the optomotor response is “color blind.” Vision Res. 36, 4025–4034. https://doi.org/10.1016/S0042-6989(96)00149-6

Schroeder, C.E., Mehta, A.D., Givre, S.J., 1998. A spatiotemporal profile of visual system activation revealed by current source density analysis in the awake macaque. Cereb. Cortex N. Y. N 1991 8, 575–592. https://doi.org/10.1093/cercor/8.7.575

Schuhmann, T., Kemmerer, S.K., Duecker, F., de Graaf, T.A., Ten Oever, S., De Weerd, P., Sack, A.T., 2019. Left parietal tACS at alpha frequency induces a shift of visuospatial attention. PloS One 14, e0217729. https://doi.org/10.1371/journal.pone.0217729

Schutter, D.J.L.G., Hortensius, R., 2011. Brain oscillations and frequency-dependent modulation of cortical excitability. Brain Stimulat. 4, 97–103. https://doi.org/10.1016/j.brs.2010.07.002

Shipp, S., Zeki, S., 1989. The Organization of Connections between Areas V5 and V1 in Macaque Monkey Visual Cortex. Eur. J. Neurosci. 1, 309–332. https://doi.org/10.1111/j.1460-9568.1989.tb00798.x

Silvanto, J., Muggleton, N., Walsh, V., 2008. State-dependency in brain stimulation studies of perception and cognition. Trends Cogn. Sci. 12, 447–454. https://doi.org/10.1016/j.tics.2008.09.004

Singer, W., 2018. Neuronal oscillations: unavoidable and useful? Eur. J. Neurosci. 48, 2389–2398. https://doi.org/10.1111/ejn.13796

Singer, W., 1999. Neuronal Synchrony: A Versatile Code for the Definition of Relations? Neuron 24, 49–65. https://doi.org/10.1016/S0896-6273(00)80821-1

Singer, W., Gray, C.M., 1995. Visual feature integration and the temporal correlation hypothesis. Annu. Rev. Neurosci. 18, 555–586. https://doi.org/10.1146/annurev.ne.18.030195.003011

Snowden, R.J., Freeman, T.C.A., 2004. The visual perception of motion. Curr. Biol. CB 14, R828-831. https://doi.org/10.1016/j.cub.2004.09.033

Strogatz, S., 2003. Synchronization: A Universal Concept in Nonlinear Sciences. Phys. Today 56, 47–47. https://doi.org/10.1063/1.1554136

Strüber, D., Rach, S., Trautmann-Lengsfeld, S.A., Engel, A.K., Herrmann, C.S., 2014. Antiphasic 40 Hz oscillatory current stimulation affects bistable motion perception. Brain Topogr. 27, 158–171. https://doi.org/10.1007/s10548-013-0294-x

Thut, G., Bergmann, T.O., Fröhlich, F., Soekadar, S.R., Brittain, J.-S., Valero-Cabré, A., Sack, A., Miniussi, C., Antal, A., Siebner, H.R., Ziemann, U., Herrmann, C.S., 2017a. Guiding transcranial brain stimulation by EEG/MEG to interact with ongoing brain activity and associated functions: A position paper. Clin. Neurophysiol. Off. J. Int. Fed. Clin. Neurophysiol. 128, 843–857. https://doi.org/10.1016/j.clinph.2017.01.003

Thut, G., Schyns, P., Gross, J., 2011. Entrainment of Perceptually Relevant Brain Oscillations by Non-Invasive Rhythmic Stimulation of the Human Brain. Front. Psychol. 0. https://doi.org/10.3389/fpsyg.2011.00170

Townsend, R.G., Solomon, S.S., Martin, P.R., Solomon, S.G., Gong, P., 2017. Visual Motion Discrimination by Propagating Patterns in Primate Cerebral Cortex. J. Neurosci. 37, 10074–10084. https://doi.org/10.1523/JNEUROSCI.1538-17.2017

Tsin, A., Betts-Obregon, B., Grigsby, J., 2018. Visual cycle proteins: Structure, function, and roles in human retinal disease. J. Biol. Chem. 293, 13016–13021. https://doi.org/10.1074/jbc.AW118.003228

Ungerleider, L.G., Mishkin, M., 1979. The striate projection zone in the superior temporal sulcus of Macaca mulatta: Location and topographic organization. J. Comp. Neurol. 188, 347–366. https://doi.org/10.1002/cne.901880302

Uusitalo, M.A., Ilmoniemi, R.J., 1997. Signal-space projection method for separating MEG or EEG into components. Med. Biol. Eng. Comput. 35, 135–140. https://doi.org/10.1007/BF02534144

v. Monakow, C., 1895. Experimentelle und pathologisch-anatomische Untersuchungen über die Haubenregion, den Sehhügel und die Regio subthalamica, nebst Beiträgen zur Kenntniss früh erworbener Gross- und Kleinhirn-defecte. Arch. Für Psychiatr. Nervenkrankh. 27, 1–128. https://doi.org/10.1007/BF02076254

van de Grind, W.A., Koenderink, J.J., van Doorn, A.J., 1986. The distribution of human motion detector properties in the monocular visual field. Vision Res. 26, 797–810. https://doi.org/10.1016/0042-6989(86)90095-7

Van Essen, D.C., Gallant, J.L., 1994. Neural mechanisms of form and motion processing in the primate visual system. Neuron 13, 1–10. https://doi.org/10.1016/0896-6273(94)90455-3

van Kerkoerle, T., Self, M.W., Dagnino, B., Gariel-Mathis, M.-A., Poort, J., van der Togt, C., Roelfsema, P.R., 2014. Alpha and gamma oscillations characterize feedback and feedforward processing in monkey visual cortex. Proc. Natl. Acad. Sci. U. S. A. 111, 14332–14341. https://doi.org/10.1073/pnas.1402773111

Varela, F., Lachaux, J.-P., Rodriguez, E., Martinerie, J., 2001. The brainweb: Phase synchronization and large-scale integration. Nat. Rev. Neurosci. 2, 229–239. https://doi.org/10.1038/35067550

Varela, F.J., Toro, A., John, E.R., Schwartz, E.L., 1981. Perceptual framing and cortical alpha rhythm. Neuropsychologia 19, 675–686. https://doi.org/10.1016/0028-3932(81)90005-1

Volgushev, M., Pernberg, J., Eysel, U.T., 2003. Gamma-frequency fluctuations of the membrane potential and response selectivity in visual cortical neurons. Eur. J. Neurosci. 17, 1768–1776. https://doi.org/10.1046/j.1460-9568.2003.02609.x

Vossen, A., Gross, J., Thut, G., 2015. Alpha Power Increase After Transcranial Alternating Current Stimulation at Alpha Frequency (α-tACS) Reflects Plastic

Changes Rather Than Entrainment. Brain Stimulat. 8, 499–508. https://doi.org/10.1016/j.brs.2014.12.004
Wakeman, D.G., Henson, R.N., 2015. A multi-subject, multi-modal human neuroimaging dataset. Sci. Data 2, 150001. https://doi.org/10.1038/sdata.2015.1
Wald, G., 1935. CAROTENOIDS AND THE VISUAL CYCLE. J. Gen. Physiol. 19, 351–371.
Wallach, H., 1935. Über visuell wahrgenommene Bewegungsrichtung. Psychol. Forsch. 20, 325–380. https://doi.org/10.1007/BF02409790
Wang, X.-J., 2010. Neurophysiological and Computational Principles of Cortical Rhythms in Cognition. Physiol. Rev. 90, 1195–1268. https://doi.org/10.1152/physrev.00035.2008
Webster, K., Ro, T., 2020. Visual Modulation of Resting State α Oscillations. eNeuro 7, ENEURO.0268-19.2019. https://doi.org/10.1523/ENEURO.0268-19.2019
Weyand, T.G., 2016. The multifunctional lateral geniculate nucleus. Rev. Neurosci. 27, 135–157. https://doi.org/10.1515/revneuro-2015-0018
Wischnewski, M., Engelhardt, M., Salehinejad, M.A., Schutter, D.J.L.G., Kuo, M.-F., Nitsche, M.A., 2019. NMDA Receptor-Mediated Motor Cortex Plasticity After 20 Hz Transcranial Alternating Current Stimulation. Cereb. Cortex N. Y. N 1991 29, 2924–2931. https://doi.org/10.1093/cercor/bhy160
Zarubin, Georgy, Gundlach, C., Nikulin, V., Villringer, A., Bogdan, M., 2020. Transient Amplitude Modulation of Alpha-Band Oscillations by Short-Time Intermittent Closed-Loop tACS. Front. Hum. Neurosci. 14. https://doi.org/10.3389/fnhum.2020.00366
Zarubin, G., Gundlach, C., Nikulin, V., Villringer, A., Bogdan, M., 2020. Transient amplitude modulation of alpha-band oscillations by short-time intermittent closed-loop tACS. bioRxiv 2020.01.23.916676. https://doi.org/10.1101/2020.01.23.916676
Zeki, S., 2015. Area V5—a microcosm of the visual brain. Front. Integr. Neurosci. 9. https://doi.org/10.3389/fnint.2015.00021
Zeki, S.M., 1978. Functional specialisation in the visual cortex of the rhesus monkey. Nature 274, 423–428. https://doi.org/10.1038/274423a0
Zeki, S.M., 1974. Functional organization of a visual area in the posterior bank of the superior temporal sulcus of the rhesus monkey. J. Physiol. 236, 549–573. https://doi.org/10.1113/jphysiol.1974.sp010452
Zrenner, C., Belardinelli, P., Müller-Dahlhaus, F., Ziemann, U., 2016. Closed-Loop Neuroscience and Non-Invasive Brain Stimulation: A Tale of Two Loops. Front. Cell. Neurosci. 10. https://doi.org/10.3389/fncel.2016.00092

ROBERTO FELIPE SALAMANCA GIRON

Engineer | Scientist | Maker | Bio-Hacker

(+41) 762262798
robertofelipe.sg@gmail.com
robertofelipesg

"What is to give light must endure burning." - Viktor Frankl -

Work Experience

EPFL — *Swiss Federal Institute of Technology, Lausanne, Switzerland, 2017-2021*

Teaching Assistant
Fundamentals of Biosensors and Electronic Biochips
Electric and Electronics Systems
Neuroscience for Engineers

campus biotech / Fondation Campus Biotech Geneva — *Campus Biotech, Center for Neuroprosthetics - EPFL, Geneva, Switzerland, 2017*

Research Engineer
Data acquisition and analysis of the effects of a visual discrimination task in a cohort of healthy participants influenced by Non Invasive Brain Stimulation.

ICM — *Brain and Spine Institute, Paris, France, 2016*

Research Engineer
Design of an electrical dynamical model of an stimulated brain embedded in a theoretical Closed-Loop system.

Data acquisition and analysis from healthy human electrophysiological recordings during a attentional task under Transcranial Electric Stimulation.

UN Universidad Nacional de Colombia — *National University of Colombia, Bogota, Colombia, 2010-2015*

Research Engineer
Mathematical model and simulation of the dynamics of Raloxifene molecules over bone bio-functionalized implants

Teaching Assistant
Radiofrequency Circuits Lab
Analysis of AC Electrical Circuits
Ethics in Biomedical & Psychsocial Research

Tech Skills

Electronics: Embedded systems (Unix), Radiofrequency & Music circuitying, FPGA (VHDL/Verilog), PCB Manufacturing & Prototyping (Eagle), Design & Simulation (Multisim).
Software: Python, R, Java, Matlab, Linux Shell, C, C++, HTML, Assembler, Latex, Logo
Others: Closed-loop, Big Data Analysis, Machine Learning, Real-time, Computer Vision, Control Theory

Education

EPFL — *Swiss Federal Institute of Technology, Lausanne, Switzerland, 2017-2021*

Ph.D. Clinical Neuro-Engineering

ESPCI PARIS PSL — *Sciences & Letters University from Paris, Paris, France, 2016-2017*

M.Eng. Bio-Engineering and Neuroscience

Université de Paris — *University of Paris, Paris, France, 2015-2016*

M.Sc. Biomedical Engineering

Universidad Nacional de Colombia Sede Bogotá — *National University of Colombia, Bogota, Colombia, 2010-2015*

B.Eng. Electronics Engineering

Research

Raffin*, Salamanca-Giron*, Hummel. (2019) Perspectives: Hemianopia – towards novel treatment options based on oscillatory activity? Neurorehabilitation and Neural Repair.
Salamanca-Giron et al. (2021) Enhancing visual motion discrimination by desynchronizing bifocal oscillatory activity NeuroImage
Salamanca-Giron et al. (2021) Cross-frequency tACS modulates EEG coupling during a motion discrimination task (In preparation)
Salamanca-Giron et al. (2021) tACS Bursts improve visual discrimination through causal links between V1 and V5 (In preparation)

Awards

2020, Baden Baden, Germany. Scholar's Travel Fellowship. NIBS International Conference
2019, Lausanne, Switzerland. Young Investigator Award. Translational Neurotechnology for Vision Symposium
2018, Providence, USA. Brown Uni. Student's Fellowship. Translational Neuroscience and Neuroengineering Workshop
2016, Paris, France. Master's Mobility Fellowship. L'Université Sorbonne Paris Cité
2015, Bogota, Colombia. Master's Degree Fellowship. Faculty of Engineering, National University of Colombia

Personal

Polyglot **(Spanish, English, French, Italian)** sportsman, founder of tech events **(e.g. Hacka-Vita),** passionate for neuroplasticty & entrepreneurship **(e.g. Forum Innovation Lausanne)** and with a deep drive to help others **(e.g. Students' Representative).**